EXPERIMENTAL CHARACTERISATION AND NUMERICAL STRESS MODELLING OF FATIGUE PERFORMANCE AND DURABILITY OF MARINE EPOXY BALLAST TANK COATINGS

A. M. ORIAIFO

PhD

2016

EXPERIMENTAL CHARACTERISATION AND NUMERICAL STRESS MODELLING OF FATIGUE PERFORMANCE AND DURABILITY OF MARINE EPOXY BALLAST TANK COATINGS

AIGBOKHAEBHO M ORIAIFO (MSc)

A thesis submitted in partial fulfilment of the requirements of the University of Northumbria at Newcastle for the degree of Doctor of Philosophy

Research undertaken in the Faculty of Engineering and in collaboration with Safinah Limited

October 2016

Abstract

Water ballast tanks (WBTs) are the most challenging areas of a merchant ship to protect and maintain against corrosion due to their size, structural complexity and operational conditions.

Prior to commercial use, WBT coatings must be 'type approved' by meeting criteria described in the International Maritime Organisation (IMO), Performance Standard for Protective Coatings for Dedicated Seawater Ballast Tanks (PSPC). Despite being 'type approved', early cracking failure of some WBT coatings has been observed in-service resulting in increased efforts from industry and scientific community to address this issue by developing a fundamental understanding of the factors influencing cracking. Typically, the cracks appear on welds where the coating is applied thickest, surface preparation is different, geometry is involved and after exposure to hygrothermal cycling conditions typically found in WBT. In addition, so called 'pure epoxies' are positioned as having superior performance in WBTs although there is no documented evidence to confirm this belief.

This study is aimed at characterising the optimum fatigue performance and durability of WBT coatings against cracking.

Test protocols commonly utilised in evaluating the performance of WBT coatings were reviewed. Factors affecting cracking of WBT coatings were prioritised for investigation. WBT coating formulations were grouped and 4 typical variants: solvent containing pure epoxy (SPE), solvent free pure epoxy (SFPE), solvent containing modified epoxy (SME) and solvent free modified epoxy (SFME) were manufactured. Each formulation was spray applied on T specimens (which had two types of surface preparation) and polytetrafluoroethylene (PTFE) panels. Free films peeled from the PTFE panels were shaped into rectangular and dog bone specimens respectively. In addition, two types of dry film thicknesses (DFT) for dog bone and T specimens were investigated.

Under laboratory conditions, a proposed fatigue test was designed to characterise and establish relationship between resistance to cracking and coating properties. In addition, thermal analysis techniques, differential scanning calorimetry (DSC), thermo-mechanical analysis (TMA) and dynamic mechanical analysis (DMA) were used to measure coating properties of free films including glass transition temperature (Tg), coefficient of thermal expansion (CTE) and storage modulus (E')

of specimens that were unaged and aged. DFTs were measured for unaged and aged T specimens. Tensile fracture strength and elongation to fracture were measured. A reanalysis with duplicate set of specimens was performed to validate the fatigue test and thermal analytical techniques. Finite element analysis (FEA) was used to simulate stress distribution as a function of coating film thickness. Statistical analysis (ANOVA test) was used to compare the mean effect of volume loss of DFTs measured before and after fatigue test.

The results of the fatigue testing produced a specific ranking twice and demonstrated the effect of hygrothermal stress on WBT formulations. SFPE was most crack resistant with fewer T specimens failing at the intersection weld and SPE was the worst. FEA modelling confirmed the increase of stress on the welded corner with increase in coating film thickness.

Thermal analysis measurement were not invariable exhibiting a mixture of increase and decrease in magnitude with subsequent exposure conditions. Tg and E' values increased significantly for SPE and SME while the reverse was for SFPE and SFME. CTE values was significantly higher for SFPE and SFME but lower for SPE and SME.

Mechanical tensile testing showed that the fracture strength of the aged specimen increased for the four formulations with SFPE showing the least increase by 2 times the unaged and SPE with the most increase by 9 times the unaged. The elongation to fracture decreased significantly with SFPE decreasing to 1.87% while other formulations including SPE decreased to approximately 1 %.

ANOVA statistics found that the amount of volume loss from DFT was significant and depended on formulation. SFPE had significantly less volume loss than others including SPE that showed the highest amount of volume loss.

The implication from this finding is that it is unsafe to generalise the performance behaviour of WBT coatings from one constituent of the formulation. Rather, comments on performance should be on the formulation as whole.

List of Contents

List of Figures

List of Tables

Acknowledgement

To date, I owe a considerable amount of gratitude and appreciation to Northumbria University and Industrial partners for the Scholarship, enormous support; continuous guidance, input and feedback that have made this project possible. Simply put, without their interest and ready assistance, this project would not have been possible.

I would like to thank the supervisory team: Dr Noel Perera, Dr Pak Sing Leung and Dr John Kian Tan for their guidance throughout the research duration.

I would like to express my gratitude to Safinah Limited most especially Dr Raouf Kattan and Mr Alan Guy (Industrial supervisor - whom I am privilege to call my friend) for the massive support offered. Also, to other industrial partners: Mr Edward Jansen of America Bureau of Shipping, Mr Richard Sloan of AkzoNobel, Dr Michael Cook of Air Product & Chemicals Inc., and Mr John Petersen of Bluewater Energy Services.

Also, to my lovely wife: Mrs Opeyemi Oriaifo, my amiable kids: Miss Eboseluimen Oriaifo and Master Oseghale Oriaifo for their endurance, support and understanding showed to me during this research period. Also to my parents, siblings and in-laws for always being there. Above all, I wish to express my sincere gratitude to God for His mercies and graces towards me.

Author's Declaration

I herein declare that the research contained in this thesis has not been submitted for any other award and that is my original contribution. I also confirm that this research fully acknowledges opinions, ideas and contributions from the work of others. This research was in collaboration with Safinah Limited as the principal industrial partner. Other partners are America Bureau of Shipping, AkzoNobel, Air Products & Chemicals, Inc., and Bluewater Energy Services.

Any ethical clearance for the research presented in this thesis has been approved. Approval has been sought and granted by the University Ethics Committee on 27th March 2014.

I declare that the word count on this thesis is 48,846 words.

Name: Aigbokhaebho M Oriaifo

Date: 31st October 2016

Nomenclature

Symbol	Definition
^{o}C	Degree centigrade
E’	Storage modulus
E’’	Loss modulus
E*	Complex modulus
G’	Shear modulus
g/L	Gram/Litre
%	Percent
m^3	Cubic metre
m^3h^{-1}	Cubic metre per hour
ms^{-1}	Metre per second
m^2	Square metre
tan δ	Tan delta
vol. %	Volume percent
µm	Microns
HALS	Hindered amine light stabilisers
mm	Millimetres
m	Metres
cP	Centipoise
mg	Milligrams
ml	Millilitres
MPa	Mega pascal
GPa	Giga pascal
Tgi	Initial glass transition temperature
Tg∞	Ultimate glass transition temperature
J	Joule
Kg	Kilograms
hr	Hours
sec	Seconds
min	Minutes
Δ	Delta
-	Minus
nm	Nanometre
PSPC	Performance standard for protective coating

CHAPTER 1

1.1 Introduction

In a marine environment, the choice of an effective coating protection system matters as it is extremely important in delaying corrosion and extending the economic life of merchant ships (such as tankers, bulkers and combinational carriers) and it is their dedicated seawater ballast tanks (WBTs) that are most challenging in this regards [1 - 6].

Corrosion is a serious problem for any structure built of steel including WBTs of merchant ships yet steel remains the economic choice for building. In WBT, corrosion is an electrochemical process that occurs following coating breakdown at locally exposed surfaces and weld joints as the unprotected steel reacts with its environment forming an oxide that is similar to the ore from which it was originally extracted. Figure 1 below shows an example of general corrosion experienced in WBT. The issue of corrosion has been recognised in the shipping industry, following considerable losses of ships suffered at sea between 1990 to the middle of 1997 - which averaged at one ship loss per month [4 - 6]. Consequently, there has been renewed focus on eliminating accelerated corrosion in WBTs of ships through the application of an effective corrosion control and better performing protective coatings [1 - 17].

Figure 1 Accelerated corrosion following coating breakdown in WBT [8]

Furthermore, the significance of an effective protective coating in WBTs has been underscored in recent ship design and building practice with the increasing dependence on high tensile steel (HTS) [1, 4, 5, 9 - 11]. Prior to 1980, mild steel was the main construction material used for building earlier ships but has seen a decline in use since 1980s. The main reason for the increased preference of HTS in ship building is the weight saving - which might amount to several thousand tonnes, cuts building costs and also enables the ship to carry more cargo [4]. Thus, for the same application, HTS plate is designed thinner than mild steel. For example, while the thickness of a mild steel side plate will range from 24 mm - 29 mm, this can be reduced to 20 mm by using HTS. However, it is now recognised [4] that the corrosion rate of HTS is similar to that of mild steel implying that HTS lacks the additional thickness offered as corrosion margin in mild steel. Therefore, there is a greater need to preserve adequately the thickness and structural integrity of this thinner HTS plating using better performing coating system to avoid accelerated diminution of scantlings especially in WBTs.

Another recent significant change that has influenced corrosion within WBTs of merchant ships is the replacement of single hulled (SH) ships with double hulled (DH) designs (which are based on the hull configuration as shown in Figure 2), following the Exxon Valdez accident in 1989 in which several thousand tonnes of oil were released when the single hull was breached. An SH ship can be described as a ship built with one hull which is a single layer of steel that directly separates the cargo internally and the ocean environment externally. The cargo sits on the inner side of the steel layer while the ocean makes contact with the opposite side. Typically, the thickness of this single layer of steel is 20-35 mm [9, 10]. Thus, the single layered hull acts as the separating barrier between the carried cargo and ocean except when the hull is accidentally compromised through collision and grounding.

The DH design applies to ships carrying liquid cargos such as crude oil and chemicals. A different design applies to ships carrying solid cargos such as iron ore and coal. They have a second hull extending for the full length of their bottom only while the both sides of the bulker remain as single hull.

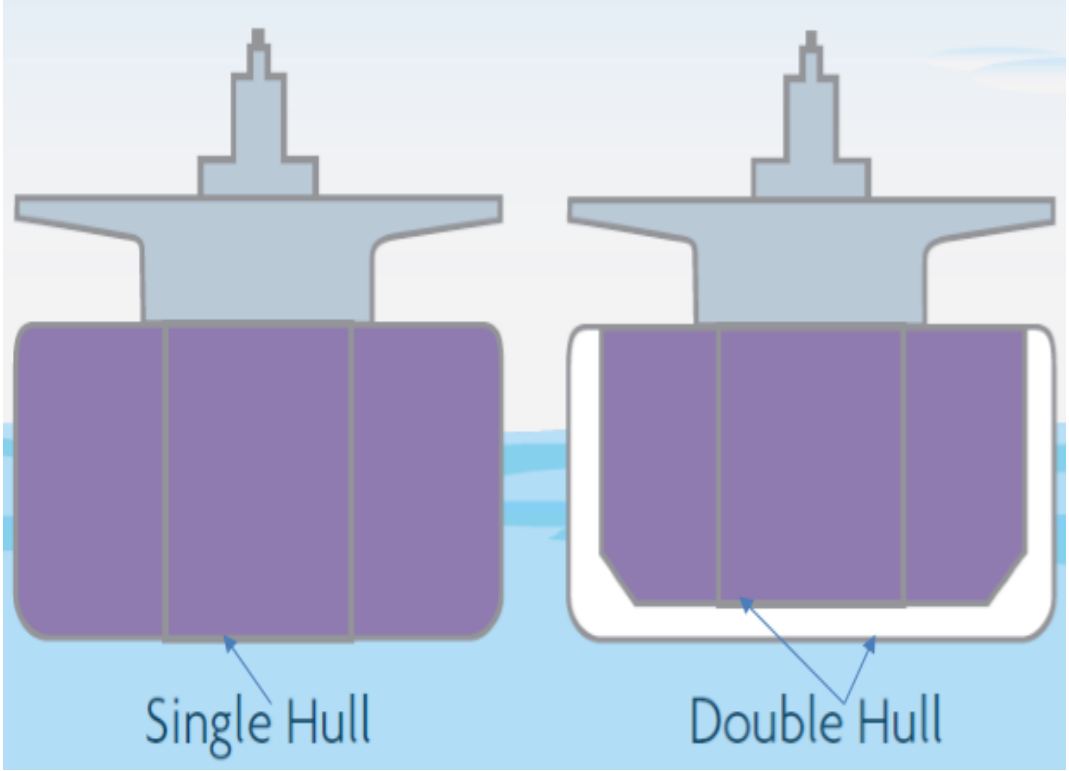

Figure 2 Configuration of single hull and double hull vessels [10]

The recent DH design has an inner hull within the outer (external) hull, thus providing two steel layers as barriers between the cargo and ocean environment. Space (in one or more separated cargo tanks) located within the inner hull is used for carrying cargo. While, the space between the inner and outer hull, which is generally 2 m wide, is segregated into tank sections for carrying only ballast seawater during the unladen voyages, (i.e. when the ship is not transporting revenue-earning cargo) and they extend for the full length of the cargo carrying area [10].

Hence, from an environmental pollution viewpoint, a DH design serves as a remedy against pollution from future ship accidents when the external hull is compromised [1, 9, 10]. However, from a corrosion standpoint, owners of DH ships will now have to maintain 225,000 m^2 or more of dedicated WBT internal spaces as against 25,000 m^2 - 125,000 m^2 in earlier SH ships [10, 12, 13]. A fundamental implication of this action is that, the size of dedicated WBTs within the DH ship to be protected and maintained has significantly increased to 2 or more times that seen in earlier SH ships built in the 1970s.

In addition, the potential for corrosion in WBTs of DH ships has inadvertently increased arising from the 'Thermos Effect' – where empty WBT spaces act as insulators allowing higher temperatures to be retained longer in warm cargo tanks [1, 4, 10, 13, 17]. This increase in temperature especially at the cargo tank/ballast tank bulkhead in conjunction with the cooler outer shell bulkhead (in the underwater regions) creates a complex set of corrosion conditions resulting in an accelerated corrosion rate of the steel in the WBTs especially in areas where the integrity of the coating films have been compromised [10, 11, 17].

Currently, the protection of ships including their WBTs is generally achieved through a coating system (which usually is a hard coating that is mostly spray applied and forms a continuous film on the substrate) plus sacrificial anodes (metals such as zinc and aluminium that are installed for consumption in preference to the surrounding steel substrate structure). However, within WBTs, sacrificial anodes do not work unless they are electrically connected – in other words immersed completely. Consequently, they are ineffective when the tanks are empty [11]. Thereby highlighting the need for an effective anticorrosive coating formulation (or paint scheme).

Typically, coating systems or coating formulations that offer protection within WBTs of DH ships are epoxy based. This choice of coating system for WBTs is now mandated by the International Maritime Organisation Performance Standard for Protective Coatings (IMO PSPC) resolution MSC.215 (82) [14]. However, over the years, epoxy systems have seen significant developmental changes based on robustness of technology shaped by environmental legislation(s) to reduce the levels of volatile organic compounds ((VOCs) - substances containing carbon and readily evaporate) as well as the removal of toxic (carcinogenic) materials from existing formulations [6, 7, 13, 15, 16]. Compliance to this legislation has resulted in the emergence of high solids and ultra-high solids content paints ($>$ 70% volume solids; VOC $\leq$ 250 g/L) displacing the traditional lower solids coatings with very high VOC levels ($\leq$ 50% volume solids; VOC $>$ 250 g/L) [7, 18]. The units of measure for VOC of paint is in grams per litre (g/L). The volume solids of paint is the ratio of the dry film thickness to the wet film thickness, expressed as a percentage. A significant

advantage during application of the higher solids paints is the ability to achieve higher film builds using fewer coats. However, there are some challenges experienced in using higher solids paints such as poor flow and levelling, and short pot life (the length of time after mixing when the paint can still be applied). The short pot life is due to the higher concentration of reactive groups in higher solids systems. This results in a faster rise in viscosity after mixing. Higher initial viscosities, especially for solvent free systems, also lead to poor atomisation as experienced during airless spray application. Specialised spray equipment with heating capability is then required to keep viscosity to usable range (for example plural component sprayer or warm single feed).

While in-service, the films of these coating systems within WBTs of DH ships are subjected to thermal cycling with temperatures as high as 85 ºC (from heated cargo in cargo tanks that share boundary plating with WBTs) and as low as 5 ºC (from intermittent immersion from sea water ballast for vessel stability) [12]. The duration of the thermal cycle depends on the trading pattern of the vessel. In addition, the films in WBTs are immersed intermittently in seawater as the ships adjust in stability. When empty, they are often subject to high relative humidity conditions, usually with high chloride levels [19] from the seawater. Consequently, the coating films of dedicated WBTs (particularly at shared heated bulkhead boundary) are subject to aggressive in-service cyclic (wet/dry, hot/cold) environmental conditions. In these conditions, which could be termed hygrothermal cycling, cracking failures are observed on welds and in corners.

Another challenge of the epoxy systems with higher solids content (in terms of failure mode) is the propensity to fail prematurely in service from embrittlement and subsequent cracking [1, 12]. Thus, this early failure principally from embrittlement adversely affects the efforts of both the shipyards, coating manufacturers and ship owners in making an effective choice prior to application. Again, the inability to reinstate or effectively repair the coating system to the initial state as at new build after the occurrence of failure further compounds this issue [1, 10, 11]. Furthermore, there are many different epoxy systems available from coating manufacturers and limited evidence from ships in service suggests that these systems have differing levels of durability and

performance [1, 2, 3, 8]. Hence, there is the need to gain an insight into the performance of WBT epoxy systems through accelerated testing prior to application as this could yield outcomes to support reformulation thereby preventing unnecessary future cost of maintenance and operation.

Prior to the application of epoxy coating systems in the WBTs of merchant ships, the performance of coating systems are evaluated by the current test protocols described in the IMO PSPC [14].

The PSPC is the latest of the IMO's response for a mandatory standard on coating performance issue for WBT. The PSPC came into force in July 2008 and aims to achieve a 15 years in-service life for the applied coating within WBTs. Thus, in Table 1 for basic coating system requirement of the PSPC, (section 1, Table 1: 1.2, page 8), the use of epoxy based systems has been mandated and passing the type approval test within the PSPC is required.

Table 1 Extract from table 1 of the PSPC mandating the use of epoxy-based system in WBT [14]

.2	Coating type	Epoxy-based systems. Other coating systems with performance according to the test procedure in annex 1. A multi-coat system with each coat of contrasting colour is recommended. The top coat shall be of a light colour in order to facilitate in-service inspection.
.3	Coating pre-qualification test	Epoxy-based systems tested prior to the date of entry into force of this Standard in a laboratory by a method corresponding to the test procedure in annex 1 or equivalent, which as a minimum meets the requirements for rusting and blistering; or which have documented field exposure for 5 years with a final coating condition of not less than "GOOD" may be accepted. For all other systems, testing according to the procedure in annex 1, or equivalent, is required.

After testing, measured data from degradation assessment of coating systems include:

- blisters and rust from mechanically induced damage to the bare steel
- dry film thickness (DFT)
- cohesive/adhesive value from pull off testing

- weight loss
- current demand and disbondment from cathodic protection
- Flexibility (measured for information only). In this context, flexibility is vaguely considered as the ability of a cured coating film on a thin panel to withstand deformation of a cylindrical mandrel without brittle failure in the form of visible crack(s).

However, in the acceptance criteria, there is no further mention of flexibility. Thus, suggesting that although the IMO PSPC recognises loss of flexibility of coating from embrittlement and subsequent cracking [in the test protocols within it] as a potential failure mode, it does not have a means of evaluating this undesirable feature.

Additionally, when in service, for ambient temperature cured epoxy coating systems, it is reported that most properties of the coating film including flexibility changes over time (with age) [15]. The ageing process affects the coating flexibility due to loss of retained volatiles, additional cross linking of residuals and leaching out of water-soluble materials leading to brittleness. Thus, recognising the effect of this ageing process, the PSPC recommends in (section 1, Table 1: 1.1, page 7) that "*the coatings for application underneath sun-heated decks or on bulkheads forming boundaries of heated spaces shall be able to withstand repeated heating and cooling without becoming brittle*". If linked with WBT environment, which is often associated with repeated variation in moisture and temperature conditions, it could be deduced that the combined effect of hygrothermal cycling (*which is fatigue related variation of moisture and temperature*) from the operating environment and tank structural complexity could strongly contribute and exacerbate embrittlement and cracking failure of applied coating films. This will occur particularly at corners of WBTs where the thicknesses of applied film are much higher than the specified 320 µm (which is the current industry recommended practice for WBTs) [11, 12, 16].

Thus, it is reasonable to investigate this complex and less understood effect of hygrothermal cycling on epoxy coating systems especially when accompanied with thermal shock. Thermal shock is a phenomenon associated with thermal

tensile stresses induced at the surface of a material by rapid thermal gradient, which could very much be the case for coating films in WBTs especially at shared bulkhead with cargo tanks. Consequently, this phenomenon will likely occur when discharging hot cargo tanks with the simultaneous ballasting of tanks with cold water.

Also, just like the IMO PSPC, there are other test protocols such as ISO 20340, NORSOK M-501, Nordtest NT Poly 185, NACE TM 0104 – 2004, NACE TM 0304 – 2004, ASTM D5894 -10 used for evaluating the performance of coating systems for marine and offshore applications [20 - 23]. The majority of the test protocols are typically focused on evaluating anti-corrosive performance properties such as resistance to corrosion creepage from coating defect(s) (which are mechanically induced through the coated surface prior to testing), blistering, weathering and cathodic protection (assessment of anticorrosive performance of a coating by depletion of sacrificial anode). Thus, by using these protocols, they do not reproduce the cracking failures seen in WBT.

1.2 Problem Statement

PSPC mandates the use of epoxy coatings in WBTs and passing the type approval tests is required

- Cracking of epoxy ballast tank coatings is seen in some ships especially on welds and in corners
- Cracking is thought to be dependent on a number of factors, amongst which are:

  Formulation: some paints are more crack resistant than others are

  Use Environment: in service conditions contribute to significant changes in properties over time
- Existing test protocols do not reproduce cracking behaviour and if they do, they do not replicate the rank order of failure as seen in practice, potentially leading to reverse correlations of performance

1.3 Research Project Aim and Objectives

1.3.1 The aim of the research project is:

- To develop a robust and reproducible test protocol capable of characterising and predicting the long term fatigue performance and durability of WBT epoxy based coating formulations with regards to embrittlement and cracking failure

In the long term, this will lead to the development of novel curing agent technology and more robust paint systems.

1.3.2 The objectives of the research project are as follows:

- To determine and understand the mechanism of coating failures in a WBT environment
- To determine critical factors affecting coating embrittlement and cracking in-service
- To study and evaluate a number of current industry test protocols used in the assessment of coating performance in marine environment
- To devise a test protocol/method that will replicate coating embrittlement and cracking in marine environment
- To classify epoxy base formulations and manufacture typical variants
- To measure and monitor the properties of the four typical epoxy based model formulations (solvent free pure epoxy (SFPE), solvent containing pure epoxy (SPE), solvent free modified epoxy (SFME) and solvent containing modified epoxy (SME)) as they are subjected to defined laboratory conditions that mimic in service changes to the coatings
- To rank the four typical epoxy based formulations after exposure to the defined test environment
- To replicate the experimental results with a re-analysis
- To simulate a model using Finite Element Analysis (FEA)
- To perform a significance test on the experimental data

1.4 Research Project Methodology

- A comprehensive literature review into the subject will be carried out in the research
- Review existing and current test protocols and methods
- Identify and prioritise the various variables affecting coating behaviour to address the problem
- Classify and agree typical epoxy based formulations
- Design prototype test conditions and appropriate test piece geometry
- Formulate, manufacture and apply four typical epoxy based coating formulations
- Setup and perform experimental testing under defined laboratory conditions and validate with a reanalysis
- To analyse experimental data with statistical test
- To simulate a model using FEA

CHAPTER 2
LITERATURE REVIEW

2.1 Water Ballast Tanks

WBTs are confined spaces found in different marine structures (or applications) such as merchant ships, oil platforms, submarines and floating wind turbines. WBTs mainly regulate stability in all these structures. Figure 3 below shows the typical locations of WBT section in an oil tanker or a chemical tanker, which carries liquid cargoes.

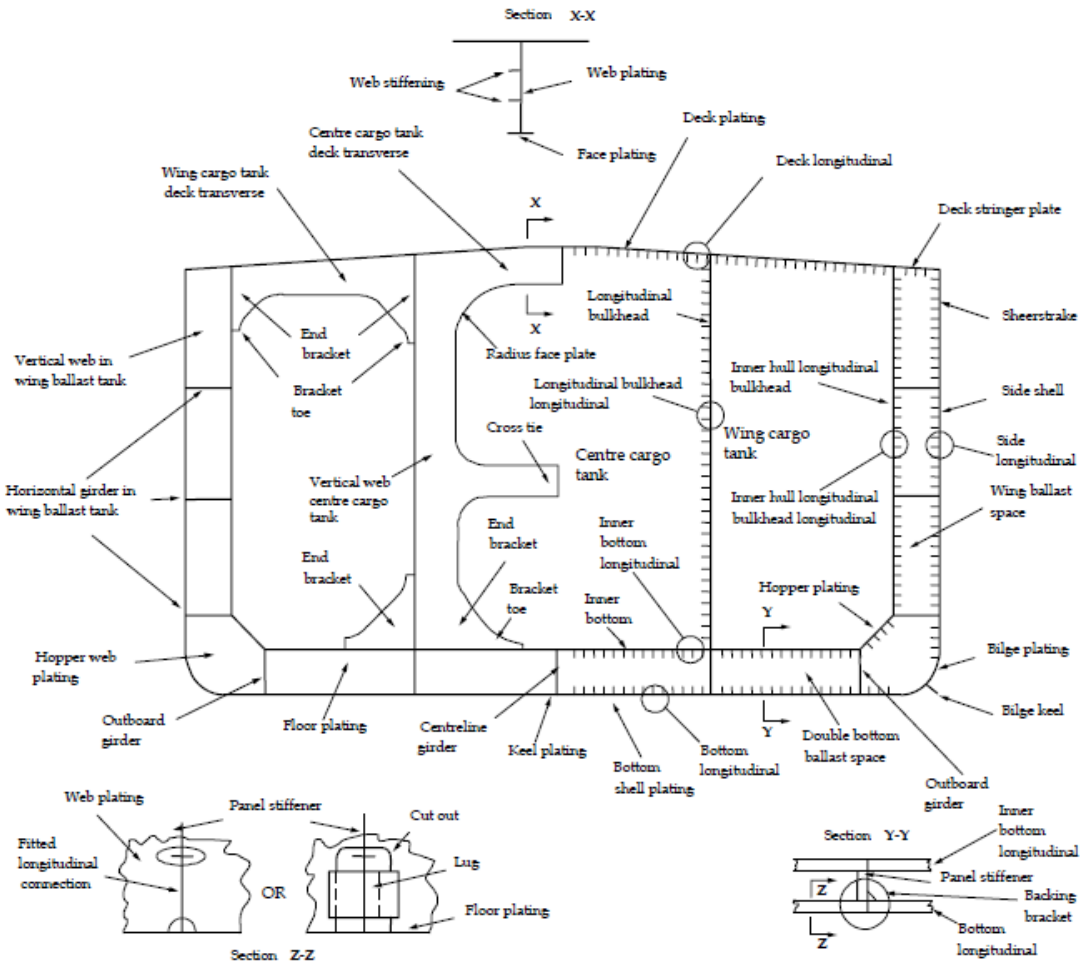

Figure 3 Typical midsection of a double hull oil tanker with two longitudinal bulkheads including nomenclature [24]

For merchant ships, WBTs are critical internal spaces that are essential to the ships as they provide the needed stability and propeller immersion through ballasting operations particularly when the ships are unladen.

2.1.1 Ballast medium

Ballast literally refers to belly load typically carried when the ship is unladen to compensate for the absence of cargo.

Other reasons for carrying ballast include:

- To provide appropriate draft
- To adjust trim
- To eliminate an inherent list
- To allow adequate rudder immersion
- To enhance manoeuvring

Figure 4 Solid (stone) ballast medium

Ballasts are primarily grouped into two: solid (dry) and liquid (wet). Before 1880, solid ballast media such as stone (shown in Figure 4), sand, roof tiles and rock were used as ballast [25]. These media were bulky and very difficult to handle especially during voyages in extreme sea conditions and resulted in long delays while carrying out ballasting or de-ballasting. These challenges drove the need for an alternative ballast medium and from the 1880s to the present day; water became the preferred medium [25].

Depending on the salt content, typical liquid ballast used in ships is of three types: fresh water (< 0.05%), brackish water (0.05-3%) and seawater (3-5% but on the average, salinity of seawater in the world's oceans is about 3.5%). Amongst these liquid ballast types, seawater is a more aggressive medium as it contains so much salt [4].

As ballast is stored in a variety of tanks, ballast operation depends on the size, configuration, and requirements of the ship as well as the complexity of the pumping and piping systems [25]. Ballast capacity using liquid ballast can range from several cubic metres in sailing boats and fishing boats to hundreds of thousands of cubic metres in large cargo carriers. For instance, large ships could carry in excess of 200,000 m^3 of ballast. Ballasting rates could range from 15,000 to 20,000 m^3h^{-1} while piping size to achieve flow velocities is between 2.6 to 3 ms^{-1}, with ballast pump capacities ranging up to 5,000 m^3h^{-1}. Furthermore, the principal advantages of liquid ballast as a choice include abundant, cheap and easily transferable using pumps.

However, this medium came with the challenge of corrosion of the structural steel tanks that ultimately led to the need for protective coatings. An early recognition of protecting interior spaces - WBTs in earlier ships with SH design against corrosion dates back to 1910 when grease was hand applied to them [16]. However, the size of internal spaces in WBTs in today's ships are much larger (approximated to eight (8) or more times) making hand application impractical.

2.1.2 Pre & post MARPOL WBTs

WBT internal spaces have been affected significantly by mandatory regulations on prevention of pollution. Notably, there have been two mandatory pollution prevention regulations: Marine Pollution 73/78 commonly referred to as MARPOL 73/78 (i.e. the 1973 MARPOL Convention and the 1978 MARPOL Protocol) and Oil Pollution Act (popularly known as OPA 90). Both regulations have also affected merchant ships with changes experienced in corrosion patterns and locations where the corrosion is found within WBT (both before and after their enactment) [26].

For the Pre-MARPOL tanks, the practice was to carry crude oil (when laden) and ballast water (when unladen) in the same tanks with total internal area of tanks typically approximated at 35,000 m^2. The corrosion pattern experienced with this type of practice was severe corrosion at the ullage space underneath deckheads where the temperature may be high and combined with frequent wetting by ballast water. In addition, significant corrosion occurred on bulkhead longitudinals and face plates of deck girders where water could be trapped.

With the enactment of MARPOL 73/78, ships were designed with segregated ballast tanks (tanks dedicated for carrying only ballast water to inhibit the discharge of oily ballast water into sea) with approximately 135,000 m^2 internal areas exposed to seawater. These were found to experience pitting and grooving corrosion on the bottom plating and other horizontal surfaces a consequence from the combination of residual water and sulphur from the inert gas systems that produce a more corrosive fluid.

Following the Exxon Valdez accident, the Oil Pollution Act (popularly known as OPA 90) was enacted which introduced the DH design as a better remedy against pollution from either collision or grounding. The post-MARPOL tanks came into existence. The internal surface area spaces of WBTs in this design had tremendously increased in size as much as two times when compared with the earlier MARPOL tanks in SH design. Additionally, the number of stiffened elements and cruciform joints has been increased significantly within WBTs to meet structural strength requirement and to make the cargo tanks a smooth

walled compartment for easy access during loading and unloading. Consequently, WBTs are the largest single areas of merchant ships protected and coated with the same coating system. Furthermore, they are more difficult to access physically and to effectively perform activities of the coating process, which requires the use of special staging and artificial lighting. Regarding corrosion type, DH operators have experienced increasingly severe microbial corrosion in addition to pitting and grooving corrosion due to the thermos effect. Thus, with the significant increase in internal surface area of WBTs in DH, ways of determining better coating system performance which will minimise unnecessary maintenance and refit costs both at new build and in-service will be highly beneficial.

2.2 Glass Transition Temperature

A significant property of WBT coatings worth reviewing is the glass transition temperature (Tg) due to its effect during coating film formation and in service. Film formation refers to the conversion of the coating from liquid into an integral solid film after application on a substrate. This enables the coated steel substrate to be usefully employed in service. It is also associated with how quickly a coated substrate can be handled, over-coated, stored, and the performance – what properties have developed by what time after application [27].

Tg is a key parameter of coating film that contributes to the understanding of film changes [28]. Tg is the transition temperature that occurs between the glassy and rubbery state in amorphous polymers such as binders used in coatings. At this temperature, the amorphous polymers gain sufficient thermal energy for motion along the polymeric chain and relax into much preferred configuration. In addition, it is typified by plotting a graph of specific volume against temperature as shown in Figure 5 [28]. A number of thermal analysis techniques including Differential scanning calorimetry (DSC), Thermomechanical analysis (TMA) and Dynamic mechanical analysis (DMA) are used to determine Tg.

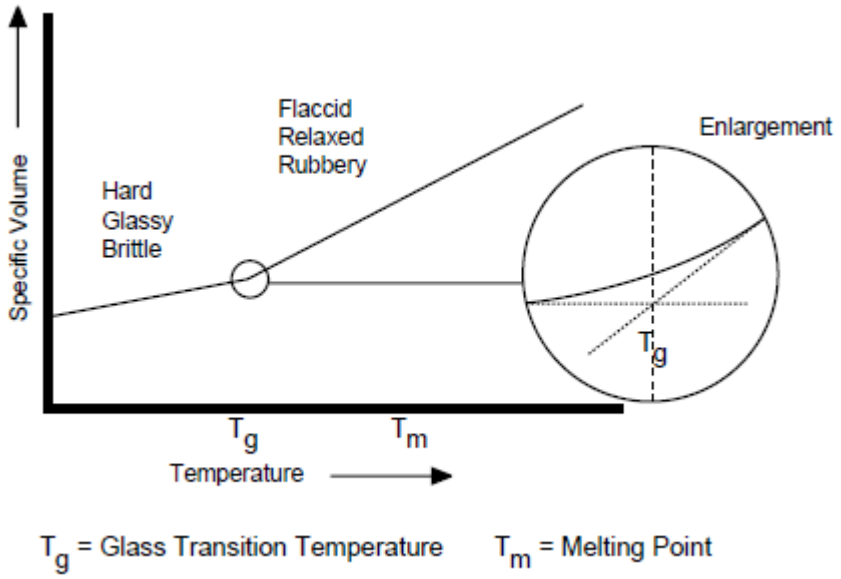

Figure 5 Phase transformation in amorphous polymers [28]

Marrion [27] stated that as the polymer is cooled to the Tg and below, the co-operative motions responsible for both translational and rotational motions in the polymer backbone essentially become frozen, and the macroscopic flow of the material no longer occurs.

Flow can only take place if the material is a thermoplastic or if it is a thermoset below its gel point. A thermoset material, such as an epoxy will not flow if it has cured past its gel point no matter what the temperature.

While in the liquid state, the viscosity behaviour (resistance to flow) of liquids is often explained using Eyrings “hole” theory, where molecular flow is achieved by series of “jumps” by molecules into unoccupied spaces or holes. The greater the number of holes, the easier the flow. Hole size and hole concentration increase with temperature. The analogous concept of free volume is a familiar and useful concept for rationalising many aspects of the behaviour of polymers.

Free volume (V_f) is one of the parameters, which affect and characterise polymeric properties. Free volume refers to the fraction of the volume not occupied by polymer. In addition, these spaces (when available) maybe

occupied by low molecular weight moieties like solvents (that are not chemically bound to the film backbone structure).

The relationship between V_f and temperature is typified by a linear gradient, which becomes steeper at coating film temperatures above its Tg. A key reason for this is the increased mobility of polymer molecules with progressive increase in temperature past the Tg (rubbery region) of the dry coating.

However, below the Tg (in the glassy region), V_f is nearly constant as the molecules of the cured coating are rigidly held. Thus, V_f increases with increase in temperature. If the film is heated above its Tg then the free volume increases. The effect is temperature driven, as there is no way free volume changes without increasing the temperature and taking it above the film Tg [28, 30, 31].

Marrion [27] also presented an investigation on the overall rate constant for the epoxy amine reaction as a function of epoxy conversion with the following explanation.

During an isothermal cure as shown in Figure 6, the Tg rises. Early on in the reaction the Tg is usually well below the cure temperature and increases only slowly. Chemical kinetic control operates in this regime. If the cure temperature is below the ultimate Tg (“also represented as T g (∞)” which is the system Tg at a conversion, x = 1), then at some conversion below x = 1 the Tg will have risen to approach the cure temperature. When this occurs, the system has transformed from viscous liquid to an amorphous solid and further reaction is controlled by diffusion. The Tg – conversion curve, particularly for epoxy-amine systems, is commonly independent of the temperature of the reaction. For each system, the Tg can therefore be taken as a measure of conversion (and also crosslink density – the number of chain segments between crosslinks per unit volume, or the average molecular weight between crosslinks). In addition and importantly, it implies that a specific and unique Tg corresponds to the gel point of the system. This is known as the gelTg.

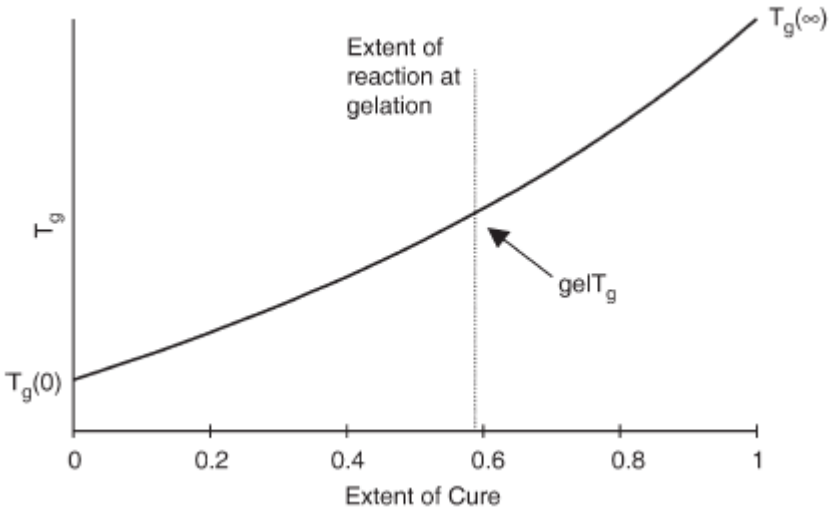

Figure 6 Typical dependence of Tg on conversion [27]

At high extents of reaction in crosslinking systems, the concentration of the residual unreacted functional groups will be low and increasingly likely to be "fixed" on the network. Thus, the final stages of reaction may be exceedingly slow or (in practical timescales) will never occur. A general rule of thumb is that the Tg of a film will reach 25-35 ^{0}C above the cure temperature [27]. In addition, Marion [27] reported that the performance of a coating is dependent on the degree of conversion. Thus, for coatings cured at ambient temperature, for example 25 ^{0}C, the Tg is therefore limited to 50-60 ^{0}C.

If insufficient conversion has been achieved at this point, the coating will likely fail prematurely. Reactions can of course continue if the temperature is subsequently increased. In addition, by selecting solvents with different volatility, the system Tg may be depressed for long enough (by solvent plasticisation) for further reaction to occur. Thus, when the solvent does eventually leave the coating (this may take years), the final Tg may reach higher temperatures in some examples up to 50 ^{0}C or 60 ^{0}C above the cure temperature [27].

For ambient temperature conditions and low temperature cure applications, some epoxy formulations are formulated with plasticiser is to aid manufacturing and application. However, it has been observed that the presence of this

constituent in the formed film after application depresses the Tg of the thermoset binders. Another intention of including such constituent is to facilitate a high degree of cure, which should be far beyond the gel point and so ensure optimal performance. In order to achieve this high degree of cure, typically benzyl alcohol (a solvent-like liquid) is sometimes incorporated into the formulations [12, 29].

The extent or completeness of cure does also affect the Tg [12]. In general, for any particular coating, the higher the extent of cure, the higher the Tg. If there is a high percentage of reactants remaining (residuals) within the network, this will tend to depress Tg with further reaction occurring later when the film is heated. At film temperatures (T) either above or below the Tg, the coating film may become significantly different. If the value of T-Tg is positive, segmental molecular activity in terms of mobility within the film is restored resulting in a stress-relaxed film. However, when T-Tg is negative the reverse is the case [28].

A summary of the effect of Tg (above and below) on coating film is shown in Table 2.

Table 2 Comparison of coating films above and below Tg [28]

No	Below Tg	Above Tg
1.	Molecular motion is restricted	Molecular motion is highly increased
2.	Coating films are hard and glassy with a propensity to break rather than deform under stress, and likely have higher internal stress	Coating films are flaccid, rubbery, stress relaxed and deform under stress
3.	Solvent retention may be high with low permeability	Solvent desorption is facilitated with high permeability

2.3 Epoxy Protective Coatings

2.3.1 Protective coatings & constituents

This type of protective coating (or paint) can be described as liquid material capable of being applied or spread (by spray, brush or roller) over a solid surface (metal substrate). After application, the coating subsequently dries or hardens by a combination of solvent loss (physical set) and/or chemical crosslinking to form a continuous adherent protective coat [32].

Spray application is the preferred means for large surface areas as it is time saving with more surface coverage.

Paint is a liquid, which on drying produces a coating that offers protection and/or colour to a surface [11]. The composition of a paint is generally made from a combination of the following constituents:

- binders (vehicle, polymers or resins or reactants – in a two pack paint such as an epoxy formulation, the epoxy base is reacted with the curing agent)
- pigments and fillers can be included in either the base or the curing agent but mostly in the base (some give colour, some such as lamellar talc and aluminium flakes give improved anti-corrosive properties)
- solvents (aid application viscosity)
- additives (including thixotropes, defoamers, wetting agents, flow modifiers and biocides) confer special properties

The below Figure 7 shows the constituents of a paint which is a common skeleton. However, not every paint will contain all of the constituents shown below; some contain more constituents while others less.

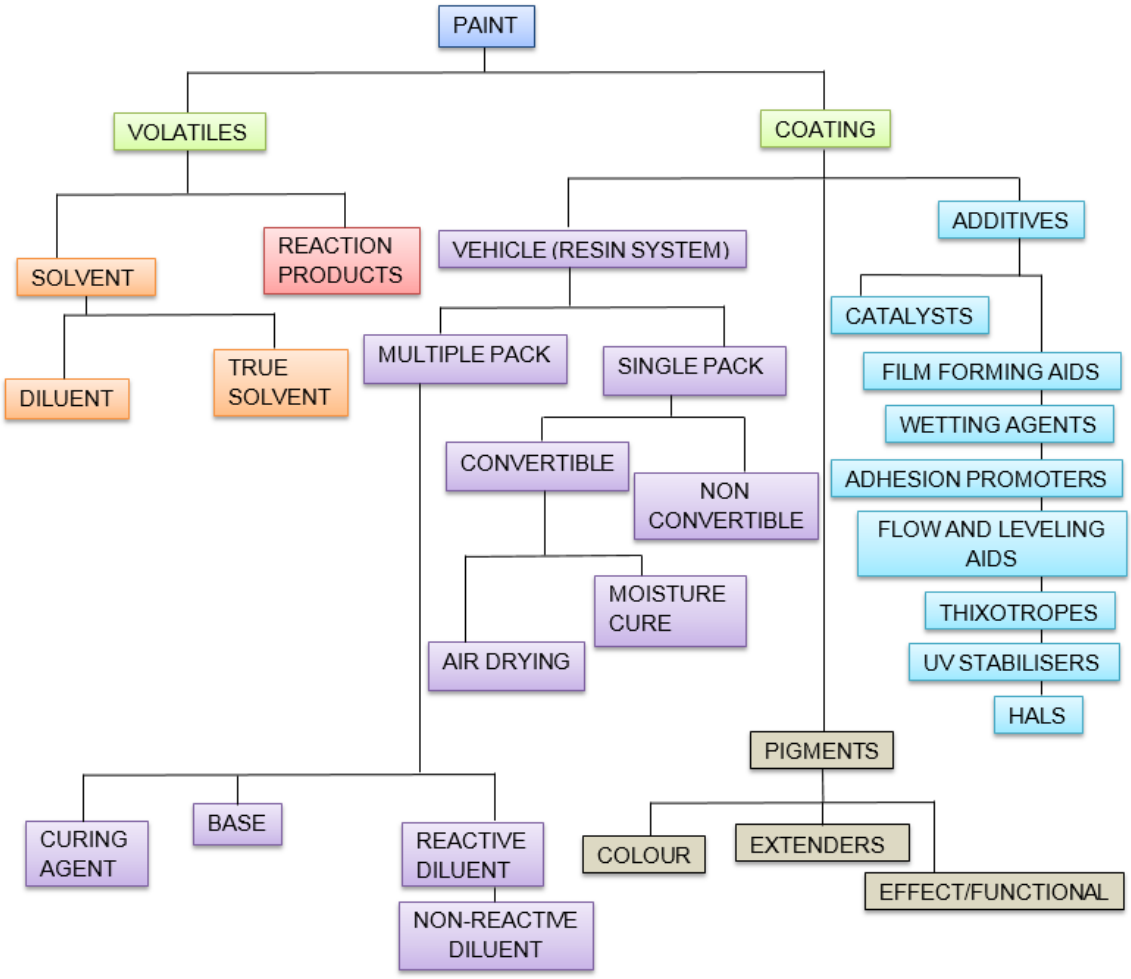

Figure 7 Constituents of a paint [27]

Binders are the main film forming part of the coating and they mainly determine the principal characteristics of the coating, which include chemical and physical properties [32]. Generally, paints are named after their base binder component for example epoxy paints and alkyd paints [11].

Typical binders of a conventional coating (i.e. ≤ 50% volume solid; VOC > 250 g/L) have a Tg and molecular weight high enough to form film. Although they might form a film, they still need to crosslink sufficiently to provide the desired performance properties. Thus, they are solids or highly viscous liquids, which require significant dilution to achieve application viscosity. Binders used for manufacturing paints are classified as thermoplastic (non-convertible) or

thermoset (convertible) [11]. This classification relates to the kind of dry film formed following the transition from the liquid paint state to the solid state after application. For a thermoplastic coating, the difference between the dry film and wet paint in can is only in the quantity of solvent content. In addition, chemically these two remain the same and if the solvent originally used is applied to a thermoplastic coating, it will soften and can re-dissolve in the solvent. In contrast, for thermoset coating, the wet paint in the can is chemically different from the dry film. Once cured or dried, thermoset coatings are unaffected by solvents used in manufacturing them [11].

Regarding reactivity for ambient temperature cure systems, these paints are typically supplied in two separate components (pack of tins or containers) which are mixed together immediately before application.

Furthermore, for thermoset coatings, the film progressively becomes more chemically complex by one of the following methods:

- reaction with atmospheric oxygen, known as oxidative crosslinking
- reaction with an added chemical curing agent to form a rigid 3 dimensional cross-linked network
- reaction with water (moisture in the atmosphere)

Ideally, following co-reaction with epoxy, the curing process should form a rigid three (3) dimensional cross-linked network. The films formed by the above methods are chemically different from the original binders and will not re-dissolve in their original solvent [11, 33]. Thus, as epoxy paints are thermoset in nature, they tend to follow the above stages of drying and ultimately the dried film acts as the protective medium for the substrate against the in service environmental conditions such as in WBTs.

2.3.2 Epoxy resin chemistry

Epoxy is a word derived from two prefixes of Greek origin namely: epi - meaning “upon, close upon (in space or time)”, and oxy - meaning “sharp, pointed; acid” [34].

The first production of epoxy resins was initiated in Europe and the United States between the late 1930s and 1940s. Pierre Castan of Switzerland and S.O Greenlee of United States were reported as the pioneers who investigated the properties and production of epoxy resin made by reacting bisphenol A with epichlorohydrin [35].

Earlier use of epoxy resin was in the dental industry and then in adhesives. The use of epoxy resin in paints came along later. Epoxy resins are regarded among the most satisfactory media for protecting structures built of steel such as ships. They are employed as primers for steel, perhaps due to the dense networks with excellent adhesion properties [27]. In the marine and coating industry, the designing and formulating of epoxy resin based paint for use in protective coating was born from the incompatibility between zinc primers and alkyds coatings.

In 1940s and 1950s, steel structures in moderately corrosive environments were protected using red lead alkyds coatings [36]. However, with the building of steel structures in severely corrosive environments, such as marine, the introduction of inorganic zinc-rich primers as first coat was necessary. Top-coating the zinc primers with alkyd coatings created challenges of incompatibility especially as zinc primers produced high alkalinity [36, 37]. Hence, the introduction of coatings that were based on epoxy resins as a spin off from the original work. The need was for a protective coating that performed better than zinc primers top coated with alkyd.

An epoxy resin typically used in paints, is a reaction product of phenol and either acetone or formaldehyde which is further condensed with epichlorohydrin. The resulting products are diglycidyl ethers of bisphenol A (DGEBA), diglycidyl ethers of bisphenol F (DGEBF) or epoxy phenolics depending on the preferred combination [36]. Figure 8 illustrates the resulting product of bisphenol A.

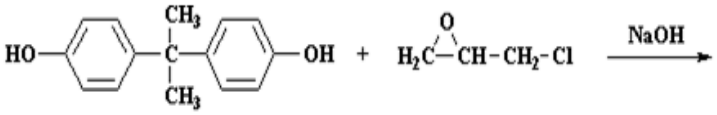

Bisphenol A Epichlorohydrin

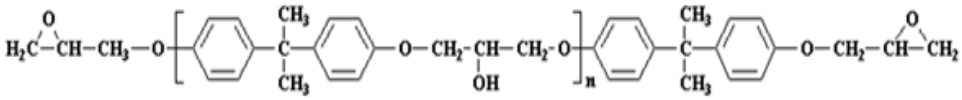

Figure 8 Chemical structure from the reaction products of bisphenol A and epichlorohydrin [38]

An epoxy resin is loosely described as a molecule containing one or more epoxy groups. There are many multifunctional epoxy resins, in fact bisphenol F resins are approximately 2.1 functional (this is the average number of reactive sites per molecule) while bisphenol A resins are approximately 1.9 functional. The reactive species at both ends of the molecule is a three membered-ring structure consisting of one oxygen atom and two carbon atoms. However, higher molecular weight epoxy resin molecules can also contain hydroxyl reactive group in the molecule.

It may be worth mentioning that all resins used in formulating paints are mixtures or blends of polymers with varying molecular weights, hence they are not pure materials [36]. This arises due to the manufacturing process that produces a number of different molecular weight materials in the same mixture. The principal physical differences between uncured epoxy resins within a family are material form and viscosity at room temperature, which can range from thin mobile liquids to solids [39]. The molecular weights of epoxy resins range from low liquid (approximately 300) to high solid (above 1000). Amongst the epoxy resins, the bisphenol F resin has a lower viscosity and is more inclined to crystallise when compared to bisphenol A types [36, 38].

However, the most commonly used resins for epoxy coatings are those based on bisphenol A. A fundamental characteristic that determines resin suitability for use is the epoxy equivalent weight (EEW). EEW is defined as the weight of

the resin per epoxide group. The equivalent weight of a polymer is used to calculate the stoichiometric ratio between the epoxy and curing agent in order to optimise the cured properties [39]. Stoichiometric ratio is an important quantitative relationship for a coating formulator; and it governs how much epoxy and curing agent is required to react with one another.

2.3.3 Curing of epoxy resins

Epoxy resins react with a number of chemical species called curing agents, curatives or hardeners with cross-linking occurring through the reaction with the epoxide group. However, the epoxy resin molecules could also react with themselves, a reaction known as homopolymerisation [40]. They convert to useful products by crosslinking or curing them with curing agents. The most versatile curing agents widely paired with epoxy resins are amines and amine derivatives. At room temperature, most amines are reactive with epoxy resins as they possess an active hydrogen. Amines for example cure with epoxy resins to yield coatings characterised by hardness, chemical resistance and excellent adhesion. However, when exteriorly exposed, coatings made from bisphenol A / bisphenol F resins have very poor weathering resistance leading to chalking – the polymer binder is broken down by ultraviolent (uv) radiation and leaving powdery pigment on the surface [27].

When selecting resin-curing agent combinations, the application or end use defines the resin characteristics that must be built into a particular system [39]. Typical amine functional curing agents used for ambient cure coating are aliphatic amines, polyamine adducts, cycloaliphatic amines, polyamides, amidoamines and ketimines. Generally, curing agents could be classified as ambient-cure and heat-cure. However, the emphasis for this research will be on ambient temperature cure systems.

Amine compounds are categorised into primary, secondary and tertiary amines. A primary amine has two reactive hydrogens, a secondary amine has one reactive hydrogen and a tertiary amine has no reactive hydrogens. Depending on the number of amine groups present in a molecule, amines are also known

as monoamine, diamine, tri-amine or polyamine. Generally, amines are classified into aliphatic and aromatic amines based on their structure.

2.3.3.1 Aliphatic amines

Aliphatic amines (polyethylene amines) such as ethylene diamine (EDA), diethylene triamine (DETA) and triethylene tetramine (TETA) were typical curing agents paired with epoxy resins. As shown in Figure 9, they are multi-functional curatives containing –NH and -NH_2 functional groups

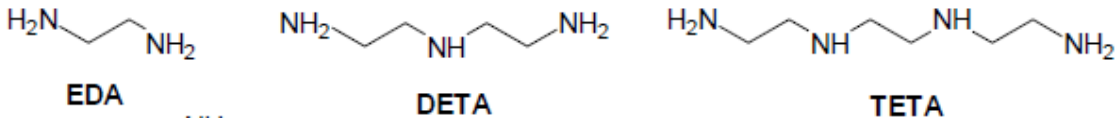

Figure 9 Chemical structure of typical aliphatic amines [41]

Aliphatic amines are capable of readily reacting with epoxide groups at ambient temperature. However, aliphatic amines present handling difficulties because of their high basicity and relatively high vapour pressure [42]. When reacted with epoxy resins, they are very exothermic (generating large amount of heat) leading to short pot life (usable life) and cure time. Under high humidity and low application temperatures, they react with carbon dioxide and moisture, commonly referred to as “amine blush” or “carbamation” giving problems with intercoat adhesion. Figure 10 illustrates the chemical reaction that occurs.

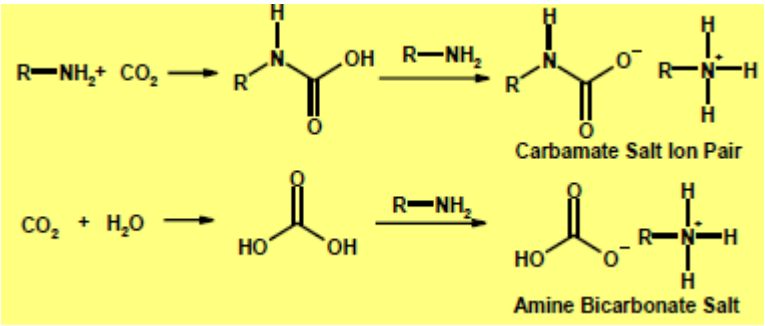

Figure 10 Chemical reaction resulting in amine blush or carbamation [41]

Additionally, blushing can promote adverse performance issues such as water sensitivity and poor overcoatability of these amine cured systems in WBT environment. During handling, aliphatic amines could be toxic posing health risk as they irritate the skin of workers who have direct contact with the products and causing dermatitis [36].

2.3.3.2 Amine adducts

In order to mitigate the reactivity and blushing effect of aliphatic amines, aliphatic amine are partially reacted with epoxy resins to yield amine adducts. This is generally prepared in the ratio of at least 2 molecules of amine to 1 molecule of di-functional epoxy resin. Adducted (or further modified) aliphatic amines have higher viscosity than aliphatic amines, longer pot life and greater mixing ratio tolerance [36]. Although they have high molecular weight and low vapour pressure resulting in less toxicity, good care is required during handling.

2.3.3.3 Mannich bases

A particular family of curing agent is mannich bases. They are formed by condensation of (aliphatic) amines, phenol (derivatives) and formaldehyde. As illustrated in Figure 11, the phenolic hydroxyl group present in these types of molecules has an accelerating effect on the epoxy-amine reaction rate. Of particular interest are Mannich bases made from cardanol, derived from cashew nut shell liquid as the phenol component. These types of products are referred to as phenalkamines.

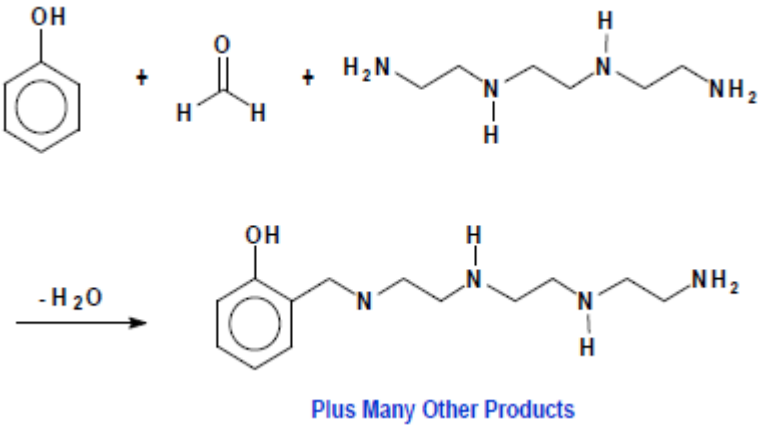

Figure 11 Chemical reaction resulting in a mannich base type [41]

Other amine curing agents include polyamide, amidoamines, aromatic amines, cycloaliphatic Amines and Ketimines.

2.3.3.4 Polyamides

The first introduction of Polyamides were in the late 1940s. As shown in Figure 12, Polyamides have been widely used and they are formed by the condensation reaction between aliphatic polyamines and dimer fatty acids. Reaction with epoxy resins generates moderate heat. Polyamides have reasonable pot life and mix-ratio tolerance. They generally require an induction time before application. New, lower viscosity, lower molecular weight, and blended materials yield higher solids that allow formulation of epoxy polyamide coatings with reduced levels of VOCs [36].

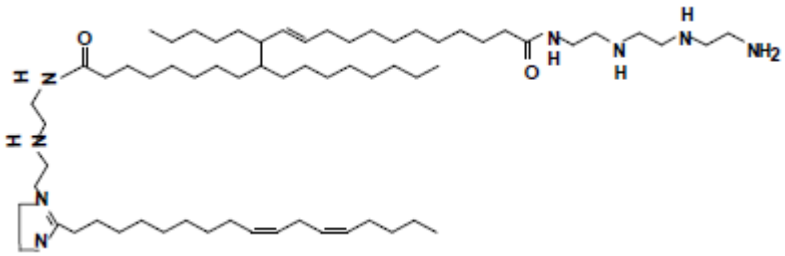

Figure 12 Chemical structure of Polyamide [41]

2.3.3.5 Aromatic amines

The word “Aromatic” is a chemical term referring to an unsaturated ring of carbon atoms. The simplest aromatic molecule is benzene. Thus, aromatic amines have the amine functional group attached to a benzene ring structure. They have good chemical resistance but very poor ultraviolet light stability resulting in chalking on exposure to sunlight. Aromatic amines are very slow to react and require an addition of accelerators or catalysts to provide a reasonable rate of reaction or higher temperatures.

2.3.3.6 Cycloaliphatic amines

Cycloaliphatic amines have a fully saturated ring structure implying that only one single chemical bond holds the carbon atoms together. Although there are several types of cycloaliphatic amines, the paint industry used only a few. As shown in Figure 13, examples include 1,2 diaminocyclohexane (DACH), isophorone diamine (IPDA), 1, 3-bis (aminomethyl) cyclohexane (1,3(1,4)-BAC) and bis (p-aminocyclohexyl) methane (PACM).

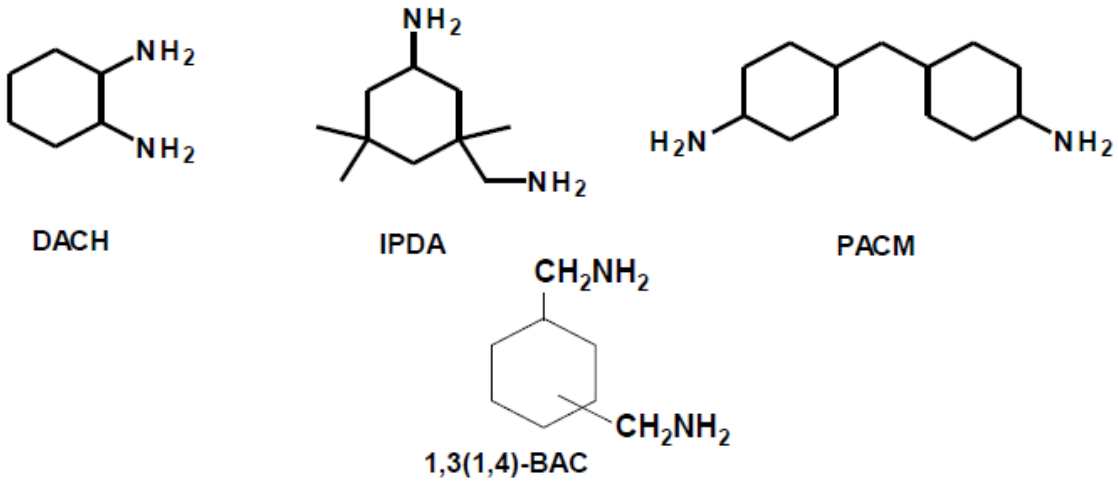

Figure 13 Chemical structure of Cycloaliphatic amine types – DACH, IPDA, BAC and PACM [41]

2.3.3.7 Ketimines

Another variant of curing agent also used for marine application and paired with high solids epoxy paints are the ketimines. As illustrated in Figure 14, Ketimines (also loosely referred to as blocked amines) are produced by reacting aliphatic amines such as DETA and TETA with ketones such as methylethyl ketone (MEK) and methylisobutylketone (MIBK). The amine resins in ketimines have almost similar behavioural properties to that of their original aliphatic amines, from which they were formed. The rationale for blocking the amine is to reduce initial reactivity hence, promoting a longer pot life. The blocked amines in the ketimines become unblocked or released for cross-link with the epoxy resin(s) only

after hydrolysis by atmospheric moisture. The process requires moisture to diffuse through the forming film to unblock the amine and the ketone (a VOC) is released from the film. However, care must be exercised during application as improper application results in thick films that may not cure completely as moisture cannot diffuse through such films.

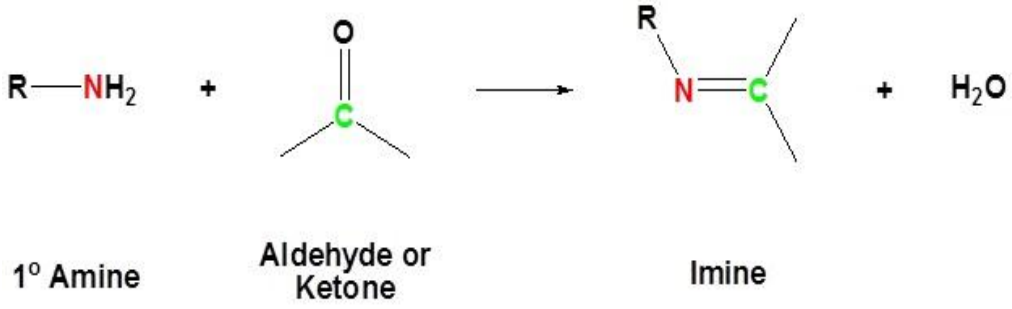

Figure 14 Chemical structure of a typical ketimine [41]

2.3.4 Epoxy coatings

With few exceptions (such as anti-fouling paints, cosmetic paints and fire retardants), the majority of coatings applied to a ship are used for anti-corrosion protection. Although, there are many types of anti-corrosion coatings, epoxy paints generally cover the greatest area on a ship, particularly when applied in WBTs [11]. Hence, epoxy paints have been available for decades with solids contents ranging from 30 -100%.

Generally, in order to provide a useful classification for paints and coatings the designation “generic type” is used. Primarily, the resin is the means for this classification. The secondary classification is typically by the curing mechanism. Thus, the generic name used to describe various types of epoxy base paints is “epoxy”.

In the 1950’s, one of the first epoxy formulations to be used on multiple areas of ships including their WBTs was coal tar epoxy. These are coatings based on amine cured epoxy resins containing coal tar. Formulations of coal tar epoxy are also found and widely used in piping, piling and waste treatment facilities because of their anticorrosive properties, high resistance to the transport of

aggressive ionic species such as chlorides or sulphates through the bulk of the paint, low water permeability and low cost per unit surface area [11, 36, 43].

With the success achieved of using this formulation, shipyards pressurised coating manufacturers for further cost reduction. The coating manufacturers responded by increasing the level of the tar and reducing the proportion of the relatively more expensive resin system [16].

Coal tar is a dark brown or black organic product extracted from the distillation of coal. Coal tar constituted about 30% of the total binder of epoxy coal tar formulation and acted as a modifying resin to alter (improve) the properties of epoxy coatings [36]. Hence, for many years in the shipping industry, the specification of coal tar epoxies was popular due to their cost effectiveness [16].

However, following concerns [11, 12, 13, 16] in the 90's raised in the industry about the toxicity of components of coal tar (such as such as 3,4 – benzopyrene that was a potential carcinogenic substances) and the difficulty of inspection in enclosed spaces such as WBTs, the International Association of Classification Society (IACS) recommended light coloured hard (tar free) coating formulations. This concern by the industry resulted in the replacement of black coal tar with lighter coloured materials such as hydrocarbon resins resulting in paints sometimes termed "bleached tar" or "modified epoxies" [16, 36].

Hydrocarbon resins, obtained from the refining of crude oil, are a variety of products added to epoxy resin to enhance properties such as moisture and ionic resistance, flexibility and wetting as well as to make them potentially more cost effective [36].

In recent years, as a follow on from IACS recommendation, light coloured epoxy coatings have been mandated and specified as the main protection system for WBTs against corrosion [16]. The preference for epoxy coatings is attributed to the excellent properties offered which include anticorrosive performance, good chemical resistance and good adhesion to substrate [40].

Epoxy WBT coatings with low solids made from high molecular weight resins (typically Bis A and polyamide) require high level of solvents to aid manufacture and subsequent application as the resins themselves were solids at room temperature [36].

However, with legislative changes and pressures to produce environmentally and user-friendly coatings, new formulations (with higher solids: solvent less or solvent frees) are being introduced with likely equal performance [36].

Solvent free coatings have been available from the early 1970's after an explosion in tanks when solvent fumes from a paint formulation ignited. They have possibly a worse health and safety profile than the lower solids paints as they contain low molecular weight materials that pose more hazard such as increased potential for skin sensitisation than higher molecular weight ones [27].

The move to higher solids content has been driven by legislation and the larger shipyards requested higher solids to meet the targeted film build at a minimum specification with reduced cost. Based on this development, higher solids epoxy coatings are becoming used increasingly and widely. They are produced by carefully selecting lower molecular weight moieties: epoxy resins and amine curing agents which when mixed together meet the target application viscosity. As experienced, the films of these high solids coatings stay wet longer as compared to the lower solids or "traditional" coatings but dry as the reactions occur.

Unlike the older (traditional) epoxy formulations with volume solids content of 50%, new formulations do not have the same record of performance as older ones that have seen extensive in service exposure over the years. Additionally, epoxy formulations have shown varying useful lives in WBTs, ranging from few months to more than 25 years, which also depended on good substrate preparation and application conditions [26]. Furthermore, the presence of diverse commercially available epoxy coatings makes the optimum selection of WBT coating quite challenging. Again, limited evidence from service shows that some seem to be more crack resistant than others are.

This has placed a new challenge on the shipping industry to find a methodology that adequately and suitably evaluate coating performance regarding embrittlement and early cracking failure prior to application in WBTs of ships.

In the paint industry, there are many different epoxy based paints available from coating manufacturers and the classification of epoxy-based paints often follow the generic names:

- pure
- modified

The classification of paint by resin type only is not useful when it comes to the performance of a paint as it ignores the effects of formulation – i.e. the contribution of all of the other components and the way in which they are put together [44]. Indeed, paint companies own literature shows difference in performance between so-called 'pure epoxies' [45, 46].

As this way of classification adopted by the paint industry is too general, a different classification approach was taken for this research that would provide an adequate representation of sample space. The approach was that paints either had film forming components that all reacted (pure) or not (modified) and contained solvent or not. Hence, paints were classified into four variants. First, they were divided mainly into two: pure epoxy and modified epoxy. These two classifications were further sub classified into solvent free and solvent containing (or solvented). Thus, epoxy coatings were grouped into four variants namely:

- solvent containing pure epoxy (SPE)
- solvent free pure epoxy (SFPE)
- solvent containing modified epoxy (SME)
- solvent free modified epoxy (SFME)

'Pure' refers to the class where all the film-forming constituents react together. They may contain epoxy reactive functional diluents. 'Modified' relates to those where not all the film-forming constituents react together. They contain non-

reactive diluents, which are usually a hydrocarbon resin that may be either solid or liquid depending on the solids content.

2.4 Issues with Epoxy Coatings

2.4.1 Embrittlement

An undesirable feature of WBT epoxy coatings recognised by the shipping industry is embrittlement. This adverse feature detracts from the protective ability of epoxy coatings as they age in the service environment. Hence, the need to understand what embrittlement could mean as it relates to WBT coatings in service.

Embrittlement of coating means change(s) taking place within the coating as it operates in service that detracts from the protective ability. The change in the coating could be either physical, chemical or both.

Ageing is another word or term used to describe embrittlement in amorphous polymers used in coatings. Struik [47] described ageing as the gradual continuation of the vitrification (a term describing when the glass transition temperature (Tg) of a recently applied coating that is curing equals the substrate temperature or environment) around the Tg. Consequently, it affects all those temperature dependent material properties that undergo drastic change at Tg. Also, during ageing the material properties change in a similar way as during cooling through the Tg. Resulting in a material, which has decreased damping as well as decreased creep and stress relaxation rates. With age, the material becomes more and more glass-like and less rubber – like. The material's feature becomes stiffer and more brittle. Although Struik [47] focused on the testing of plastics, it was recommended that ageing should be considered when testing polymers, especially in predicting long-term performance.

Perera [48] concluded that physical ageing induced changes to the coating properties. These changes are determined by the in-service environmental conditions which represents the difference between the real Tg of coating film

(affected by relative humidity) and the ageing temperature and the coating composition such as structure and cross link density of the binder (i.e. the degree of bonding between the epoxy resin and amine curing agent), and pigmentation [48]. The key challenge identified and unresolved was the relationship between physical ageing phenomenon, coating composition and the long-term durability of coatings in practise.

Recently, the IMO PSPC [14] and Det Norske Veritas (DNV) [26] have reaffirmed the need to understand and eliminate coating embrittlement in WBTs with the following respective quotes:
"Coatings for application underneath sun-heated decks or on bulk heads forming boundaries of heated spaces shall be able to withstand repeated heating and/or cooling without becoming brittle".
"*It is due time that the shipping industry together with the paint/coating manufacturers start investigation of how coating flexibility changes with time due to ageing processes. The behaviour of coatings under simulated ballast tank deckhead conditions is primarily of interest".*

Although the PSPC attributes "*brittle*" to aged coating film commonly fatigued (due to in-service WBT environmental conditions) from hygrothermal cycling, the word "*brittle*" does not identify the cause for the problem. It simply means the characteristic of a material that fails in tension with little or no elongation on exceeding the proportionality limit while undergoing tensile testing which is more appropriately applied to an elastic material (metal) unlike in this case a viscoelastic material (coating film). The environment setup of a tensile testing equipment is unable to appropriately capture the ageing effect of coating films, which is highly relevant in determining performance. In addition, with viscoelastic materials, strain is rate or time dependent [49].

Based on this premise in this research, it seems appropriate to recommend a suitable terminology – *thermal fatigue resistance*. Thermal fatigue resistance would represent the effect of the repeated cycling of an adhered coating film above and below its Tg from two temperature extremes resulting in the degradation of the film, which manifests in the form of cracks particularly at the

weld corners where much higher dry film thickness is seen in WBTs than ideal. Thus, adopting this recommendation would facilitate the establishment and delivery of an enhanced testing protocol for evaluating and selecting durable coating systems prior to their application in WBTs.

Furthermore, the limited literatures specific to WBT coatings, especially concerning the assessment of coatings to cracking and embrittlement/loss of flexibility with age suggests that this subject area will be quite challenging. Hence, it is highly important to the scientific community and industry to better understand and address this issue.

2.4.2 Cracking failure of epoxy coatings

While in service, cracking failure of a coating refers to the breakdown of an intact dry coating film before the anticipated useful life in the form of cracks that penetrate at least one layer of the coating system [7]. Cracking is a damage that occurs to coating in service. Cracking can occur for several reasons including excessive film thickness leading to film shrinkage from over-application, poor product formulation, incorrect over-coating intervals, thermal cycling and poor surface preparation especially at welds [16, 21]. Other damages to coating include wear and tear, mechanical damage and poor adhesion between substrate and coating [50]. Cracking is considered an undesirable feature from embrittlement or loss of flexibility of the protective coating as the coating ages. In addition, it is considered a principal factor resulting in subsequent corrosion and diminution of ship's structural substrate especially in WBTs [10]. The IACS manual [8] supports this view by stating that this problem is, therefore, very similar to that of local pitting corrosion, where, if early remedial action is missed, the overall integrity of the structure will be put at risk. As the consequence of corrosion is serious and expensive to the shipping industry, there is renewed effort in combating early corrosion through emphasis on effective coating protection [1-17, 26, 51].

In terms of the asset value and integrity of merchant ships, a key reason for scrapping them is the poor condition of their WBTs and it is widely accepted in the industry that good condition of the coatings in WBTs contribute to the ship

longevity. However, they are very demanding in the application and maintenance of protective coatings against corrosion. Hence, over the years, various organisations both governmental and non-governmental have taken approaches independently in some cases and collectively in other cases to restore confidence and safety of these vessels at sea by introducing guidelines and requirements on preventing pollution and more importantly focusing on the durability of protective coatings.

A number of classification societies have increased their involvement in corrosion protection of ships due to high level of premature coating failure recorded during inspection and investigation. In addition, the recent emphasis and involvement is linked to the economic savings and benefits that quality coatings can offer over the lifetime of the ship as steel renewal is both expensive and time consuming [8, 17, 51]. On another hand, quality coatings will assist in a better forecasting of maintenance as well as delaying onset corrosion [11].

The IACS manual [8] reaffirms this by stating that the maintenance of this corrosion protection system throughout the lifespan of the ship (from the keel laying to the scrapping) is an important element in the initial choice of materials and continues to be a measure of the structural integrity of the ship.

For WBT coatings as shown in Table 3, classification societies during inspection assign three separate conditions to coatings: good, fair, poor as a basis for subsequent examinations. These conditions are part of the classification scope of work due to the IACS Unified Requirement (UR) “Hull Surveys” [26]. If the inspection of the coating film falls far below good condition (as in the case of poor) then an annual enhanced survey is likely prescribed. “Good” refers to the coating condition with only minor spot rust < 3% coating breakdown on areas or < 20% on welds and edges [8, 24]. Fair relates to the condition with local breakdown at weld connections and edges of stiffeners, light rusting over 20% or more of areas under consideration, but less than defined for poor condition. Poor means the condition with general breakdown of coating is 20% or more of areas or hard scale at 10% or more of areas under consideration [8, 52]. In

addition, Good condition could mean no maintenance for 3 years, fair condition could mean maintenance required in 3 years and poor could signify maintenance required annually [52].

Table 3 IACS clarification of coating conditions: "GOOD", "FAIR" AND "POOR" [8]

	GOOD (3)	**FAIR**	**POOR**
Breakdown of coating or area rusted (1)	< 3%	3 – 20 %	> 20%
Area of hard rust scale (1)	-	<10%	≥ 10%
Local breakdown of coating or rust on edges or weld lines (2)	< 20%	20 - 50%	> 50%
Notes (1) % is the percentage of the area under consideration or of the "critical structural area" (2) % is the percentage of edges or weld lines in the area under consideration or of the "critical structural area" (3) spot rusting i.e. rusting in spot without visible failure of coating			

The implication of poor WBT condition to ship owners includes frequent dry-docking for repair, loss of revenue; increase in down time and in extreme cases loss of lives at sea. Hence, in order to mitigate this impact, the maritime industry and stakeholders are demanding the application of better quality epoxy coatings in WBTs of ships that have endured an enhanced performance testing before application.

2.5 Development of Stress in Epoxy Coatings

Askheim et al. [15] stated that the cracking propensity of WBT coatings is due to stress within the coating film that arise from a combination of the following four factors:

(a) Shrinkage a result from chemical curing during cross linking – this is inherent and a consequence of the reaction

(b) After gelation, loss and migration of low molecular moieties such as solvents, plasticisers, accelerators, binder extenders and unbound catalysts during the curing process. Some of these moieties are lost during application and film formation while that of others occur after complete cure

(c) Strain transferred or transported from the steel substrate

(d) Impacts from the environmental conditions such as temperature changes, water immersion, wet and dry cycling, heating from the sun and cooling at night) especially in a cyclic manner

Although, Askheim et al. [15] examined the cracking of two epoxy coatings using a 4-point bend test on flat test specimens (applied coating on steel substrates) after accelerated ageing, further investigation was suggested to establish a standard method for testing the long-term durability of coating properties regarding loss of flexibility with ageing.

Mills and Elliasson [12] disagreed with Askheim et al. [15] on the transportation of strain from the steel substrate to the coating but agreed with the other factors suggested by Askheim et al. [15]. Mills and Elliasson [12] suggested that the difficulty in addressing cracking of WBT coating arises from the numerous factors influencing cracking. This adds to the problem complexity as some of the variables interact with other variables, and could not be treated in isolation.

Perera [53] recognised that stress could affect the adhesion of coating and/or cohesion and provoke delamination and/or cracking. This study made a major contribution to the failure of coatings. Perera [53] concluded that stress is

developed through all stages of coating life so it was the sum of all contributing factors (some tensile and others contractile) that defined the total stress and subsequent strain. Perera [53] linked good adhesion with restricted movement of the dried coating film as the origin of stress and outlined three main factors that provoked stress in organic coating as follows:

(a) Film formation – Internal stress (internal stress starts developing after vitrification)

(b) Variation in temperature – thermal (thermal stress arises in coated substrate system from temperature mismatch between the coating and the substrate as well as different cycling conditions. The thermal expansion coefficients of coatings and substrate are not similar or close)

(c) Variation in relative humidity – hygroscopic (Similarly, a mismatch between the expansion coefficient of the coating and the substrate system (during water absorption and desorption) gives rise to hygroscopic stress.

The stress derived from the combined effect of temperature and humidity refers to hygrothermal stress.

Perera [53] presented how the development of stresses could also depend on the specific formulation by considering effects of the following coating components: pigmentation, pigment volume concentration (PVC), critical pigment volume concentration (CPVC), solvents and different binder systems.

Although Perera [53] did not specifically address the conditions encountered by WBT coatings, the factors confirmed the general views that stress in WBT coatings arises from the combination of the above listed factors. However, Perera [53] did not consider the leaching effect of water-soluble materials from the coating when immersed.

Mills and Elliasson [12] further suggested that ageing of the WBT coating from both thermal and wet/dry cycling (from mechanical fatigue) was responsible for diminishing the coating's protective ability. Thus, the coating eventually succumbs to failure in the form of cracking.

Ringsberg [50] stated that the endurance limits of most metals decreased in the presence of a corrosive environment. Similarly, thermal fatigue under the influence of a corrosive environment such as seawater can be very harsh on WBT coatings. Thus, emphasising the potential role played by the combined cycling between seawater and temperature especially from rapid thermal differential that could exacerbate cracking failure.

2.5.1 Cyclic stress in WBT environment

Environmental conditions in WBTs simply describe a combination of two conditions: hygroscopic cycling (wet/dry conditions brought about by ballasting and de-ballasting) and thermal cycling (hot/cold) within the tanks. Thus, wet/dry cycling and cold/hot cycling is associated with fatigue processes because there are elements of stress cycling from both tensile and compressive stresses, which damage the coating and result in changes to the film with age. The combined cycling is typically termed hygrothermal cycling and its consequence is hygrothermal stress [31].

Hygrothermal stress is a source of stress that WBT coatings continuously encounter in service. Temperature and moisture or heat and humidity are always present environmentally in WBTs. Hence, it is worth considering together their impact on WBT coatings.

WBTs coating films alternately take up and desorb water in response to ballast changes in order to maintain an equilibrium condition with the environment [12, 30]. When WBT coating films are immersed (i.e. in ballast conditions), the films absorb or take up water and are likely to swell. However, this is not to any substantial extent.

This action of water absorption puts the film in compressive stress. The absorbed water will depress the Tg as it acts like a plasticiser but the precise amount will be formulation dependent. A similar condition is experienced when

heat is transferred from the carried cargo (in the cargo hold) into WBTs. The coating films also expand in response to the heat producing compressive stress.

WBT coatings when de-ballasted experience desorption and the adhered film tries to contract resulting in tensile stress [13, 31]. The film does not actually contract, if it did, there would be no stress. Stresses are generated because the film cannot contract. A similar effect is demonstrated at low temperatures. The effect of either tensile stress or compressive stress acting alone is not as damaging as the combined effect of the constant alternating of these two components of stress above and below the coating's Tg, in addition to initial shrinkage stress during film formation [31].

The significant changes brought upon the coating structure by the net effect of hygothermal cycling can be summarised as follows:

- Loss of residual solvent and/or loss of external unreacted plasticisers
- Leaching of water soluble constituents
- Additional cross linking from residual reaction and subsequent shrinkage (in film thickness only)
- Increased coating stiffness (modulus) and Tg

All of these changes to WBT coating film may significantly contribute to cracking and the gradual inability to protect effectively the substrate with age.

Zhang et al. [54] stated that the high temperature within ballast tanks in DH ships (from cargo temperatures of 60 ºC) remained longer than 10 hr during which the internal stress of the coating may be dissipated through post curing and viscous-elastic behaviour. A possible explanation is that the temperature of the coating may increase and exceed the glass transition temperature Tg resulting in stress relaxation within the polymer. Also, the retained longer temperature duration confirms the thermos bottle effect.

Mills and Elliasson [12] reported how one epoxy WBT coating containing hydrocarbon resins was seen to "sweat" when the opposite cargo tank carried caprolactam at 85 °C. A puddle of the hard, amber resin was exuding and dripping during a single 28 days voyage.

Gunter [55] confirmed experimentally that wetting and immersing periods found mainly in all of water/air zones was an important factor for consideration in coating performance tests. The research focused on evaluating coating performance of hydraulic structures from undercoat corrosion using test panels with a scribe mark (or mechanical damage) initiated at the top face of the cured coating film and continued to the bare panel surface.

WBTs, even when empty, contain water (with silt in other cases) in their bottom structural plating. They have condensing humidity most of the time. With DH ships, the elevated temperature of the cargo potentially increases the corrosion rate within the ballast tanks, doubling it for every 10 ^{0}C rise in temperature. Thus, if the average temperature of WBT is 20 ^{0}C warmer than before, the corrosion rate would likely quadruple [13, 56].

Some particular areas in WBT are more prone to cracking of coating especially welds, edges and details with difficult access [12, 13, 24].

Several researchers [11 - 13, 16, 50, 53 - 55] have agreed that the proper selection and choice of a coating scheme should be tailored to suit the specified in-service and environmental conditions as different coatings respond differently to the influence of the environment. Some exhibit more fatigue resistance than others when cycled from low to high temperatures [50].

2.5.2 Components of stress in epoxy coatings

Generally, stresses in coatings are classified as either tensile or compressive and they may play a counterproductive role to performance.

2.5.2.1 Tensile stress

Tensile stress is developed when the WBT coating film would like to contract but cannot as it is fixed effectively at both ends. Such could occur from either film formation (solvent evaporation and curing process) or cold (low temperature) exposure. Commonly, WBT coatings are applied in the liquid state by a combination of airless spray and brush application. Upon applying the coating to the substrate, solidification

subsequently follows. Solidification, or drying, occurs by a simultaneous combination of chemical cross-linking and solvent evaporation. The resultant effect of coating solidification is shrinkage in the plane. If the coating is a free film, it will shrink unrestricted. However, for a film adhered to a substrate that has sufficient strength and thickness, it will be unable to shrink freely in the plane of the substrate. The restricted in-plane shrinkage results in in-plane biaxial tensile stress.

2.5.2.2 Compressive stress

Compressive stresses occur from expansion of adhered WBT coating film in response to either elevated temperature or high relative humidity. As was the case with tensile stress, changes from expansion to the adhered film from compressive stress are restricted. Thus, a strain is produced in the film as a consequence of restriction in the plane, which opposes adhesion and cohesion. If great enough, the strain can lead to coating failure. However, for coatings of low enough Tg, the application of compressive stresses may actually lead to dissipation of the total stress especially at film temperature much above the Tg as segmental molecular mobility is restored within the film [57].

Perera [53] observed that coated substrate when immersed in water initially developed compressive hygroscopic stress that was followed by its decrease. In addition, the removal of the immersed coated substrate induced and developed high tensile hygroscopic stress before it declined. Also stated was the time it took to approach zero stress, which depended on the coating type. Perera [53] recommended considering both tensile and compressive stress when designing coatings for service exposure.

2.5.2.3 Internal stress

The in service or environmental stresses that affect a coating are in general well known but their effects are not well quantified. Less understood are the internal stresses that develop in the paint film as it

adjusts from the wet film to the dry film and then more slowly to those gradual molecular changes that accompany (or more accurately produce) the aging process. These stresses are usually tensile in nature, especially those that originate during film formation and cure. These stresses make up a substantial, if not the paramount, component of the total stress. They are often unaccounted for by those who use, specify, or formulate coating systems [57].

Several publications refer to internal stress of solvent containing coatings as follows: cure stresses, residual stresses, shrinkage stresses, film formation stresses, solvent removal stresses [12, 13, 15, 53, 57 - 59]. An applied and cured coating may have the required flexibility when recently applied and for a few years afterwards. Then due to cyclic conditions such as temperature variation and intermittent immersion, the more volatile and low molecular weight components are lost by either evaporation or washed away [26], resulting in subsequent diminishing coating flexibility with higher potential to crack.

Thus, some researchers attribute cracking in coating films to shrinkage stresses (internal stresses) alone generated and developed from curing when the initial matrix volume of the coating shrinks from loss of migratory species such as solvents and binder extenders [12].

Croll [60] measured internal stress in an acrylic thermoplastic (non-convertible system which dries physically by solvent evaporation without further chemical reaction) polymer solvent system (polyisobutylmethacrylate (PIBM) dissolved in toluene solvent) at ambient conditions (23 ºC & 50% relative humidity (R.H)) using the applied thin steel substrate as cantilever. Croll [60] concluded that internal stress was independent of coating thickness and initial solvent concentration. The thickness of the coating ranged from 10-100 µm however higher thicknesses were not considered. The maximum coating thickness used in the experiment is less than one – third the standard recommended for WBT coatings. However, this is in contrast to

thermoset (convertible system which dries by both solvent loss and chemical reaction) coating films where there is some evidence that internal stress is likely to increase with coating thickness [61,62]. In addition, Croll [60] used steel gauge stock of 0.1-0.25 mm thick indicating that the effect on thicker substrates was unconsidered. With thicker substrates, a different conclusion could have emerged.

After application of a coating, the solvent evaporates from the wet film leaving available spaces for the polymer to occupy. However, as solidification takes place, movement by contraction is allowed only in the thickness dimension of the applied coating while movement in the remaining dimensions (plane) is restricted by adhesion between the film and substrate. Croll [60] also stated that, depending on the type of polymer, any stress present after curing would have an adverse effect on the body of the coating with the occurrence of crazing or brittle failures. The IACS manual [24] confirms this by stating that a better understanding of the different coating systems and the possible limitations of each system will assist in the prevention of unnecessary and undetected corrosion. Thus, confirming the need to investigate different epoxy formulations.

Following from the above, some other publications have emerged including:

Negele and Funke [63] agreed that internal stress by curing shrinkage was the main reason for cracking and checking. Checking is a type of coating failure where break(s) primarily occur on the coating film similar to that seen in cracking failure. However, unlike cracking failure, the breaks described as checking only appear on the film surface without penetrating the full depth of the coating film thickness. In a recent study, Zhang et al. [54] refuted this postulation and suggested that cracking of coatings (in epoxy-based paints) manifested from thermal stress accumulated during ballasting operation.

Zhang et al. [54] performed thermal cycling test along with Thermo-Mechanical Analysis (TMA) to obtained parameters such as thermal coefficient of expansion. Epoxy coatings (mainly supplied by two different manufacturers) and spray applied on T-bars were experimented. There were five types of epoxies; however, the precise formulations were unknown. Dry film thicknesses (DFT) (as much as 1500±50 μm) were considered. From the thermal cycling test, the conclusion was that thicker coatings had more propensity to cracking. Yuly and Salem [64] agreed and stated that it took longer time for low DFT coatings to reach the peak of the internal stress and no failures occurred at low DFT when compared to high DFT as same level of exposure.

Furthermore, Zhang et al. [54] also suggested that the performance characteristic of coating is highly dependent on its surroundings (the in-service environment). Also, stated (after performing a pull off test on immersed coatings) is that the cohesive strength of coatings decreased with increase in the immersion period because the absorbed water severed hydrogen bonds resulting in coating degradation.

Researchers suggesting internal stress from cure and shrinkage as the only reason for cracking of coating films tend to draw this conclusion by (linking or comparing) the solvent loss to internal stress developed while assuming the coating film to be perfectly elastic. Another area not considered is the relationship or influence of thicker coatings that are applied on thicker substrates as majority of the reviewed experiments were performed using either free films or very thin coated substrates. The reality is that the coating film on very thin substrate is relieving its own internal stress through shrinking while transferring the stress to a substrate with insufficient strength when curling. Hence, conclusions based on this approach cannot be relied on for adherent coatings especially those with thicker films and substrates.

Mills and Elliasson [12] hypothesised by stating that the initial elongation of freshly applied coatings for the majority seems high enough, maybe due to the film being well plasticised by the retained solvents. However, it is unclear whether this applies to all new formulations. There are doubts about the performance of these coatings as they are relatively new in service applications such as the WBTs of double hull ships.

2.6 Performance Testing and Test Protocols

The performance of materials (such as coatings, steel structures, plastics) in their service environments continues to raise significant interest and concern especially when the materials are intended for more extreme environmental conditions [65]. Thus, a relevant approach to understanding and anticipating material behaviour with regards to performance is to expose or subject the materials to some form of testing which could be either natural (field testing) or artificial (accelerated testing in laboratory).

While field testing (particularly in the form of weathering) could give the desired understanding as the materials are exposed to the same conditions but this form of testing takes a very long time to yield the outcome. Other disadvantages include relative high cost, inability to adequately control variables leading to large data scatter, size of the model (test samples) relative to the in-service full size (real structure) and difficulty of undertaking interim inspections [66]. In view of these disadvantages, accelerated testing is favoured.

Accelerated (artificial) testing takes a shorter period to deliver indicative results that could provide a good insight to the behaviour of the materials [67]. In term of exposure conditions, accelerated testing employs several conditions also known as set exposure conditions. The set exposure conditions particularly temperature and relative humidity could be used either alone or combined as well as could be employed at a constant or cyclic rate. While temperature seems less challenging to control, relative humidity is quite challenging in this regards. These set conditions also apply to WBT coatings.

Test protocols are written standards containing set exposure conditions employed in the marine industry for evaluating and predicting the durability of coatings in terms of performance. Typical evaluated performance include corrosion resistance, weathering and immersion resistance.

Significant drivers for the application of test protocols include:

- The demands for better performance and longer asset life from coating improvements have led to the introduction and modification of several test protocols.
- Increasing legislative pressure on VOC emission reduction from coatings has required the development of new formulations.

Based on the above drivers, test protocols used by the industry have evolved from static exposure testing to cyclic exposure testing.

A static test protocol is an exposure of coated test specimen(s) to only one environmental set condition. Test specimens are subject to one particular exposure for example a hot salt spray (ASTM B117, ISO 7253:1996). Salt spray was one of earliest method to be introduced and used around 1914. Then in 1939, the neutral salt spray technique was incorporated into ASTM B117 [68, 69].

Cyclic test protocols subject test sample(s) to more than one set exposure condition and the samples are alternated between them. For WBT coating assessment, cyclic test protocols are more relied on and applied because better correlation within service performance could be achieved.

2.7 Review of Existing Test Protocols

Test protocols commonly employed to assess the performance of WBT coatings include: ASTM D5894 10 [70], ISO20340:2009 (E) [71], NORSOK M 501 [72], NORD-TEST NT POLY 185 [73], NACE TM0304-2004 [74], NACE TM0104-2004 [75] and IMO PSPC [14]. These protocols are also used in different marine applications with seawater environmental zones including marine atmosphere, splash/spray, tidal, deep ocean, shallow ocean and mud.

2.7.1 ASTM D5894-10 - (Standard practice for cyclic salt fog/UV exposure of painted metal)

ASTM D5894-10 subjects test panels to cyclic corrosion testing by alternating UV/Condensation cycles and wet/dry salt fog cycles. The UV/Condensation cycle is a 4 hr exposure using UVA-340 nm at 60 ^{o}C. This UV exposure is then followed by a 4 hr condensation exposure at 50 ^{o}C, using UVA-340 lamps. The duration for the UV/Condensation exposure cycling is 1 week (168 hr). The cycled test specimens from the UV/Condensation cycling are then transferred for fog/dry cycling. The fog chamber runs a cycle of 1 hr at ambient temperature and 1 hr dry-off at 35 ^{o}C. The duration for this cycle is 1 week (168 hr). The electrolyte employed in the fog chamber is dilute solution of 0.05% sodium chloride and 0.35% ammonium sulphate. This type of electrolyte suggests that the test is more applicable to onshore applications. The dimensions of the specified flat specimen are 150 mm by 75 mm.

The above protocol could be described as a cyclic corrosion test where a weathering exposure is alternated with an electrolyte exposure. The usage of a flat test specimen to simulate a cracking test for WBTs seems unsuitable, as the occurrence of any cracking failure on any flat surface/area is extremely uncommon in service when compared against power-tooled welds at corners. As this method does not take into account film thickness or surface preparation, it is not considered suitable for the testing of ballast tank coatings where these are considered to be significant variables. Again, the application of UV is unrealistic as WBTs have very little exposure to UV.

2.7.2 ISO 20340:2009 (E) (Paints and varnishes – Performance requirements for protective paint systems for offshore and related structures)

ISO 20340:2009 (E) deals with performance requirements of paint systems applied on offshore and related structures. This standard specifies additional test requirements over and above those specified in ISO 12944-6 for corrosivity category C5-M (marine & offshore environment). In addition, ISO 20340 is applied in qualifying structure(s) of category Im2 (immersed in seawater). The dimensions of the specified test panel are 150 mm by 75 mm by 3 mm. The

specified surface preparation is by grit blasting to at least Sa 2.5. The recommended maximum thickness of each coat on each panel is as follows: less than 1.5 x the nominal dry film thickness (NDFT) if the NDFT is ≤ 60 µm, less than 1.25 x the NDFT if the NDF is > 60 µm. The conditioning period is in accordance with ISO 3270 (temperature: 23±2 ^{o}C and relative humidity: 50±5%) for 7 days or 1 week. The test panel is horizontally scribed parallel to one of the width sides. The scribe dimension is 50 mm long, 2 mm wide, 12.5 mm from each long edge of the panel and 25 mm from the bottom (short) edges of the panel. ISO 20340 qualification tests used in the assessments of coating performance include ageing resistance, cathodic disbonding and seawater immersion. The ageing resistance is a cyclic exposure test consisting of UV/Condensation, Salt Spray and sub-zero dry out. An exposure cycle for one (1) week (168 hr) includes the following:

- Starts with 72 hr exposure of UV/Condensation: alternating periods of 4 hr UV exposure at 60±3 ^{o}C and 4 hr for condensation exposure at 50±3 ^{o}C
- Followed by 72 hr salt spray in accordance with ISO 9227 at 35±2 ^{o}C using 5% sodium chloride electrolyte
- 24 hr of exposure to low temperature at -20±2 ^{o}C

Also, it is advised to rinse the panels with deionised water between the salt spray and low temperature exposure but avoid drying them. Also, this -20±2 ^{o}C low temperature of the panels is required to be achieved within 30 min. Duration of exposure for the test panels is 25 cycles or 4200 hr (25 weeks).

ISO 20340 and ASTM D5894-10 are cyclic corrosion tests. The distinguishing characteristic between these two standards is the freeze cycle in ISO 20340. Another distinct feature of ISO 20340 test specimens is the introduction of a mechanical damage through a scribe marking. The mechanical damage would drive a different failure mode from cracking which is corrosion. A corrosion assessment is performed on the scribed specimen by removing all loose/corroded areas at a number of predefined points along the scribe and averaging to obtain the final Figure. The analysis of this corrosion assessment could be considered to be subjective as it depends on the judgement of the operator.

Common to both the ISO 20340 and ASTM D5894-10 test protocols is the alternate exposure of the test specimen to UV/Condensation and salt spray cycles. The weekly test durations for UV/Condensation and salt spray exposures as shown in ASTM D5894-10 have been reduced in ISO 20340 to 72 hr (3 days instead of the 7 days interval as in ASTM D 5984). The overall test protocol duration is longer for ISO 20340, extending to 25 weeks when compared to 6 or 12 weeks for ASTM D5894-10.

The incorporation of UV light in the test also negates and undermines the kind of in service exposure as seen in WBTs. Finally, flat specimens (grit blasted to Sa 2.5) employed in ISO 20340 tests are highly unlikely to produce cracking failure of WBT coatings as they lack the required geometry as explained earlier (the vast majority of the cracking failure reported occur at corners on power tooled welds).

2.7.3 NORSOK STANDARD M-501 (Surface preparation and protective coating)

NORSOK M-501 is targeted towards offshore and associated facilities such as bottom-founded installations, ships, floating structures. This test attempts to address different coating system functional requirements in offshore corrosion protection, such as prefabrication primers, deck systems, passive fire protection and linings including ballast coatings. NORSOK M-501 is more prescriptive about paint application (number of coats, stripe coating and DFT) when compared to ISO 20340. In addition, NORSOK M-501 prescribes pre-blasting preparation on sharp edges, fillets and corners by rounding and smoothing whilst welds are prepared by grinding. In this test, coating system 3B refers to coatings applied to WBTs. The performance testing of the protective coating is similar and in accordance with ISO 20340 as enumerated before. So in essence the NORSOK test for WBTs is a reflection of ISO 20340. Also, the IMO PSPC MSC 215(82) pre-qualification or performance testing has been accepted as an alternative qualification method for ballast tank coatings (coating system 3B) employed by NORSOK M-501. Therefore, NORSOK M-501 shares the same

highlighted issues with ISO 20340 and IMO PSPC MSC 215(82) when applied to performance testing of WBT coatings.

2.7.4 NORDTEST Method NT POLY 185 (Determination of flexibility and fatigue resistance of aged ballast tank coatings)

NORDTEST NT POLY 185 is intended to determine flexibility and fatigue resistance of aged ballast tank coatings. The test piece is a flat steel substrate with a length of 150 mm and 30 mm in width and 3 mm in thickness. Coating thickness is specified at about 300 µm on both sides of the test piece. The ageing test consists of three stages: immersion conditioning, air conditioning and damp heat cycling. One cycle of the test consists of three stages, which are completed in one week:

- 72 hr exposure to artificial seawater immersion at 40 ^{o}C
- 24 hr air conditioning exposure at 23 ^{o}C and relative humidity is 50%
- 72 hr damp heat including condensation according to IEC 68230 combined with temperature interval 20-90 ^{o}C

Maximum exposure time shall be 12 weeks (12 cycles) and mechanical testing after every three weeks.

Mechanical testing is achieved through either a four point bending or cylindrical mandrel bending test.

(a) Static bend test using 4 point bend machine is carried out on aged specimens until they break. The strains are set below 4%. However, with higher strains, the equipment is unusable.

(b) Cyclic fatigue testing is recommended for higher strains of 1%, 0.7% and 0.4% for cycles including: 100, 200 and 300. The machine displacement is performed in 10 sec at selected strains.

This test protocol is intended for assessing coating flexibility with a flat test specimen. This test protocol does not take into consideration thicker coating films, i.e. above 300 µm or more. The test mentions the blasting of test

specimen but does not say specifically to what cleanliness. In addition, the test lacks the structural geometry in a WBT where the majority of coating breakdown by cracking is reported in areas other than a flat plate.

2.7.5 NACE TM0304-2004 (Offshore platform atmospheric and splash zone maintenance coating system evaluation)

NACE TM0304-2004 is targeted at the offshore platform maintenance coatings. This test protocol contains seven test types including rust creepage resistance, edge-retention, thermal cycling resistance, seawater immersion resistance test, cathodic disbondment, flexibility, and impact resistance.

The rust creepage resistance test is in accordance with ASTM D 5894 but the electrolyte is replaced with synthetic seawater that represents an offshore environment. Test panels are scribed for UV exposure. Test duration of 12 weeks is recommended. Performance is determined by measurement of rust creepage from a scribe marking. The test specimen is flat with dimension: 150 mm by 76 mm by 4.75 mm.

The Edge-Retention test uses a 90^{o} aluminium substrate bar with a curvature of 0.7± 0.1 mm. Dimension: Long = 150 mm, 19 mm by 19 mm by 3.18 mm.

Thermal cycling resistance test is performed on a coated C-Channel block (dimension: 76 mm by 50 mm by 3.18 mm) in which the coating is post cured at 60 ^{o}C for one week before undergoing the thermal cycling. A cycle is carried out in two hours at an upper temperature of 60 ^{o}C and a lower temperature of -30 ^{o}C. Test duration is at least three weeks or 252 thermal cycles.

Seawater Immersion Resistance test: Test specimens are cleaned by blasting to Sa 2.5 before coating application. Coated test specimens, cured at room temperature for one week, are immersed in synthetic seawater at 40±2 ^{o}C. Coating adhesion is evaluated by either a pull-off test in accordance with ASTM D 4541 on test specimens without holiday or wet coating disbondment test that uses test specimen with circular holiday in the coating film. Dimension of the flat specimen is 150 mm by 76 mm by 4.75 mm.

Flexibility testing is carried out on the coated panels that have been post cured at 60^{o}C for one week using a fixed radii mandrel bending machine as described in NACE RP0394. The dimensions of flat test specimen are: Length = 150 mm, Width = 12.7 to 25 mm, Thickness = at least 10 times coating system DFT.

Most of the testing in this protocol is carried out on flat specimens except in the edge retention and thermal cycling resistance tests. Dry out cycles are not included in any of the tests (when compared to ISO 20340) except for a sub-zero temperature cycle which is used in the thermal cycling resistance test. The sub-zero temperature cycle is highly unrepresentative of WBT exposure temperature. The test specimen does not incorporate welds and power tooled preparation by grinding at the corners as seen in service. Rather the prescribed surface preparation of the C-channel test piece is a near white metal blast cleaning only. In addition, the angle of the C-channel is undefined which may lead to the use of various test specimen which may be similar but provide different result. Bending test specimens by mandrel bending also does not replicate in service conditions as higher strains than expected are observed to be applied by this test.

2.7.6 NACE TM0104-2004 (Offshore platform ballast water tank coating system evaluation)

NACE TM0104-2004 is a test protocol specifically dedicated to ballast water tank coatings of offshore platforms. As a test protocol, NACE TM0104-2004 has three tests, which are similarly to NACE0304-2004. These tests are edge retention, seawater immersion resistance and cathodic disbondment. In addition to these three tests, it also includes dimensional stability, ageing stability, thick film cracking and hot/wet cycling which is only for Floating Production Storage and Off-loading (FPSO) Structures.

The Dimensional Stability test is intended to track a coating system's swelling or shrinkage on immersion. Room temperature cured free films are immersed in synthetic seawater at 40±2 ^{o}C for 12 weeks. The changes in length, width and mass of the free films are measured.

Aging Stability test: Test specimens that have been cured are exposed to an ageing test by seawater immersion for 12 weeks at 40±2 ^{o}C. Thereafter, flexural strain is obtained on fixed radii mandrel bending for both the aged and non-aged test specimens. The rationale is to compare the aged test specimens against the non-aged/control test specimens. The flat test specimen dimensions are: Length = 150 mm, Width = 12.7 to 25 mm, Thickness = at least 10 times coating system DFT.

Thick-Film Cracking test: In this case, the test specimen used is the same test specimen employed in the thermal cycling resistance test for NACE TM304-2004. However, for this test protocol, the test specimen is immersed in synthetic seawater at 40±2 ^{o}C for 12 weeks. Thereafter, the coating system is assessed for cracks.

Hot/Wet cycling: The test is intended to assess coating performance by simulating wet/dry exposures, which may be encountered in ballast tanks on a Floating Production Storage and Offloading (FPSO) vessels. This is a cyclic salt-fog test carried out in accordance with ASTM G 85-A5. This test alternates cycles of 3 hr wet at room temperature and 3 hr dry at 60 ^{o}C. Flat test specimens with vertical scribe on one side are used for this test. Their dimensions are: 150 mm by 76 mm by 4.75 mm.

Amongst the four tests, two (aging stability and hot/wet cycling) employ flat test specimens while the others (dimensional stability and thick-film cracking) employ free film and C-channel specimens respectively. The use of the flat specimen and free film is unrepresentative of the in service location where cracking is observed in WBT. All the other tests except the hot/wet cycling test can be linked to a static exposure condition test. However, the hot/wet cycling test assesses corrosion from rust creepage of the mechanically induced damage.

2.7.7 IMO PSPC MSC 215 (82) (Performance standard for protective coatings for dedicated seawater ballast tanks in all types of ships and double-side skin spaces of bulk carriers)

Amongst, the test protocols already discussed, the IMO PSPC [14] is the latest specifically targeted at coating performance in WBTs of ships. The goal of PSPC is to achieve a useful coating life of 15 years in good condition with maintenance [14].

From 1990 to 2000, the shipping industry continuously focused on the consequences of corrosion and increasingly demanded better performance from protective coatings used for corrosion control [6, 7, 11, 16]. These concerns led to the introduction to an amendment of the International Convention for Safety of Life At Sea Convention (SOLAS) in Chapter II Part A-1 Regulation 3-2, which specified the need for protective coatings for dedicated ballast tanks and double-sided skin space of bulk carriers in compliance with the PSPC mandated by the IMO [11]. IMO responded to the need of members of International Association of Classification Societies (IACS) and other stake holders through the adoption and amendments made to the SOLAS 74/78 by resolution 216 (82) of the Maritime Safety Committee (MSC) on page 3. One of such stakeholders that set the pace for a standard for the protective coatings in WBTs was the Tanker Structure Cooperative Forum (TSCF). Shell International Marine formed the TSCF in 1983 as a group with initial members as ship owners and class societies but its current membership also include oil majors and coating producers [76].

The group's rationale is to share experience and knowledge on technical matters concerning the performance of tanker structures in service. From the shared experience, several publications have emerged in the shipping industry. One of such publication in 2002 was the TSCF guidelines for WBT coating systems and surface preparation, which set the foundation for the IMO PSPC [7]. By including the IMO PSPC into SOLAS, WBT coating has attained a similar importance and level as mandatory ships safety equipment. Generally as acknowledged in successive forms, the SOLAS Convention is the most important of all international treaties regarding the safety of merchant ships. As

a direct response to the RMS Titanic disaster, SOLAS Convention was adopted in 1914 and it had revised versions in 1929 and 1948 respectively. Another version was adopted in 1960 and the latest version in 1974 [4]. The IMO PSPC exceeds and renders more precisely each classification society's own standard as well as the existing "Unified Requirement Z8," issued by the IACS in 1990 and revised 1995 [77]. Hoppe [78] presents a comprehensive overview on the development of IMO PSPC including the meeting outcomes of the various committees. The approval of the PSPC was in December 2006 and its first adoption was in 1st July 2008. The requirement is now mandatory and applies to protective coatings in WBT of all type of ships of not less than 500 gross ton and double side skin spaces arranged in bulk carriers of 150 m in length and above [14, 77].

The PSPC requirement can be summarised as selection, application and maintenance of protective coatings within WBTs. The requirement defines coating practices such as shown in the Table 4 below:

Table 4 Contents of coating specification

Scheme for (ref. SOLAS Reg. II-1/3-2)	**Items to be described in specification**
General (Tri-Partite Agreement)	The yard's, owner's and coating manufacturer's agreement on the specification
Selection of coating	Coating type – epoxy based, other alternative systems
	Coating Pre-qualification test
	Definition of coating systems, including number of applied coats and minimum/maximum variation in NDFT with 90/10 rule

Scheme for (ref. SOLAS Reg. II-1/3-2)	Items to be described in specification
Application of coating	Surface preparation (primary and secondary) including preparation for edges and welds, surface cleanliness and profile requirements (e.g. blasting to Sa. 2.5 with profile between 30-70 µm)
	Environmental conditions in terms of maximum allowable air humidity in relation to air and steel temperatures during surface preparation and coating application
	Also, environmental conditions for coating application shall conform to coating manufacturers specification
	Other practice prescribed include dust quantity, water soluble salts and oil contamination
Maintenance of coating	In service maintenance, repair and partial recoat

This requirement and the accompanying IACS Procedural Requirement (PR) 34 has brought more awareness of the importance of protective coating practices that have been long neglected in the shipbuilding/shipping industries. However, the long-term impact of the PSPC on the industry is yet to be seen as it is still early days.

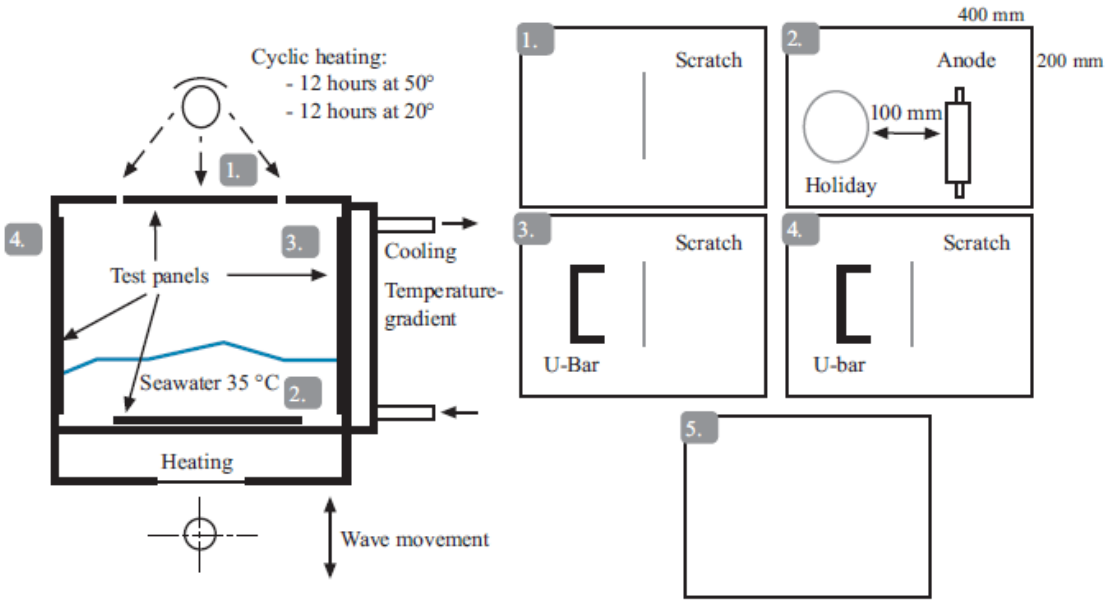

Figure 15 Schematic of wave tank laboratory testing for ballast tank coatings [14, 79]

According to the IMO PSPC, one of the methods of accepting a coating system for application in WBTs is to undergo a pre-qualification in a laboratory test (also known as type approval). The test facilities, test panels, test duration and acceptance criteria to be achieved are described in the PSPC. However, there is no data or requirement to adequately benchmark coating embrittlement in WBTs from the current proposed coating pre-qualification test. For the test; two principal tests chambers are recommended for coating testing. They are, the use of a wave tank chamber (as shown in Figure 15) to simulate supposed service conditions inside a ballast tank, and the use of a condensation chamber to simulate condensing condition.

After performing the PSPC testing from both chambers, one of the measured data to be reported is coating flexibility which is highlighted in MSC 82/24Add.1 Annex 1&2, section 2.2.4 and stated as follows: "*flexibility modified according to panel thickness (3 mm steel, 300 µm coating, 150 mm cylindrical mandrel gives 2% elongation) for information only*". Although, the PSPC has mentioned and acknowledged the need for a flexibility test for assessing WBT coatings, it does not have a specified test method in this regards.

The PSPC recommended acceptance criteria from these tests are relating to blistering which is a different form of coating degradation to cracking. Also, the PSPC pre-qualification standards evaluates mainly anti-corrosive coating properties such as delamination from mechanically induced damage made from a scribe marking, under film cutting from corrosion and in other cases water resistance and UV resistance.

This issue seems more complicated because of the different WBT epoxy coating formulations. These coatings respond differently when used in service. Some develop and show early cracking failure whilst others do not when operating in the same environmental conditions.

Similarly, the Performance Standard for Protective Coating for Cargo Oil Tanks of Crude oil Tankers (PSPC-COT), whose test protocols are based on or adopted from the PSPC, also shares and contains the same short falls of the PSPC test protocols already mentioned especially the flexibility testing.

Thus, these concerns indicate that there is a need to investigate different WBT epoxy coating formulations (types) further on cracking failure. Most especially the changes that occur in the coating film that significantly brings about loss of its applied (flexibility or ductility) properties with respect to coating life. Det Norske Veritas (DNV) [26] and IMO PSPC [14] confirms this in the below two quotes respectively:

"*It is due time that the shipping industry together with the paint/coating manufacturers start investigation of how coating flexibility changes with time due to ageing processes. The behaviour of coatings under simulated ballast tank deckhead conditions is primarily of interest".*
"Coatings for application underneath sun-heated decks or on bulk heads forming boundaries of heated spaces shall be able to withstand repeated heating and/or cooling without becoming brittle".

Also, in practice however, Safinah Limited has reported [80] that PSPC pre-qualified WBT coatings (i.e. the coatings that have passed the PSPC pre-

qualification test) can suffer early or premature in service failure especially in the form of cracks around structural areas such as corners, edges, welds and joints of WBTs as the applied coating ages. Cracking tend to occur at the corners where the film thicknesses are much more than the PSPC recommended and these areas are mostly powered tooled.

To conclude briefly, the majority of the reviewed test protocols (above) are considered unsuitable for reasons such as:

- lack of conditioning period
- inappropriate geometry of test specimen as majority use flat panel and flat areas in service are where cracking of coating are rarely found
- uv exposure
- use of free films
- focus on anti-corrosive performance (blistering and creepage) only
- inappropriate immersion times

This section on the review of existing test protocols has been published [81]. Thus, highlighting the need for a testing protocol/method to assess embrittlement of WBT coatings. Following the reviewed literatures and test protocols, the following section summarises in a detailed tabular form, those factors considered to affect cracking of coating in WBTs and their relative importance.

2.8 Summary of Factors Affecting Cracking of Coatings in Water Ballast Tanks

2.8.1 Following literature survey and industry consultation, critical factors affecting cracking of coating in WBTs as considered are listed in Table 5 below:

Table 5 Critical factors affecting cracking of coating in WBTs

Critical factors	Comments/rationale
Geometry	T shaped steel substrates are the preferred test piece. They have the necessary geometry to produce out of plane stresses. Cracking is rarely seen on flat plate. Instead, it is prevalent in corners and on welds where the substrates are not flat. Hence, it is necessary to design a test piece, which takes into account the location and geometry of the cracks seen in practice.
Surface preparation	Power tooled welds are reported to fail prematurely. Adjacent areas that are grit blasted have different adhesion characteristics and experience much less failure. In keeping with practice, welds of the T substrates will be power tooled to St 3.0 as the mostly observed areas of cracking. Other areas adjacent to the welds will be grit blasted to Sa 2.5.
Coating application	In keeping with practice, welds should be stripe coated with brush and subsequent coats applied by airless spray. The areas where cracking and failure are seen are thicker than the target specification of 320 µm. This is due both to the stripe coats that are applied to welds and edges, and also to the complex geometry compared to a flat plate which means that multiple passes are applied by spray and stripe coating to build up the required thickness on the surrounding areas.
Coating scheme and stripe coats	Vast majority of failures occur where the coating or the paint is thickest. Test schemes on test piece must include 2 and 3 times the standard 320 µm thickness specified by the IMO PSPC. Stripe coating must be included. Schemes to be applied as two coats, as in practice. Rationale as above.

Critical factors	Comments/rationale
Conditioning period	Water ballast tanks are painted at block stage – i.e. before erection and before launch. Depending on the shipyard, after application process is completed, the WBT coating film may not enter service (ballasted and de-ballasted conditions) for anywhere between 3-12 months. Therefore, it may be 3-12 months before the ship enters service. This means that there is 'dry conditioning' period prior to launch. During this dry conditioning period, the coating is considered likely to have reached its ultimate Tg at the cure temperature. After launch, the ship will travel in a ballasted condition to pick up the first cargo. This could be considered as a 'wet conditioning' period and could be as long as 4 weeks. This wet conditioning period could remove water soluble materials such as solvents and unreacted species from the film. Plasticisation by water could also result in further cure and some relaxation of internal stresses in the film. Thus, wet conditioning and dry conditioning are suggested as part of the proposed fatigue test.
Cyclic sea water immersion	Immersion removes water soluble materials and can produce swelling of the WBT coating film. Subsequent exposure to air allows solvents to leave film. Both exposure conditions will result in volumetric shrinkage and stress development. As above, immersion removes water soluble materials from the film such as unreacted species and solvents. It also may reduce internal stress by plasticising the film. Alternating immersion and drying out induces cyclic stresses in the film and is an important aspect of fatigue testing where repeat cycles contribute to failure.
Immersion times	It is important to allow sufficient time for the film to become sufficiently saturated with water. 1 week immersion is suggested for wet conditioning.
Effects of temperature variation	High temperatures of 100 ºC is required to replicate in-service conditions. It is important to cycle the temperatures above and below the glass transition temperature (Tg) of the coating film to maximise stress development. Temperatures in ballast tanks change as the hot cargoes are discharged and the tanks filled with colder seawater. Depending on the type of cargo carried, temperatures of 70-90 ºC may be required but locally the temperature could be slightly more. Cyclic temperatures variations will contribute to fatigue failure of the paint and so should feature in the fatigue test. Ideally, the temperature should be cycled above and below Tg to maximise stress development.

Critical factors	Comments/rationale
Test timescales	It is important to let the test run until failures occur. Setting an arbitrary limit at the beginning may be counterproductive.

2.8.2 Non-Critical factors affecting cracking of coating in WBTs as considered following literature survey and industry consultation are listed in Table 6 below:

Table 6 Non-critical factors affecting cracking of coating in WBTs

Non-critical factors	Comments
UV exposure	Not relevant and unrepresentative of ballast tanks.
Mandrel bend test (Cylindrical and Conical)	Is not relevant to the challenges or in service conditions found in ballast tanks
Free (self-supporting) film measurements	The use of free (or self-supporting) films not appropriate. Stresses are different when attached to a substrate especially thinker ones and producing flawless or defect-free self-supporting film is extremely difficult.
Sub-zero temperatures	Not relevant to ballast tanks. In addition, this problem occurs without exposure to such low temperatures. Often used as an accelerating test condition but its purpose is not clearly defined.
Un-aged films	Only of use as a benchmark for the initial condition, but not necessarily an indicator of performance after ageing.
Stresses in steel	Not considered to be a significant factor as the stresses in the steel are not transmitted through to the paint film.
Salt spray tests	Not relevant to a ballast tank.
Oven drying as sole part of ageing protocol	Does not remove water soluble materials from the coating films.
Flat panel tests	Does not provide the required geometry to produce out of plane stresses.
Hydrostatic pressure	Not considered important but is also an area where little information exists.

CHAPTER 3
METHODOLOGY

3.1 Introduction

Having examined the literature including existing test protocols/methods, identified and prioritised factors as part of the knowledge gathering phase, now it is suitable to continue by explaining the design, development and choice of coating formulations, test specimen design and coating process.

3.2 Design of Epoxy Formulations

As stated previously, the protection of WBTs in merchant ships is now mandatory and typically achieved by the application of epoxy coating formulation(s). The preference for the application of epoxy formulations stems from the unique properties offered which include excellent barrier protection, chemical and corrosion resistance as well as being compatible with the substrate and primers containing zinc.

For marine applications, epoxy-coating formulations for ambient temperature cure are typically formulated as two-component systems with each component containing a binder type (i.e. “part A” and “part B”).

Part A is typically composed of the following basic constituents: the epoxy resins, additives such as pigments, diluents (either reactive or non-reactive), defoamer, thixotrope, wetting agents and solvents, which are mainly added to reduce viscosity during manufacturing, handling and application.

Part B often just contains amine curing agent and solvent but may contain pigments.

The combination of part A and part B in specified mix ratios makes up the coating formulation system for application. The simplest formulations may combine a single epoxy resin with the curing agent, more-complex ones will

include multiple epoxy resins, modifiers and curing agents to develop the desired properties.

As earlier stated, epoxy paints have a great number of different compositions. They have in common a basic composition of binder, pigment and solvent or diluent. They are applied as a liquid and on drying convert to solid.

Furthermore, the importance of every constituent of an epoxy-based formulation cannot be overemphasised as binders, pigments, solvents and additives (such as defoamers, thixotropes, wetting agents) all have a significant role to perform. In the solvent containing epoxy based formulation, the solvent constituent not only plays a key role during manufacture but also during film formation and drying. In contrast to the solvent containing formulations, solvent free epoxy formulations are developed without such solvents but for similar application properties to offer the same performance.

Therefore, this study has attempted to compare and contrast solvent containing based epoxy systems with their solvent free counterparts. The actual formulations for the part A and part B employed in this research project are outlined in Table 7 below.
The four types of part A paints, which are typical representative models of WBT epoxy anti-corrosive formulations, are:

- solvent containing pure epoxy (SPE)
- solvent free pure epoxy (SFPE),
- solvent containing modified epoxy (SME)
- solvent free modified epoxy (SFME)

They have in common similar type of constituents such as epoxy resins and pigments/extenders combination. Additional information from the data sheets on the four formulations is detailed in appendix II.

Furthermore, there are three part B types listed below:

- ❖ Ancamine 2519 ® - modified cycloaliphatic amine adduct with benzyl alcohol
- ❖ Ancamine 2712M ® – mixed aliphatic - cycloaliphatic amine no benzyl alcohol 100% solids
- ❖ Cardolite NX-4709E ® - phenalkamine

Air Products & Chemicals, Inc. produced and supplied the first two types of part B (curing agents) above while AkzoNobel supplied the last one. Additional information on the three curing agents is on data sheets shown in appendix III.

Table 7 below shows the constituents of the formulations for SPE, SFPE, SME and SFME accompanied with variants of curing agent.

The coating properties adjusted in each formulation included % solids by volume, % solids by weight, stoichiometry, pigment volume concentration (PVC) and mix ratio by weight. The obtained values were adjusted using Interform (AkzoNobel's in-house formulation software) to meet application viscosity particularly for airless spray without further dilution. Each coating corresponding to each paper formulation was subsequently manufactured at AkzoNobel.

Table 7 Constituents in the four formulations

Constituents	**Pure epoxy**		**Modified epoxy**	
Part A	**Solvent containing (SPE)**	**Solvent free (SFPE)**	**Solvent containing (SME)**	**Solvent free (SFME)**
Epoxy resin	bisphenol A	bisphenol F	bisphenol A	bisphenol F
Reactive Diluent	None	Yes	None	None

Constituents	**Pure epoxy**		**Modified epoxy**	
Part A	**Solvent containing (SPE)**	**Solvent free (SFPE)**	**Solvent containing (SME)**	**Solvent free (SFME)**
Non-reactive diluent	None	None	Solid hydrocarbon resin	Liquid hydrocarbon resin
Pigments	Yes	Yes	Yes	Yes
Fillers	Yes	Yes	Yes	Yes
Thixotrope	Yes	Yes	Yes	Yes
Wetting agent	Yes	Yes	Yes	Yes
Solvents	Xylene/butanol (3:1 ratio by volume)	None	Xylene/butanol (3:1 ratio by volume)	None
% solids by volume	71	98	65	99
% solids by weight	83	98	79	99
Pigment Volume Concentration (PVC)	28	11	26	9
Stoichiometry (epoxy:amine)	1:0.90	1:0.85	1:0.70	1:0.80

Constituents	**Pure epoxy**		**Modified epoxy**	
Part A	**Solvent containing (SPE)**	**Solvent free (SFPE)**	**Solvent containing (SME)**	**Solvent free (SFME)**
Mix ratio by weight	7.11:1	3.87:1	4.83:1	5.19:1
Volatile Organic Content (VOC) grams/litre (g/L)	264	23	297	6
Part B	**Curing agents**			
	SPE	**SFPE**	**SME**	**SFME**
Ancamine 2519 ®	Yes			
Ancamine 2712M ®		Yes		Yes
Cardolite NX-4709E ®			Yes	

3.2.1 Choice of constituents in formulations

3.2.1.1 Epoxy resins

As shown in Table 7, the solvent free formulations (SFPE & SFME) had higher volume solids, which is approximately 100% when compared to the solvent containing formulations (SPE & SME) at 71% and 65% respectively. SFPE & SFME contained liquid bisphenol F epoxy while SPE & SME had liquid bisphenol A epoxy. Early versions of the four model formulations were based on low molecular weight liquid bisphenol

A epoxy resin. However, during handling and subsequent demonstration (demo) spray application using airless spray, it was observed that the choice of the liquid bisphenol A epoxy resin was much more suitable for the solvent containing formulations. The solvent frees containing the bisphenol A epoxy resin had much higher viscosity and shorter pot life that resulted in application challenges during airless spraying. Other challenges include decreased transfer efficiency, poor surface appearance from reduced flow and levelling. Hence, in order to mitigate these challenges regarding resin choice, the SFPE & SFME formulations were reformulated by replacing the low molecular weight liquid bisphenol A epoxy resin (which had an equivalent epoxy weight (EEW) of 188) with a lower molecular weight liquid bisphenol F epoxy resin having EEW of 169. The viscosity of liquid bisphenol A epoxy resin at 25 °C was 12,500 cP while that of liquid bisphenol F epoxy resin was 4,500 cP.

3.2.1.2 Extenders pigments and colouring pigments

The extender pigments and colouring pigments used in formulating were in the form of powders. For most formulations including those for this research project, they are mostly the second largest volumetric component of the paint film after the binder volume. Extender pigments such as mica and barytes are inert and are used to enhance properties such as anticorrosive performance. Colouring pigments such as titanium dioxide are also inert but these are added for colour purpose. These properties were considered in the selection of pigments/extenders and fillers for the epoxy base formulations. Titanium dioxide was included to provide colour while talc, mica and barytes (inert extenders) were included to make up the required pigment volume. The PVCs are 27.88%, 26.21%, 10.65% and 8.96% for SPE, SME, SFPE and SFME respectively.

3.2.1.3 Diluents

In formulating solvent free coating systems for marine application such as merchant ships, one of the routes used in reducing the paint's

viscosity to that suitable for spray application is the inclusion of diluent(s) into the formulation. Diluents have a much lower viscosity than the epoxy resins in the formulation, thus, they aid application particularly in solvent free formulations. The incorporated diluent could be either reactive or non-reactive.

(a) Reactive diluent

Reactive diluents contain functional groups and can react into the formulation. Diluents can be mono-functional or multifunctional, depending on how many reactive groups they contain. However, the focus will be on a mono-functional diluent as it was the type incorporated into the SFPE formulation. Reactive diluents are made by reacting alcohol (or acid) with epichlorohydrin. Commonly used mono-functional types include cresyl glycidyl ether and Epodil 748, a C_{12} – C_{14} glycidyl ether as illustrated in Figure 16. As an epoxy functional diluent, Epodil 748 reacts with the amine-curing agent and forms part of the network. Epodil 748 was used for adjusting the SFPE formulation (with a very high solids by volume) to meet the targeted application viscosity for the airless spray pump. The viscosity of the Epodil 748 at 25 °C was 12 cP. The functionality of Epodil 748 is approximately 1. The other formulations (SPE, SME and SFME) do not contain the reactive diluent - Epodil 748.

C_{12-14} Glycidyl Ether
R = $C_{12}H_{25}$ to $C_{14}H_{29}$

Figure 16 C12-14 Glycidyl ether [41]

(b) Non-reactive diluents

Other constituents used in the manufacture of some formulations are the non-reactive diluents. Unlike the reactive diluents, the non-reactive diluents do not react into the film rather they sit between molecular chains. The modified epoxy formulations (SME & SFME) contained non-reactive diluents. The non-reactive diluents were hydrocarbon resins, which are derived from crude oil. The physical state of the hydrocarbon resins varies from liquid to high Tg solid. Solid hydrocarbon in the form of capsules was incorporated into the SME while that used in the SFME was liquid. Softening point for the solid hydrocarbon resins range from 90–140 ^{0}C.

3.2.1.4 Thixotropes

Thixotropes play a key role in coating formulations by aiding film formation and structure build through conferring anti-sagging and anti-slumping properties once the film has been applied. They are mostly supplied in powder form. They could be classed as inorganic and organic. Examples of the inorganic thixotropes include bentone clays, organoclays, and synthetic silicas. Examples of common organic types are castor oil derivatives and polyamides. Many require some dispersion and activation at high process temperature and careful formulation procedure(s) are necessary to avoid seeding “false body” or loss of thickening efficiency.

Polyamide wax thixotropes (Crayvallac MT and Disparlon 6650) were used for formulating. They both required temperatures up to 55 °C or more for activation to occur. A possible hold period of 15–30 min was required during activation. Crayvallac MT was incorporated into the solvent free formulations (SFPE and SFME) while Disparlon 6650 was used in the solvent containing formulations (SPE and SME).

3.2.1.5 Solvents

Solvents such as xylene and butanol, which are in liquid form also, play this role of lowering viscosity when incorporated at manufacturing. Following this principle in formulating, SME and SPE were balanced with a mixture of xylene and butanol in a ratio 3:1 by volume at VOC levels under 300 g/L to 65% and 71% solids by volume respectively while the SFPE and SFME do not contain any mixture of xylene/butanol.

3.2.1.6 Curing agents

While there are three basic types of epoxy resins (Bis A, Bis F and epoxy phenolic novolacs), there is a vast range of curing agents for formulators to choose from. Similar to the base epoxy resin, amine-curing agents have different structures, rate of cure, functionalities and viscosities. The basic reason for choosing or creating an amine-curing agent for an epoxy formulation hinges on: cost, required performance and processing equipment without sacrificing compatibility. As mentioned previously, the three curing agents used are as follows:

- Ancamine 2519 ® (Modified cycloaliphatic amine adducted with benzyl alcohol)
- Ancamine 2712M ® (Mixed aliphatic - cycloaliphatic amine no benzyl alcohol 100% solids)
- Cardolite NX-4709E ® (Phenalkamine)

3.2.2 Manufacture of coating formulations

3.2.2.1 High speed disperser

After generating paper formulations using the Interform software, the constituents for SPE, SME, SFPE and SFME were ordered and used in manufacturing the respective coating formulation. At the manufacturing stage, a typical laboratory high-speed disperser (HSD) as shown in Figure 17 was used to mechanically perform the manufacture of the four epoxy based coating formulations. It consists of a circular disc with vane

teeth affixed to a shaft, held vertically centred in an upright position and rotated at high speed. Blade tip speed ranged to 24 ms^{-1}.

The shaft of the HSD was lifted and a suitable size container was placed at the HSD base. Then the shaft was lowered to the specified position enabling the respective constituents to be loaded into the container. The respective formulation constituents such as epoxy resins, pigments, fillers and additives were scale weighed and loaded into the pail at specified intervals. With pigments, those with the hardest were added first and followed by others. The agglomerated pigment particles (in powder form) were reduced in size and dispersed or mixed into the epoxy resin (which wetted the pigment particles) using the HSD. Using HSD, the pigments/extenders and fillers were dispersed into the epoxy binder to particle size of approximately 50 µm, which was the target fineness of grind. The process involves mechanically breaking the agglomerated particles apart, wetting their surfaces, and creating a different surface such that they do not reaggreagate [27].

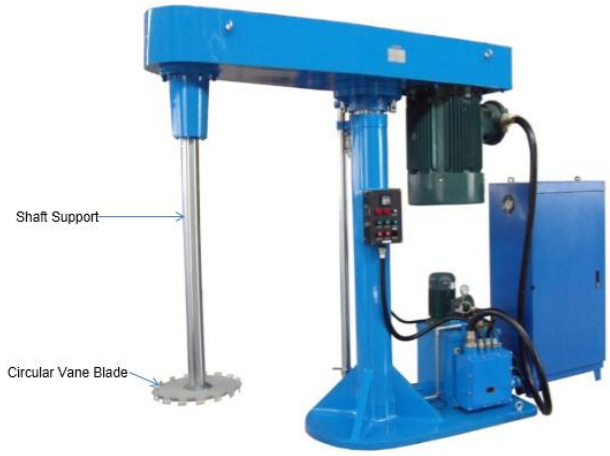

Figure 17 High speed disperser [82]

The HSD operates by a “shearing” principle [83], which occurs below the circular vane teeth blade as fresh layers are forced down by the vortex as with outward movement to the top of the vortex shown in Figure 18.

Thus, nearest the blade the high shear disperses the agglomerates as well as inducing the self-attrition mechanism, whilst the lower viscosity away from the blade ensures the mobility of the material necessary to continuously reintroduce mill-base into the dispersing region [27].

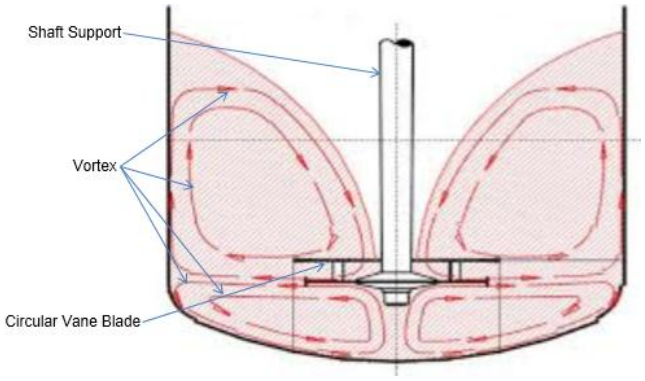

Figure 18 Vortex movement above and below circular vane blade [84]

After completing the manufacture of SPE, SFPE, SME & SFME, they were filtered through a 250 µm mesh screen. Next, they were poured into 5 L pails and stowed in flammable storage cabinet prior to mixing and application. Thus, allowing the manufactured formulations to stand for some time before application.

Several other preliminary tests including viscosity check, Beck Koller (BK) drying time and hold up were conducted before each formulation was scaled up to 20 L. Hold up was checked using a sag index bar and later after airless spray application.

3.3 Design of Test Specimen

To gain insight into the performance of the WBT coating formulations under defined laboratory conditions, two types of test specimens - T specimen(s) and free film specimen(s) - were designed and created. The T specimens were T sectional steel substrates with adherent film applied on them. Unlike the T specimens with adherent films on steel substrate only, the free film specimens were created from two substrate types: adhered substrates and release

substrates. The adhered substrates were T sectional steel substrates while the release substrates were polytetrafluoroethylene (PTFE) tape on glass panels. Thus, regarding the creation of the free films from the type of substrate utilised for applying the film, there were two variant of free film specimens. One variant of the free films known here as 'non-self-supporting free film specimens' were created from the adherent film of T sectional steel substrates that had been cured at ambient temperature and subsequently subjected to fatigue testing. Whereas the other variant of free film specimens known here as 'self-supporting free film specimens' were created from films applied on PTFE panels which had been cured at ambient temperature only.

3.3.1 T specimens

Literature survey and industry experience indicate that cracking failure of WBT epoxy based coating occurs locally at corners even when the coating film on the other WBT areas such as the flat surfaces are intact (as shown in Figure 19).

Figure 19 Pictorial view of coating failure at corners of WBT in-service

In addition, as WBTs are complex structures with extensive amount of welding and connections, a T sectional substrate (i.e. a welded intersection of a web plate and flange plate as shown in Figure 20 & 21) from mild (normal) steel was considered a suitable test specimen to investigate the effect and influence of geometry as well as surface preparation.

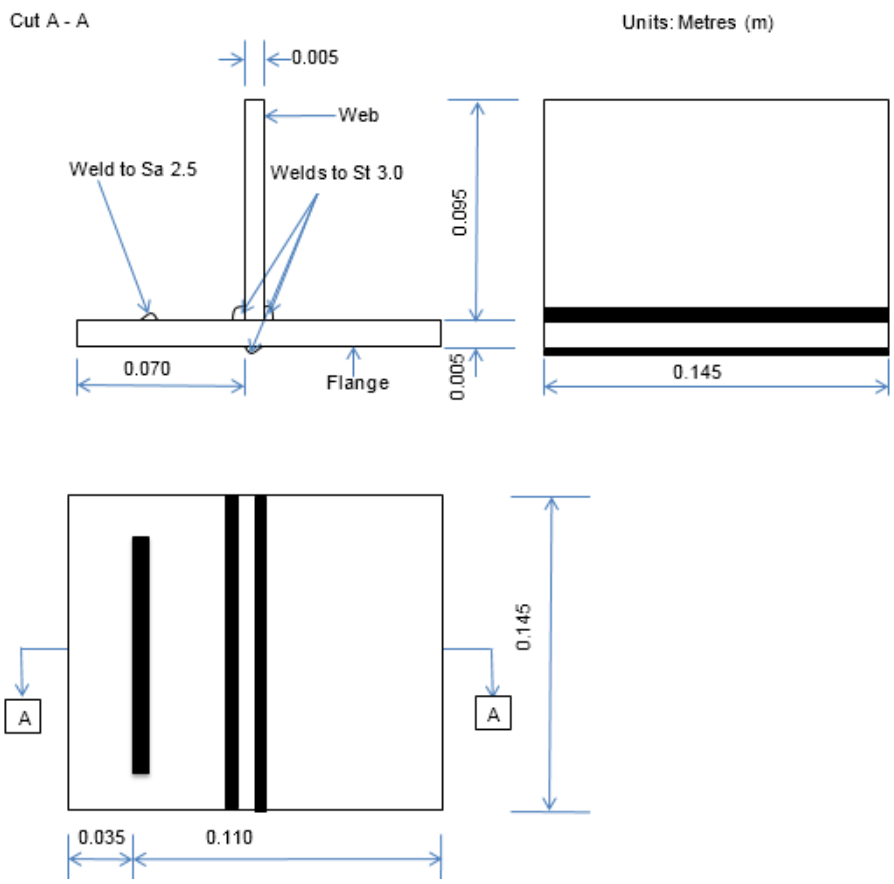

Figure 20 Drawing of T sectional substrate in multi-view: 1st angle projection

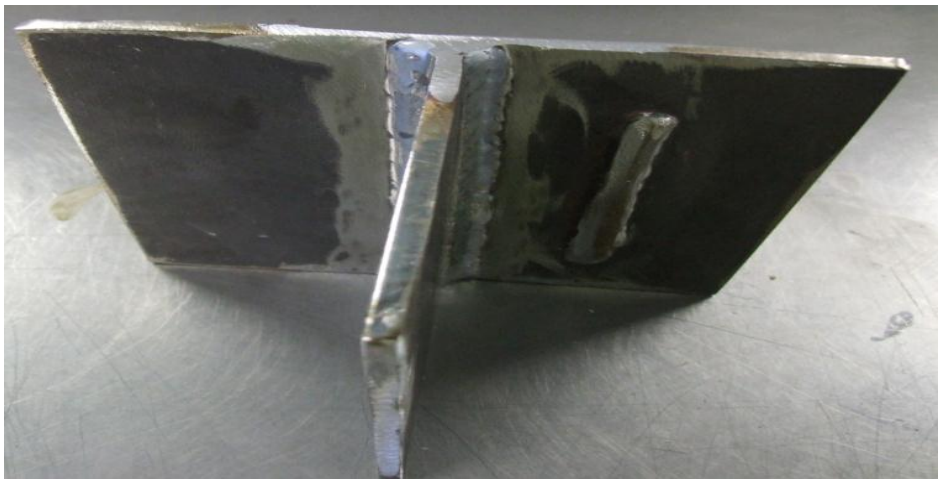

Figure 21 Pictorial view of the "as received" bare T sectional substrate

A T sectional substrate made from mild steel had typical tensile material properties as shown in Table 8.

Table 8 Typical tensile mechanical property of the mild steel [50]

Material Property	Mild Steel
Yield Stress, σ_y (0.2)	378 MPa
Young's modulus, E	208.1 GPa
Poisson's ratio, ν	0.3

Furthermore, a T sectional substrate comprised of a flange plate with a web plate that are shop welded together as shown in Figure 21. As shown in Table 9, the dimensions (length (L), width (W) and depth (D)): L x W x D of the T specimen flange plate are (0.145 m x 0.145 m x 0.005 m) and the web plate dimensions are (0.145 m x 0.005 m x 0.095 m).

Table 9 Sectional dimensions of T specimen

Sectional Dimension				
Sectional Index	Depth of Section (m)	Width of Section (m)	Thickness	
			Flange (m)	Web (m)
T 0.145 x 0.145	0.145	0.1	0.005	0.005

These dimensions have been chosen based on the amount of test specimens that the laboratory test rig (oven and tank) can accommodate (i.e. available room) and to have a reasonable number of representative sample spaces for evaluation.

T specimens were created by taking the T sectional steel substrates through the coating process as explained in section 3.4. A set of twenty-four (24) T

specimens were utilised for the first run of the fatigue test and a reanalysis was achieved using another set of 24 T specimens. Thus, forty-eight (48) T specimens in total were utilised in the laboratory test rig for the fatigue testing as described in section 4.1.

3.3.2 Free film specimens

3.3.2.1 Non-self-supporting free film specimens from T specimens

One variant of free film specimens created is the 'non-self-supporting free film specimens'. The non-self-supporting free film specimens (mostly in flakes) were created from the adherent films on T specimens; which had been subjected to the fatigue test based on hygrothermal cycling. Hammering and chiselling process was used to detach or remove the flakes of free films (which were mostly in the form of irregular shaped quadrilateral with irregular cross sections) from the T specimens.

3.3.2.2 Self-supporting Free Film Specimens released from Polytetrafluoroethylene panels

152.4 X 101.6 mm glass panels covered with polytetrafluoroethylene (PTFE) tape were utilised to create the other variant of free films referred here as 'self-supporting free film specimens'. Following the coating process described in section 3.4, the ambient temperature cured free films were peeled off (detached) from the PTFE tape surface. Appropriate shaped specimens were cut out from the peel of self-supporting free films for thermal analysis (DSC, DMA and TMA) and mechanical analysis (uniaxial tensile analyser) as discussed in section 4.2 and section 4.3. Specimens for thermal analysis and mechanical analysis were cut out of the spray applied films cured at ambient temperature after two days of cure. A pair of tweezers, a razor blade, a slide rule and a knife were used to cut out specimens utilised for thermal analysis. While specimens utilised for mechanical analysis were cut using a punch mould.

3.4 Coating Process

Worthy of special mention here is the fabrication of ships such as tankers. Tankers are a collection of near-identical welded tanks, possessing a pumping and pipeline systems, with an engine generating power to turn a propeller and deflect water across a rudder at the rear, and a flared bulbous bow forward that assists progress through the water [85]. If shipbuilding is reviewed, the stages can be listed as follows:

- plate treatment
- plate cutting
- panel production
- preassembly production
- sub-section assembly and painting
- block assembly and painting
- block erection and painting
- outfit quay and painting

One of the crucial stages of this build process is the coating process [86 - 88]. The coating process represents all activities that involve taking the bare steel through to a coated object ready to be gainfully employed in service. However, block coating has been identified as a bottleneck in the fabrication process and consequently is a critical time constraint on overall production [86, 87].

For WBT, the sequence of the coating process can be loosely visualised or represented as shown in Figure 22.

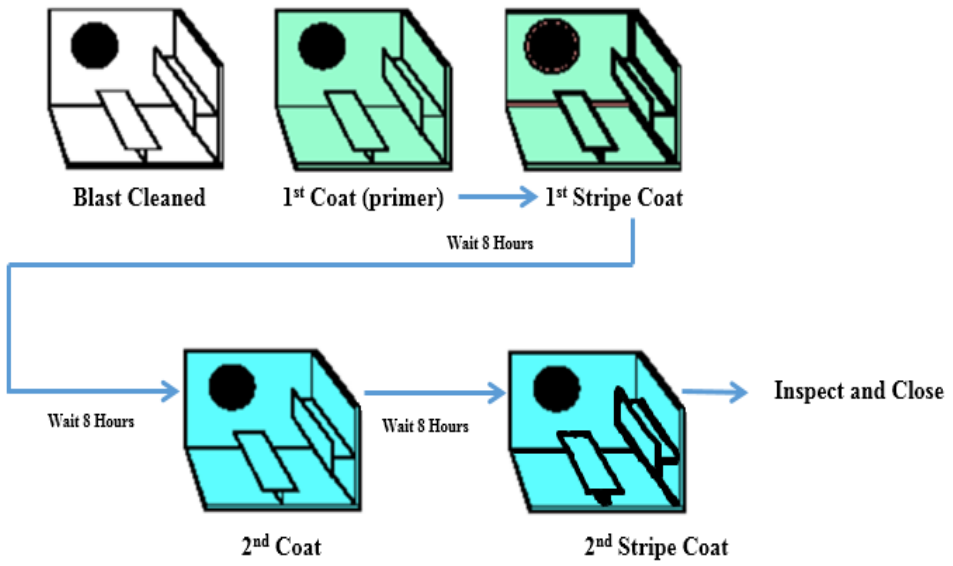

Figure 22 Coating application sequence for WBT

Thus, if an epoxy formulation is considered as the protective coating, then the first coat is applied to a specific dry film thickness using airless spray. After the first coat has satisfactorily cured, the tank is inspected and uncoated spots coated (touch up). However, for structural critical areas within the tank where it is extremely difficult to achieve appropriate film thickness, stripe coats are applied with brush or roller as illustrated in Figure 23. Typical critical areas for stripe coating in WBTs are:

- backs of stiffeners
- welds
- ladders and hand rails
- areas of difficult access (corners)
- cut outs i.e. scallops

Figure 23 Typical critical areas striped coated in a WBT

After the application of the stripe coats and inspection carried out, the second coat, which is usually a different colour from the first coat, is applied using airless spray. After the second coat is satisfactorily cured, the second stripe coat is applied. Lastly, measurements of dry film thickness are taken when the coating film is sufficiently cured at ambient temperature.

3.4.1 Surface preparation

One of the most important procedures of the coating process considered during new building of ships is quality surface preparation as a high number of coating failures could be attributed to inappropriate surface cleaning and preparation [8]. Quality surface preparation is also strongly recommended during repair and maintenance prior to coating application. There are several types of surface preparation techniques as outlined below:

- Hand chipping
- Power tooling cleaning, needle-gun, chipping gun, rotary grinders, wire and brushes

- Water-jetting
- Ultra-high-pressure water jetting
- Slurry blasting
- Water-jetting with grit injection
- Ultra-high-pressure water-jetting with grit injection
- Dry ice blasting
- Sodium-bicarbonate (Baking Soda) blasting
- Blast cleaning
- Magnesium de-scaling
- Sponge-jet blasting

IACS [8] extensively described each method of surface preparation. Amongst the methods listed above, blast cleaning was confirmed as the workhorse for corrosion prevention systems. Other attributes of blast cleaning presented include most cost effective method, service life expectancy in excess of 10 years. However, appropriate choice of blasting type specific to case should be considered.

For surface cleaning after erection, there are two common types of cleaning specified by IMO PSPC for WBT: blast cleaning where practicable or power tooling. It recommends preparation in critical areas by thorough blasting to Swedish standard Sa 2.5 or power tooling to St 3.0 but typically by power tooling.

- Sa 2.5 Very thorough blast cleaning: "*When viewed without magnification, the surface shall be free from visible oil, grease and dirt and shall be free from mill-scale, rust, paint coatings and foreign matter. Any remaining traces of contamination shall show only slight stains in the form of spots or stripes*".

- St 3.0 Power tool cleaning: "*It is a mechanical technique of surface preparation involving equipment such as abrasive grinding wheels, power sanders, power chipping hammer. It removes adherent mill scale, rust, all visible coatings and contaminants to bare metal substrate*".

In line with industry practice, the sequences of surface preparation for the pre-primed T substrate specimen are discussed further below.

3.4.1.1 Solvent cleaning

As a preliminary step before abrasive blasting, the as received bare T sectional substrates were degreased using Acetone solvent and a hand brush to clean and remove surface contaminants such as grease, oil or dirt. A contaminant is described as any substance that prevents a coating film from adhering to the steel substrate. The degreased bare T sectional substrates were stowed in a pail containing silica gel prior to abrasive blasting. Similarly, the 152.4 X 101.6 mm glass panels covered with PTFE were cleaned using Acetone solvent and a rag. They were also stowed away in pails having silica gel awaiting spray application.

3.4.1.2 Abrasive blasting

After solvent cleaning or degreasing the bare T sectional substrates and PTFE panels, only the bare T sectional substrates required abrasively blasting. Abrasive blasting was carried out using wheelabrator ventus blaster, shown in Figure 24.

Figure 24 Wheelabrator blaster

Abrasive blasting is essential for the adhesion of the coating to its substrate. The process creates roughened surface and helps remove any contaminants left on the surfaces of the substrate. There are two types of abrasive blasting: shot blasting and grit blasting. The essence of abrasive blast is to ensure the substrate surface has the required roughness to facilitate proper adhesion of the coating. Following industry practice specified by IMO PSPC, the surfaces of the T sectional substrate were grit blasted to Sa 2.5 using the wheelabrator blaster. Subsequently, the peaks and troughs of the blast profile created on the surfaces of the T sectional substrates were visually evaluated using a comparator gauge shown in Figure 25 to ensure that the blast profile was within the specified IMO PSPC 30-75 µm.

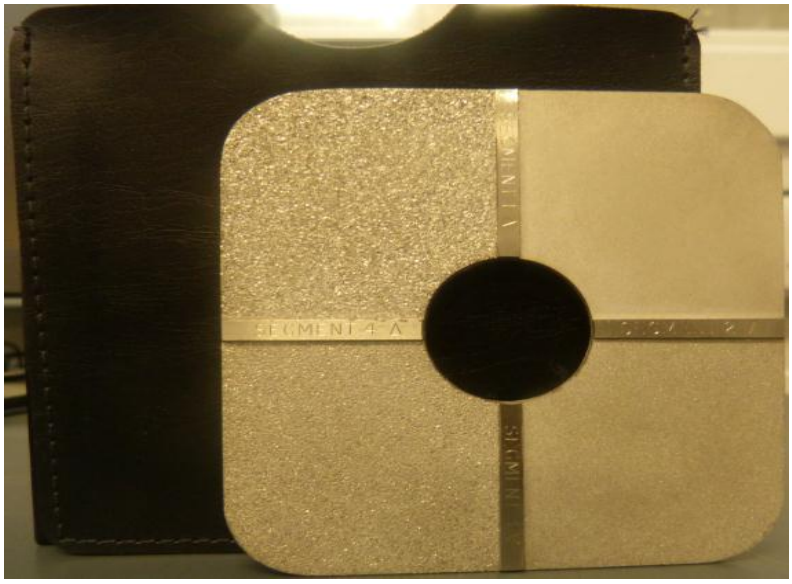

Figure 25 Comparator gauge

3.4.1.3 Power tooling

As reported earlier in the literature survey, for ships in service, cracking failures of WBT coatings are found to initiate on coated welds of steel substrates especially at corners (critical areas) that are normally cleaned by power tooling, spray applied and stripe coat included. This cleaning leaves a smooth profile surface, which could lead to inferior adhesion

after coating application at these critical areas. In addition, it is highly likely that including stripe coating will lead to higher film build at such corners than on the flat surfaces of the WBTs. A power tool with an attached disk is normally used to grind around welded corners in shipyards at new building especially for block surfaces prior to coating application.

To simulate and understand the effect of surface preparation and high film build on welds, it was proposed and agreed that a T sectional substrate had four welds. Two at both sides of the web and flange plate intersection, the next on the topside surface of the flange running directly above the web and the remaining weld at the underside surface of the flange – 0.035 m (i.e. 35 mm) away from the web. The surfaces of all the T sectional substrate including their welds at the underside of the flange (specifically that 0.035 m away from the web) were surface prepared by grit blasting to Sa 2.5, leaving a coarse adhesion surface for coating. While the welds at the intersection corners and the topside surface of the flange were prepared (or cleaned) by power tooling to St 3.0, leaving a smooth adhesion surface for coating. This is shown in Figure 26.

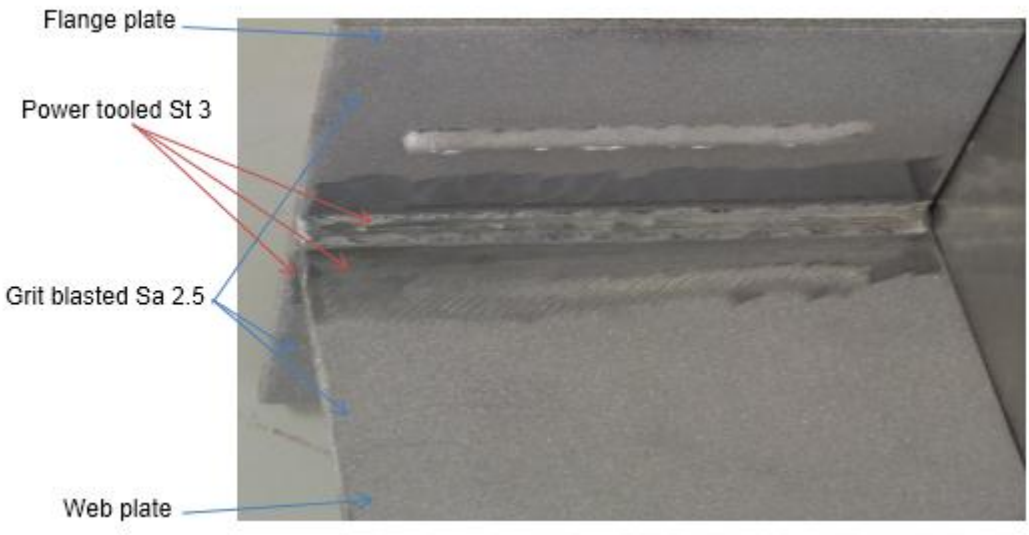

Figure 26 Areas of T sectional substrate with Sa 2.5 and St 3 surface preparations

3.4.2 Coating application

An adequate film thickness is also essential for anti-corrosive coatings such as epoxy-based formulation to perform and offer the desired protection to the substrate. Under thickness of the applied coating will lead to widespread spot rusting.

3.4.2.1 Wet film thickness:

As shown in Table 10, the wet film thicknesses (WFTs) of the paints were calculated and converted to the targeted dry film thickness (DFT) prior to coating application. This acted as a guide to the quantity of WFT required during application to reach the specified DFTs of 640 µm and 960 µm. The relationship between WFT and DFT is expressed in eq 1 as follows:

$$\textbf{\textit{WFT}} = DFT / (\%\ solids\ by\ volume) \qquad \textbf{(1)}$$

Table 10 Calculated WFTs for the four coating formulations

Targeted dry film thickness (µm)	**WFT of WBT coating formulations (µm)**			
	SPE	**SFPE**	**SME**	**SFME**
640 (i.e. 2 x 320)	640/0.707 = 905	640/0.978 = 654	640/0.652 = 982µm	640/0.994 = 644
960 (i.e. 3 X 320)	960/0.707 = 1358	960/0.978 = 982	960/0.652 = 1472	960/0.994 = 966

During the coating application, the actual value for the WFT on the surface(s) of the T specimen and PTFE panels were obtained using a hexagonal notch type gauge immediately after the coating had been applied. This type of gauge (also called “comb gauge”) comprises of two ends that are on the same plane and progressively deeper notched

steps in between both ends. As shown in Figure 27, each step is labelled by numbers representing the distance in mils or microns between the steps and the plane created by the two ends.

Figure 27 Wet film thickness gauge

The gauge was firmly pressed (in a perpendicular direction) into the wet film of the T specimen and later withdrawn. This was also the case for the spray applied PTFE panels. The wet film thickness was considered as that between the last wetted step and the next adjacent higher one, which was dry. Several measurements were taken over an area. In addition, the WFT gauge was cleaned using a rag after every measurement. The values of the WFT were unrecorded but served as an indication for quality control during paint application.

3.4.2.2 Methods of coating application:

As both industry experience and literature survey confirmed that cracking failure of coatings occurs particularly at welded corners which were power tooled with higher dry film thicknesses than ideal, six (6) T specimens were considered as a representative group for each of the four coating formulations. As an example using the SPE formulation, 6 T specimens were spray applied with SPE formulation. Three (3) of the six (6) T specimens represented the 640 µm (had twice the recommended standard 320 µm DFT) while the remaining three (3) represented the 960 µm (had thrice the recommended standard 320 µm DFT) dry film

thickness. The same approach regarding number of representative specimens and specified film thicknesses was utilised for other formulations: SFPE, SME and SFME. Furthermore, the same approach was utilised in applying the respective WBT coating formulations on the PTFE panels.

In accordance with IMO PSPC section 4.4 Table 1: 1.4 - 1.5 on application shown in Table11, the liquid coating was applied in two spray coats and two stripe coats to better attain the targeted value of the specified film thickness for the T specimens. The sequence of application was:

- spray apply 1st coat
- brush apply 1st stripe coat to welds
- spray apply 2nd coat
- brush apply 2nd stripe coat to welds

Table 11 Extract from table 1 of the PSPC on coating application process in WBT [14]

.4	Job specification	There shall be a minimum of two stripe coats and two spray coats, except that the second stripe coat, by way of welded seams only, may be reduced in scope where it is proven that the NDFT can be met by the coats applied, in order to avoid unnecessary over-thickness. Any reduction in scope of the second stripe coat shall be fully detailed in the CTF. Stripe coats shall be applied by brush or roller. Roller to be used for scallops, ratholes, etc., only. Each main coating layer shall be appropriately cured before application of the next coat, in accordance with coating manufacturer's recommendations. Surface contaminants such as rust, grease, dust, salt, oil, etc., shall be removed prior to painting with proper method according to the paint manufacturer's recommendation. Abrasive inclusions embedded in the coating shall be removed. Job specifications shall include the dry-to-recoat times and walk-on time given by the manufacturer.
.5	NDFT (nominal total dry film thickness)[4]	NDFT 320 µm with 90/10 rule for epoxy-based coatings; other systems to coating manufacturer's specifications.

Similarly, two spray coats were spray applied on the PTFE panels for each of the four formulations. However, as the PTFE panels were flat without welds on, the first and the second strip coating by brush was omitted from their coating process. Generally, airless spray application

was used to apply the coat to the T sectional substrates and PTFE panel substrates in multi-passes. The airless sprayer comprised of a handheld spray gun, spray tip guard, spray tip (as shown in Figure 28), pump, suction system, high-pressure filter and high-pressure fluid hose. Airless spray is a coating application method whereby atomisation (breaking up liquid paint into small droplets) is achieved without using compressed air. The liquid paint is mechanically pumped under high pressure through the spray tip. The flow rate of the paint (the amount of paint applied) is determined by the tip size and pressure. The tip also creates the fan width (pattern). Thus, it is essential to make an appropriate choice of tip for a particular application.

A Graco 621 spray tip was chosen for the spray application. Graco spray tips normally come with three digits. The first digit to the left represents half of the fan width while the last two digits represent the orifice size in thousandths of an inch.

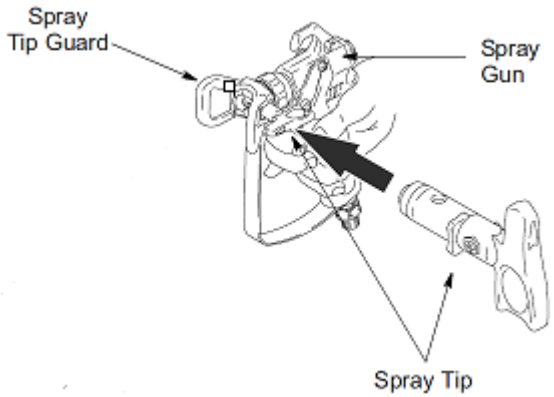

Figure 28 Schematic of an airless sprayer [89]

So using a 621 spray tip resulted in a 304.8 mm fan width and 0.5334 mm orifice. The spray gun was held at an approximate distance of 304.8 mm relative to the substrate surface(s).

The spray application was carried out in an enclosed spray booth at AkzoNobel. Conditions during spray application were recorded daily with average temperature and relative humidity conditions at 19 ^{0}C and 32%

respectively. In addition, brush application was used for stripe coating mainly at welded corners of the T specimens to achieve the targeted film build and follow industry practice. Figure 29 shows a T specimen that has been spray applied and stripe coated at the welded corners.

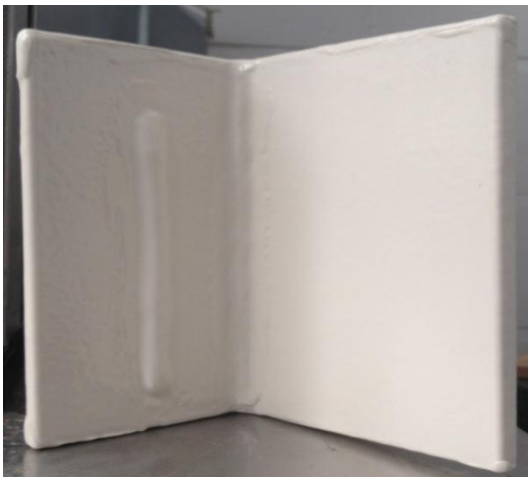

Figure 29 Coated T specimen

3.4.2.3 Dry film thickness:

Following industry practice, the DFT of the coated T specimens were determined after a week of ambient cure, using an Elcometer 496 gauge, which is an electronic gauge with an extension lead as the measuring sensor. The Elcometer 496 gauge was set to zero on a smooth steel substrate and calibrated using appropriate shims placed on the smooth steel substrate (as shown in Figure 30). The DFT readings were taken from several locations on all surfaces of the T specimens including that shown in Figure 31 and then recorded. In addition, at the end of the fatigue test, DFT readings were again taken from several locations on the surfaces of the T specimens. The difference in DFTs were evaluated using a statistical method discussed in section 5.6.

Figure 30 Calibration shims

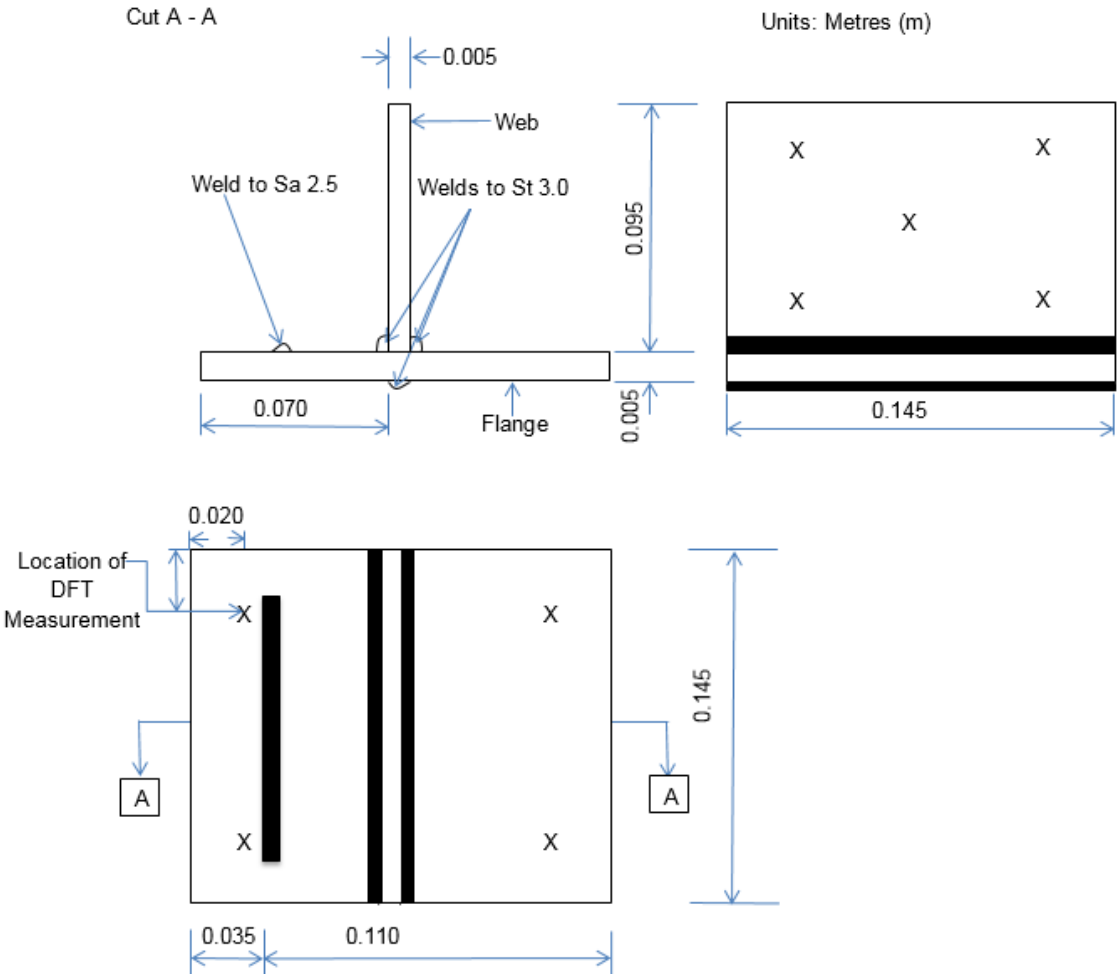

Figure 31 Locations for DFT measurements on T specimen in multi-view: 1st angle projection

In accordance with ASTM E 376 - 96 and practice [90], DFT measurements by the Elcometer gauge were taken 0.020 m (or 20 mm) from the corners and the edges. In addition, the accuracy of DFT measurements obtained using electromagnetic gauges (such as Elcometer gauge) could be influenced by certain parameters including profile of substrate and edge effects. As the Elcometer gauge was calibrated on a smooth surface plate, it implies that the roughened profile on the T substrate surface was unaccounted for. Therefore, as recommended by ISO 19840 [91], a correction value of 25 µm for medium profile was allowed and applied to each DFT reading obtained. To avoid influence from edge effects, measurements were only obtained from 0.020 m from an edge.

3.4.2.4 Edge preparation

After spray application, there is the tendency for the liquid coating to pull back from welded corners and sharp edges resulting in less than the targeted DFT. The primary approach for film build used to compensate for probable thinner layer of coating at these areas is to either stripe coat typically by brush/roller application for corners or by dipping for edge corners. In like manner, the T specimens were dipped and stripe coated to build film thickness at the edges.

3.4.3 Ventilation and curing:

After completing the spray application in the spray booth, the coated T specimens and the coated 152.4 X 101.6 mm glass PTFE panels were moved after coating application to appropriate location(s), which had the required ventilation to allow for proper curing and drying at ambient temperature condition. The process was in accordance with ASTM D 1640 – 03 “Standard test methods for drying, curing, or film formation of organic coatings at room temperature” [92].

3.4.4 Labelling

On curing at ambient temperature, each of the specimens (T sectional substrates with the adherent film and the 'self-supporting free films' detached from the PTFE panels) were labelled with a marker. A label is illustrated on a T specimen in Figure 32.

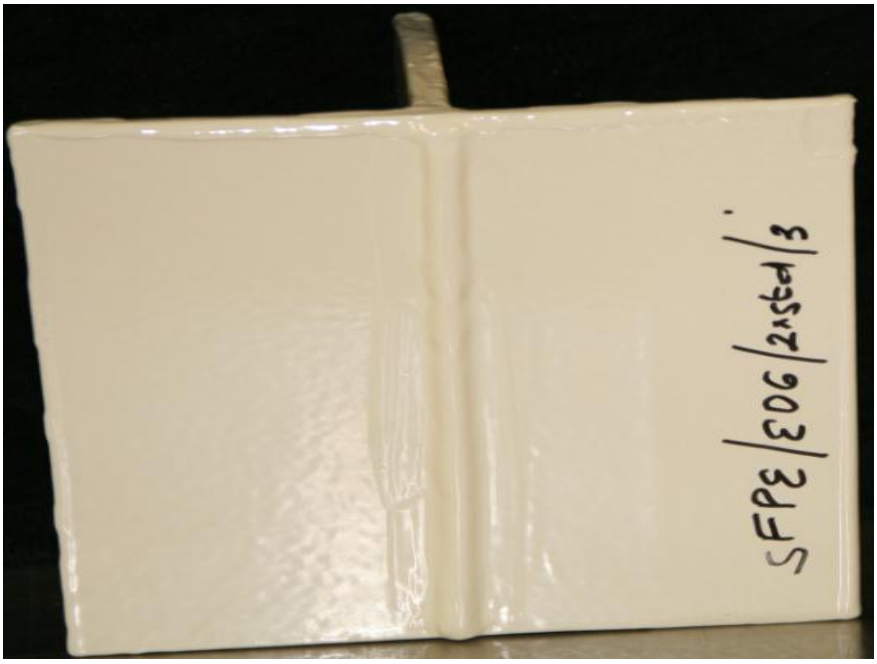

Figure 32 Label on one of the adherent film of the T specimen

CHAPTER 4
EXPERIMENTAL CHARACTERISATION OF COATING FORMULATIONS

4.1 Fatigue Testing of T Specimens

Having previously established in chapters one and two that the exposure of coatings within WBT to hygrothermal cycling (i.e. the combination of hygroscopic cycling (wet/dry conditions brought about by ballasting and de-ballasting) and thermal cycling (hot/cold)) creates fatigue conditions particularly when accompanied with rapid thermal gradient, a fatigue test was considered. The essence of the fatigue test was to investigate the performance of the four WBT formulations regarding their fatigue resistance against cracking failure (at geometric areas such as corners with higher film build than ideal) when exposed to the same defined laboratory conditions.

The term hygrothermal deals with the effects of moisture and heat on materials. It is also related to the interaction and combined effect of moisture and heat between a system and its environment. A system can be viewed as anything: a volume of material, a shipbuilding assembly, and the coated substrate surfaces within dedicated seawater ballast tank (WBT) of a ship. These environmental conditions - moisture and heat - are synonymous with WBT environment and their combined effect on protective coatings in WBT could occur in a cyclic manner in levels significant for consideration especially with the double hull (DH) design.

Simply put, the factors that govern fatigue failure by hygrothermal cycling could be summarised as follows:

- the number of cyclic rates – the higher the number of cycles, the more likely the material is to fail
- the level of stress development - in the case of viscoelastic materials such as coating film, very rapid tensile stress development represents the worst case

- ❖ Cycling above and below Tg of coating film increases tensile stresses in the film
- ❖ thicker films are more likely to develop more stress than thinner films as internal temperature distribution will depend on size and shape
- ❖ the level of defects in the film

Based on this premise with regards to cracking especially in areas related to higher film thickness and specific geometries (corners with welds), the fatigue test established on hygrothermal cycling was designed to characterise the performance of T specimens (i.e. T sectional substrates with adherent films of the four formulations: SPE, SFPE, SME and SFME respectively). The performance of each epoxy formulation with both twice – and – thrice the standard 320 µm DFT on T specimens were evaluated by exposing them to hygrothermal cycling to simulate likely environmental conditions in WBT.

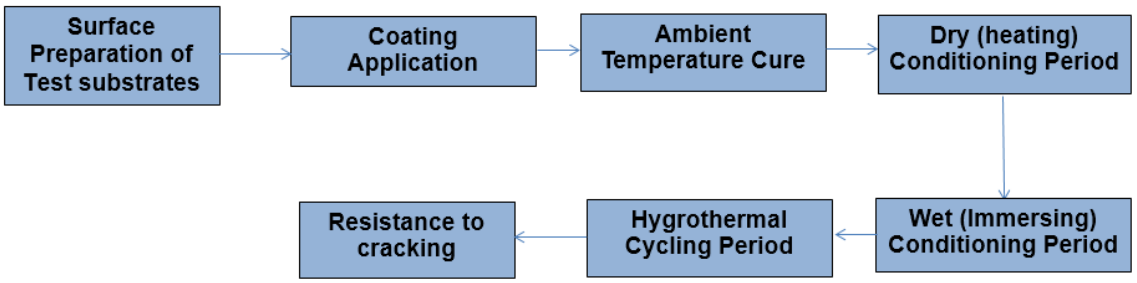

Figure 33 Process flow chart for the fatigue test

The fatigue test consisted of a conditioning period and a cycling period which the T specimens were subjected to. Figure 33 above shows the process flow for the fatigue test. As newly applied coating films cured at ambient temperature can contain retained solvents, residual functional groups and/or both, a conditioning time-period (dry and wet) was included in the fatigue test to drive additional residual reaction and cure in the film. Thus, taking the ambient cured film to a more likely state of total cure. That way retained solvent and other volatile materials would have been driven out of the film.

The main components of the laboratory test rig used to perform the fatigue test were an oven and a tank that contained artificial seawater. The fatigue test

cycled T specimens between the artificial seawater inside a tank and the heat in an oven under defined laboratory set conditions.

The tank (as shown in Figure 34) with dimensions, L x W x D: 0.855 m x 0.500 m x 0.515 m contained artificial seawater with 3.5% salt composition. The ambient temperature of the artificial seawater was 23±3 ^{0}C.

Figure 34 Immersion tank

The oven, as shown in Figure 35, has an internal confined space also known as a chamber within which specimens were exposed only to dry temperature condition using preheated air. The interior dimensions of the Memmert UF160 plus oven, L x W x H are: 0.560 m x 0.400 m x 0.720m. The oven temperature for dry conditioning of the T specimens was set at 50 ºC while the oven temperature for the hygrothermal cycling of the fatigue test was set at 100 ºC following the completion of the conditioning time-period. The oven held a maximum number of specimens, which made up a set during a specific fatigue test. Two sets of T specimens were subjected to the fatigue testing.

In the first instance, a set of twenty-four (24) T specimens were evaluated by the fatigue test. Six (6) T specimens represented each of the formulations. Out of which, three (3) of the 6 representative specimens had twice the recommended standard dry film thickness (i.e. 640 µm) while the remaining had thrice the standard dry film thickness (i.e. 960 µm) spray applied. It was anticipated that such DFTs could give an insight into the effect of higher film thickness. At the end of the fatigue test for set 1, a reanalysis (or repeat)

experiment with another set of 24 T specimens (herein known as set 2) was also performed. Thus, the oven accommodated twenty-four (24) T specimens for set 1 during a fatigue testing as shown in Figure 35.

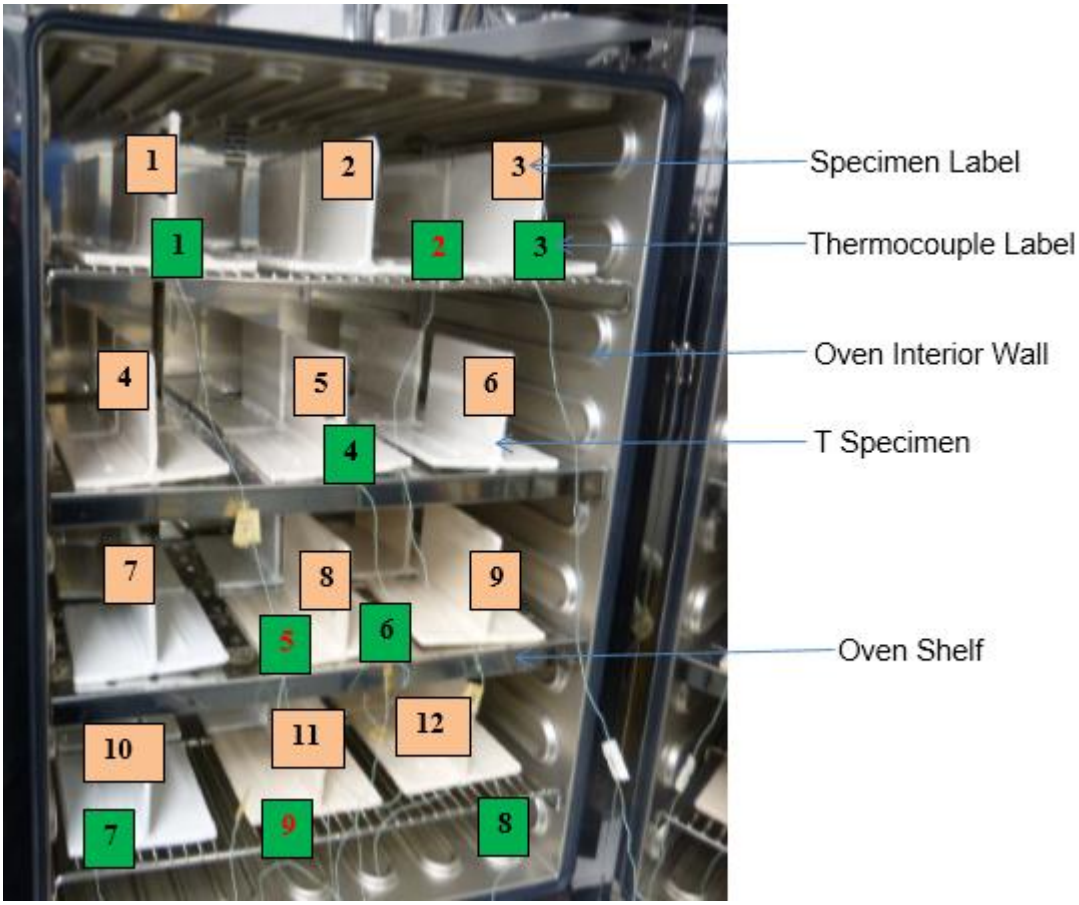

Figure 35 Oven with the coated T specimens

Other components of the laboratory fatigue test rig include: a laptop, thermocouple wires and two loggers (one of the logger (designated as logger1) had eight (8) thermocouple channels while the other (designated as logger 2) had one (1) thermocouple channel as shown in Figure 36 and 37 respectively.

The colour codes used in Figure 35 above for T specimens and thermocouples are defined as follows**:**

- *Orange filled box represents specimens*
- *Green filled box represents thermocouples*

- *Green filled box with black number represents thermocouple monitoring the surface temperature of specimen*
- *Green filled box with red number represents thermocouple monitoring the air temperature of oven*

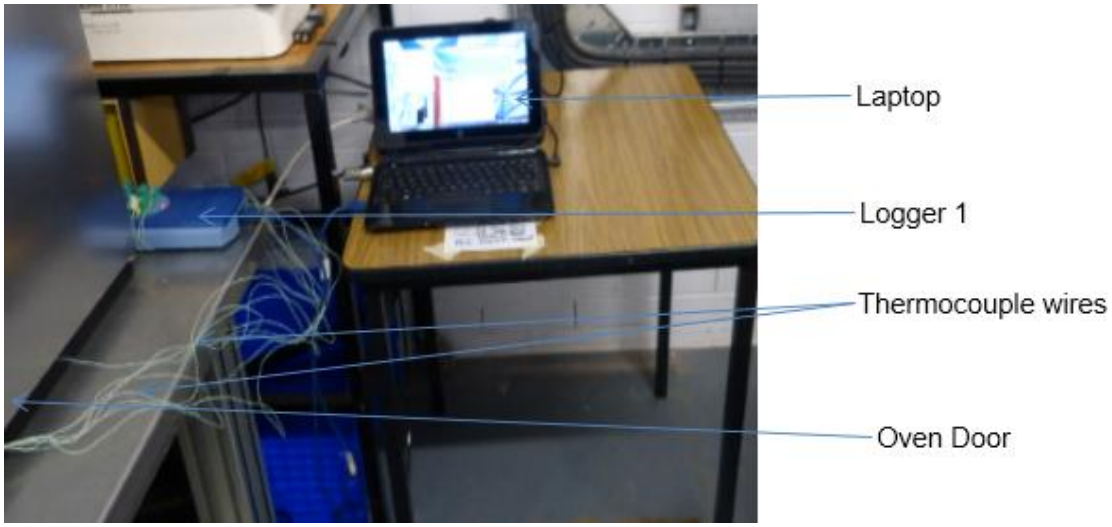

Figure 36 Logger 1 with connected thermocouples and the laptop

Figure 37 Logger 1 & 2 with connected thermocouple(s)

4.1.1 Conditioning of T specimens

4.1.1.1 Dry conditioning

Prior to dry conditioning by heating in an oven, the ambient cured T specimens were visually examined for surface defects such as cracking, crocodiling, aligatoring and checking on the coating film. Subsequently, the T specimens without defects were placed in the oven for one (1) week at a temperature of 50 ^{o}C.

4.1.1.2 Wet conditioning

After 1 week of 50 ^{o}C dry conditioning, the T specimens were removed from the oven and surface(s) visually examined for cracking failure or other surface defects. After inspection, T specimens without crack(s) were immediately transferred to the tank containing artificial sea water for complete immersion at temperature of 23±3 ^{o}C for one (1) week.

Following the end of the conditioning period (dry and wet conditioning), the T specimens were visually inspected again for surface defects before they were exposed to a sequence of hygrothermal cycling between artificial seawater and dry heat as described below. Thus, ensuring that only T specimens showing no crack(s) progressed for hygrothermal cycling from the conditioning period.

4.1.2 Hygrothermal cycling of T specimens

4.1.2.1 Details of the sequence for one cycle of the fatigue test are as follows:

- All T specimens were completely immersed in the artificial seawater (SWI) at 23±3 °C for *2 hr*
- At the end of the immersion period, the T specimens were transferred into the oven at 100±2 °C to be heated for *2 hr*
- At the end of the 2 hr heating, the T specimens are transferred from the oven to the artificial sea water at 23±3 °C to be completely immersed for *2 hr*

- ❖ At the end of this immersion period, the T specimens are then transferred from the artificial seawater back to the oven *at 100±2 °C* for approximately *17.5 hr*

(1 Cycle = 2 hr @ 23±3 °C SWI + 2 hr @ 100±2 °C + 2 hr @ 23±3 °C SWI + 17.5 hr @ 100±2 °C)

4.1.2.2 Transfer period:

- ❖ *Ten (10) minutes was used as a transfer time of the T specimens* between the oven and artificial seawater during each run.

The hygrothermal cycling was repeated following the above sequence and transfer period until failure of coated T specimen(s) was observed. Failure is defined as the numbers of cycles at which crack(s) and/or related surface defect such as checking, crocodiling and aligatoring appears on a T specimen specifically on the coated weld intersection of the underside flange and web plates.

4.1.3 Assessment

The conditioned T specimens were visually inspected for crack failure before and after the conditioning period (dry and wet). Prior to being cycled, T specimens showing no crack(s) after exposure to the conditioning period were progressed for hygrothermal cycling. Similarly, the cycled T specimens were visually inspected for crack failure after the completion of each hygrothermal cycling sequence (i.e. at the end of each artificial seawater immersion sequence or prior to placing them in the oven). The number of cycles to failure was recorded. Cycled T specimens showing no crack(s) after an exposure to this sequence were returned for additional hygrothermal cycling.

4.2 Thermal Analysis of Free Film Specimens

Prior to practical use, another means utilised in characterising, investigating and predicting the likely behaviour of a wide range of materials including coating

films is through the application of thermal analysis. The rationale for using thermal analysis arises from the dominant role that temperature plays as an exposure condition in the use environment for most materials. Therefore, thermal analysis is an important technique used in evaluating a material's response to changes in temperatures.

For coating film(s), thermal analysis is quantitative and can be used to monitor the glass transition temperature (Tg) which can be related to the cross-link density. Thermal analysers commonly used in determining cross-link density from measuring Tg include: differential scanning calorimetry (DSC), dynamic mechanical analysis (DMA) and thermal mechanical analysis (TMA) [93 – 95].

4.2.1 Differential scanning calorimetry (DSC) measurement

Differential scanning calorimetry (DSC) is a frequently used piece of analyser (or equipment) for the thermal characterisation of paint and coating films since the 1970s. DSC analyser evaluates the heat flow effect (i.e. the changes in heat flow to or from the coating specimen) as the temperature of the specimen is ramped up in a very precisely controlled linear rate. Ramp depicts the rate of change in temperature over time. Thus, DSC analyser measures the heat flow into or from a DSC specimen that is cooled, heated or isothermally held when compared to a reference. A DSC specimen is a cramped crucible containing specific amount of a material (for example, coating film) with a known mass while a reference is an empty crucible that is cramped.

Typically, the glass transition temperature (Tg) from a temperature scan of a DSC specimen is commonly measured and assigned in accordance to ASTM E1356, "Standard Test Method for Assignment of the Glass Transition Temperatures by Differential Scanning Calorimetry" [96].

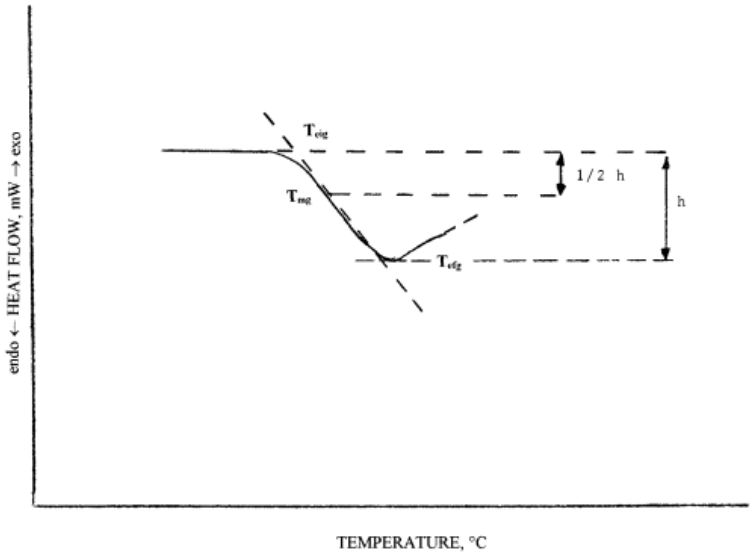

Figure 38 DSC Tg calculation at midpoint of inflection [96]

As illustrated in Figure 38, a critical transformation point of interest in a typical DSC thermogram (which is the output curve derived from a DSC) is the Tg. Although the Tg is a range of temperature rather than a single temperature, it is a widely accepted practice in industry to report a single temperature value which is read from the midpoint of the temperature range based on ASTM E1356 [96]. Also shown in Figure 38 are other points on the DSC thermogram where Tg could be assigned such as the onset temperature and the end temperature. The Tg relates to chain mobility which is different for each coating formulation. The thermal event for determining Tg is endothermic (heat consuming). Therefore, the Tg is observed based on the characteristic inflections on the measured curve resulting from changes in heat flow during the transition.

The DSC 200 F3 Maia was used to perform the temperature scan and determine the Tg of the DSC specimens which are cramped crucibles containing ambient temperature cured films from the formulations: SPE, SFPE, SME and SFME respectively. The DSC analyser has a temperature range between -170 °C to 600 °C, heating rates: 0.001 K/min to 100 K/min and cooling rates: 0.001 K/min to 100 K/min (depending on temperature). Figure 39 provides both side and top views of the DSC specimens and reference.

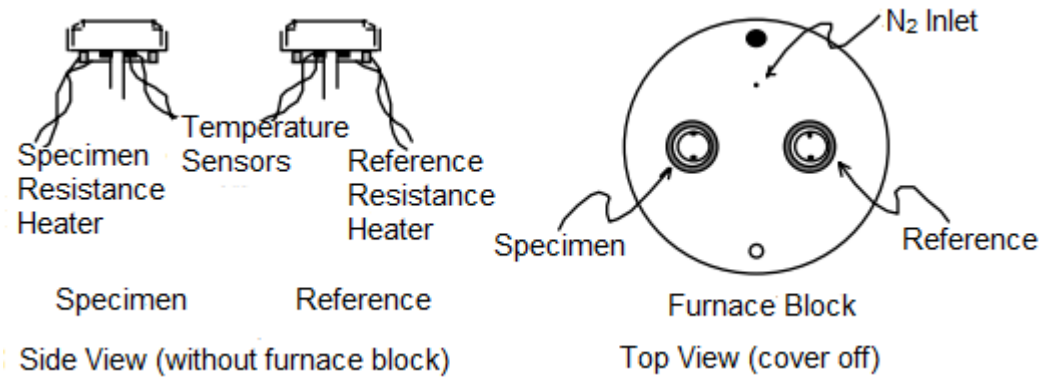

Figure 39 Schematic showing DSC specimen and reference holder [97]

An aluminium crucible with pan of internal base diameter 5.5 mm and aluminium lid were used during specimen preparation and temperature scan. The pan of aluminium crucible had a mass of 24 mg and the aluminium lid was approximately 16 mg. A pair of tweezers was used to cut out two or three small pieces from self-supporting free films to make up a DSC specimen with mass of approximately 10 mg. The 10 mg mass of specimen was placed inside the aluminium pan with the lid placed on top of it and sealed using the press. A small hole was made in the lid using a 0.35 mm diameter needle. The purpose of the hole is to prevent pressure build up inside the aluminium pan/lid assembly which could result in anomalies in obtained data. An empty pan (known as the reference specimen) and those containing specimens of the four formulations were placed on the carousel in the DSC chamber. The DSC specimens including the reference were located adjacent to each other. Whilst inside the DSC 200 F3 Maia, the DSC specimens and reference absorbed heat inside the furnace from the sensor on which they are placed.

Nitrogen (N_2) was used as a purge gas (dry and non-reactive gas) at a flow rate of 20 ml/min. The use of a purge gas such as nitrogen improves the thermal characteristics of the chamber and removes any gas lost from the DSC specimens.

The DSC specimens were taken through or subjected to the below temperature scan as the thermal program: cooled to -50 °C and then heated to 210 °C at a ramp of 20 °C/min. Two runs of temperature scan were carried out: an initial

scan and a re-scan. The re-scan of the DSC specimens followed the same temperature scan as the initial. Prior to analysing the DSC specimens in the laboratory, all DSC specimens were stowed at ambient temperature conditions in separate 127 x 88.9 mm polyethylene plastic bag with a re-sealable zip lock.

Although DSC analysis is widely used to determine Tg with advantages including the ability to use small weights of specimen (for example 10 mg), other thermal analysers such as DMA and TMA are also used for the same purpose of obtaining Tg. However, these may give different values as the process and method used by each analyser type is different.

4.2.2 Dynamic mechanical analysis

Dynamic mechanical analysis ((DMA), also known as Dynamic Mechanical Thermal Analysis (DMTA)) is a thermal analysis technique which can be used to determine the Tg of coating films. The DMA uses a technique where a small deformation (or strain) is applied to a specimen (of known geometry) in a cyclic way with increasing temperature or frequency. Small strains are applied to prevent permanent or plastic deformation.

Similar to the DSC analysers, DMA analysers have been utilised for characterising coating films since the 1970s. A further advantage of the DMA analyser if compared to the DSC analyser is the ability to also measure other dynamic properties such as storage modulus (E'- tensile modulus or G' – shear modulus), loss modulus (E'') and damping (tan delta (tan δ)) as a function of frequency, temperature or time. However, the DMA analyser does not provide information on yield or fracture as such information is commonly obtained from a mechanical tensile analyser.

DMA analysers operate in several modes of deformation such as compression, bending (single cantilever, dual cantilever and three-point bend), shear sandwich and tension over multiple frequencies and temperature control. In addition, each of the deformation mode utilises a specific fixture that is also referred to as geometry.

In a DMA test, the DMA specimen is subjected to sinusoidal stress resulting in a sinusoidal strain of pre-selected amplitude. Put in another way, an oscillating force is applied to the specimen and the resultant displacement of the specimen is measured. Also, the test determines the stress and the phase angle difference between applied strain and resultant measured stress. For an ideal elastic material, there is no phase shift as there is an instantaneous stress response to the applied strain. However, Newtonian fluid and viscoelastic materials respond differently. For Newtonian fluids, there is a phase shift of 90^0, while viscoelastic materials exhibit an intermediate response (lagging by some phase angle). Obtained parameters such as maximum applied strain (ε), maximum measured stress (σ) and phase shift (δ) are used for calculating dynamic properties.

In viscoelastic materials, the storage modulus (E') is a measure of the elastic response and can be represented in eq 2 as follows:

$$E' = (\sigma^0/\varepsilon^0) \cos \delta \quad \textbf{(2)}$$

The loss modulus is a measure of the viscous response and can be represented in eq 3 as:

$$E'' = (\sigma^0/\varepsilon^0) \sin \delta \quad \textbf{(3)}$$

The loss tangent, also commonly referred to as tan δ is the most significant parameter which is the ratio of energy lost (viscous component) to the energy stored (elastic component) per deformation cycle, (i.e. E"/E') and represented in eq 4 as:

$$E''/E' = \sin \delta / \cos \delta = \tan \delta \quad \textbf{(4)}$$

The relationship between these parameters E', E" and tan δ can be represented in an Argand diagram. Thus, the complex modulus E* is defined with a real (storage - E') and imaginary (loss - E") components respectively.

Similar to the DSC analyser, there are several ways in the industry of measuring and assigning Tg for a DMA analysis including Tg at onset storage modulus, E', Tg at the peak of tan δ (as illustrated in Figure 40) and Tg at the peak of the loss modulus, E".

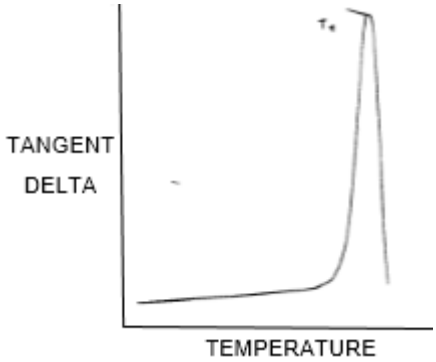

Figure 40 DMA Tg calculation at tan δ peak [98]

Typically, Tg is measured and assigned in accordance to ASTM E1640 - 13, "Standard Test Method for Assignment of the Glass Transition Temperature by Dynamic Mechanical Analysis" [98]. In line with industry practice, the corresponding temperature at the peak of tan δ curve has been adopted in specifying and reporting Tg for DMA analyses carried out in this research project.

4.2.2.1 DMA Analysers

Two types of DMA analysers and loading fixtures were utilised to evaluate the behaviour of free film specimens prepared from the four coating formulations: SPE, SFPE, SME and SFME. One of the DMA analysers was an RSA G2 rheometer (TA Instrument) while the other was a DMA 8000 (PerkinElmer). The two fixtures are: tension and single cantilever respectively.

(a) RSA G2 rheometer DMA analyser

The RSA G2 rheometer DMA analyser mainly consist of a servo motor, a force convention oven (or furnace), specimen fixture, a temperature controller and a force rebalance transducer (FRT). Both the motor and transducer have separate linear variable differential transducers (LVDT). The RSA G2 DMA was equipped with a thin film fixture (clamp) in tension and was used in measuring parameters of the self-supporting free films. Data were collected over -50 °C to 200 °C range every 30 sec

using 3 °C/min temperature ramp. A deformation frequency of 1 Hz and an initial strain of 0.05% were used. All measurements were conducted in a dry nitrogen environment.

The cross-sectional dimensions of the DMA specimen: self-supporting free film are approximately 30 mm long (l), 6-10 mm wide (w), and 0.3-1.3 mm thick (t). The DMA specimens were cut using a knife and a slide rule. Thus, each DMA specimen was clamped at the bottom and the top. After clamping, the furnace was put in place to completely enclose the tension fixture and the DMA specimen that was subjected to tension as illustrated in Figure 41.

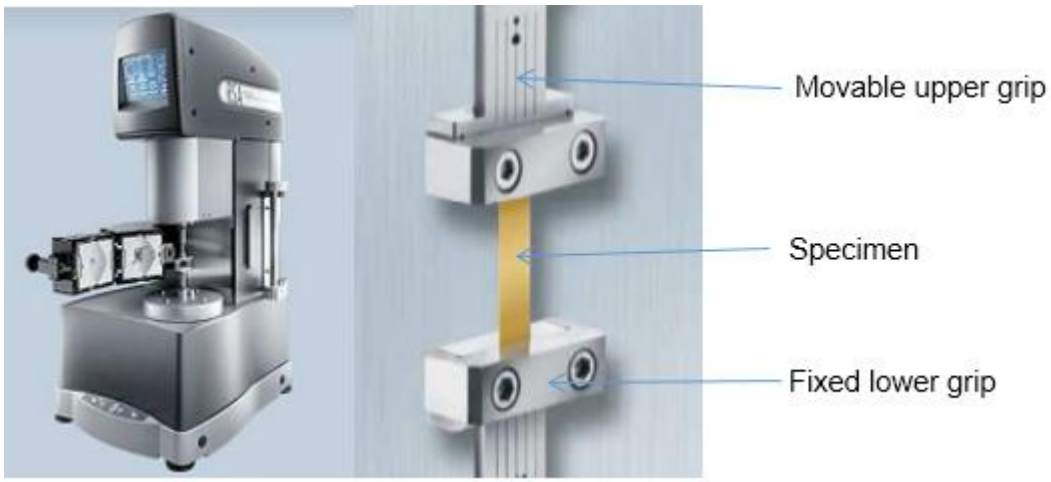

Figure 41 Tension fixture of RSA G2 rheometer analyser

This mode as shown in Figure 41 was used for testing two variant of DMA specimens of self-supporting free films: unaged (i.e. free films specimens cured at ambient temperature only) and aged (i.e. free film specimens cured at ambient temperature followed by stressing or exposing them to defined laboratory conditions). The defined laboratory conditions are based on the fatigue testing using the same principle of hygrothermal cycling as described for T specimens in section 4.1. A summary of the laboratory exposure conditions for the DMA specimens of self-supporting free films is described in Table 12.

Table 12 Description of exposure conditions of free film specimens

	Description of the Exposure Conditions
1.	Unaged film: (only cured at ambient temperature which served as reference)
2.	Heat stressed: (cured at ambient temperature followed with conditioning at 50±2 ^{0}C dry constant heating in an oven for 1 week)
3.	Wet stressed: (cured at ambient temperature followed by conditioning at 50±2 ^{0}C dry constant heating in an oven for 1 week and a further 1 week complete immersion in artificial seawater tank at 23±3 ^{0}C)
4.	Hygrothermal cycling (HTC) stressed: (cured at ambient temperature followed by conditioning at 50±2 ^{0}C dry constant heating in an oven for 1 week with another 1 week complete immersion in artificial seawater tank at 23±3 ^{0}C and a further hygrothermal cycling between the oven at 100±2 ^{0}C and artificial seawater tank 23±3 ^{0}C for 1 day)
5.	Hygrothermal cycling (HTC) stressed: (cured at ambient temperature followed by conditioning at 50±2 ^{0}C dry constant heating in an oven for 1 week with another 1 week complete immersion in artificial seawater tank at 23±3 ^{0}C and a further hygrothermal cycling between the oven at 100±2 ^{0}C and artificial seawater tank 23±3 ^{0}C for 1 week)

As illustrated in Table 13, the labels on the DMA specimens of self-supporting free films for the four formulations exposed to the conditions described in Table 12 above are as follows:

Table 13 Labels on exposed specimens: self-supporting free films

Exposure Condition	Designation on Self-supporting Free Film
Reference films	SPE New R, SME New R, SFPE New R and SFME New R
Heat stressed films	SPE New 1, SME New 1, SFPE New 1 and SFME New 1
Wet stressed films	SPE New 2, SME New 2, SFPE New 2 and SFME New 2
Hygrothermal stressed 1	SPE New 3, SME New 3, SFPE New 3 and SFME New 3
Hygrothermal stressed 2	SPE New 4, SME New 4, SFPE New 4 and SFME New 4

Prior to analysing the DMA specimens by tension mode in the laboratory, all DMA specimens were stowed at ambient temperature conditions in separate 127 x 88.9 mm polyethylene plastic bag with a re-sealable zip lock.

Thus, twenty (20) self-supporting free films of DMA specimens were analysed for glass transition temperature (Tg), tan δ and storage modulus (E') using the RSA G2 rheometer DMA analyser.

(b) DMA 8000 (PerkinElmer)

The other DMA analyser utilised was a PerkinElmer DMA 8000. The PerkinElmer DMA 8000 consisted of a drive temperature controller, a furnace, a drive shaft, a specimen fixture and a high sensitivity displacement detector LVDT. The DMA 8000 analyser exhibits similar operational features and working principles as the RSA G2 rheometer analyser. In addition, the DMA 8000 analyser had the additional

capability of using Material Pockets made from stainless steel to support DMA specimens that were non-self-supporting with irregular cross-section which was the case for the flakes of free films created from the cycled T specimens following fatigue testing as described in section 4.1.

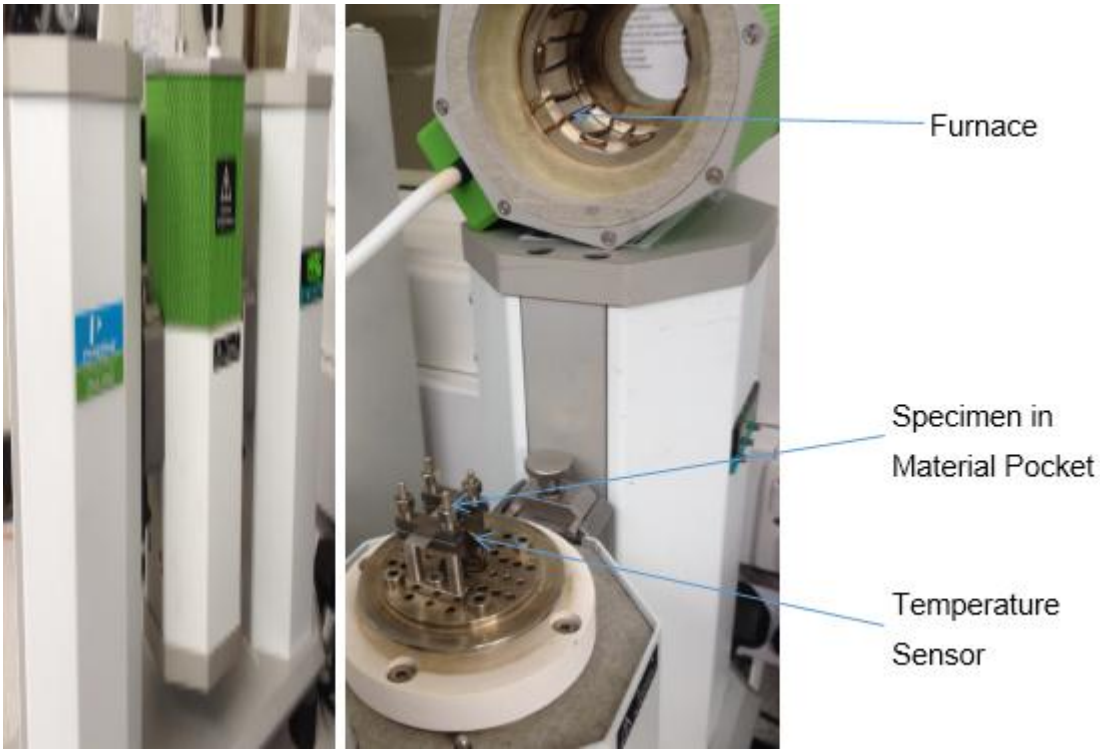

Figure 42 Single cantilever fixture for DMA analysis

As illustrated in Figure 42, DMA 8000 (PerkinElmer) analyser was equipped with a bending fixture: single cantilever, which was used in measuring properties of the non-self-supporting free films encapsulated in a Material Pocket. Material Pockets are typically designed for use only in a bending fixture such as the single cantilever. A sheet of Material Pocket was folded along the pre-fold to make an angle of approximately 90° between its inner faces. The folded material pocket was placed on a scale and the scale tared. Non-self-supporting free films of each formulation was placed on the flat horizontal face of the material pocket and weighed scale. Approximately a 100 mg of non-self-supporting free film of each formulation was utilised. The two faces of the material pockets were folded together and crimped using a table vice. The DMA

specimen: non-self-supporting free film encapsulated in a material pocket was reweighed to determine and confirm the weight of the encapsulated specimen. The DMA specimens used in DMA 8000 were labelled Hygrothermal stressed 3. As shown in Figure 42, the DMA specimen was clamped into the bending single cantilever fixture of DMA 8000. The DMA furnace was put in place to completely enclose the bending fixture with DMA specimen. Data were collected over 25 °C to 200 °C range every 30 sec using 3 °C/min temperature ramp. A deformation frequency of 1 Hz and an initial strain of 0.05% were used. All measurements were conducted in a non-nitrogen environment. Similar DMA properties as that of self-supporting free film specimens were analysed for with the non-self-supporting free film specimens.

Thus, sixteen (16) DMA specimen: non-self-supporting free film encapsulated in a Material Pocket were analysed for Tg, tanδ, E' and E" using the DMA 8000 analyser. In addition, as the Material Pocket was made of steel, the storage modulus of the Material Pocket alone (i.e. without any specimen) was evaluated using same temperature scan input conditions as that for the non-self-supporting free films.

4.2.3 Thermo-mechanical analysis

Similarly, Thermo-Mechanical Analysis (TMA) was also used to determine the Tg of self-supporting free film specimens with similar labels used for the DMA. In contrast to the DMA, rather than apply dynamic load, TMA applies a constant static load to a material or a specimen. It defines Tg with regards to the change in the coefficient of thermal expansion as the polymer specimen goes from glassy to rubbery with the associated change in free molecular volume. Thus, it measures the physical effect i.e. the expansion or change in dimension.

Typically, in accordance to ASTM E1545 - 05, "Standard Test Method for Assignment of the Glass Transition Temperature by Thermomechanical Analysis", the Tg from a temperature scan of a TMA specimen is commonly measured and assigned [99]. Following a plot of Displacement against temperature, the Tg is located at the intercept of the two curves as shown in

Figure 43. This method was used in assigning Tg for the TMA specimens. In addition, the coefficient of linear thermal expansion was assigned at the onset Tg in the glassy region of the curve.

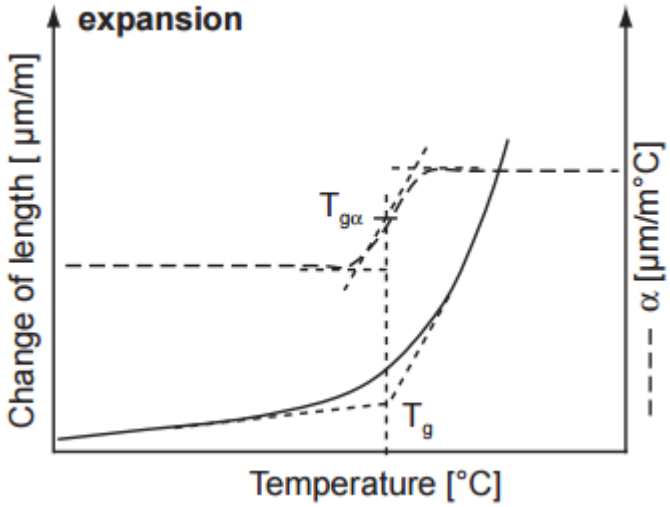

Figure 43 TMA Tg calculation at the intercept of the two curves [99]

The TA Instruments Q400 TMA was used to evaluate both the Tg and the coefficient of linear thermal expansion (CTE) of the formulations: SPE, SFPE, SME and SFME. The TA Instruments Q400 TMA consists mainly of a furnace, a specimen stage, a force motor and a linear variable differential transducer (LVDT). It provides several deformation modes including expansion, tension, three-point bending and penetration. Amongst these available deformation modes, expansion measurement was specifically performed. The expansion measurement yields Tg and CTE of a material. It utilised a flat-tipped standard expansion probe, which was placed on the specimen (that had been positioned on the stage using tweezers). The furnace was placed to completely enclose the specimen, which was subjected to a temperature program. The probe movement recorded specimen expansion. Figure 44 shows a TA Instruments Q400 TMA.

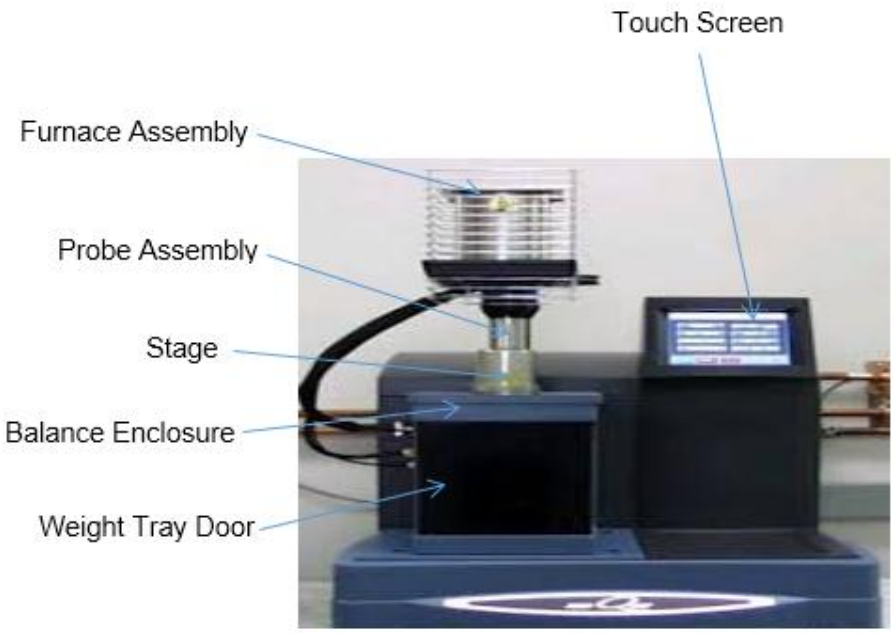

Figure 44 Parts of a TA Instruments Q400 TMA

The TA Instruments Q400 TMA was calibrated at 5 °C/min with reference materials tin and zinc. The cell constant was calibrated using silver wire. The film-fibre probe was used for specimen measurements. Approximately 8 mm long, 4 mm wide, 0.7 mm thick free film specimens of each formulation was cut using a razor blade to form TMA specimens. TMA specimens were placed on a flat specimen platform and the expansion probe was placed to rest on the surface of the TMA specimens under loading. The TMA furnace was put in place to completely enclose the expansion probe with TMA specimen. The specimens were ramped from -120 to 250 °C at 5 °C/min. Force and preload of 0.05 N were used. The purge gas was nitrogen with a flow rate of 50 ml/min. A closer view of the stage is shown in Figure 45 below:

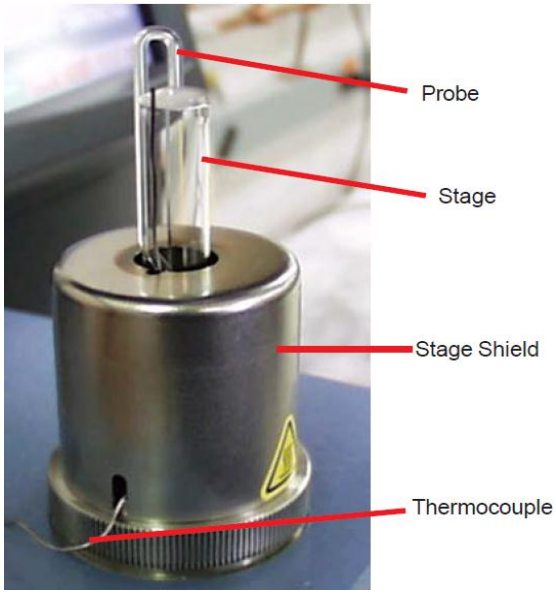

Figure 45 Stage and probe arrangement of a TA Instruments Q400 TMA

4.3 Mechanical Analysis of Free Film Specimens

In material characterisation, another significant means utilised in understanding the anticipated behavioural response of a material from an encounter with stress is mechanical analysis. Hence, this section offers insight into mechanical analysis of the four WBT coating formulations using free film specimens shaped as dog bones that were subjected to uniaxial tension testing.

In a typical mechanical analysis, the material is subjected to a mechanical load, which results in a deformation. The resultant deformation depends on several factors including the size and shape of the material. The basic concepts governing physical properties in a mechanical analysis are: elasticity, plasticity (ductility) and toughness. Elasticity is the ability of a material to deform temporarily under mechanical load and subsequently return to its original shape once the mechanical load is removed. Plasticity is the capacity of a material to deform permanently without failure under mechanical load. Toughness is the capacity of a material to absorb shocks without unexpected failure. Generally, a popular technique of mechanical analysis utilised in evaluating a material's physical properties is the universal testing analysers. The universal testing analyser has several deformation fixtures and modes including axial (tensile or

compressive) and flexural. The uniaxial tensile deformation mode is very common in studying the physical or mechanical properties of a material as the analyser pulls the material apart. In uniaxial tensile testing also known as 'pull to break' testing, there are two grips for the specimen: one stationary (fixed member) and the other movable (movable member carrying a second grip that moves away at a constant rate). The uniaxial tensile analyser measures the displacement of the gripped specimen and load through the load cell attached to the top position of the movable grip. The testing from a uniaxial tensile analyser is destructive.

Following the end of testing, a load versus displacement curve is produced from which an engineering stress versus engineering strain curve is generated.
Engineering stress (σ_e) refers to the applied mechanical load divided by the original area of the material as expressed in eq 5. The unit of engineering stress is expressed as MPa (i.e. 1 x 10^6 N/m^2)

$$\sigma_e = P/A_o \quad \textbf{(5)}$$

Where P is the applied mechanical load and A_o is the original cross sectional area of the specimen normal to the direction of loading.

Engineering strain (ε_e) is the ratio of the deformation of the material (or change in length, ΔL) to the original dimension of the material as represented in eq 6. The unit of engineering strain is dimensionless.

$$\varepsilon_e = \Delta L/L_o \quad \textbf{(6)}$$

Where ΔL is the deformation or change in length and L_o is the original specimen dimension along a single axis.

Instron 5969 Uniaxial Tensile Analyser

In this research project, the uniaxial tensile analyser utilised for evaluating self-supporting free film specimen (shaped as dog bone) was an Instron 5969. The Instron 5969 is screw driven with a 500 N static load cell and it is a

displacement controlled load frame, which means that the crosshead is lowered or raised by turning screws. Strain was measured using a non-contact video-extensometer with a field gauge length of 25 mm. Strain is measured typically using a contact extensometer. However, a specific advantage of the video extensometer over the traditional contact extensometer is the ability to be utilised in testing up to break without damage. Other advantages include the non-initiation of premature failure and the non-distortion of delicate test specimens.

Some of the important parts of the uniaxial tensile analyser are shown in Figure 46 below.

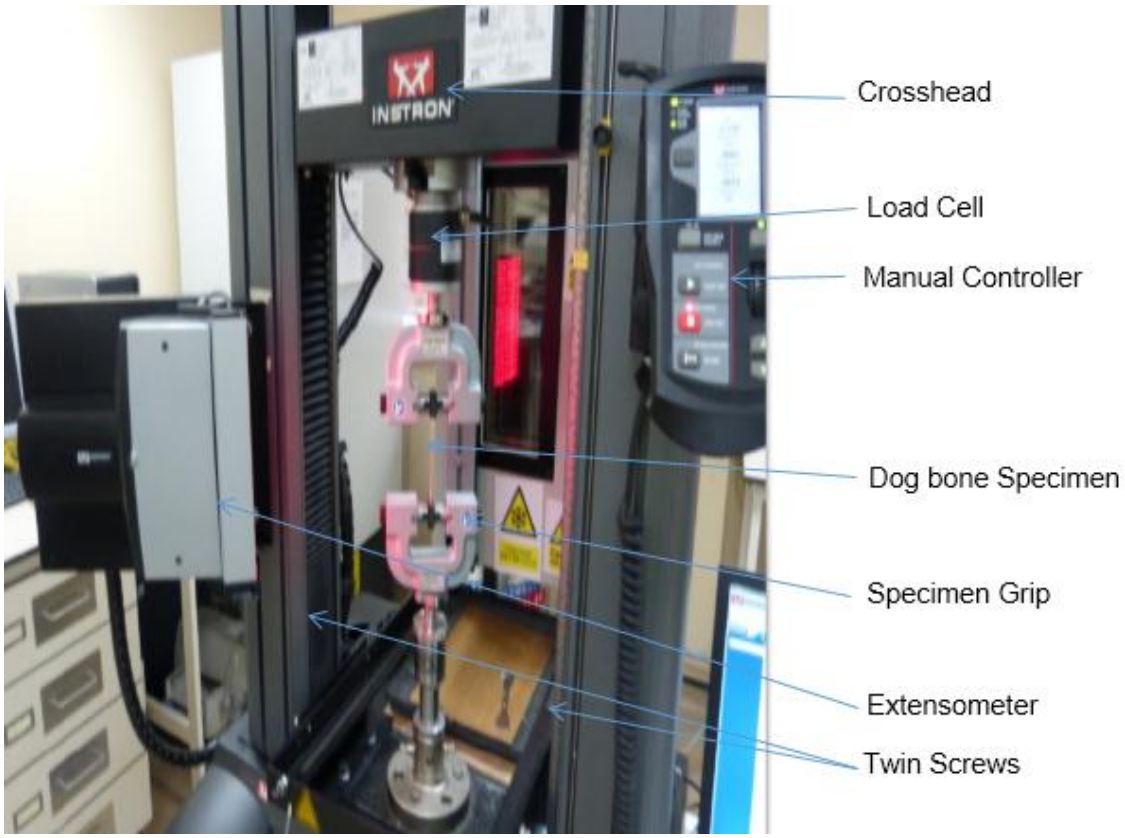

Figure 46 Main parts of the uniaxial tensile analyser

The testing speed of the crosshead (displacement rate) is 5mm/min. The tensile properties of the four WBT coating formulations were determined in accordance to the standard method ASTM D 638 – 02a “Standard Test Method for Tensile Properties of Plastics” [100]. This standard covers the determination of tensile properties including elongation to fracture, yield strength, tensile strength and

young's modulus (stiffness) of reinforced and unreinforced plastics. Hence, elongation to fracture and tensile strength were recorded during the uniaxial mechanical testing for this research.

After spray application of WBT coating formulations on PTFE panels, self-supporting free films were peel off after cure for two days at ambient temperature. The peeled off self-supporting free films were shaped into dog bone specimens using a punch mould. Each dog bone specimen had two basic regions: shoulder (or grip section) and neck. The shoulders of the dog bone specimen had larger cross section than the neck to enable adequate gripping on the uniaxial tensile analyser. The neck region with a reduced cross section is intended to localises stress and ensure failure occurs ideally at the middle of the dog bone specimen during uniaxial testing. The dry film thicknesses of the dog bone specimens were typically: 640 µm and 960 µm. As shown in Figure 47, the cross section of the dog bone specimens approximately are: 138 mm (length) X 25 mm (width) X 0.64 – 0.96 mm (thickness).

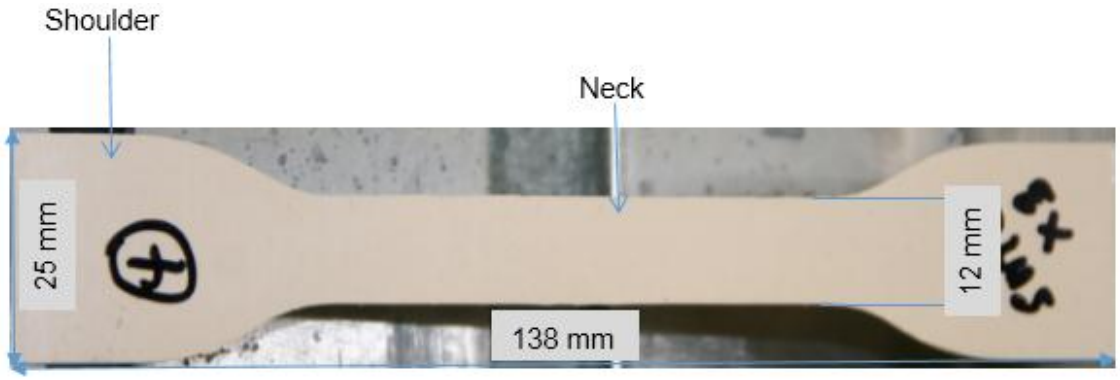

Figure 47 Cross sectional dimension of a dog bone specimen

Participants of both unaged and aged dog bone specimens of each coating formulation were investigated. Unaged dog bone specimens were cured at ambient temperature only while aged ones were cured at ambient temperature followed by oven heating at 100 ºC. Following the two days ambient temperature cure of the self-supporting free films used in forming the dog bone specimens, one set of dog bones specimens (unaged) were further cured at ambient temperature only for one week while the other set of dog bone

specimens (aged) were post cured in an oven at 100 ºC for one week. Herein, the unaged dog bone specimens are known as reference while the aged ones are referred to as heat stressed. Prior to mounting each dog bone in the uniaxial tensile analyser, a marker pen was used to place two marks (in the form of dots) with a gauge length of 25 mm on the neck region of the dog bone specimen. The average thickness of each dog bone was obtained from triplicate position readings taken between the markings of the gauge length using a micrometre.

Prior to uniaxial tensile testing, each dog bone specimen was placed in the grips of Instron 5969 as shown in Figure 46. Alignment of the each dog bone specimen was considered and slippage relative to the grips was avoided. For a specific dry film thickness and coating formulation, triplicate dog bone specimens of both unaged and aged were tested. Tensile properties were determined from an average of the triplicate test for each specific dry film thickness and coating formulation. Forty-eight (48) dog bone specimens were investigated using uniaxial tensile testing that was conducted at ambient laboratory conditions.

4.4 Reanalysis

Having completed the fatigue testing and thermal analysis using specimens for set 1, specimens for set 2 were evaluated with fatigue testing and thermal analysis. The essence of subjecting specimens of set 2 to the similar conditions was to compare and validate the performance of the four formulations from two separately performed fatigue testing and thermal analysis.

4.5 Statistical Analysis

An IBM statistical product and service solution (SPSS) was the statistical package used. The SPSS data editor comprised of the data view tab and the variable view tab.

The statistical method used in analysing the experimental data was analysis of variance (ANOVA). ANOVA is applied to study or determine relationship

between variables (i.e. the dependent variable and the independent variable) [101, 102, 103]. The dependent variable is the outcome and the independent variable is the number of parameters, which in this case, four parameters (SPE, SFPE, SME and SFME) were studied. Following a statistical analysis using ANOVA, a test statistics, the *F-ratio* is produced that compares the amount of systematic variance (SS_M) in the data to the amount of unsystematic variance (SS_R). The P value test is the statistical significance of the obtained test data. Any “P value” less than .05 (within 95% confidence interval) indicates that the respective model is statistically significant. The Levenes’s test determines if the variation is similar or different between groups. When Levene’s test is statistically significant, it means there are differences in variation between the groups. The 95% confidence interval offers a measure of the precision with which the true population differences is estimated [102, 103]. Two statistical analyses using ANOVA were conducted to determine the mean effect of volume loss from DFT measurements taken before and after the fatigue test; and the mean effect of the fatigue test on the four formulations. Hinton [103] provides further explanation of the theory and parameters of ANOVA.

CHAPTER 5
EXPERIMENTAL RESULTS

5.1 Fatigue Test

This section presents the results from investigating T specimens of the four formulations (SPE, SFPE, SME and SFME) subjected to a designed fatigue test proposed for industry. Figure 48 shows the observation of cracks at different stages of the fatigue testing for the evaluated four formulations.

5.1.1 Set 1: T specimens

Failure of a coating formulation occurred with the appearance of visible crack(s) as T specimens were subjected to the designed fatigue test.

Comparing the T specimens for the four formulations: SPE was the least crack resistant as cracks were observed after 1 cycle at the weld intersection of all 6 specimens representing this formulation. The cracks observed were much bigger in size compared to those seen and reported on other formulations: SME, SFME and SFPE. In addition, the cracks ran both in the parallel and perpendicular directions along the intersection weld as shown in Figure 48a. As observed after chiselling off the coating films from the T specimens at the end of the fatigue test, brown rust, the by-product of corrosion was present on the T sectional steel substrates. Thus indicating that the cracks after initiation propagated through the dry coating film thicknesses to the substrate.

The SME specimens demonstrated more resistance when compared to SPE specimens but developed cracks before SFME and SFPE specimens. SME withstood 42 cycles before cracks appeared on the intersection welds of all the 6 T specimens representing this formulation. The cracks ran parallel along the weld toe at the intersection of the flange and web plates as shown in Figure 48b. The cracks after initiation also propagated through the coating dry film thicknesses to the T sectional steel substrates as there was evidence of steel corrosion after chiselling off the films from the T specimens.

Comparing T specimens coated in SFME and SFPE as shown in Figure 48c and 48d respectively, the observed cracks appeared at 59 cycles. The cracks

were observed on all 6 T specimens representing SFME while only 2 of the SFPE specimens showed cracks. Worthy of mention is that the visible cracks on the T specimens of SFME and SFPE were just on the surface of the films. The micro cracks did not propagate through the film to the substrate as there was no evidence of brown rust from steel corrosion observed. Thus, SFPE was the most crack resistant amongst the four formulations as this formulation still had 4 T specimens from the 6 without cracks.

Although failure by cracking occurred in all the formulations, overall, SFPE, the solvent free pure epoxy having just 2 failures out of 6 T specimens, is the most crack resistant, followed by SFME. The next less crack resistant formulation (following the solvent free formulations) is SME and the SPE is the least crack resistant of them all.

Based on the fatigue testing from hygrothermal cycling, the performance of the four formulations from the most crack resistant to the least crack resistant was observed and distinguished as follows:

- **SFPE > SFME > SME > SPE**

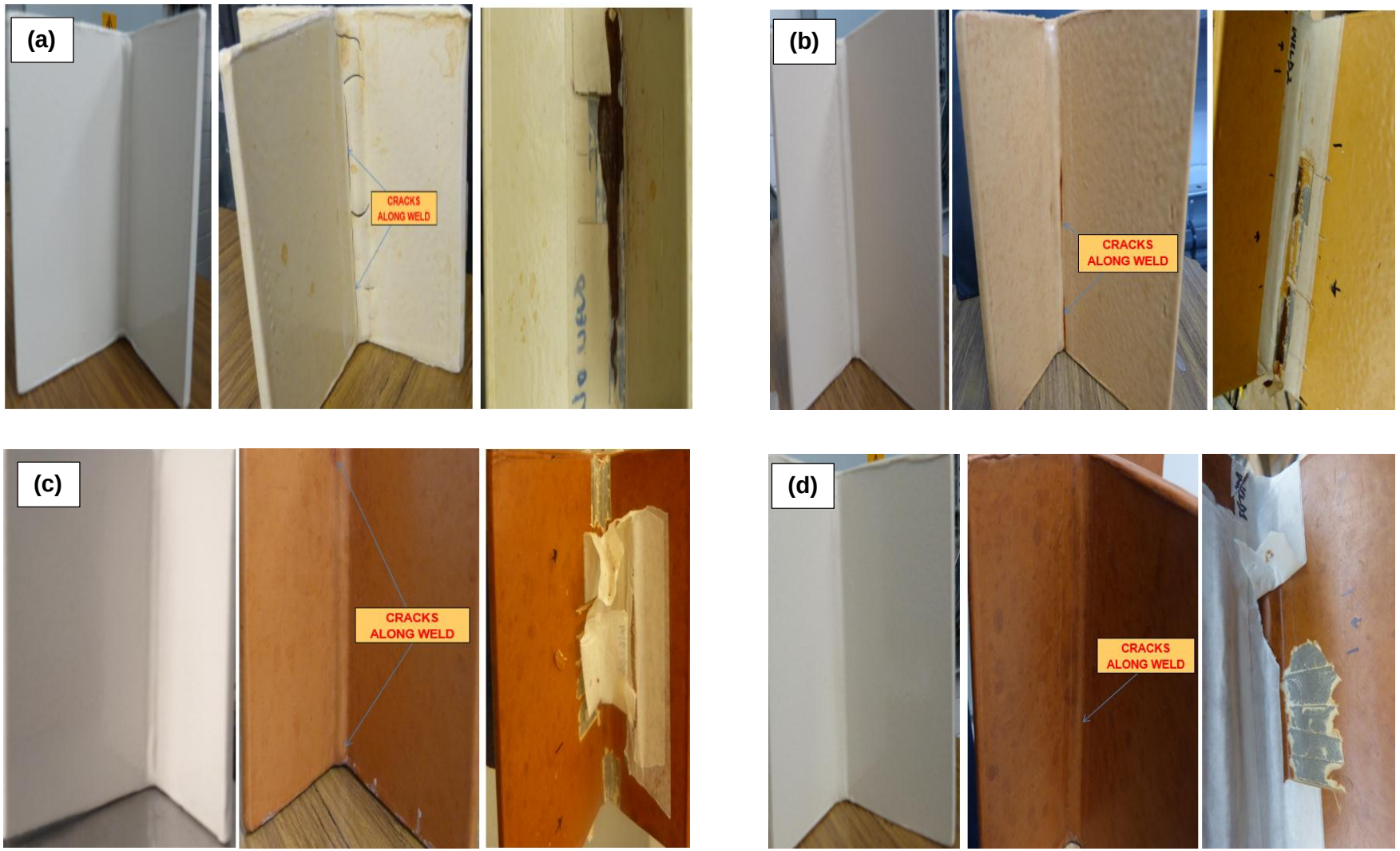

Figure 48 T specimens before and after fatigue testing (a) SPE after 1 cycle (b) SME after 42 cycles (c) SFME after 59 cycles (d) SFPE after 59 cycles

5.2 Thermal Analysis of Free Film Specimens

This section presents the results from investigating free film specimens of the four formulations (SPE, SFPE, SME and SFME) for both ambient temperature cured and that subjected to the fatigue test and subsequently temperature scan using thermal analysers. Figures 49 to 52 show the obtained results following the temperature scan from DSC, Figures 55 to 64 illustrate that from DMA and Figures 70 to 71 show that for TMA.

5.2.1 Differential scanning calorimetry – Glass transition temperature

The glass transition temperature (Tg) of DSC specimens from the four formulations was determined first using differential scanning calorimetry (DSC) after 16 days of cure at ambient temperature. The Tg is a function of the extent of cure and reaches a maximum temperature Tg∞, when the specimen has fully cured (or when no further cure is possible). Thus, the value of Tg∞ obtained for each coating formulation from the re-scan indicated the maximum Tg for each formulation as the initial Tg value (Tgi) was either well below or above that of Tg∞.

Figures 49 through 52 show the plots of heat flow as a function of temperature. The initial temperature scan versus the re-scan is represented in two different colours for each graph with the respective formulation shown. On each graph, cursors were positioned on either side of the transition where the heat flow curve was linear and ideally, where the 1st derivative curve was flat. Onset and Midpoint Tg parameters were read from the transition inflections on the initial scan and re-scan (also referred to as second heating).

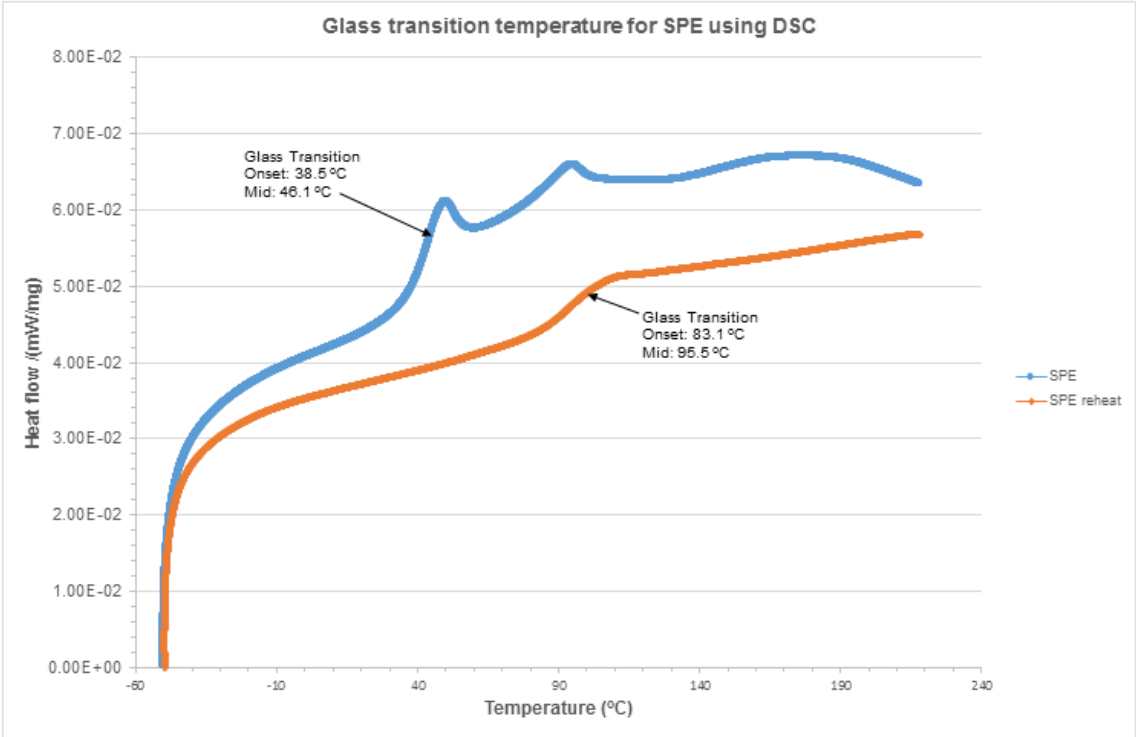

Figure 49 Differential scanning calorimetry curve for SPE formulation

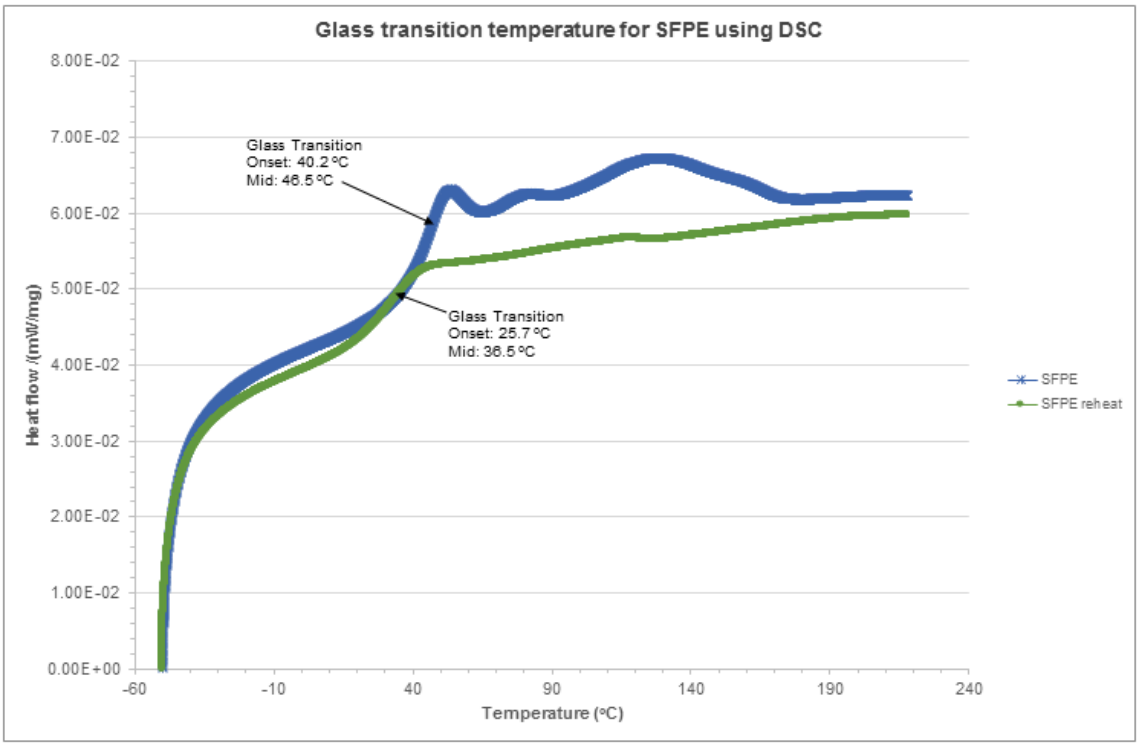

Figure 50 Differential scanning calorimetry curve for SFPE formulation

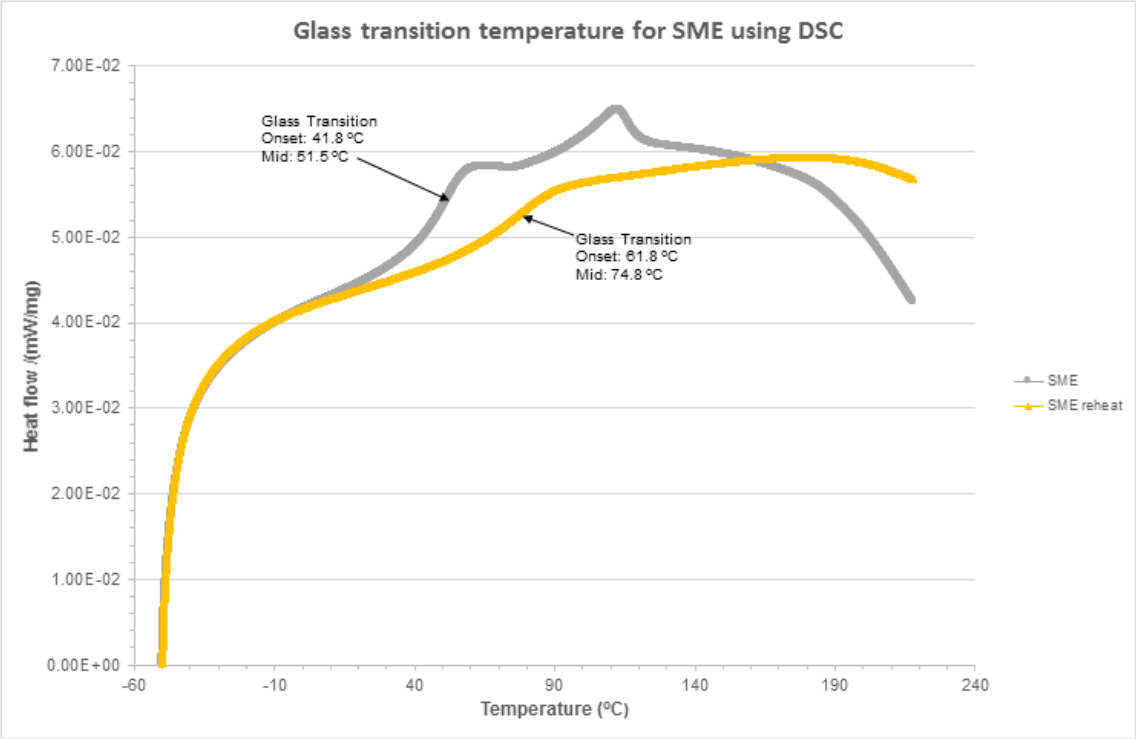

Figure 51 Differential scanning calorimetry curve for SME formulation

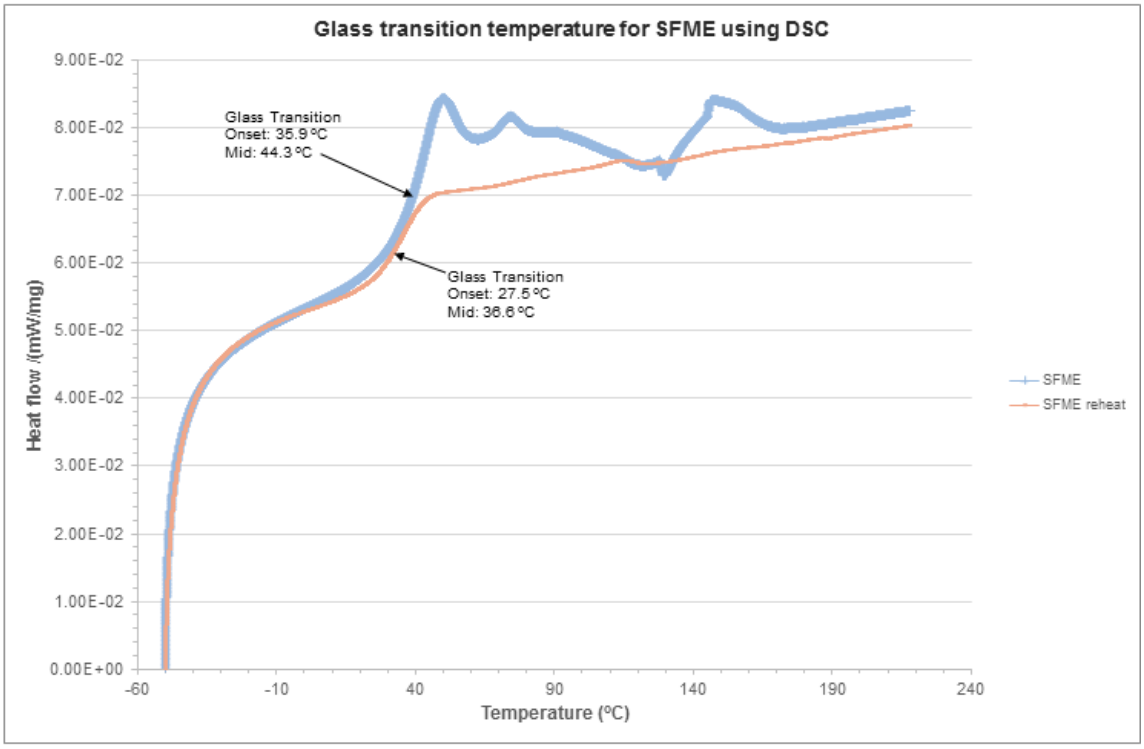

Figure 52 Differential scanning calorimetry curve for SFME formulation

Presented in Figure 53 is the bar chart plot of initial temperature scan (Tgi) and re-scan (Tg∞) for SPE, SME, SFPE and SFME.

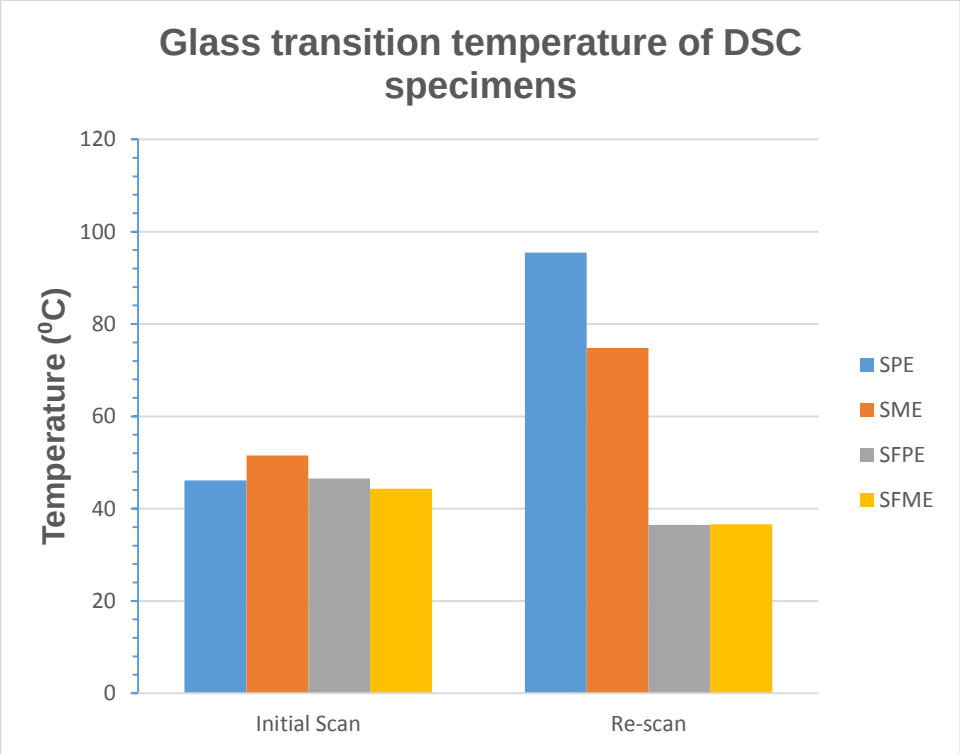

Figure 53 Bar chart plot of Tg values measured for the four formulations using DSC

Table 14 below presents a summary of the initial temperature scan and re-scan Tgs for the four formulations from Figures 49 – 52. The difference between the initial and re-scan Tgs (**Δ**Tgs) is included in Table 14 for comparison.

Table 14 Tg values measured for all formulations using DSC

Formulations		**Initial scan Tgi (°C)**	**Re-scan Tg∞ (°C)**	**(Tg∞ -Tgi) ΔTg (°C)**
Pure Epoxy	Solvent Containing (SPE)	46.1	95.5	49.4

Formulations		Initial scan Tgi (°C)	Re-scan Tg∞ (°C)	(Tg∞ -Tgi) ΔTg (°C)
	Solvent Free (SFPE)	46.5	36.5	-10
Modified Epoxy	Solvent Containing (SME)	51.5	74.8	23.3
	Solvent Free (SFME)	44.3	36.6	-7.7

As shown above, the Tgs from the initial scan for the four formulations range from 44.3 °C to 51.5 °C. SME (a solvent containing formulation) demonstrated the highest Tg magnitude while SFME (a solvent free formulation) showed the lowest. Tg magnitudes (values) for SPE (the other solvent containing formulation) and SFPE (the other solvent free formulation) were between that of SME and SFME. Thus, the range of Tg magnitudes from the initial scan are relatively close indicating that the formulations have been cured at ambient temperature. This is consistent with the view that the maximum Tg will be approximately 25 °C to 35 °C above the cure temperature [27]. However, the ranking order from Tg values from highest to lowest for the initial scan using DSC is as follows:

SME > SFPE ≈ SPE > SFME

With the re-scan, the Tg∞ values ranged from 36.5 °C as the lowest to 95.5 °C as the highest. SPE and SME demonstrated values that shifted much above that observed for SFPE and SFME. A comparison of **Δ**Tgs showed that SPE and SME exhibited significant increases in Tg value.

For SPE and SME, the Tgs from the initial scan were 46.1 °C and 51.5 °C respectively while there was a rise to 95.5 °C and 74.8 °C respectively for the re-scan. Comparing the two solvent containing formulations, there is a much higher shift in Tg position for SPE following the re-scan.

In contrast, both solvent free formulations: SFPE and SFME showed a small change in the re-scan from the initial scan. The change was a negative shift that was inconsistent with the typical change observed. Tgs from the initial scan for SFPE and SFME were 46.5 °C and 44.3 °C respectively then dropping in the re-scan to 36.5 °C for SFPE and 36.6 °C for SFME. Thus, the ranking order from Tg∞ values from highest to lowest for the re-scan using DSC is as follows:

SPE > SME >> SFME ≈ SFPE

The higher ΔTg value for SME and especially SPE strongly suggests that there was a considerable or significant amount of retained solvent and/or unreacted functional groups in the SPE film after initial ambient temperature cure. For the SPE film, following the re-scan, additional reaction and solvent loss was driven resulting in a higher cross-link density and significantly higher Tg than that of the initial scan. Also, this higher ΔTg value of the SPE film (which is twice that shown by the SME film) could represent a likelihood of increased internal stress (shrinkage stress) which probably could be retained within the film as residual stress. Thus, such significant level of residual stress from film formation when present could be detrimental to the performance of the coating film later when in service as the film has limited threshold to sustain addition external stress from its environment.

SFPE demonstrated the lowest ΔTg with a value of -10 °C followed by SFME at -7.7 °C. This decreased trend below the initial Tg following the re-scan could be regarded as unusual and at present there is no known mechanism for explaining it. However, a possible explanation for this behaviour may be either that one or more of the constituents in the SFPE and SFME formulation exuded after the initial scan or plasticisation occurred which depressed the re-scan Tg. For SFPE and SFME formulations, the significant lower ΔTg value could indicate a low internal stress, which could offer more room to accommodate external stress during use.

Therefore, it will be interesting to see what bearing a significant increase in ΔTg value or a decrease in ΔTg value could mean to the performance of coating especially regarding embrittlement and premature cracking failure when

exposed to fatigue (cycling) testing in a laboratory or in-service. A summary of Tg and Tg∞ values are illustrated in Table 15.

Table 15 Summary of glass transition temperature, Tg using DSC

Initial Scan	SME > SFPE ≈ SPE > SFME
Re-scan	SPE > SME >> SFME ≈ SFPE
ΔTg	SPE >> SME > SFME > SFPE

5.2.2 Dynamic mechanical analysis

This section presents the DMA results from set 1: DMA specimens (self-supporting free films and non-self-supporting free films) of the four formulations. Prior to the DMA tensile mode testing, self-supporting free films were exposed to similar defined laboratory conditions of the fatigue test as described in (section 4.2.2, Table 12). The tensile dynamic mechanical properties of the four formulations are shown in Table 16 and Table 18 for the same specimen exposure conditions labelled: reference (ambient cured), heat stressed, wet stressed and hygrothermal stressed. Generally, the specimens demonstrated a single Tg with a broad rubbery plateau. Twenty (20) DMA specimens from the four formulations were evaluated and compared.

(a) Glass transition temperature Tg of self-supporting free films

Presented in Figure 54 is the bar chart plot of Tgs as a function of the exposure conditions for SPE, SME, SFPE and SFME formulations.

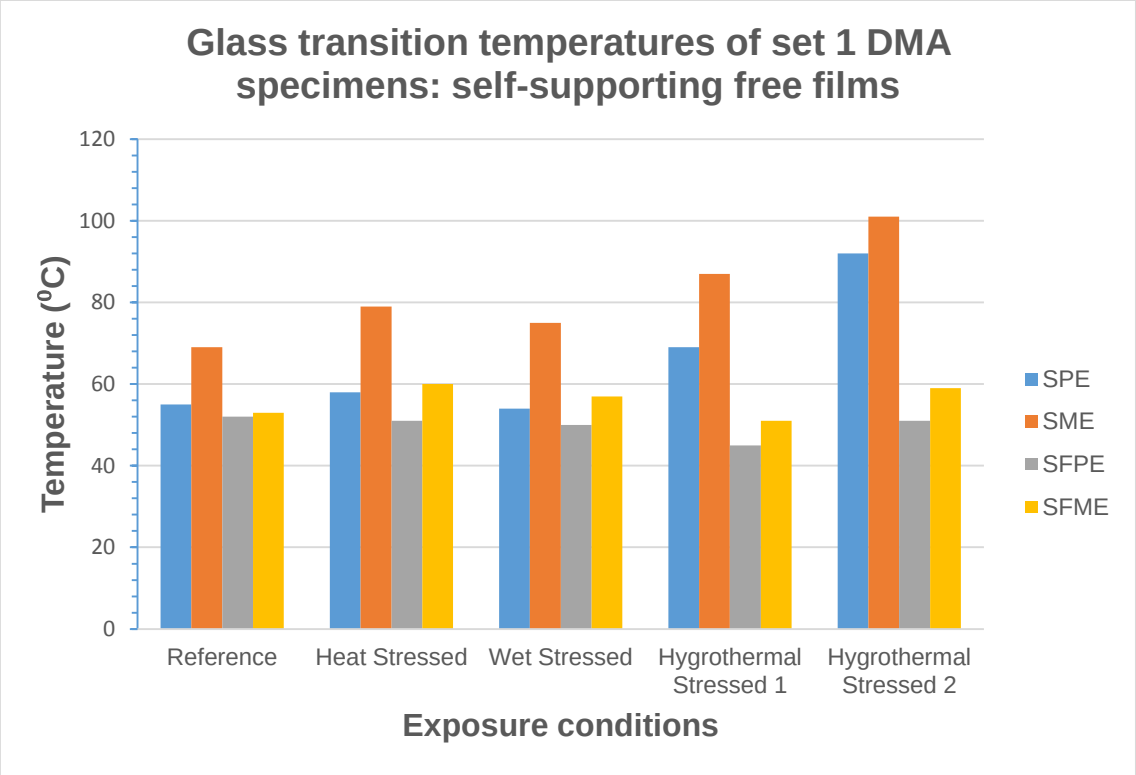

Figure 54 Bar chart plot of Set 1: Tg values measured for unaged and aged self-supporting specimens using DMA

For DMA self-supporting specimens labelled reference (i.e. cured at ambient only), it was observed that the values of Tg ranged from 52 °C to 69 °C. SME exhibited the highest Tg while SFPE showed the lowest. Both SPE and SFME showed the Tg values of 55 °C and 53 °C respectively. The following Tg trend emerged:

SME > SPE > SFME ≈ SFPE

This initial ranking from the DMA self-supporting specimens labelled reference when compared to that obtained using the DSC for the initial scan does not agree. However, results from both analyses for the initial scan show a consistency for ranking SME formulation as having the highest Tg. Also, shown in Table 16 is the Tg values.

Table 16 Set 1: Tg values obtained for unaged and aged self-supporting specimens using DMA

Formulations / Exposure Conditions		Set 1 DMA specimens: Self-supporting Free Films (°C)				
		Unaged	Aged			
		Reference (Ambient Cured)	Heat Stressed	Wet Stressed	Hygro-thermal Stressed 1	Hygro-thermal Stressed 2
Pure Epoxy	Solvent Containing (SPE)	55	58	54	69	92
	Solvent Free (SFPE)	52	51	50	45	51
Modified Epoxy	Solvent Containing (SME)	69	79	75	87	101
	Solvent Free (SFME)	53	60	57	51	59

For the DMA self-supporting specimens labelled heat stressed (i.e. cured at ambient temperature followed by heating at 50 °C for 1 week), it was observed that the Tg values ranged between 51 °C and 79 °C with SFPE displaying the lowest and SME exhibiting the highest. On this occasion, SPE and SFME presented Tgs between those of SME and SFPE. The following Tg trend was drawn:

SME > SFME > SPE > SFPE

Except for SFPE, this ranking does not agree with that of the other formulations obtained from the DSC ranking for the re-scan.

For the DMA self-supporting specimens labelled wet stressed (i.e. cured at ambient temperature followed by heating at 50 °C for 1 week followed by sea water immersion for 1 week), the ranking is similar to that obtained from the specimens, which were only heat stressed. The Tg trend was as follows:

SME > SFME > SPE > SFPE

However, the wet stressed specimens exhibited a minor decrease in Tg values compared to the Tg values from the heat stressed specimens. This decrease in Tg values is attributed to a likely plasticisation effect.

The DMA self-supporting specimens labelled hygrothermal stressed 1 (i.e. cured temperature at ambient followed by heating at 50 °C for 1 week followed by sea water immersion for 1 week followed by hygrothermal cycling between heat at 100 °C and sea water immersion for 1 day) exhibited a slightly different ranking as follows:

SME > SPE > SFME > SFPE

The DMA self-supporting specimens labelled hygrothermal stressed 2 (i.e. cured at ambient temperature followed by heating at 50 °C for 1 week followed by sea water immersion for 1 week followed by hygrothermal cycling between heat at 100 °C and sea water immersion for 1 week) exhibited a similar ranking as did the hygrothermal stressed 1 specimens. The ranking in this case is follows:

SME > SPE > SFME > SFPE

Overall, in all exposure conditions for this DMA analysis, SME consistently exhibited the highest Tg while SFPE constantly exhibited the lowest. The Tg values for the solvent containing formulations: SPE and SME increased significantly when heated and cycled at 100 °C. This significant increase in Tg values between the (unaged specimen) and hygrothermal stress 2 specimens (aged specimen) indicate additional loss of solvent and further cross linking. However, this was not the case for the solvent free formulations: SFPE (which had almost constant Tg value) and SFME (which had a very small increase of Tg value) between the reference and hygrothermal stress 2 specimens. A summary of Tg values using DMA is illustrated in Table 17.

Table 17 Summary of glass transition temperature, Tg using DMA

Reference	SME > SPE > SFME > SFPE
Heat Stressed	SME > SFME > SPE >SFPE
Wet Stressed	SME > SFME > SPE > SFPE
Hygrothermal Stressed 1	SME > SPE > SFME > SFPE
Hygrothermal Stressed 2	SME > SPE >> SFME > SFPE

(b) Tensile storage modulus of self-supporting free films

The modulus from tensile testing is an important property of materials including coatings, which directly reflects the rigidity or stiffness of the material. The moduli from tension deformation mode using the tensile fixture on DMA specimens (i.e. self-supporting free films) are reported here. The below Figure 55 shows the plot of tensile storage modulus (E') obtained in the rubbery region as a function of specimen exposure conditions.

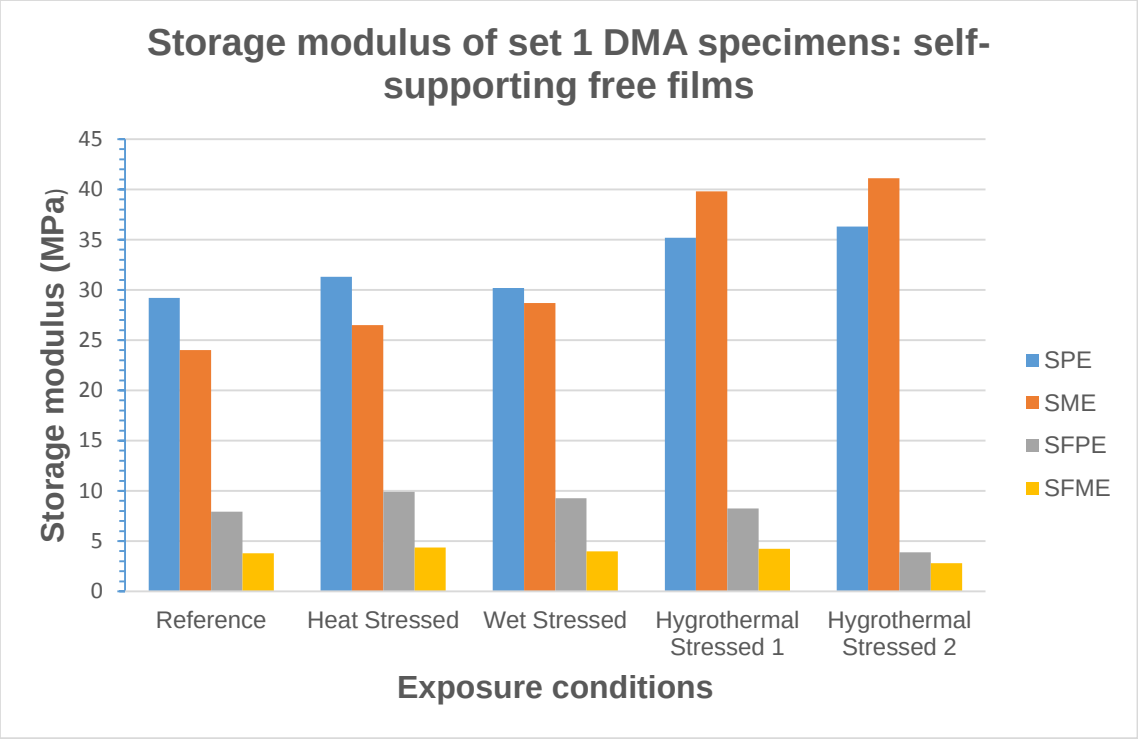

Figure 55 Bar chart plot of set 1: tensile storage modulus values measured for unaged and aged self-supporting specimens using DMA

For the DMA self-supporting specimens labelled reference shown in Figure 55, SPE exhibited the highest storage modulus (E') while SFME showed the lowest. SME and SFPE exhibited E' values between SPE and SFME. The trend for E' was as follows:

SPE > SME > SFPE > SFME

For the DMA self-supporting specimens labelled heat stressed, SPE and SME were observed to display significantly higher E' than SFPE and SFME. SPE showed the highest E' while SFME displayed the lowest E'. SME and SFPE displayed E' values between SPE and SFME. Thus, the following trend for E' was noted for the DMA self-supporting specimens labelled heat stressed:

SPE > SME > SFPE > SFME

This trend for E' from the DMA self-supporting specimens labelled heat stressed was the same as that seen for the reference ones.

For the DMA self-supporting specimens labelled wet stressed specimens, a similar trend as the reference and heat stress ones was observed:

SPE > SME > SFPE > SFME

For the DMA self-supporting specimens labelled hygrothermal stressed 1 specimens, there was a slight change in the trend as follows:

SME >SPE >> SFPE > SFME

It was observed that SPE and SME increased significantly in E' values. SME increased much more compared to SPE. Unlike SPE and SME, SFPE and SFME exhibited a small drop and a slight increase respectively.

Again, for the DMA self-supporting specimens labelled hygrothermal stressed 2 specimens, the following same trend as that of hygrothermal stressed 1 specimens was observed:

SME >SPE >> SFPE > SFME

In addition, the E' values for SPE and SME of hygrothermal stressed 2 specimens increased slightly while that of SFPE and SFME decreased significantly when compared to those specimens of hygrothermal stressed 1. This decrease in E' value was most apparent for SFPE.

The observed increase in storage modulus (E') for SPE and SME can be attributed to the higher content of pigments, fillers (rigid particles) resulting in an increased pigment volume concentration (PVC) when compared to SFPE and SFME. The PVCs are 27.88%, 26.21%, 10.65% and 8.96% for SPE, SME, SFPE and SFME respectively. SFPE and SFME presented very low storage modulus as reference specimens, which dropped significantly following hygrothermal cycling for one week. Furthermore, if the E' values obtained for reference specimens are compared to those obtained for hygrothermal stressed 2 specimens, it could be deduced that there is a significant affect to E' values following the exposure of specimens to 100 ºC for one week.

Also observed as in Table 18 for the hygrothermal stressed 1 specimens and the hygrothermal stressed 2 specimens, the obtained E' values for SPE and SME seem to have levelled. However, this was not the case for SFPE and SFME that required further exposure to 100 ºC of hygrothermal cycling to achieve stabilisation.

Table 18 Summary of set 1: tensile storage modulus E' at the rubbery region for unaged and aged self-supporting specimens using DMA

Formulations \ Exposure Conditions		Set 1 DMA specimens: Self-supporting Free Films (MPa)				
		Unaged	Aged			
		Reference (Ambient Cured)	Heat Stressed	Wet Stressed	Hygro-thermal Stressed 1	Hygro-thermal Stressed 2
Pure Epoxy	Solvent Containing (SPE)	29.2	31.3	30.2	35.2	36.3
	Solvent Free (SFPE)	7.92	9.92	9.26	8.26	3.90
Modified Epoxy	Solvent Containing (SME)	24.0	26.5	28.7	39.8	41.1
	Solvent Free (SFME)	3.80	4.35	3.97	4.23	2.79

A summary of storage modulus (E') values using DMA is illustrated in Table 19.

Table 19 Summary of tensile storage modulus E' using DMA

Reference	SPE > SME > SFPE > SFME
Heat Stressed	SPE > SME > SFPE >SFME
Wet Stressed	SPE > SME > SFPE > SFME
Hygrothermal Stressed 1	SME > SPE >>SFPE > SFME
Hygrothermal Stressed 2	SME > SPE >> SFPE > SFME

(c) Tan delta (δ) of self-supporting free films

Figures 56 through 64 provide overlays comparing the E' and tan δ values as a function of temperature obtained for the four formulations (SPE, SME, SFPE and SFPE) after exposure to different defined laboratory conditions. However, comments will be based only on the corresponding Tg of tan δ peak values as E' values were earlier discussed in section 5.2.2b.

Figure 56 shows tan δ values as a function of temperature for SPE after different exposures (reference, heat stressed, wet stressed and hygrothermal stressed). Tan δ is the ratio of the mechanical dissipation energy to stored energy. As observed in Figure 56, there was change in tan δ signals of SPE formulation occurring between 40 to 120 ^{o}C, which represented the ranges over the Tg. The peak height of each tan δ signal corresponds to a Tg value. As shown, the obtained Tg values corresponding to the peak tan δ was different for the four exposure conditions. The peak height of tan δ was highest for SPE New 4 (hygrothermal stressed 2 exposure) corresponding to 92 ^{o}C while it was lowest for SPE New 1 (heat stressed exposure) corresponding to 58 ^{o}C. This trend indicates the effect from the ageing process that induces loss or release of retained solvents and additional crosslinking of residuals following post cure. Ideally as observed for SPE, this process resulted in shifting of the height of the peak tan δ with the corresponding Tg to higher temperature magnitudes especially after heating at 100 ^{o}C for one week. The difference in Tg value between SPE New R and SPE New 4 (i.e. initially unaged and ultimately aged) was 37 ^{o}C (an increase of 67.3%). In addition, the tan δ signals of SPE New R and SPE New 2 (wet stressed) exhibited a reduced magnitude compared to SPE New 4, a consequence of the retained solvent(s) and residuals that retained much of the applied deformational energy and only allowing a small part to be dissipated at the interface. As expected SPE New 2 had a damping less than SPE New 1 because of further plasticisation from immersing in seawater. Therefore, the tan δ ranking of SPE formulation with corresponding Tg from highest to lowest is as follows:

SPE New 4 > SPE New 3 > SPE New 1 > SPE New R ≈ SPE New 2

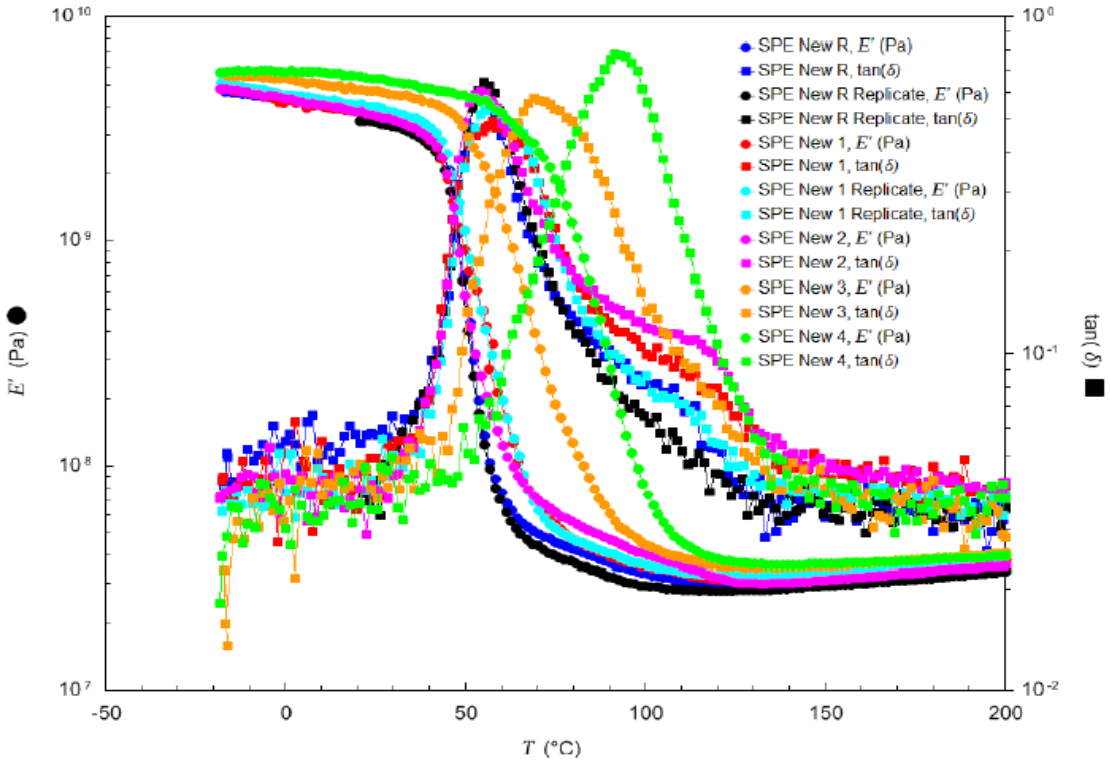

Figure 56 D.M.A Overlay of tensile storage modulus Vs temperature curve for SPE formulation

Similar to SPE in Figure 56 above, Figure 57 shows tan δ values as a function of temperature for SME after exposure to different conditions. As observed in Figure 57, there was change in tan δ signals of SME formulation occurring between 30 to 130 °C, which represented the ranges over the Tg. The peak value was highest for SME New 4 (hygrothermally stressed 2) corresponding to 101 °C while it was lowest for the SME R (reference) corresponding to 69 °C. Again, this trend agrees with the effect of the ageing process that is evident as exposure progressed with the application of heat. There was shifting of the tan δ peak heights with corresponding Tg values to higher temperature magnitudes (especially after heating at 100 °C for one week). The difference in Tg value between SME New R and SME New 4 was 32 °C (an increase of approximately 46.4%). This observation is a consequence following the release of retained solvent and further cross-linking of residuals. SME New 2 had a damping less than SME New 1 because of further plasticisation from immersing in seawater. The tan δ ranking of SME formulation with corresponding Tg from highest to lowest is as follows:

SME New 4 > SME New 3 > SME New 1 > SME New 2 > SME New R

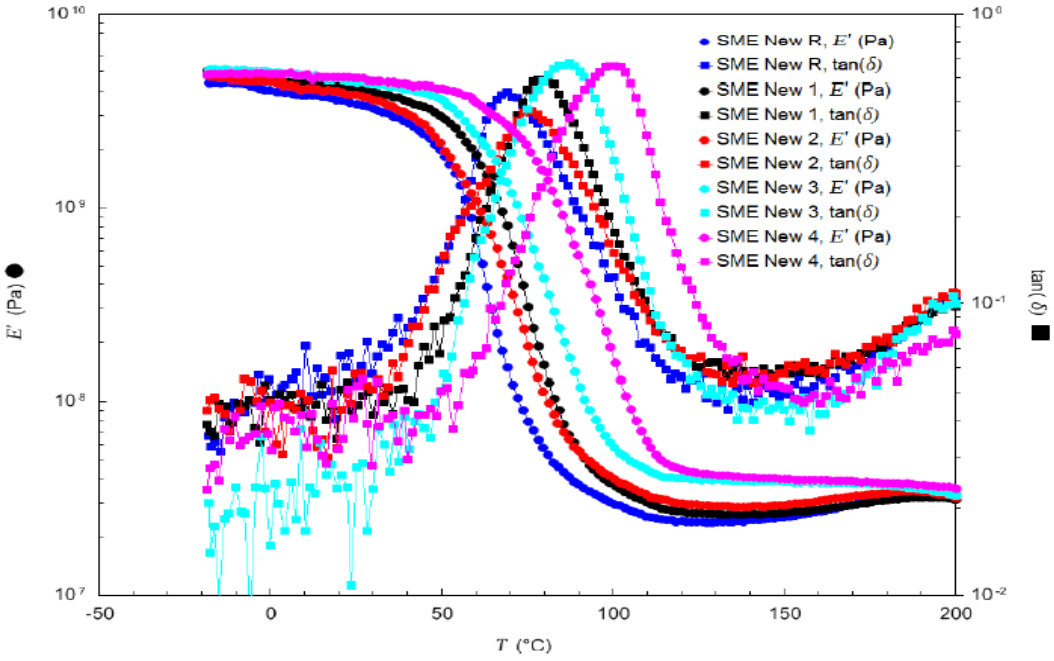

Figure 57 D.M.A Overlay of tensile storage modulus Vs temperature curve for SME formulation

Figure 58 shows tan δ values as a function of temperature for SFME after exposure to different defined laboratory conditions. As observed in Figure 58, there was change in tan δ signals of SFME formulation occurring between 20 to 90 °C, which represented the ranges over the Tg. The peak height of tan δ was highest for the SFME New 4 (hygrothermally stressed 2) corresponding to 59 °C while it was lowest for SFME New 1 (heat stressed) corresponding to the highest Tg at 60 °C. Except for SFME New 4, the height for peak tan δ of SFME New R (reference) was higher than SFME New 1, SFME New 2 (wet stressed) and SFME New 3 (hygrothermally stressed 1). However, the corresponding Tg value for SFME New R was the lowest as expected. SFME New 3 exhibited an unusual behaviour with a drop in corresponding Tg value from the peak tan δ height. This behaviour was attributed to further plasticisation from the wet exposure. The difference in Tg magnitude between the SFME New R and SFME New 4 was 6 °C (an increase of 11.3%). In general, this trend indicates less effect of the ageing process on SFME as the increase in Tg between exposure conditions was small, an indication of less change for SFME after

initial cure (with less residual reactants and less crosslinking) compared to that seen for SPE and SME with similar progressive exposures. In addition, SFME contained liquid diluent that seemed to remain within the coating matrix following the exposure conditions. The tan δ ranking of SFME formulation with corresponding Tg from highest to lowest is as follows:

SFME New 4 > SFME New 1 > SFME New 2 > SFME New R > SFME New 3

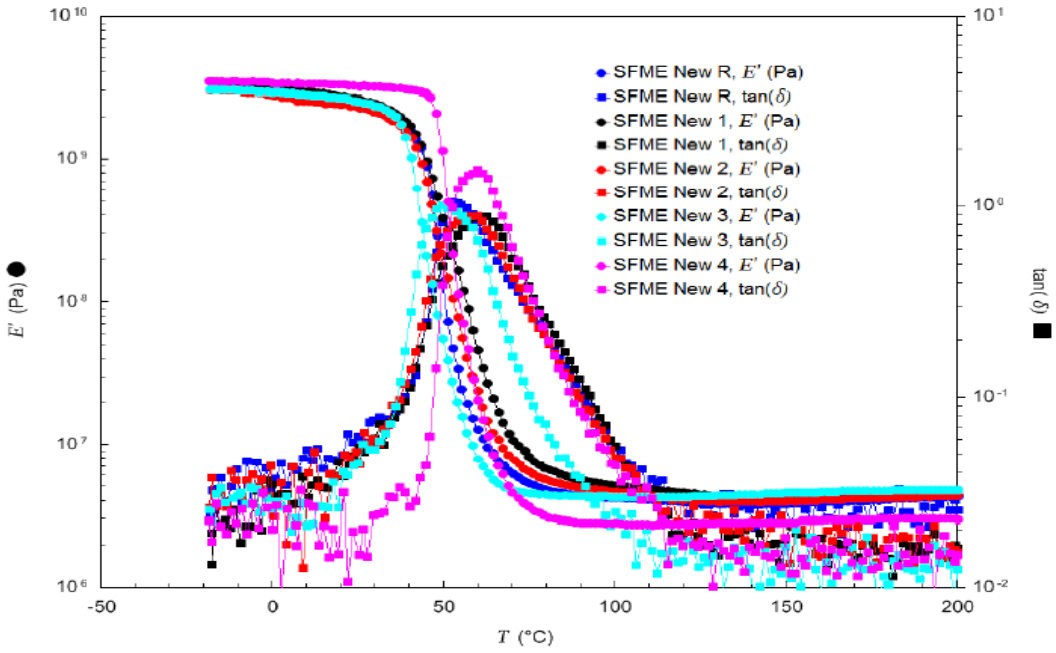

Figure 58 D.M.A Overlay of tensile storage modulus Vs temperature curve for SFME formulation

Figure 59 shows tan δ values as a function of temperature for SFPE after exposure to different defined laboratory conditions. There was change in tan δ signals of SFPE formulation occurring between 25 to 90 °C, which represented the ranges over the Tg. The peak height of tan δ was highest for the SFPE New 3 (hygrothermally stressed 1) corresponding to 45 °C while it was lowest for SFPE New 2 (wet stressed) corresponding to 50 °C. The heights for peak tan δ of SFPE New 3 and SFPE New 4 (hygrothermally stressed 2) were higher than those of SFPE New R (reference), SFPE New 1 (heat stressed), and SFPE New 2. However, the corresponding Tg magnitude for SFPE New 3 was the lowest. Similar to SFME New 3, SFPE New 3 exhibited an unusual behaviour with a drop in corresponding Tg value from the peak tan δ height. This

behaviour was attributed to further plasticisation from the wet exposure. The difference in Tg value between the SFPE New R and SFPE New 4 was -1 ºC (a decrease of 2%). In general, this trend indicates little or no effect of the ageing process on SFPE when compared to that seen for SFME, SME and particularly SPE. A potential reason is that, SFPE contained reactive diluent that reacted and remained within the coating matrix following the progressive exposure conditions. The tan δ ranking of SFPE formulation with corresponding Tg from highest to lowest is as follows:

SFPE New R > SFPE New 1 ≈ SFPE New 4 > SFPE New 2 > SFPE New 3

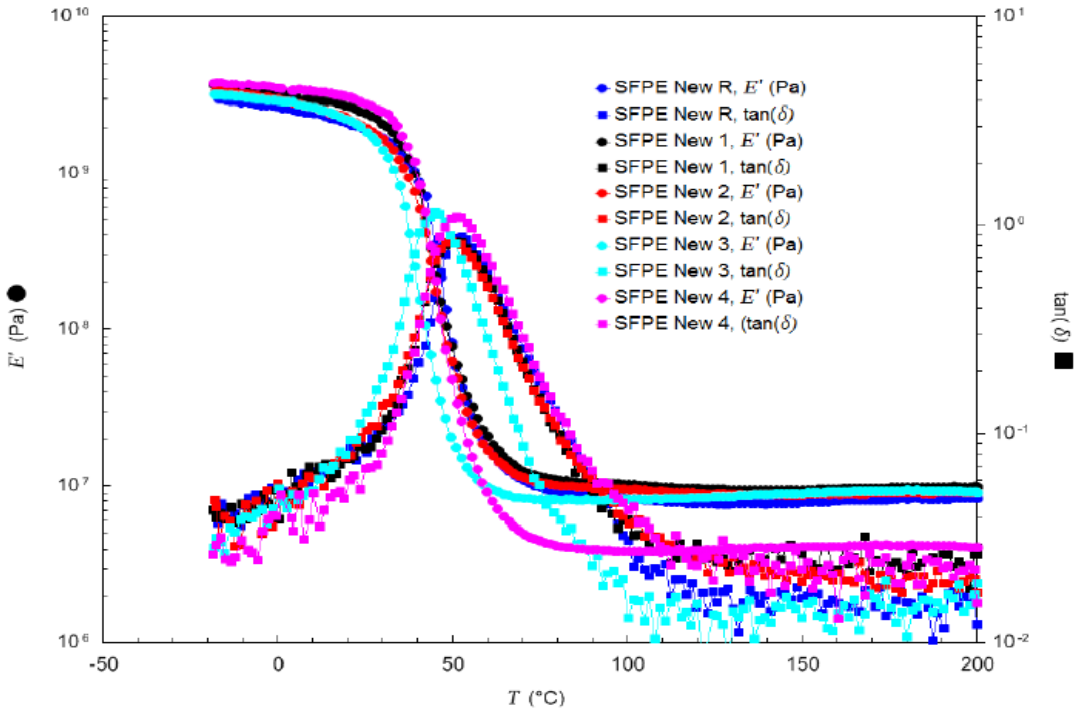

Figure 59 D.M.A Overlay of tensile storage modulus Vs temperature curve for SFPE formulation

Figure 60 shows tan δ values as a function of temperature in a combined plot of the four formulations for reference exposure condition. There was change in tan δ signals occurring between 30 to 110 ºC, which represented the ranges over the Tg. The peak height of tan δ was highest for SFME New R corresponding to 53 ºC while it was lowest for SME New R corresponding to 69 ºC. Although the height for peak tan δ for SPE New R and SME New R was below that of SFME

New R and SFPE new R, both had corresponding Tg magnitudes greater than those for SFME New R and SFPE new R. The tan δ ranking for this combination with corresponding Tg from highest to lowest is as follows:

SME New R > SPE New R > SFME New R ≈ SFPE New R

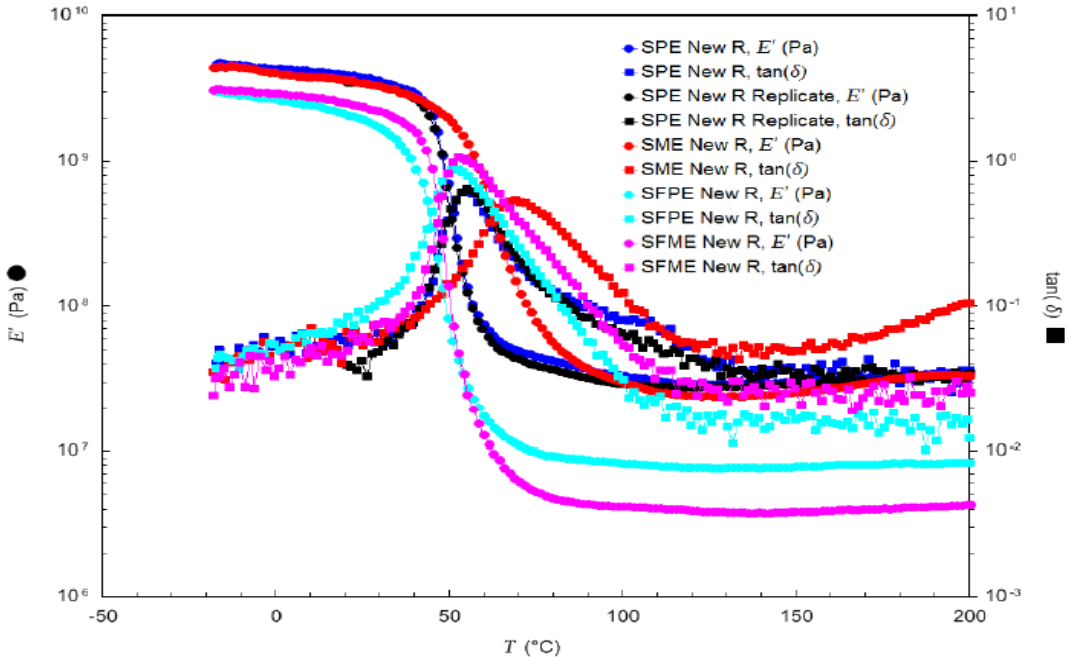

Figure 60 D.M.A Overlay of tensile storage modulus Vs temperature curve for the four formulations - reference

Figure 61 shows tan δ values as a function of temperature in a combined plot the four formulations for heat stressed exposure condition. There was change in tan δ signals occurring between 30 to 120 °C, which represented the ranges over the Tg. The peak height of tan δ was highest for SFME New 1 corresponding to 60 °C while it was lowest for SPE New 1 corresponding to 58 °C. Although the height for peak tan δ for SPE New 1 and SME New 1 was below those of SFME New 1 and SFPE new 1, only SFPE New 1 had corresponding Tg value less than SPE New 1, SME New 1 and SFME new 1. SPE New 1 and SME New 1 damped less than SFPE New 1 and SFME New 1 because both had retained solvents and residual reactants that required a temperature above 50°C to induce further reaction. The tan δ ranking for this combination with corresponding Tg from highest to lowest is as follows:

SME New 1 > SFME New 1 > SPE New 1 > SFPE New 1

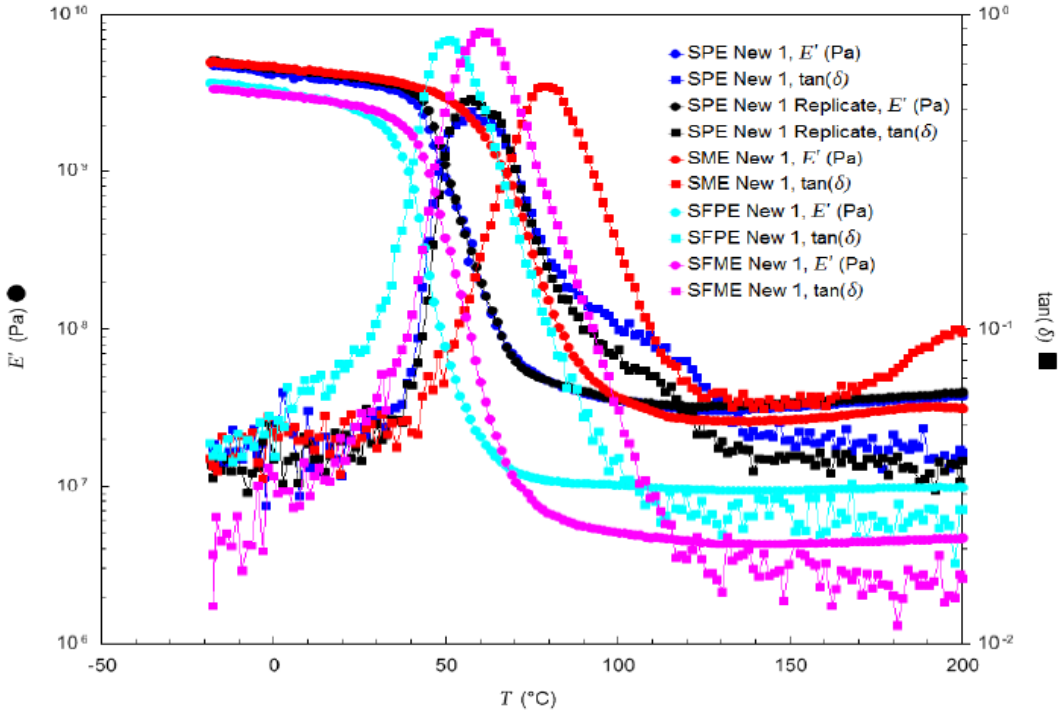

Figure 61 D. M.A Overlay of tensile storage modulus Vs temperature curve for the four formulations - dry heat stressed

Figure 62 shows tan δ values as a function of temperature in combining the four formulations: SPE, SME, SFPE and SFME exposed to wet stressed condition. There was change in tan δ signals occurring between 30 to 120 °C, which represented the ranges over the Tg. The peak height of tan δ was highest for SFME New 2 corresponding to 57 °C while it was lowest for SME New 2 corresponding to 50 °C. Although the heights for peak tan δ for SPE New 2 and SME New 2 were below that of SFME New 2 and SFPE new 2, only SFPE New 2 had corresponding Tg value less than SPE New 2, SME New 2 and SFME new 2. Similar to the heat stressed condition, the tan δ ranking for this combination with corresponding Tg from highest to lowest is as follows:

SME New 2 > SFME New 2 > SPE New 2 > SFPE New 2

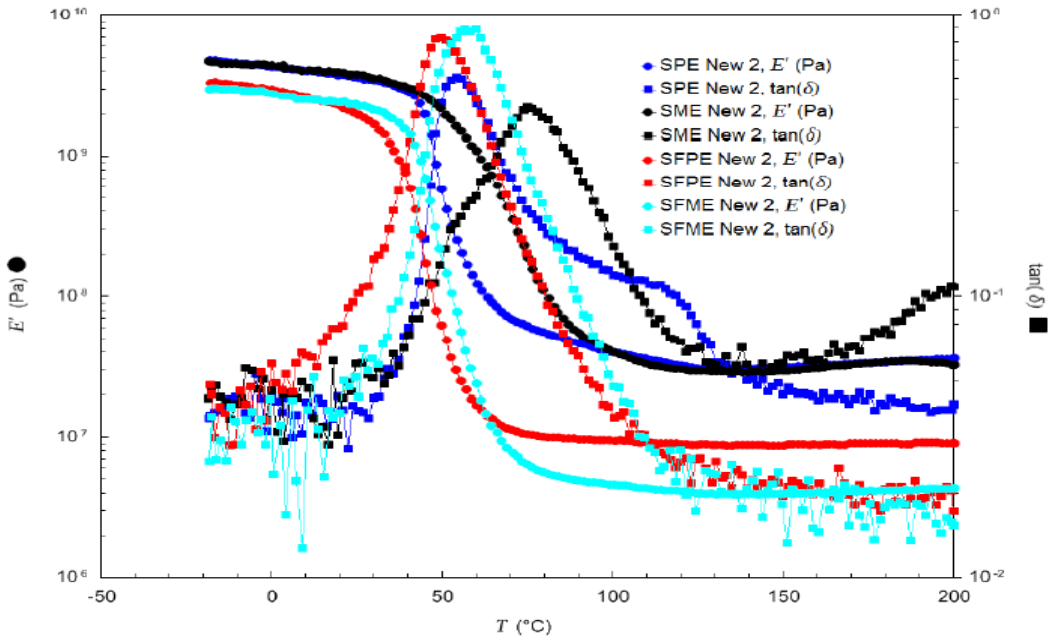

Figure 62 D. M.A Overlay of tensile storage modulus Vs temperature curve for the four formulations - wet stressed

Figure 63 shows tan δ values as a function of temperature in combining the four formulations: SPE, SME, SFPE and SFME for a particular define laboratory exposure condition: hygrothermal stressed 1. There was change in tan δ signals occurring between 20 to 120 ^{o}C, which represented the ranges over the Tg. The peak height of tan δ was highest for SFPE New 3 corresponding to 45 ^{o}C while it was least for SPE New 3 corresponding to 69 ^{o}C. Although the height for peak tan δ for SPE New 3 and SME New 3 was below that of SFME New 3 and SFPE new 3, both SPE New3 and SME New 3 had corresponding Tg values greater than SFME New 3 and SFPE new 3. This observation suggests that the less cross-linked formulations (SPE New 3 and SME New 3) at ambient cure are ageing more during progressive exposure than others that are much cross-linked (SFPE New 3 and SFME New 3). The tan δ ranking for this combination with corresponding Tg from highest to lowest is as follows:

SME New 3 > SPE New 3 > SFME New 3 > SFPE New 3

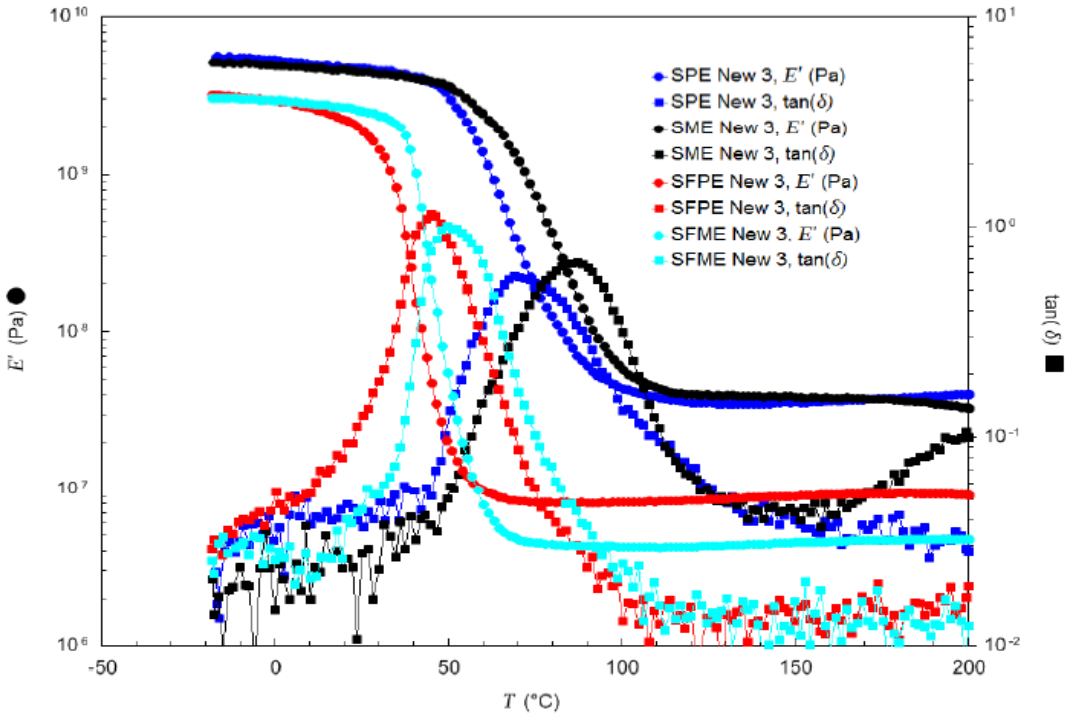

Figure 63 D. M.A Overlay of tensile storage modulus Vs temperature curve for the four formulations – hygrothermally cycled stressed 1

Figure 64 shows tan δ values as a function of temperature in combining the four formulations: SPE, SME, SFPE and SFME exposed to hygrothermal stressed 2 condition. There was change in tan δ signals occurring between 20 to 130 °C, which represented the ranges over the Tg. The peak height of tan δ was highest for SFME New 4 corresponding to 59 °C while it was lowest for SME New 4 corresponding to 101 °C. Although the height for peak tan δ for SPE New 4 and SME New 4 was below that of SFME New 4 and SFPE new 4, both SPE and SME had corresponding Tg values greater than SFME New 4 and SFPE new 4. This observation is similar to hygrothermal stressed 1. The tan δ ranking for this combination with corresponding Tg from highest to lowest is as follows:

SME New 4 > SPE New 4 > SFME New 4 > SFPE New 4

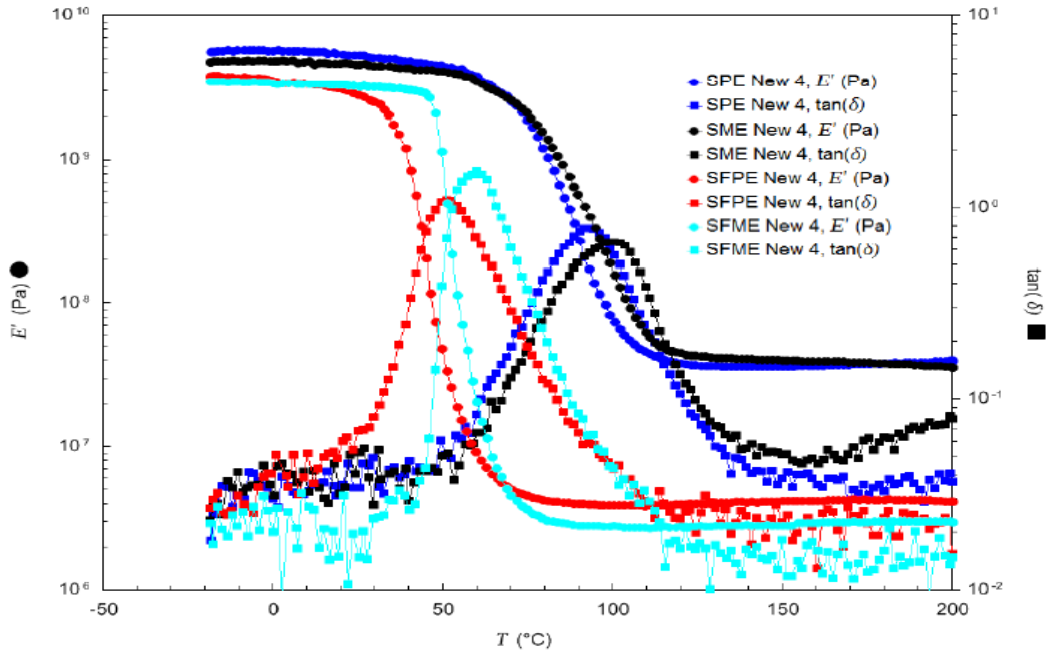

Figure 64 D. M.A Overlay of tensile storage modulus Vs temperature curve for the four formulations – Hygrothermally cycled stressed 2

(c) Glass transition temperature Tg of non-self-supporting free films

Presented in Figure 65 is the bar chart plot of Tgs as a function of the fatigue exposure condition for SPE, SME, SFPE and SFME.

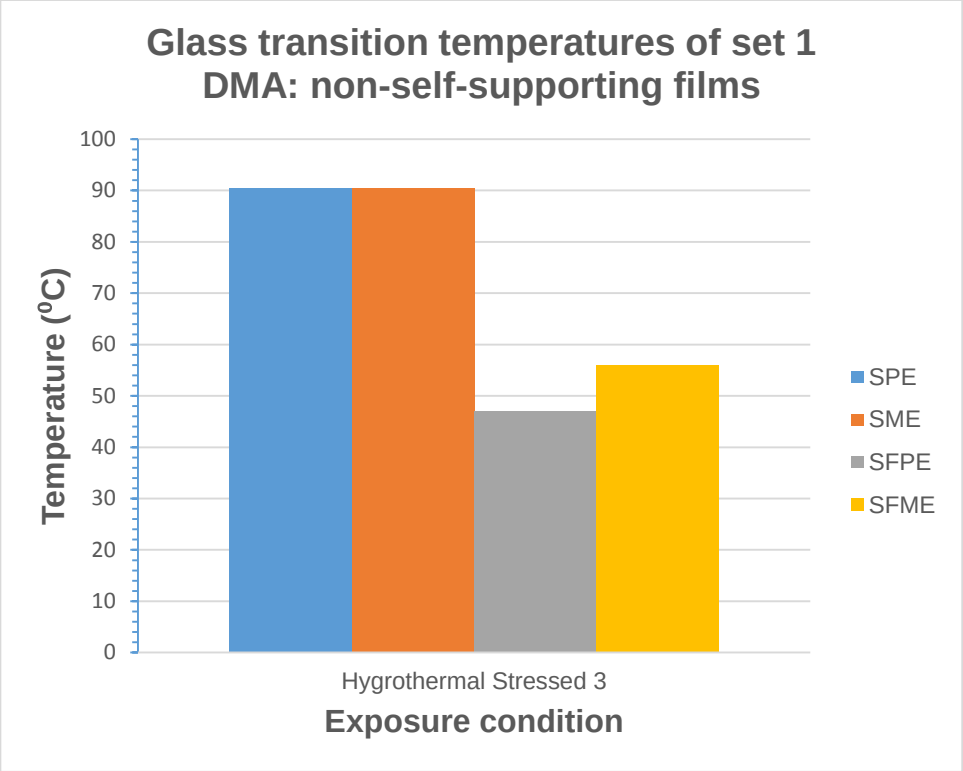

Figure 65 Bar chart plot of set 1: Tg values measured for the non-self-supporting specimens using DMA

For DMA non-self-supporting specimens (i.e. flakes removed form cycled T specimens and labelled as hygrothermal stressed 3), it was observed that the values of Tg averaged from two temperature scan ranged from 47 °C to 90.5 °C. Both SPE and SME exhibited same Tg which was the highest while SFPE showed the lowest. SFME showed Tg value of 56 °C. The following Tg trend was drawn:

SPE ≈ SME > SFME > SFPE

As shown in Figure 66, this ranking from the DMA non-self-supporting specimens (labelled as hygrothermal stressed 3) compares to that from the DMA self-supporting specimens (labelled as hygrothermal stressed 2), which were also hygrothermal stressed for a much shorter period.

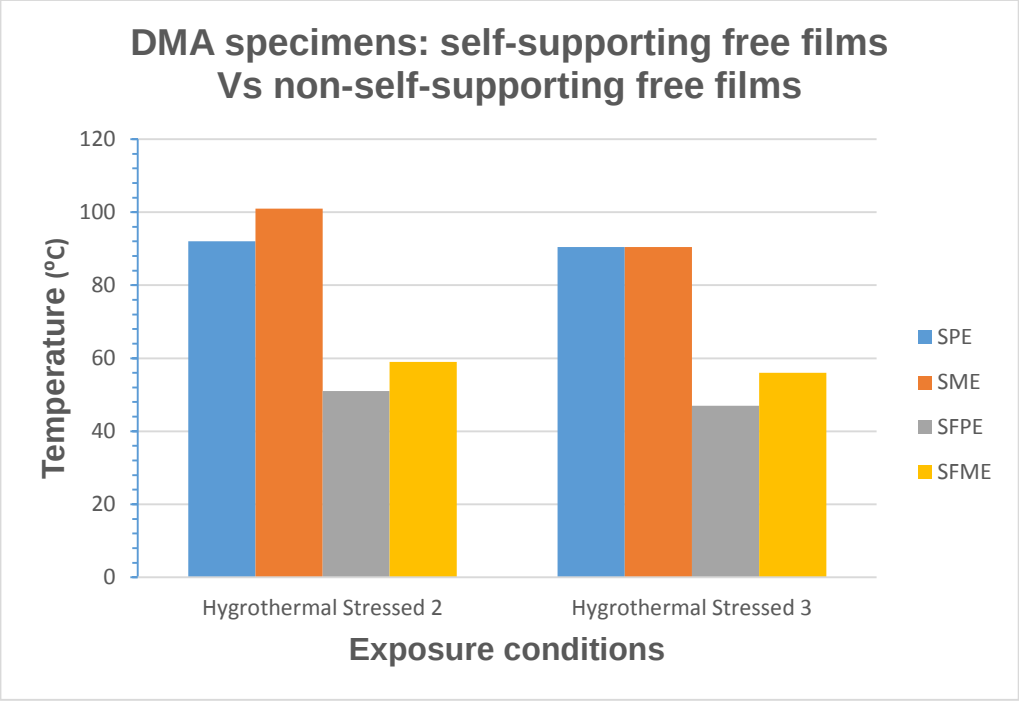

Figure 66 Bar chart plot of set 1: Tg values for self-supporting specimens Vs non-self-supporting specimens using DMA

In addition, except for SME whose Tg increased slightly for the self-supporting specimens, the Tg values obtained for the non-self-supporting specimens are reasonably close to those obtained for the self-supporting specimens despite two different types of DMA modes of deformation (i.e. tension and bending) and fixtures were utilised. Thus, there is very good agreement with both DMA modes of deformation and fixtures as SPE and SME exhibited the higher Tg values while SFPE and SFME exhibited much lower Tg values than SPE and SME. Also, shown in Table 20 is the Tg values.

Table 20 Set 1: Tg values obtained for non-self-supporting specimens using DMA

Formulations \ Exposure Conditions		Set 1 DMA specimens: Non-Self-supporting Free Films (°C)
		Aged
		Hygrothermal Stressed 3
Pure Epoxy	Solvent Containing (SPE)	90.5
	Solvent Free (SFPE)	47
Modified Epoxy	Solvent Containing (SME)	90.5
	Solvent Free (SFME)	56

A summary of Tg values using DMA is illustrated in Table 21.

Table 21 Summary of glass transition temperature, Tg using DMA

Hygrothermal Stressed 3	SPE ≈ SME >> SFME > SFPE

(d) Bending storage modulus of non-self-supporting free films

The moduli from bending deformation mode using the single cantilever fixture on DMA specimens (i.e. non-self-supporting free films) are reported here. The below Figure 67 shows the plot of storage modulus (E') obtained in the rubbery region as a function of specimen exposure condition.

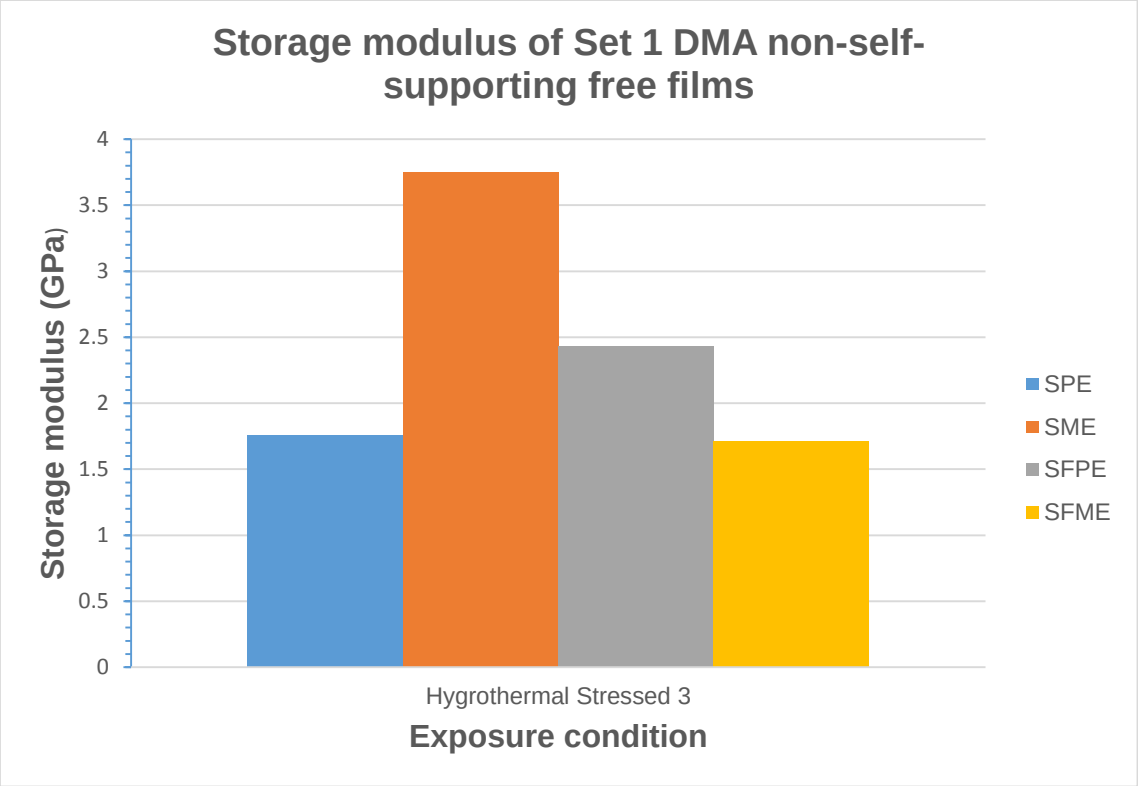

Figure 67 Bar chart plot of set 1: storage modulus values measured for non-self-supporting specimens using DMA

For the DMA non-self-supporting specimens shown in Figure 67, it was observed that SME exhibited the highest storage modulus (E') and SFME showed the lowest. SPE and SFPE exhibited E' values between SME and SFME. The trend for E' can be deduced as follows:

SME > SFPE > SPE > SFME

This ranking from the DMA non-self-supporting specimens is different to that from DMA self-supporting specimens, which were hygrothermal stressed. However, the ranking agrees in both cases that SME has the highest E' value and SFME has the lowest E' value. In addition as shown in Figure 68, the E' values for the non-self-supporting specimens are much more than those obtained for the self-supporting specimens which could be attributed to the two different types of DMA modes of deformation (i.e. tension and bending), steel Material Pocket (MP) and fixtures utilised.

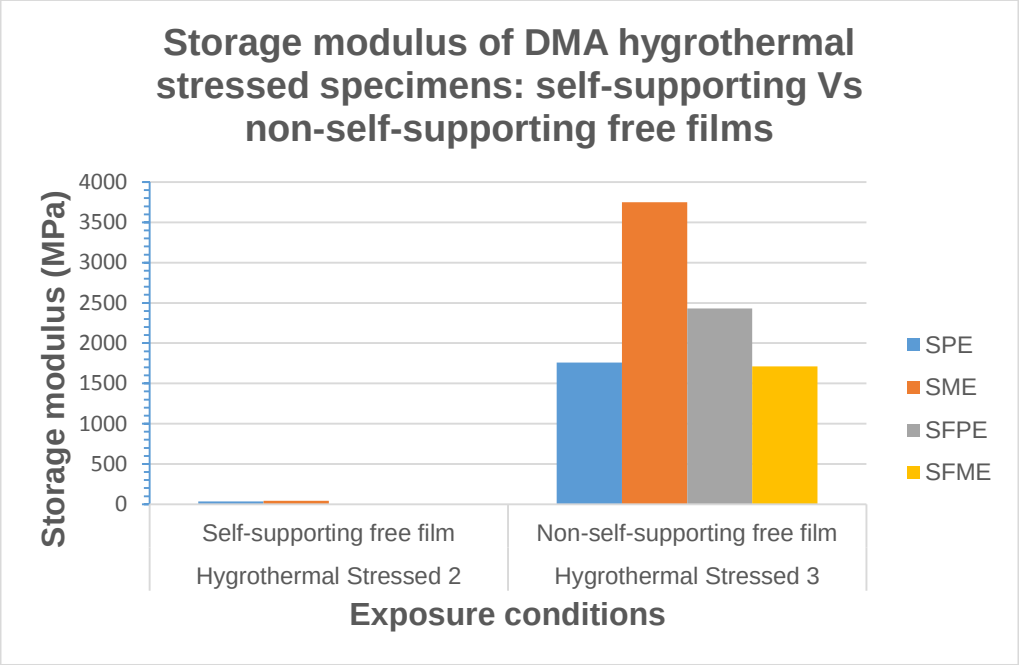

Figure 68 Bar chart plot of Storage modulus values measured for self-supporting and non-self-supporting specimens

As shown in Table 22, the average moduli of the steel MP obtained from duplicate DMA temperature scans was 43100 MPa (or 43.1 GPa). For SPE, SME, SFPE and SFME formulations, the average moduli obtained from duplicate temperature scan were 1760 MPa, 3750 MPa, 2430 MPa and 1710 MPa (or 1.76 GPa, 3.75 GPa, 2.43 GPa and 1.71 GPa) respectively. Although, this value of 43.1 GPa obtained from DMA testing is much less compared to typical quoted value of 208 GPa [50]; which relates to the elastic modulus of steel from uniaxial tensile testing, it does indicate that the stiffness of the steel MP was much more than that of the DMA specimens: non-self-supporting free films. Furthermore, as the average moduli of the non-self-supporting free films ranged 1.71 GPa to 3.75 GPa, it was impossible to subtract moduli of the films from that of the steel MP: 43.1 GPa. Comparing the E' data obtained from both DMA mode of deformations, it is clear that the steel MP significantly influenced the obtained E' values for the non-self-supporting free films. Again, as the steel MP does not exhibit any transitions within the DMA temperature scan and significantly influence the E' values, the E' obtained from this method should be

used with caution and could be unbeneficial for ranking performance of coating films.

Table 22 Set 1: E' values obtained for non-self-supporting specimens and steel material pocket using DMA

Formulations \ Exposure Conditions		Set 1 DMA specimens: Non-Self-supporting Free Films (GPa)
		Aged
		Hygrothermal Stressed 3
Pure Epoxy	Solvent Containing (SPE)	1.76
	Solvent Free (SFPE)	2.43
Modified Epoxy	Solvent Containing (SME)	3.75
	Solvent Free (SFME)	1.71
Support	Steel Material Pocket	43.1

A summary of E' values using DMA is illustrated in Table 23.

Table 23 Summary of the storage modulus, E' using DMA

Hygrothermal Stressed 3	SME > SFPE > SPE > SFME

5.2.3 Thermo-mechanical analysis

(a) Glass transition temperature

As illustrated in Figure 69 and Table 24, one of the measurements obtained from the TMA was Tg. For specimens of TMA labelled reference, it was observed that the values of Tg ranged from 48.5 °C to 53.6 °C. SFME exhibited the highest Tg while SFPE showed the lowest. SPE and SME showed Tg values of 50.7 °C and 52.5 °C. The following Tg trend was drawn:

SFME > SME > SPE > SFPE

Comparing this ranking of reference specimens from the TMA to reference specimens of either the DSC or the DMA showed that there was no agreement between the rankings.

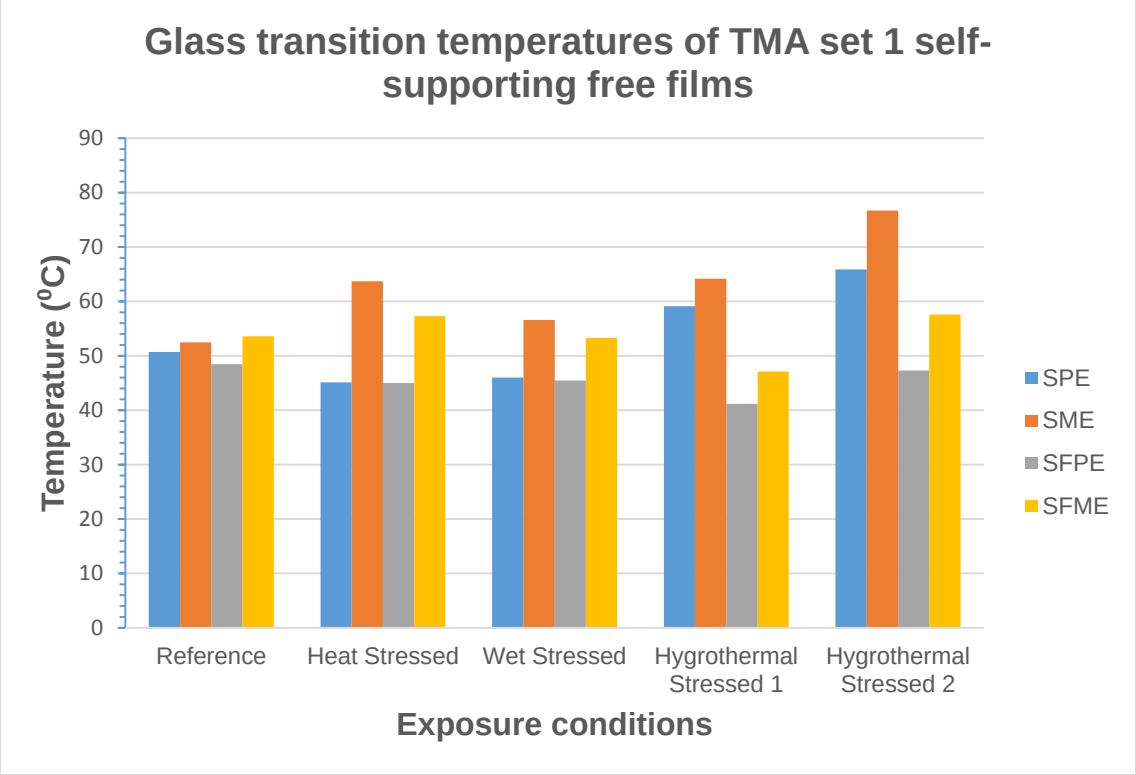

Figure 69 Bar chart plot of Tg measured using TMA

Table 24 Values of glass transition temperature (Tg) measured using TMA

Formulations / Exposure Conditions		Set 1 TMA specimens: Self-supporting Free Films (°C)				
		Unaged	Aged			
		Reference (Ambient Cured)	Heat Stressed	Wet Stressed	Hygro-thermal Stressed 1	Hygro-thermal Stressed 2
Pure Epoxy	Solvent Containing (SPE)	50.7	45.1	46.0	59.1	65.9
	Solvent Free (SFPE)	48.5	45.0	45.5	41.2	47.3
Modified Epoxy	Solvent Containing (SME)	52.5	63.7	56.6	64.2	76.7
	Solvent Free (SFME)	53.6	57.3	53.3	47.1	57.6

For the TMA specimens labelled heat stressed, it was observed that the Tg values ranged between 45.0 °C and 63.7 °C with SFPE displaying the lowest and SME exhibiting the highest. Also, SPE and SFME presented Tgs between those of SME and SFPE. The following Tg trend was drawn:

SME > SFME > SPE > SFPE

This ranking correlated closely to that obtained from the DMA ranking that were heat stressed.

For the TMA specimens labelled wet stressed, the ranking is similar to that obtained from the TMA specimens which were heat stressed. Also, the ranking is similar to that from DMA ranking for wet stressed. The following Tg trend was drawn:

SME > SFME > SPE > SFPE

For the TMA specimens labelled hygrothermal stressed 1, the ranking exhibited was as follows:

SME > SPE > SFME > SFPE

This ranking from TMA was different from the wet stressed. However, the position of SME and SFPE were consistent with earlier reported TMA ranking for heat stressed and wet stressed. Furthermore, the TMA ranking for hygrothermal stressed 1 was consistent with DMA ranking for hygrothermal stressed 1.

For the TMA specimens labelled hygrothermal stressed 2, the ranking exhibited is as follows:

SME > SPE > SFME > SFPE

It was observed that this ranking from TMA for hygrothermal stressed 2 was consistent with TMA ranking for hygrothermal stressed 1.

Table 25 illustrates the summary of the glass transition temperature Tg using TMA.

Table 25 Summary of glass transition temperature, Tg using TMA

Reference	SFME > SME > SPE > SFPE
Heat Stressed	SME > SFME > SPE >SFPE
Wet Stressed	SME > SFME > SPE > SFPE
Hygrothermal Stressed 1	SME > SPE > SFME > SFPE
Hygrothermal Stressed 2	SME > SPE > SFME > SFPE

(b) Coefficient of thermal expansion

Table 26 and Figure 70 showed the magnitudes of coefficient of thermal expansion obtained using TMA. Figures 71 shows the combined TMA plot. For specimens of TMA labelled reference, the magnitudes of CTE ranged from 53.3-74.4 µm/m°C. SFPE exhibited the highest CTE while SPE showed the lowest. SME and SFME showed CTE magnitudes of 56.6 µm/m°C and 63.6 µm/m°C respectively. The following CTE trend was established:

SFPE > SFME > SME > SPE

This ranking for CTE of reference specimens from the TMA is different to that obtained using either the DSC or the DMA as the process measured are different.

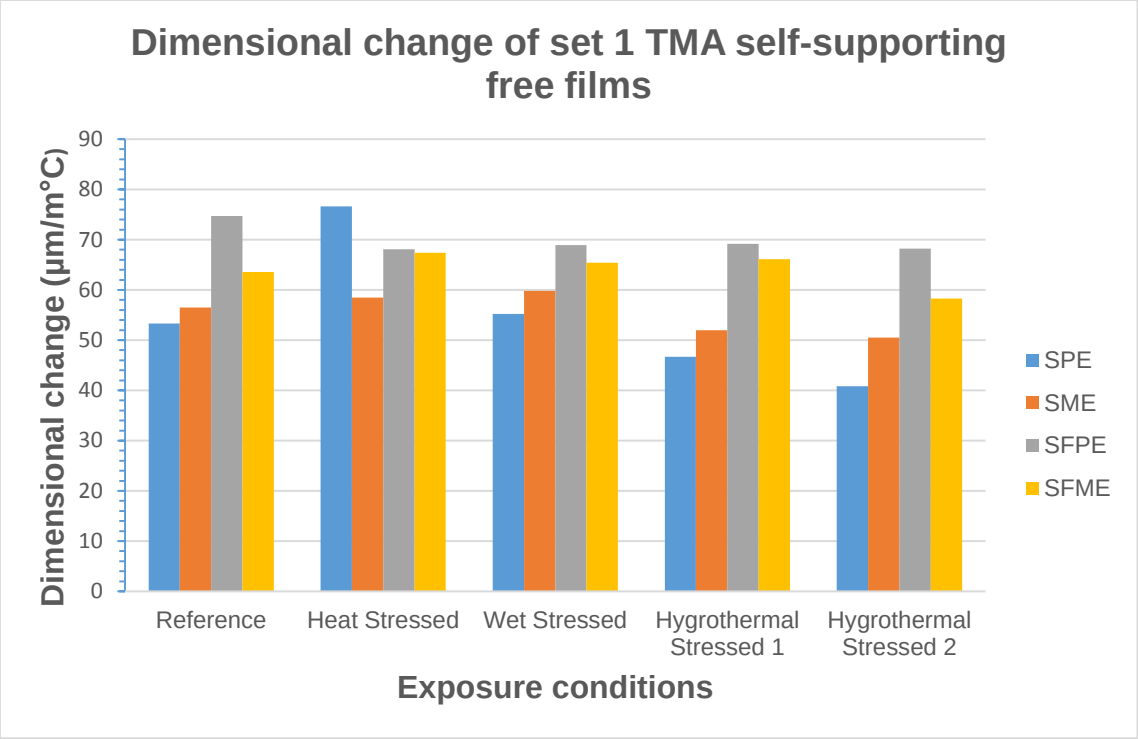

Figure 70 Bar chart plot of CTE measured using TMA

Table 26 Values of coefficient of thermal expansion (CTE) measured using TMA

Formulations \ Exposure Conditions		Set 1: TMA specimens: Self-supporting Free Films (µm/m°C)				
		Unaged	Aged			
		Reference (Ambient Cured)	Heat Stressed	Wet Stressed	Hygro-thermal Stressed 1	Hygro-thermal Stressed 2
Pure Epoxy	Solvent Containing (SPE)	53.3	76.6	55.2	46.7	40.8
	Solvent Free (SFPE)	74.7	68.1	68.9	69.2	68.2
Modified Epoxy	Solvent Containing (SME)	56.5	58.5	59.8	52.0	50.5
	Solvent Free (SFME)	63.6	67.4	65.4	66.1	58.3

For the TMA specimens labelled heat stressed, it was observed that the CTE values ranged between 58.5 µm/m°C and 76.6 µm/m°C with SME displaying the lowest and SPE exhibiting the highest. Also, SFPE and SFME presented CTE values between those of SPE and SME. The following CTE trend was established:

SPE > SFPE > SFME > SME

This ranking is not in agreement with that from the TMA ranking for reference specimens.

For the TMA specimens labelled wet stressed, the ranking is similar to that obtained from the reference TMA specimens and dissimilar to those obtained from the heat stressed ones. The following CTE trend was established:

SFPE > SFME > SME > SPE

For the TMA specimens labelled hygrothermal stressed 1, the ranking exhibited was as follows:

SFPE > SFME > SME > SPE

This TMA ranking from hygrothermal stressed 1 specimens was consistent with the TMA ranking for both wet stressed and reference specimens.

For the TMA specimens labelled hygrothermal stressed 2, the ranking exhibited was as follows:

SFPE > SFME > SME > SPE

The TMA ranking for hygrothermal stressed 2 was consistent with TMA ranking for reference, wet stressed and hygrothermal stressed 1 specimens. Furthermore, it emerged that SFPE and SFME had higher CTEs in most exposure cases considered while SPE and SME had less CTEs when compared to SFPE and SFME. Table 27 illustrates the summary of the CTE using TMA.

Table 27 Summary of coefficient of thermal expansion, CTE using TMA

Reference	SFPE > SFME > SME > SPE
Heat Stressed	SPE > SFPE > SFME >SME
Wet Stressed	SFPE > SFME > SME > SPE
Hygrothermal Stressed 1	SFPE > SFME > SME > SPE
Hygrothermal Stressed 2	SFPE > SFME > SME > SPE

Figure 71 provides a combined TMA plot of dimensional change for coefficient of thermal expansion as a function of temperature obtained for the four formulations after exposure to different defined laboratory conditions.

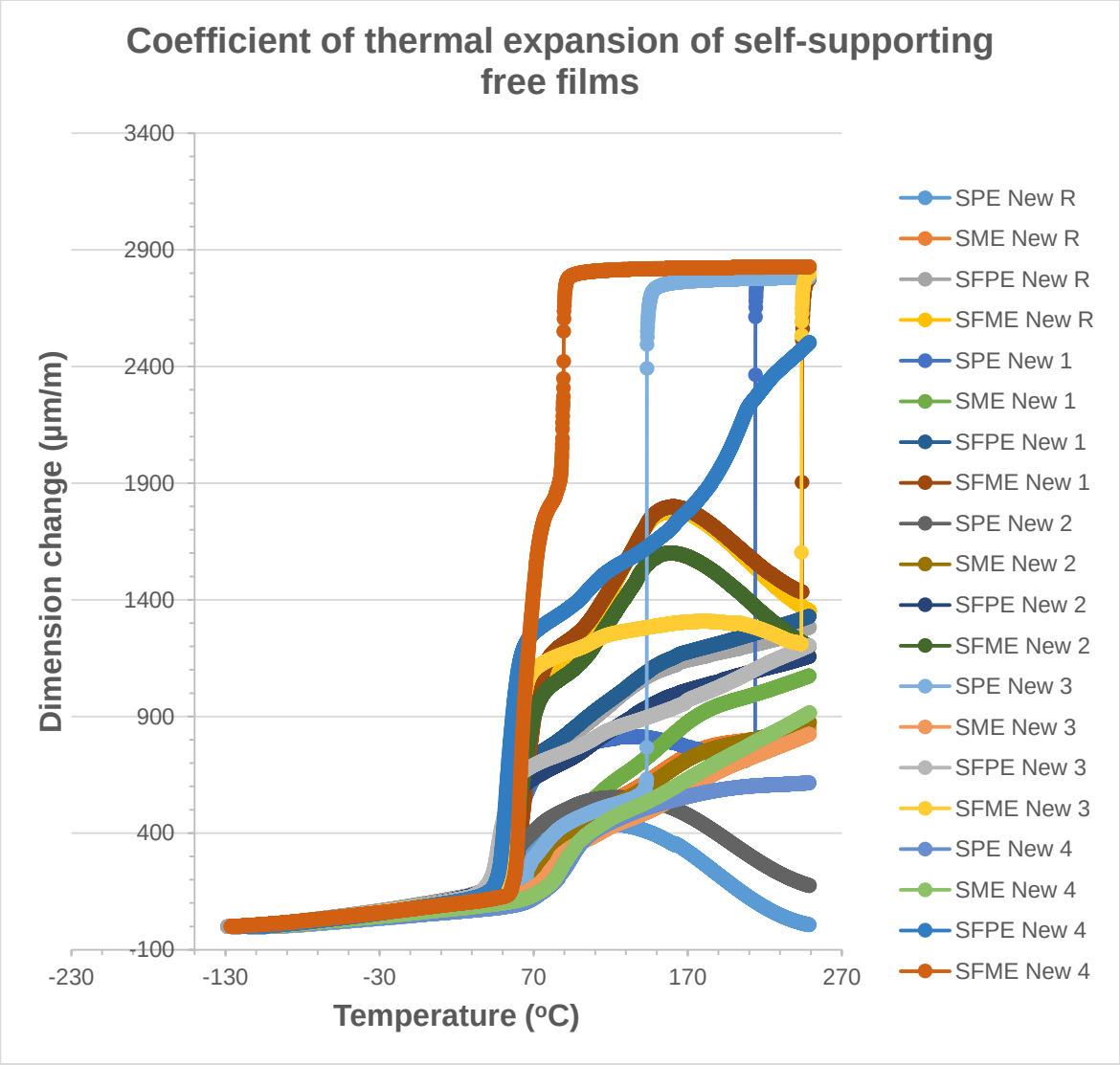

Figure 71 Overlay plot of CTE measured using TMA for set 1 free films

The average CTE from the exposure conditions are 69.82 µm/mºC, 64.16 µm/mºC, 55.46 µm/m ºC and 54.52 µm/m ºC for SFPE, SFME, SME and SPE respectively. Comparing the average CTE of each formulation to the CTE of structural steel (12 µm/m ºC) [104], it was observed that the difference (or mismatch) in CTE are 58.82 µm/m ºC, 52.16 µm/m ºC, 43.46 µm/m ºC and 42.52 µm/m ºC for SFPE, SFME, SME and SPE respectively. In relating the mismatch CTE values to the result obtained from the fatigue test in sections 5.2.1 and 5.4.1, a plausible conclusion is that the mismatched CTE had the least effect on SFPE with the highest magnitude. On the contrary, SPE with the lowest

average mismatched CTE was adversely affected by cracking after one cycle of the fatigue test. As the top temperature for the fatigue test was at 100 ^{o}C, SFPE and SFME will be stress relieved because this top cycling temperature is much above their ultimate Tg of less than 60 ^{o}C as recorded from the thermal analysers. Thus, implying that SFPE and SFME were in the rubbery region where there is increased molecular motion within the coating matrix. In contrast, the ultimate Tgs of SPE and SME reached 90 ^{o}C and above for the DMA and DSC thermal analysers. Thus, indicating that SPE and SME are likely to be within the glassy region where there is limited molecular movement. In conclusion, formulations (SFPE and SFME) with higher CTE and more mismatched magnitude to steel performed much better than those (SPE and SME) with lower CTE and less mismatch magnitude.

5.3 Mechanical Tensile Testing

This section presents the results from investigating dog bone free film specimens of the four formulations: SPE, SFPE, SME and SFME at 640 µm and 960 µm DFTs. Two variants of dog bone specimens were evaluated. One set were cured at ambient temperature only while the other set was cured at ambient temperature followed by 100 ºC temperature. The results from the mechanical analysis of the dog bone specimens are engineering stress versus engineering strain curves. Figures 72 and 73 showed the obtained results following uniaxial tensile testing of the specimens cured at ambient temperature and those specimens further cured at 100 ºC temperature in an oven after ambient temperature cure. The ambient temperature cured dog bones were labelled reference and the ones cured further at 100 ºC temperature were labelled heat stressed. Thus, two sets of specimens with two types of DFTs: 640 µm and 960 µm of both reference and heat stressed exposure conditions were investigated. Tensile properties from the uniaxial testing reported are as follows: elongation to fracture and tensile strength at fracture.

5.3.1 Elongation at fracture of self-supporting dog bone specimens

Presented in Figure 72 is the bar chart plot of Elongation to fracture as a function of the exposure conditions for SPE, SME, SFPE and SFME formulations.

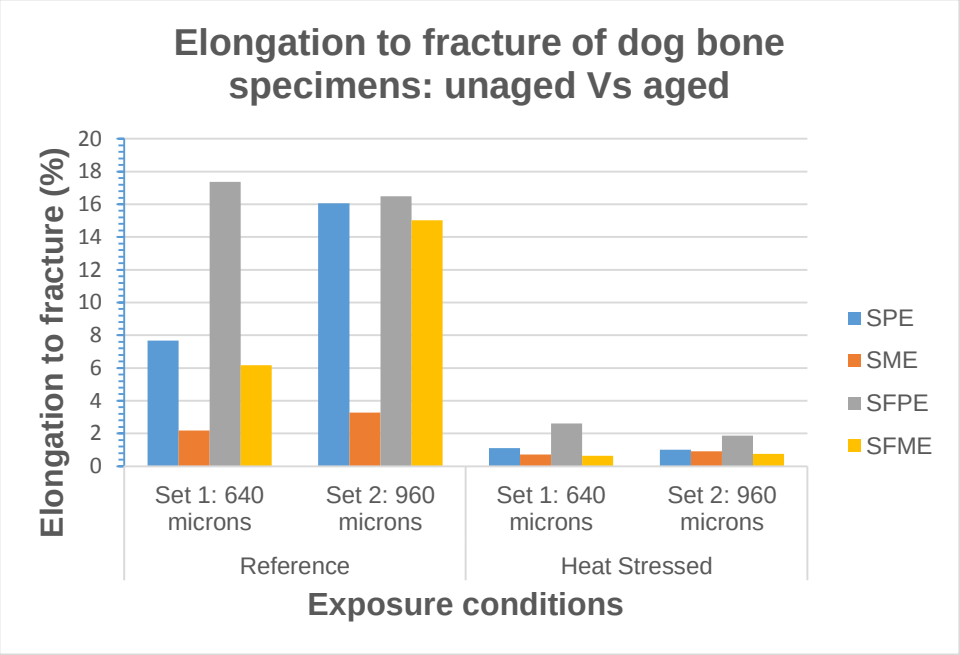

Figure 72 Bar chart plot of Set 1 and Set 2: elongation at fracture for unaged and aged dog bone specimens using uniaxial tensile analyser

For dog bone specimens labelled reference (i.e. cured at ambient temperature only) in set 1, it was observed that the values of elongation to fracture (ε_b) for 640 µm DFT ranged from 2.18% to 17.36%. SFPE exhibited the highest while SME showed the lowest. Both SPE and SFME showed the elongation at fracture values of 7.67% and 6.16% respectively. The following elongation at fracture trend was established:

SFPE > SPE > SFME > SME

For set 2 specimens of dog bone labelled reference, it was observed that the values of elongation at fracture for 960 µm DFT ranged from 3.27% to 16.49%. SFPE exhibited the highest while SME showed the lowest. Both SPE and SFME

showed the elongation at fracture values of 16.05% and 15.02% respectively. The following elongation to fracture was drawn:

SFPE > SPE > SFME > SME

The ranking of both set 1 and set 2 dog bone specimens for reference exposure condition with DFTs of 640 µm and 960 µm compares very well with good agreement.

For dog bone specimens labelled heat stressed (i.e. cured at ambient temperature followed by heating at 100 ºC temperature) in set 1, it was observed that the values of elongation at fracture for 640 µm DFT ranged from 0.64% to 2.61%. SFPE exhibited the highest while SFME showed the lowest. Both SPE and SME showed the elongation at fracture values of 1.11% and 0.72% respectively. The established trend for elongation to fracture trend was as follows:

SFPE > SPE > SME > SFME

For set 2, dog bone specimens labelled heat stressed, it was observed that the values of elongation at fracture for 960 µm DFT ranged from 1.87% to 0.76%. SFPE exhibited the highest while SFME showed the lowest. Both SPE and SME showed the elongation at fracture values of 1% and 0.91% respectively. The trend of elongation at fracture established was:

SFPE > SPE > SME > SFME

The ranking of both set 1 and set 2 dog bone specimens for heat stressed exposure condition with DFTs of 640 µm and 960µm compares very well with good agreement. However, the ranking of reference and heat stressed dog bone specimens are slightly different with SME and SFME interchanging position. Interestingly, following heating at 100 ºC of the dog bone specimens with 640 µm and 960 µm DFTs, their elongation to fracture decreased significantly to less than 3% indicating a pattern of likely similar behaviour of the four coating formulations.

5.3.2 Tensile strength at fracture of self-supporting dog bone specimens

Presented in Figure 73 is the bar chart plot of tensile strength at fracture as a function of the exposure conditions for SPE, SME, SFPE and SFME formulations.

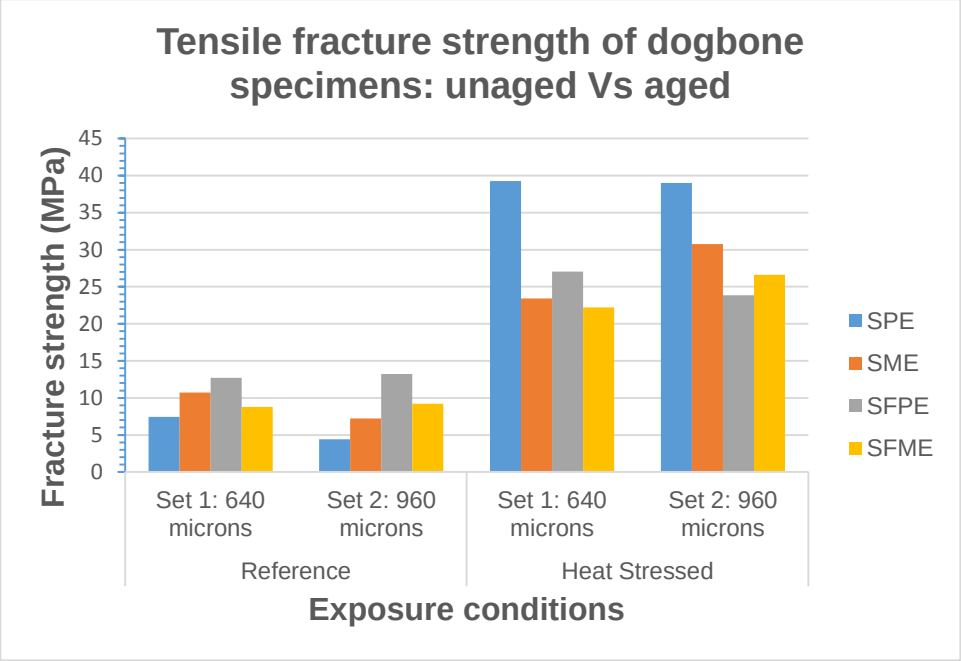

Figure 73 Bar chart plot of set 1 and set 2: tensile strength at fracture for unaged and aged dog bone specimens using uniaxial tensile analyser

For dog bone specimens labelled reference in set 1, it was observed that the values of tensile strength for 640 µm DFT ranged from 7.45 MPa to 12.7 MPa. SFPE exhibited the highest while SPE showed the lowest. Both SME and SFME showed tensile strength values of 10.71 MPa and 8.77 MPa respectively. The following tensile strength trend was drawn:

SFPE > SME > SFME > SPE

For set 2, dog bone specimens labelled reference, it was observed that the values of tensile strength for 960 µm DFT ranged from 4.42 MPa to 13.22 MPa. SFPE exhibited the highest while SPE showed the lowest. Both SME and SFME

showed tensile strength values of 7.21 MPa and 9.2 MPa respectively. The following elongation at fracture trend was drawn:

SFPE > SFME > SME > SPE

The ranking of both set 1 and set 2 dog bone specimens for reference exposure condition with DFTs of 640 µm and 960 µm was slightly different. However, the position for SFPE and SPE were consistent in both case.

For dog bone specimens labelled heat stressed in set 1, it was observed that the values of tensile strength for 640 µm DFT ranged from 22.19 MPa to 39.27 MPa. SPE exhibited the highest while SFME showed the lowest. Both SME and SFPE showed tensile strength values of 23.4 MPa and 23.07 MPa respectively. The following elongation at fracture trend was drawn:

SPE > SFPE > SME > SFME

For set 2, dog bone specimens labelled heat stressed, it was observed that the values of tensile strength for 960 µm DFT ranged from 23.84 MPa to 39.03 MPa. SPE exhibited the highest while SFPE showed the lowest. Both SME and SFME showed tensile strength values of 30.78 MPa and 26.61 MPa respectively. The following tensile strength trend was drawn:

SPE > SME > SFME > SFPE

The ranking of both set 1 and set 2 dog bone specimens for heat stressed exposure condition with DFTs of 640 µm and 960 µm are not in agreement. However, the position of SPE in both cases is consistent.

Reanalysis

5.4 Fatigue Test

Having completed the fatigue testing of set 1: T specimens, another set of twenty-four (24) T specimens were prepared and evaluated with the designed fatigue test. The rationale of the reanalysis was to replicate the first set of result obtained from set 1: T specimens. Set 2: T specimens with the four

formulations: SPE, SFPE, SME and SFME were subjected to the fatigue test and the results are presented in this section. Figure 74 shows the observation of cracks at different stages of the fatigue testing for the evaluated four formulations.

5.4.1 Set 2 specimens

For set 2 T specimens, failure of the coating formulation is demonstrated with the appearance of visible crack(s) from the fatigue test.

Comparing the specimens for the four formulations: SPE is the least crack resistant as cracks were observed after 1 cycle at the weld intersection of all six specimens representing this formulation. The cracks observed were much bigger in size compared to those seen and reported on other formulations: SME, SFME and SFPE. Also, the cracks ran both in the parallel and perpendicular directions along the intersection weld as shown in Figure 74a. The cracks after initiation propagated through the coating film (irrespective of the thickness) to the steel substrate as brown rust, the by-product of corrosion, was observed after full immersion.

The SME specimens demonstrated more resistance when compared to SPE specimens but developed cracks before the SFME and SFPE specimens. SME withstood 37 cycles before cracks appeared on the intersection welds of all the six specimens representing this formulation. The cracks ran parallel along the weld toe at the intersection of the flange and web plates as shown in Figure 74b. The cracks after initiation propagated through the coating film to the steel substrate as there was evidence of steel corrosion after full immersion.

Also, comparing specimens coated in SFME and SFPE as shown in Figures 74c and 74d respectively, cracks were observed to appear at 60 cycles. The cracks were observed on all 6 specimens representing SFME while only 2 of the SFPE specimens showed cracks. Worthy of mention is that the cracks shown on the specimens of SFME and SFPE were just on the surface of the films. The micro cracks did not propagate through the film to the substrate as there was no evidence of brown rust from steel corrosion observed. Thus, SFPE was the

most crack resistant amongst the four formulations as this formulation still had 4 specimens from the 6 without cracks.

Although failure by cracking occurred in all the formulations, overall, SFPE, with the solvent free pure epoxy having just 2 failures out of 6 specimens, is the most crack resistant, followed by SFME. The next less crack resistant formulation (following the solvent free formulations) is SME and the SPE is the least crack resistant of them all.

Based on the hygrothermal cycle testing, the performance of the four formulations from the most crack resistant to the least crack resistant was observed and distinguished as follows:

- **SFPE > SFME > SME > SPE**

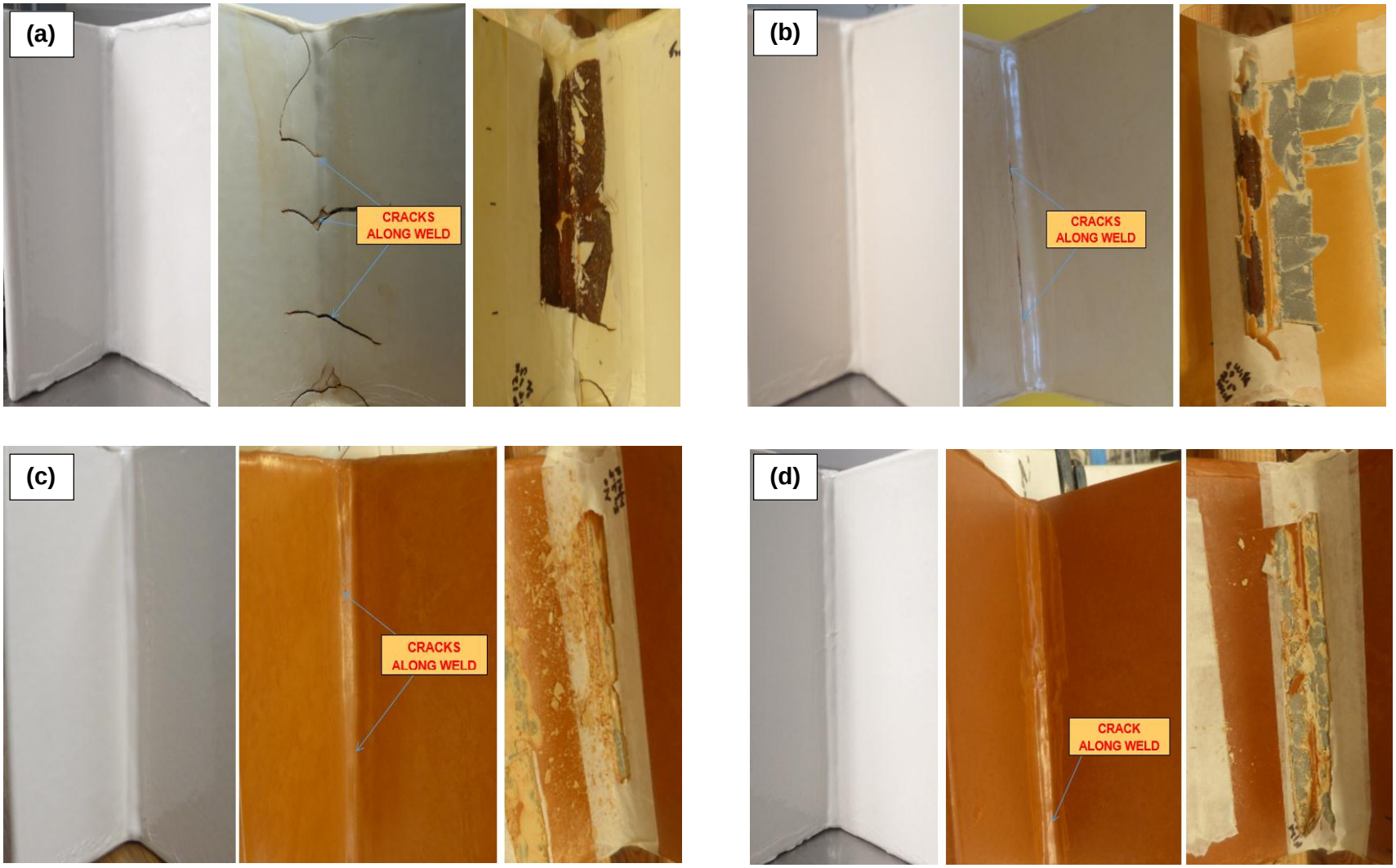

Figure 74 T specimens before and after fatigue testing (a) SPE after 1 cycle (b) SME after 37 cycles (c) SFME after 60 cycles (d) SFPE after 60 cycles

After ranking the specimens from set 1 by exposing them to the designed fatigue test based on hygrothermal cycling, a second set of specimens (set 2 specimens) were prepared and cycled to replicate this fatigue test. Figure 75 shows the comparison and ranking of the four formulations characterised for set 1 and set 2 T specimens.

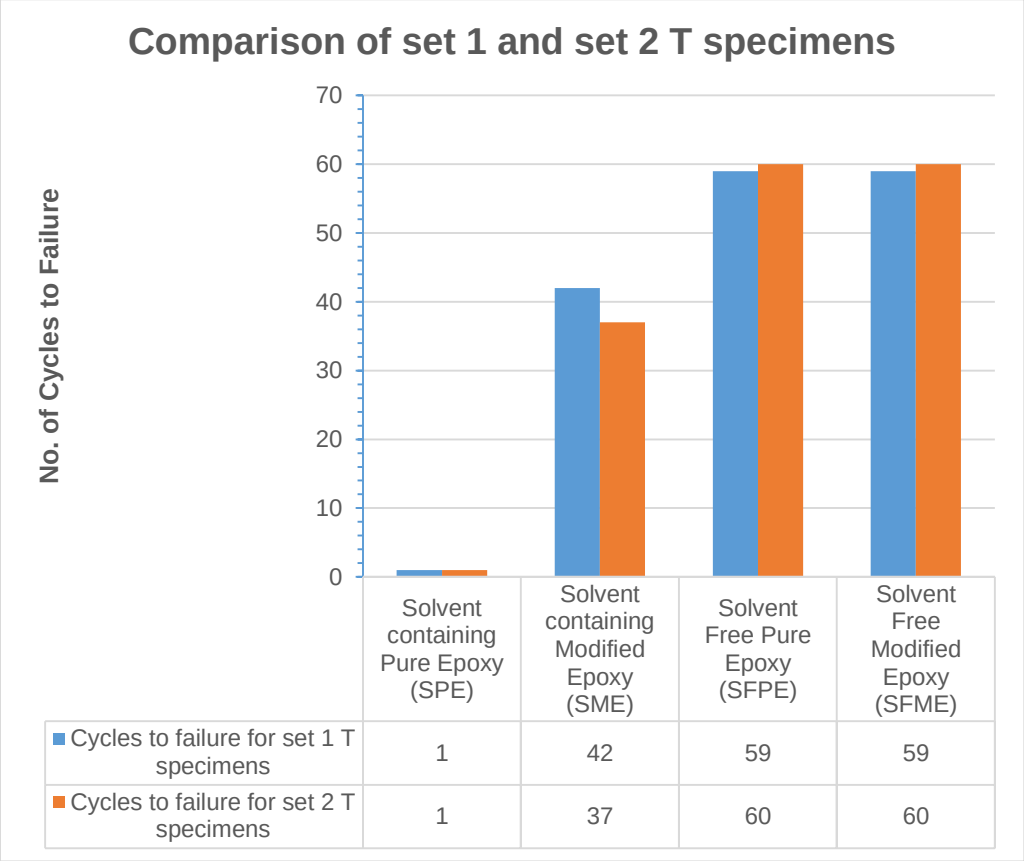

Figure 75 Comparison of number of cycles to failure for the four formulations

Furthermore, Table 28 below summarises the outcome from the exposure of T specimens to the fatigue test for set 1 and set 2.

Table 28 Summary of fatigue testing: comparison of number of cycles to failure for the four formulations from set 1 and set 2 T specimens

Formulation	D.F.T (µm)	Hygrothermal Cycle (2 hr @ 23±3 °C SWI + 2 hr @ 100±2 °C Oven + 2 hr @ 23±3 °C SWI + 17.5 hr @ 100±2 °C Oven) : 1 cycle per day												
		0	5	10	15	20	25	30	35	40	45	50	55	60	65
SPE	640	1													
	960	1													
SFPE	640													59, 60	
	960													59, 60	
SME	640									37	42				
	960									37	42				
SFME	640													59, 60	
	960													59, 60	

Cracks to substrate Surface cracks

In both set 1 and 2, cracks occurred on the power tooled welds with higher film thickness than the 320 µm specified by the IMO PSPC. The occurrence of these cracks at the intersection corner relates and confirms the influence of geometry and higher film thickness as seen in WBT where it is extremely difficult to achieve appropriate spray application.

The replicated test using set 2: T specimens has demonstrated strong agreement that correlates with the earlier findings for set 1: T specimens. The results from the fatigue test for set 1 and set 2 T specimens has established that this fatigue test can be relied on to rank or distinguish between coating formulations regarding resistance to cracking. The correlation indicates a more precise means to determine premature or early cracking in WBT coating formulations under defined laboratory conditions.

5.5 Thermal Analysis of Free Film Specimens

Following the completion of thermal analysis with set 1 free film specimens, a repeat thermal analyses was performed on another set of free film specimens (referred as ‘set 2 free film specimens’). The set 2 free film specimens were exposed to the fatigue test prior to the thermal analyses. This section presents the results obtained from investigating set 2 free film specimens of the four formulations: SPE, SFPE, SME and SFME. Figures

76 to 91 show the obtained results following the temperature scan from DMA and Figures 92 to 96 show that for TMA.

5.5.1 Dynamic mechanical analysis

The DMA results for the four epoxy based formulations presented includes Tg and tensile storage modulus of self-supporting free film specimens; and the Tg and bending storage modulus of non-self-supporting free film specimens. The set 2 self-supporting free films specimens were exposed to defined laboratory conditions as described in section 4.2.2 with a modification in the conditioning temperature (post cure temperature). The conditioning temperature was increased from 50 °C to 100 °C. The rationale for this modification was to investigate the effect of temperature on the ranking produced for the ultimate Tg and moduli properties of the formulations. It was thought that this change could accelerate the test duration while at the same time ensuring that the self-supporting free film specimens attained their ultimate cure by driving out solvent and causing further residual reaction especially for the solvent containing formulations. Lastly, it was considered beneficial to observe the level of plasticisation from wet stress exposure (after heat stress exposure) whether it would differ or remain the same for both conditioning temperatures. The tensile dynamic mechanical properties of the four formulations for Set 2 specimens (self-supporting free films) are shown in Table 31 and Table 35 for the exposure conditions labelled: reference (ambient cured), heat stressed, wet stressed and hygrothermal stressed. Generally, the specimens demonstrated a single Tg with a broad rubbery plateau.

(a) Glass transition temperature Tg of self-supporting free films

Presented in Figure 76 is the bar chart plot of Tgs as a function of the exposure conditions for SPE, SME, SFPE and SFME.

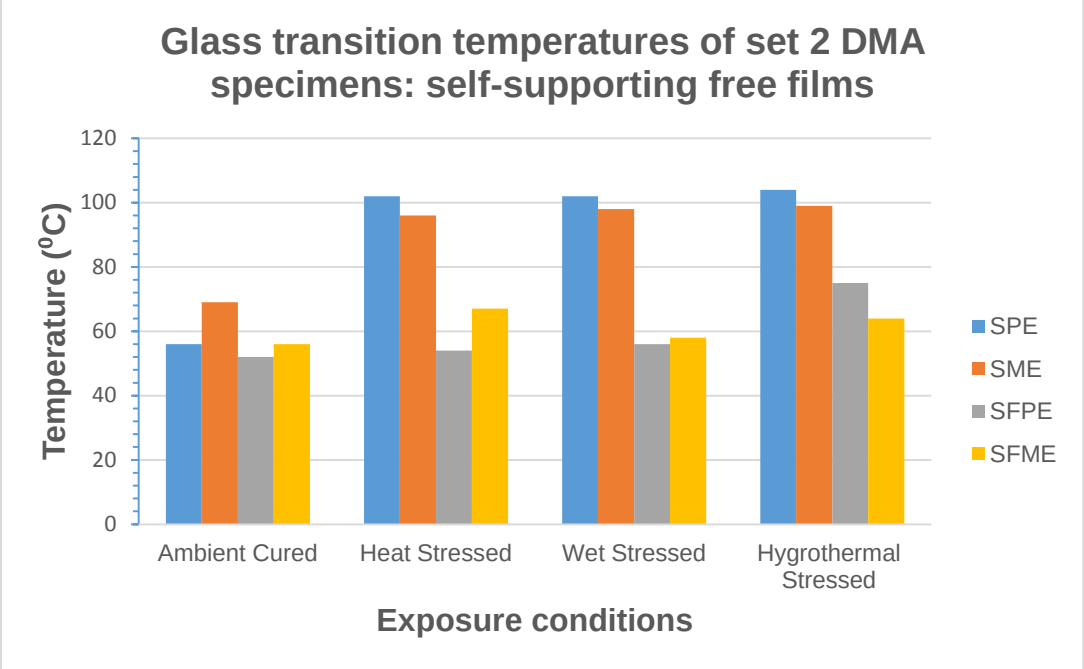

Figure 76 Bar chart plot of Tg values measured for the four formulations using DMA

For DMA self-supporting specimens labelled reference (ambient cured only), it was observed that the values of Tg ranged from 52 °C to 69 °C. SME exhibited the highest Tg while SFPE showed the lowest. Both SPE and SFME had Tg value of 56 °C. The following Tg trend was drawn:

SME > SPE ≈ SFME > SFPE

This ranking of set 2 reference specimens from the DMA is in agreement with that obtained for set 1 reference specimens. Also, both set 1 and set 2 reference specimens show a consistency for ranking SME formulation as having the highest Tg value. Table 29 presents the Tg values from subsequent exposure conditions.

Table 29 Tg values obtained for the four different exposure conditions using DMA

Formulations \ Exposure Conditions		Set 2 DMA specimens: Self-supporting Free Films (°C)			
		Unaged	Aged		
		Reference (Ambient Cured)	Heat Stressed	Wet Stressed	Hygro-thermal Stressed
Pure Epoxy	Solvent Containing (SPE)	56	102	102	104
	Solvent Free (SFPE)	52	54	56	76
Modified Epoxy	Solvent Containing (SME)	69	96	98	99
	Solvent Free (SFME)	56	59	58	64

For the DMA self-supporting specimens labelled heat stressed, it was observed that the Tg values ranged between 54 °C and 102 °C with SFPE displaying the lowest and SPE exhibiting the highest. On this occasion, SME and SFME presented Tgs between those of SPE and SFPE. The following Tg trend was established:

SPE > SME >> SFME > SFPE

The ranking was different from that of DMA self-supporting specimen of set 1 labelled heat stressed. As expected, the Tg values and ranking of heat stressed specimen of set 2 was similar to that obtained for DMA self-supporting specimens labelled hygrothermal stressed 1 and hygrothermal stressed 2 of set 1 except that SME formulation of set 1 displayed the highest value. With change in conditioning temperature of post cure from 50 °C to 100 °C, the formulations did not required subsequent exposures to reach their ultimate Tg except for SFPE and SFME that experienced difficulties with clamping specimens and likely second overlapping Tg. Nevertheless, it is possible to find similarities in the obtained data and conclude that the coating formulations studied in both DMA experimental analysis was the same.

For the DMA self-supporting specimens labelled wet stressed of set 2, the ranking is similar to that obtained from the heat stressed specimens of set 2. The ranking is also closely related to that of hygrothermal stressed 1 and

hygrothermal stressed 2 specimens of set 1. The following Tg trend was drawn:

SPE > SME >> SFME > SFPE

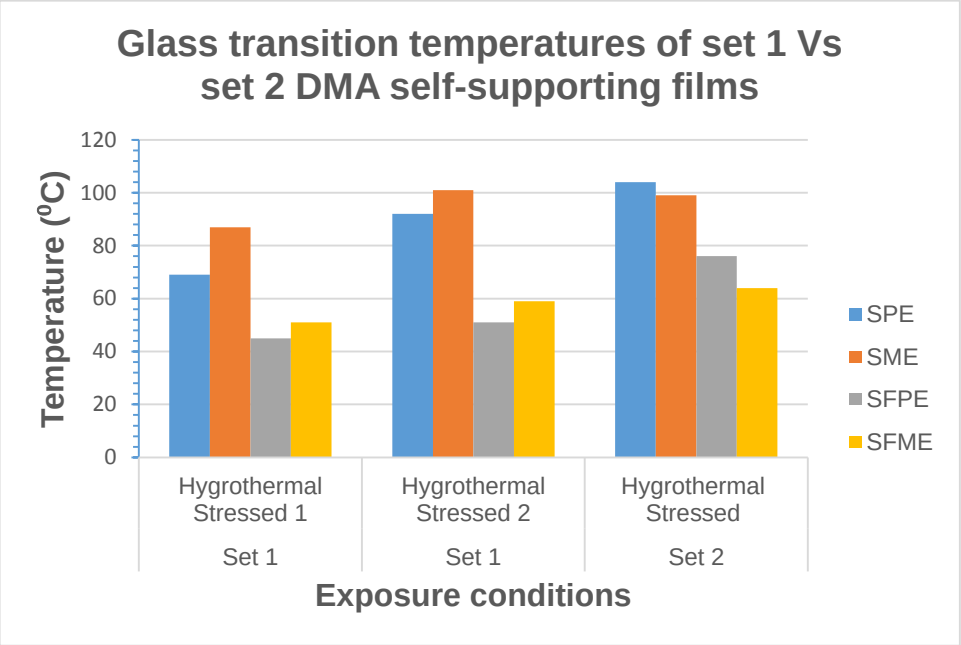

Figure 77 Bar chart plot of Tg values for set 1 Vs set 2 self-supporting films using DMA

In addition, only SFME for wet stressed specimens of set 2 exhibited a decrease in Tg value which could be attributed to difficulties with clamping the specimen and likely second overlapping Tg at lower temperature. Furthermore, unlike specimens post cured at 50 °C where there was an effect of plasticisation, the effect of plasticisation following wet stress exposure was not apparent in specimens post cured at 100 °C.

The set 2 DMA self-supporting specimens labelled hygrothermal stressed exhibited a ranking as follows:

SPE > SME > SFPE > SFME

The ranking is different from that of hygrothermal stressed 1 and hygrothermal stressed 2 specimens of set 1 as specimens of set 2 had increased in Tg than those for set 1. Notably, SPE and SFPE were more affected by post curing at 100 °C than SME and SFME. Overall, it was

confirmed that after post curing the specimens at 100 °C, the Tg had reached an ultimate (maximum) temperature as it remained approximately levelled especially for the SPE and SME while SFPE and SFME experienced an increase for hygrothermal stressed exposure because of a likely second Tg from clamping. A summary of Tg values using DMA is illustrated in Table 30.

Table 30 Summary of glass transition temperature, Tg using DMA

Reference	SME > SPE ≈ SFME > SFPE
Heat Stressed	SPE > SME >> SFME >SFPE
Wet Stressed	SPE > SME >> SFME > SFPE
Hygrothermal Stressed	SPE > SME > SFPE > SFME

(b) Tensile storage modulus of self-supporting free films

The below Figure 78 shows the plot of tensile storage modulus as a function of exposure conditions.

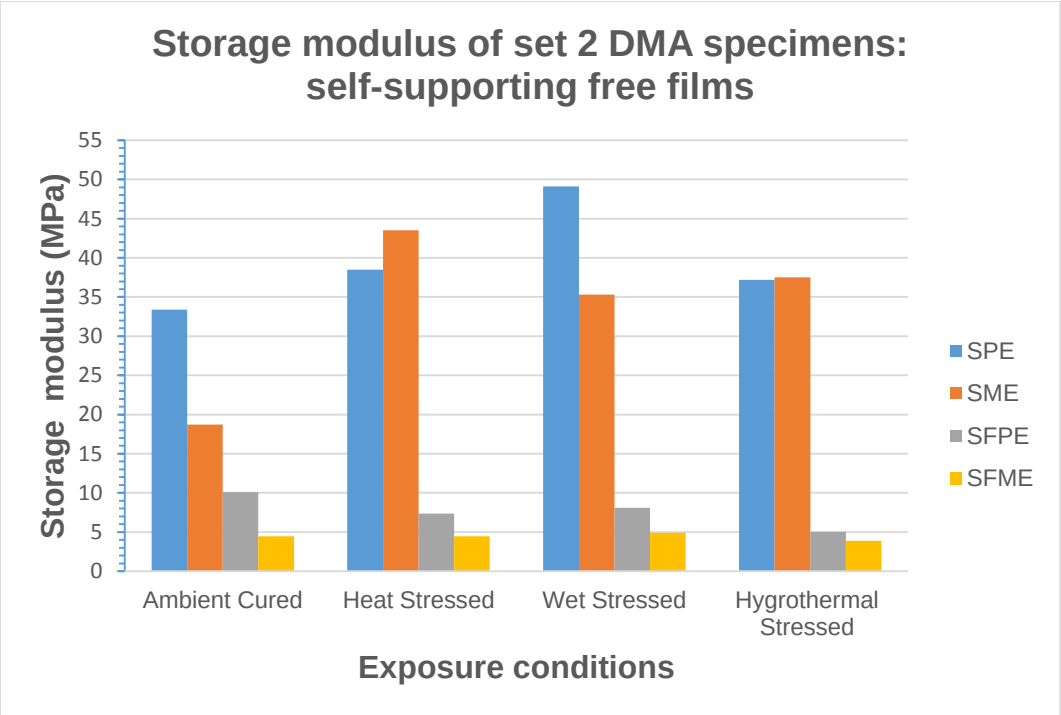

Figure 78 Bar chart plot of tensile storage modulus values of set 2 specimens using DMA

For the DMA self-supporting specimens labelled reference, it was observed that the SPE exhibited the highest E' and SFME showed the lowest. The trend below for storage modulus (E') was established:

SPE > SME > SFPE > SFME

This ranking trend of set 2 reference specimens from the DMA is in agreement with that obtained for set 1 DMA reference specimens. Also, both set 1 and set 2 reference specimens show a consistency for ranking SPE formulation as having the highest E' value.

For the DMA self-supporting specimens labelled heat stressed, SME and SPE were observed to display significantly higher E' value than SFPE and SFME. SME showed the highest E' value while SFME displayed the lowest E'. Thus, the following trends for E' of heat Stressed specimens was established:

SME > SPE >> SFPE > SFME

Furthermore, this ranking is also in agreement with that of hygrothermal stressed 1 and hygrothermal stressed 2 specimens of set 1.

For the DMA self-supporting specimens labelled wet stressed, the following trend was concluded:

SPE > SME >> SFPE > SFME

This ranking is in agreement with that of wet stressed specimens of set 1.

For the DMA self-supporting specimens labelled hygrothermal stressed, the following trend was observed:

SPE ≈ SME >> SFPE > SFME

This ranking is closely related to that obtained for DMA self-supporting specimens labelled hygrothermal stressed 1 and hygrothermal stressed 2 of set 1 as shown in Figure 79.

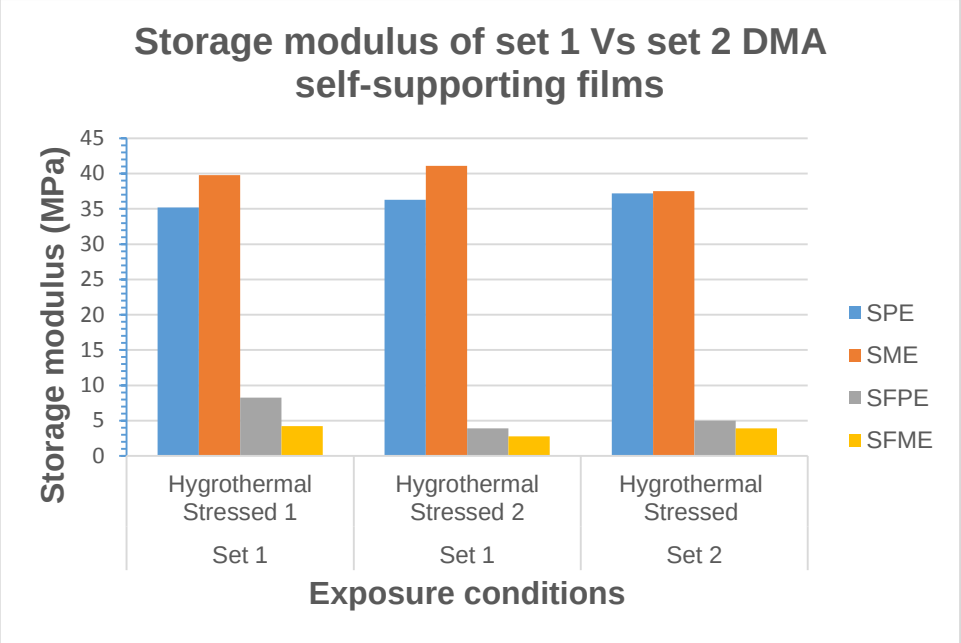

Figure 79 Bar chart plot of tensile storage modulus of set 1 Vs set 2 specimens using DMA

Also, in this ranking SPE and SME formulations displayed approximately equal E' value. As previously stated, the observed increase in storage modulus for SPE and SME can be attributed to the higher content of pigments, fillers (rigid particles) resulting in an increased pigment volume concentration (PVC) when compared to SFPE and SFME. SFPE and SFME presented very low storage modulus at reference condition, which dropped slightly following other exposure conditions.

Also, observed as in Table 31 was the reduction in storage modulus value for SPE which levelled off with that recorded for SME following hygothermal cycling exposure. For SFPE and SFME, it was observed that the modulus was relatively close and much less than those for SPE and SME.

Table 31 Summary of Set 2: tensile storage modulus E' taken at the rubbery region for unaged and aged specimens using DMA

Formulations \ Exposure Conditions		Set 2 DMA specimens: Self-supporting Free Films (MPa)			
		Unaged	Aged		
		Reference (Ambient Cured)	Heat Stressed	Wet Stressed	Hygro- thermal Stressed
Pure Epoxy	Solvent Containing (SPE)	33.4	38.5	49.1	37.2
	Solvent Free (SFPE)	10.1	7.34	8.10	5.01
Modified Epoxy	Solvent Containing (SME)	18.7	43.5	35.3	37.5
	Solvent Free (SFME)	4.45	4.46	4.90	3.90

A summary of the ranking based on the obtained tensile storage modulus values using DMA is illustrated in Table 32.

Table 32 Summary of tensile storage modulus E' using DMA

Reference	SPE > SME > SFPE > SFME
Heat Stressed	SME > SPE >> SFPE >SFME
Wet Stressed	SPE > SME >> SFPE > SFME
Hygrothermal Stressed	SPE ≈ SME >> SFPE > SFME

(c) Glass transition temperature Tg of non-self-supporting free films

Presented in Figure 80 is the bar chart plot of Tgs as a function of the fatigue exposure condition for SPE, SME, SFPE and SFME formulations.

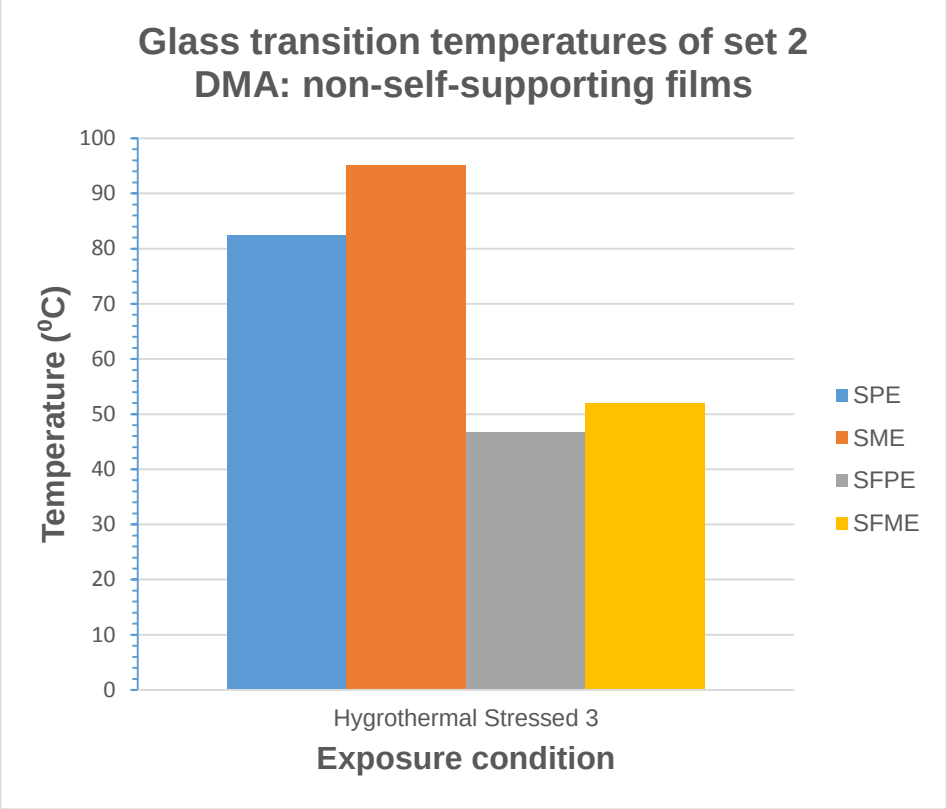

Figure 80 Bar chart plot of Set 1: Tg values measured for the non-self-supporting specimens using DMA

For set 2 DMA non-self-supporting specimens (i.e. flakes removed form cycled T specimens and labelled as hygrothermal stressed 3), it was observed that the values of Tg averaged from two temperature scan ranged from 46.6 °C to 95 °C. SME exhibited the highest Tg value while SFPE showed the lowest. SPE and SFME showed Tg value of 82.5 °C and 52 °C respectively. The following Tg trend could be drawn:

SME >SPE > SFME > SFPE

As shown in Figure 81, this ranking of Tg compares reasonably with that from set 1 DMA non-self-supporting specimens which was also subjected to the fatigue testing. Unlike set 1 DMA non-self-supporting specimen where SPE and SME had approximately equal Tg value, SME for set 2 DMA non-self-supporting specimens had a slightly higher value; which changed the ranking order in this case.

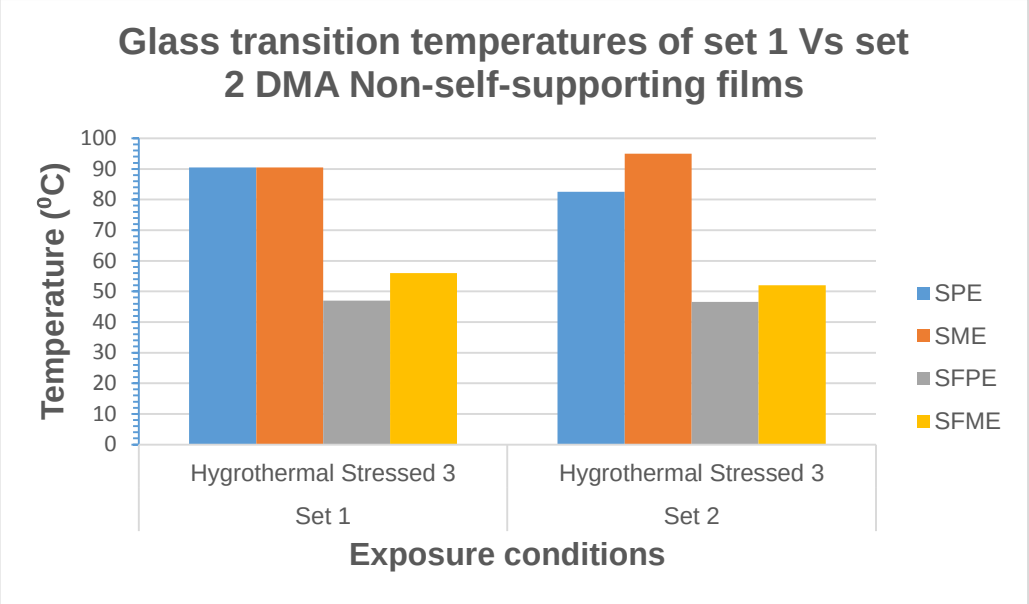

Figure 81 Bar chart plot of Set 1 Vs Set 2: Tg values of non-self-supporting specimens using DMA

In addition, following hygrothermal stressed, the Tg values obtained for both the non-self-supporting specimens and self-supporting specimens of set 2 are reasonably close to those obtained for set1 despite two different types of DMA modes of deformation (i.e. tension and bending) and fixtures were utilised. Thus, there is very good agreement with both DMA modes of deformation and fixtures as SPE and SME exhibited the higher Tg values while SFPE and SFME exhibited much lower Tg values than SPE and SME. This trend and data similarities show that the steel material pockets that encapsulated the DMA non-self-supporting specimen had no influence on the obtained Tg values and using this method yields Tg values that compare very well to those obtained from DMA self-supporting specimens for tension mode. This finding also suggests that the coating formulations studied are the same for both DMA modes of deformation. Also, shown in Table 32 is the Tg values.

Table 33 Set 2: Tg values obtained for non-self-supporting specimens using DMA

Formulations \ Exposure Conditions		Set 2 DMA specimens: Non-Self-supporting Free Films (°C)
		Aged
		Hygrothermal Stressed 3
Pure Epoxy	Solvent Containing (SPE)	82.5
	Solvent Free (SFPE)	46.5
Modified Epoxy	Solvent Containing (SME)	95
	Solvent Free (SFME)	52

A summary of Tg values using DMA is illustrated in Table 34.

Table 34 Summary of glass transition temperature, Tg using DMA

Hygrothermal Stressed 3	SME > SPE >> SFME > SFPE

(d) Bending storage modulus of non-self-supporting free films

The moduli from bending deformation mode using the single cantilever fixture on DMA specimens (i.e. non-self-supporting free films) are reported here. The below Figure 82 shows the plot of storage modulus (E') obtained in the rubbery region as a function of specimen exposure condition.

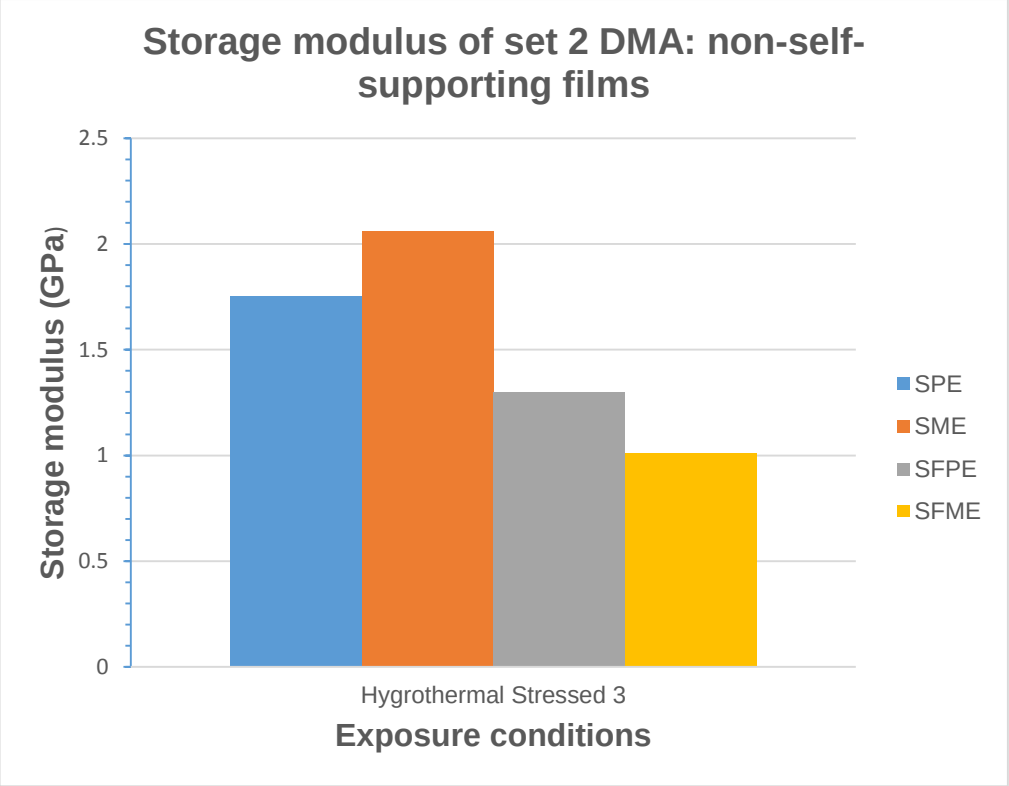

Figure 82 Bar chart plot of Set 1: Storage modulus values measured for non-self-supporting specimens using DMA

For the DMA non-self-supporting specimens shown in Figure 82, it was observed that the SME exhibited the highest storage modulus (E') and SFME showed the lowest. SPE and SFPE exhibited E' values between SME and SFME. The trend for E' was as follows:

SME > SFPE > SPE > SFME

As illustrated in Figure 83, this ranking from the DMA non-self-supporting specimens of set 2 is different to that from set 1. However, the ranking agrees in both cases that SME has the highest E' value and SFME has the lowest E' value. In addition, the E' values for the DMA non-self-supporting specimens are much more than those obtained for the DMA self-supporting specimens which could be attributed to the two different types of DMA modes of deformation (i.e. tension and bending), steel Material Pocket (MP) and fixtures utilised.

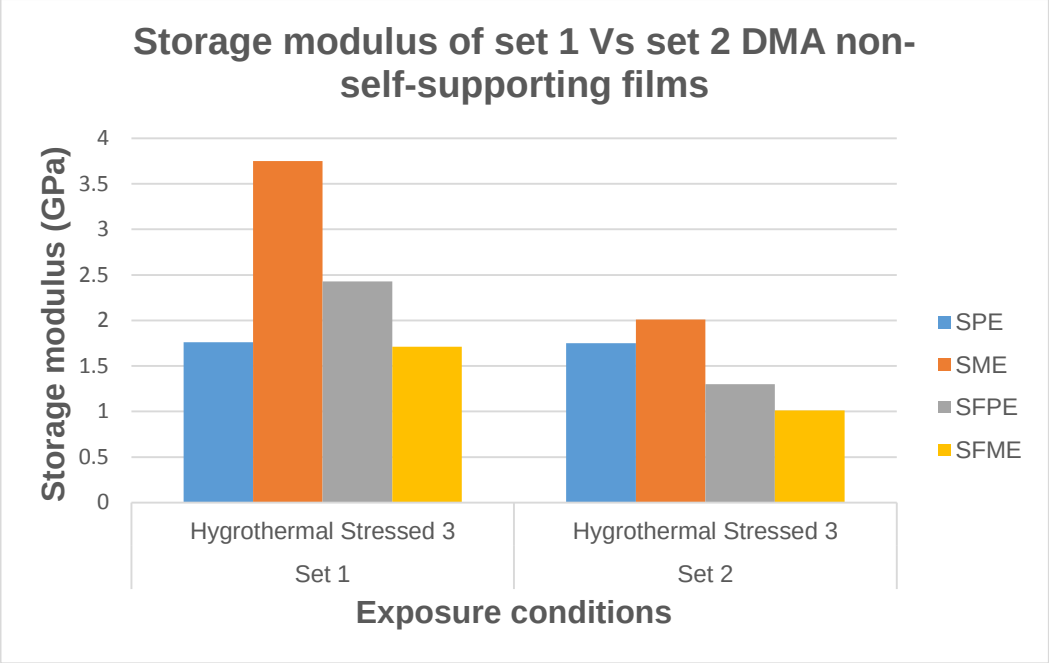

Figure 83 Bar chart plot of Storage modulus values measured for the four formulations using DMA

As shown in Table 35, the average modulus of the steel MP obtained from duplicate DMA temperature scans was 43.1 GPa while the average moduli obtained from duplicate temperature scan of set 2 for SPE, SME, SFPE and SFME were 1.75 GPa, 2.01 GPa, 1.3 GPa and 1.01 GPa respectively. Although, this value obtained from DMA test is much less compared to typical quoted value of 208 GPa [50]; which relates to the elastic modulus of steel from tensile testing, it does indicate that the stiffness of the steel MP was much more than the DMA specimens: non-self-supporting free films. Furthermore, as the average moduli of the non-self-supporting free films ranged 1.01 GPa to 2.01 GPa, it was impossible to subtract moduli of the films from that of the steel MP: 43.1 GPa. Comparing the E' data obtained from both DMA mode of deformations, it is clear again that the steel MP significantly influenced the obtained E' values for the non-self-supporting free films of set 1 and set 2. Again, as the steel MP does not exhibit any transitions within the DMA temperature scan and significantly influence the E' values, the E' obtained should be used with caution and could be unbeneficial for ranking performance of coating films.

Table 35 Set 1: E' values obtained for non-self-supporting specimens and steel material pocket using DMA

Formulations \ Exposure Conditions		Set 2 DMA specimens: Non-Self-supporting Free Films (GPa)
		Aged
		Hygrothermal Stressed 3
Pure Epoxy	Solvent Containing (SPE)	1.75
	Solvent Free (SFPE)	1.30
Modified Epoxy	Solvent Containing (SME)	2.01
	Solvent Free (SFME)	1.01
Support	Steel Material Pocket	43.1

A summary of E' values using DMA is illustrated in Table 36.

Table 36 Summary of the ranking for storage modulus, E' using DMA

Hygrothermal Stressed 3	SME > SPE > SFPE > SFME

Figures 84 through 91 provide an overlay comparing the E' properties as a function of temperature obtained for the four formulations after exposure to fatigue testing for the reference, heat stressed, wet stressed and hygrothermal stressed conditions respectively.

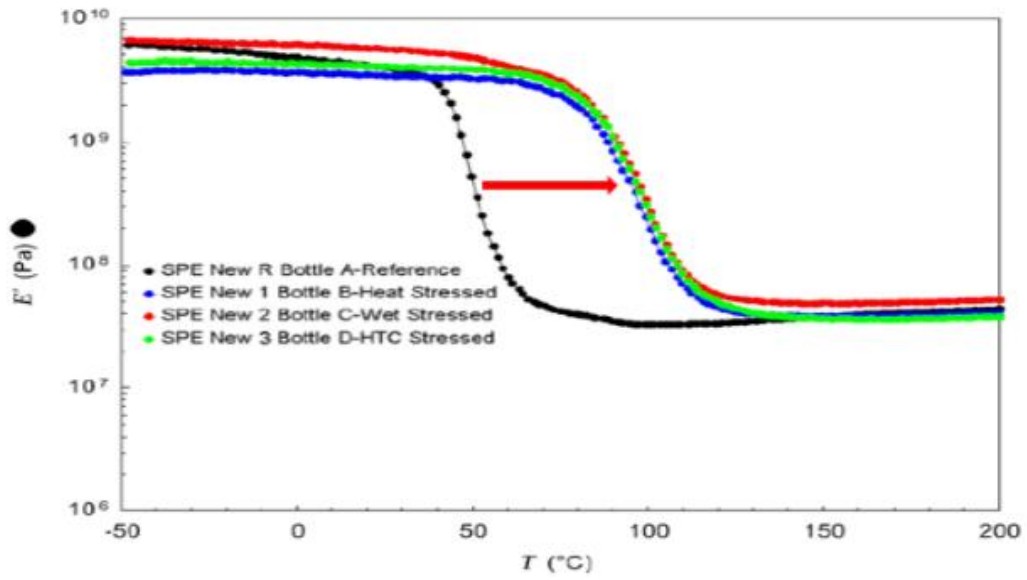

Figure 84 D.M.A Overlay of tensile storage modulus Vs temperature curve for SPE formulation

Figure 84 shows an overlay comparing the E' values as a function of temperature for SPE after exposure to different conditions (reference, heat stressed, wet stressed and hygrothermal stressed). As observed in Figure 84, there was change in E' signals of SPE formulation occurring between 40 to 120 ^{o}C, which represented the ranges over the Tg. Except for the reference (SPE New R), there was a substantial shift in signal after exposure to 100 ^{o}C for other exposure conditions as shown by the red arrow direction to the right. This trend indicates the effect of the ageing process (physical ageing) due to loss or release of retained solvents and additional crosslinking of residuals following post cure. In addition, the E' signals of SPE New 1, SPE New 2 and SPE New 3 were on the same path with negligible shift.

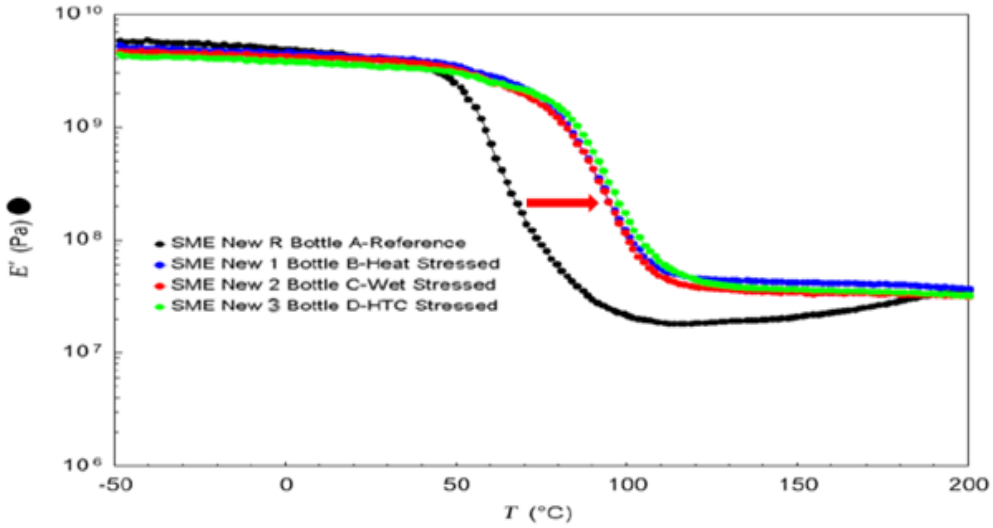

Figure 85 D.M.A Overlay of tensile storage modulus Vs temperature curve for SME formulation

Figure 85 shows an overlay comparing the E' values as a function of temperature for SME after exposure to different conditions (reference, heat stressed, wet stressed and hygrothermal stressed). As observed in Figure 85, there was change in E' signals occurring between 55 to 110 ^{o}C, which represented the ranges over the Tg. Similar to SPE, there was a shift in signal after exposure to 100 ^{o}C (for SME New 1, SME New 2 and SME New 3) as shown by the red arrow direction to the right. However, the shift was less than that observed for SPE in Figure 84. Similarly, this trend indicates the effect of the ageing process (physical ageing) due to loss or release of retained solvents and additional crosslinking of residuals following post cure. In addition, the E' signals of SME for heat stressed, wet stress and hygrothermal stressed were on the same path with negligible shift.

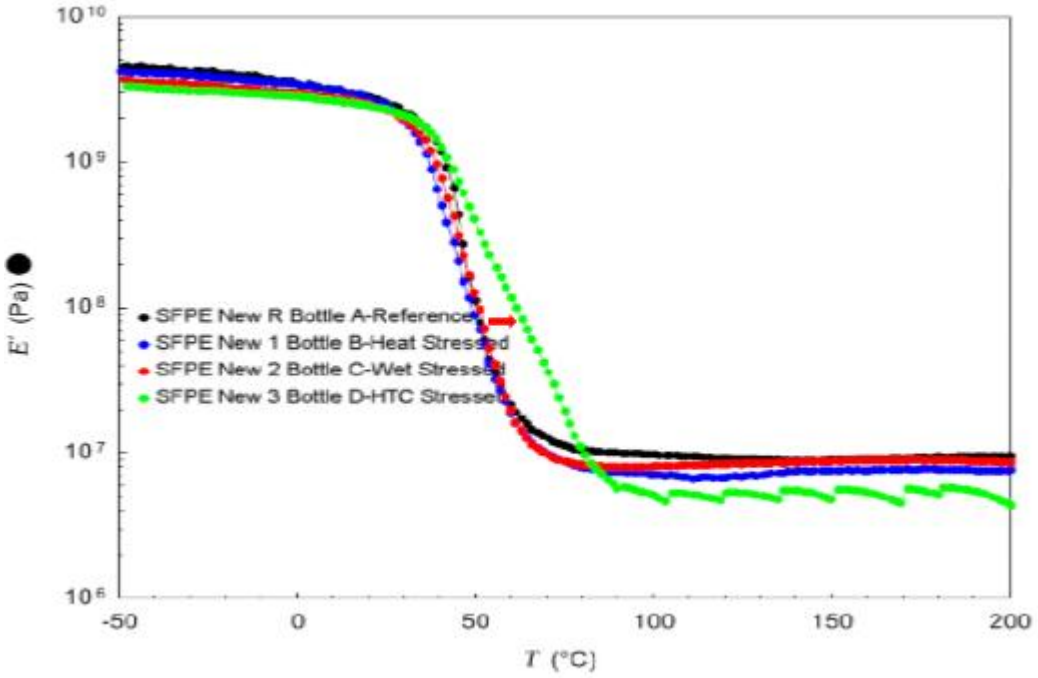

Figure 86 D.M.A Overlay of tensile storage modulus Vs temperature curve for SFPE formulation

Figure 86 shows an overlay comparing the E' values as a function of temperature for SFPE after exposure to different conditions (reference, heat stressed, wet stressed and hygrothermal stressed). As observed in Figure 86, there was change in E' signals of SFPE formulation occurring between 30 to 80 ^{o}C, which represented the ranges over the Tg. Except for the SFPE New 3, the others seem to be ageing at the same rate as shown by the red arrow direction with a slight shift to the right. Although this trend indicates the effect of the ageing process (physical ageing) due to additional crosslinking of residuals following post cure at 100 ^{o}C, it does show that the rate and capacity to change is less in SFPE after initial ambient cure.

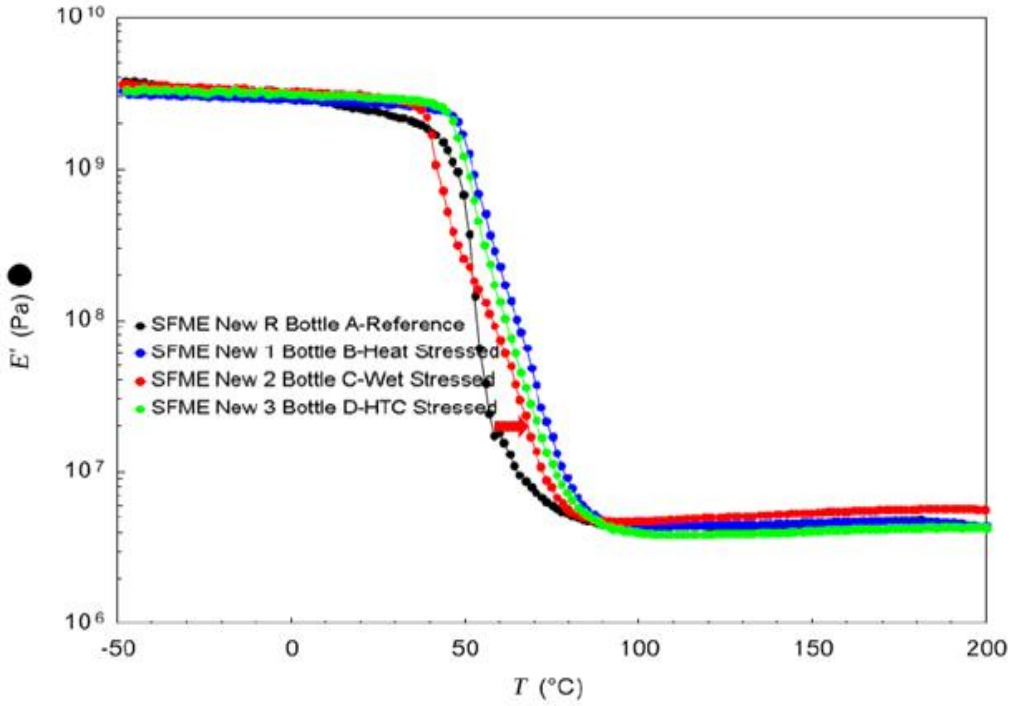

Figure 87 D.M.A Overlay of tensile storage modulus Vs temperature curve for SFME formulation

Figure 87 shows an overlay comparing the E' values as a function of temperature for SFME after exposure to different conditions (reference, heat stressed, wet stressed and hygrothermal stressed). As observed in Figure 87, there was change in E' signals of SFME formulation occurring between 40 to 85 ^{o}C, which represented the ranges over the Tg. Except for SFME New R New, there was a slight shift in signal of other exposure conditions after exposure to 100 ^{o}C as shown by the red arrow direction to the right. Again, this trend indicates the effect of the ageing process (physical ageing) due to additional crosslinking of residuals following post cure. In addition, it demonstrates that the rate and capacity to change is less SFME after initial ambient cure.

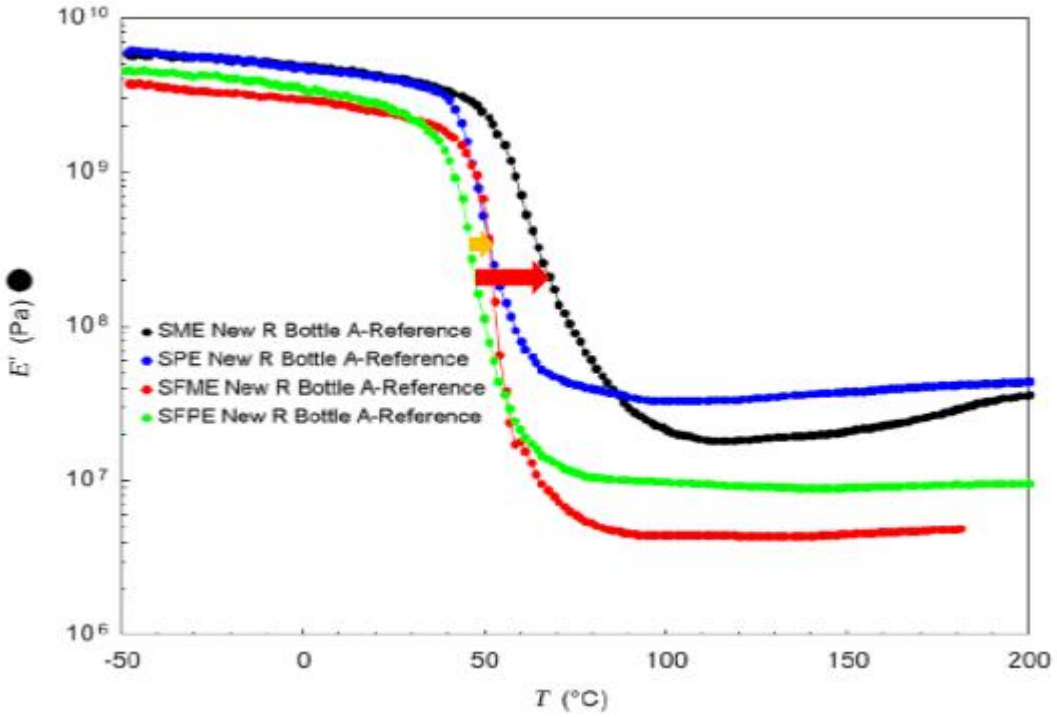

Figure 88 D.M.A Overlay of tensile storage modulus Vs temperature curve for the four formulations – reference

Figure 88 shows an overlay comparing the E' values as a function of temperature for the four formulations for reference condition. As observed in Figure 88, there was change in E' signals for the formulations occurring between 45 to 75 ^{o}C, which represented the ranges over the Tg. Except for SFPE, there was a shift in signal for the other formulations: SPE, SME and SFME. As indicated by the orange arrow direction to the right, SPE and SFME shifted slightly from SFPE. In contrast, as indicated by the red arrow direction to the right, SME shifted more from SFPE than SPE and SFME. In addition, SPE seems to shift slightly to the right from SFME. Again, this trend indicates the effect of the ageing process due to loss or release of retained solvents and additional crosslinking of residuals. Furthermore, the signals suggested that SPE and SME exhibited more rate and capacity to change following post cure.

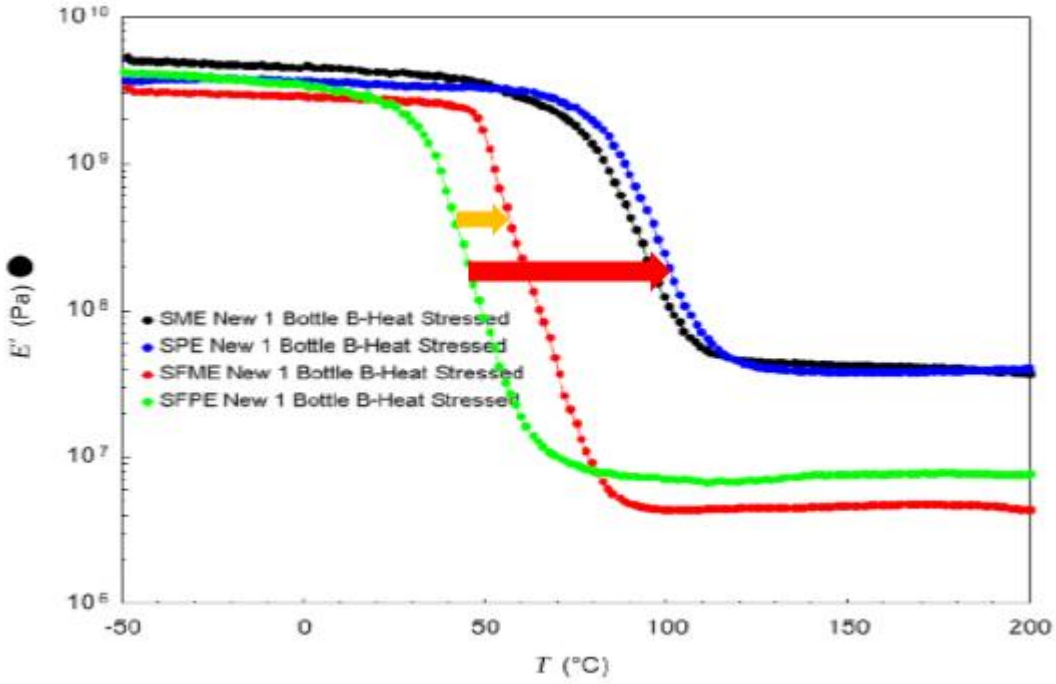

Figure 89 D. M.A Overlay of tensile storage modulus Vs temperature curve for the four formulations – dry heat stressed

Figure 89 shows an overlay comparing the E' values as a function of temperature for the four formulations for heat stressed condition. As observed in Figure 89, there was change in E' signals for the formulations occurring between 35 to 110 ^{o}C, which represented the ranges over the Tg. Except for SFPE, there was a shift in signal for other formulations: SPE, SME and SFME. As indicated by the orange arrow direction to the right, SFME shifted slightly from SFPE. In contrast, as indicated by the red arrow direction to the right, SME and SPE shifted significantly from SFME and more from SFPE. In addition, SPE shifts slightly to the right from SME. Comparing the four formulations for the dry heat stressed condition, SPE and SME shifted significantly to the right from SFPE and SFME. Again, this trend indicates the effect of the ageing process due to loss or release of retained solvents and additional crosslinking of residuals. Furthermore, the signals demonstrated that SPE and SME exhibited more rate and capacity to change following post cure.

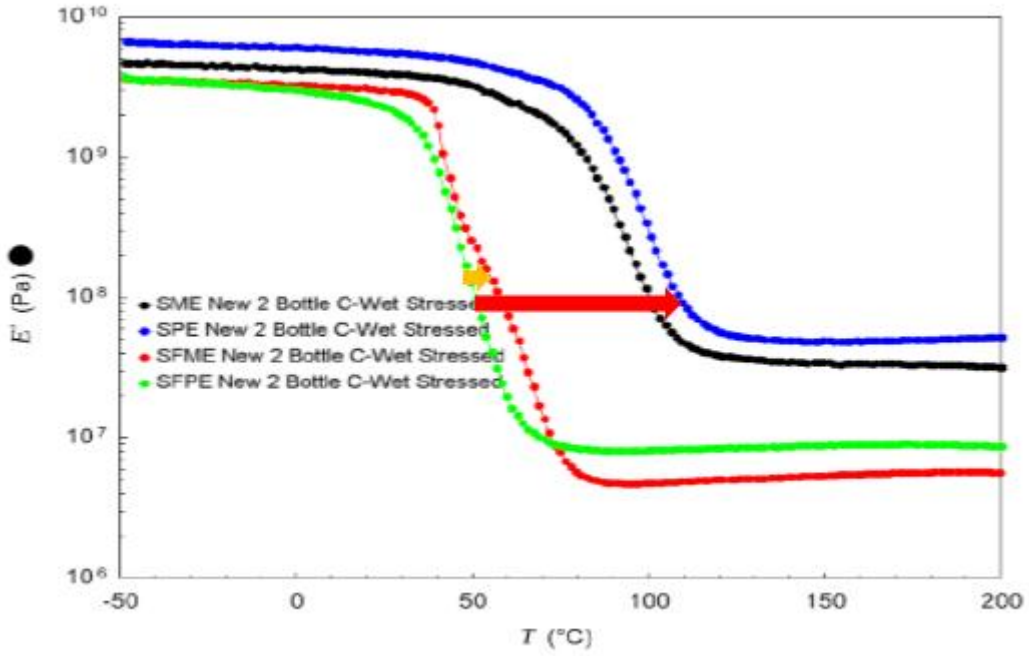

Figure 90 D. M.A Overlay of tensile storage modulus Vs temperature curve for the four formulations – wet stressed

Figure 90 shows an overlay comparing the E' values as a function of temperature for the four formulations for wet stressed condition. As observed in Figure 90, there was change in E' signals for the formulations occurring between 40 to 110 ^{o}C, which represented the ranges over the Tg. Except for SFPE, there was a shift in signal for the other formulations: SPE, SME and SFME. As indicated by the orange arrow direction to the right, SFME shifted slightly from SFPE. In contrast, as indicated by the red arrow direction to the right, SME and SPE shifted significantly from SFME and more from SFPE. In addition, SPE shifted slightly to the right from SME. Comparing the four formulations for this exposure condition, SPE and SME shifted significantly to the right from SFPE and SFME. Again, this trend indicates the effect of the ageing process due to loss or release of retained solvents and additional crosslinking of residuals. Furthermore, the signals demonstrated that SPE and SME exhibited more rate and capacity to change following post cure.

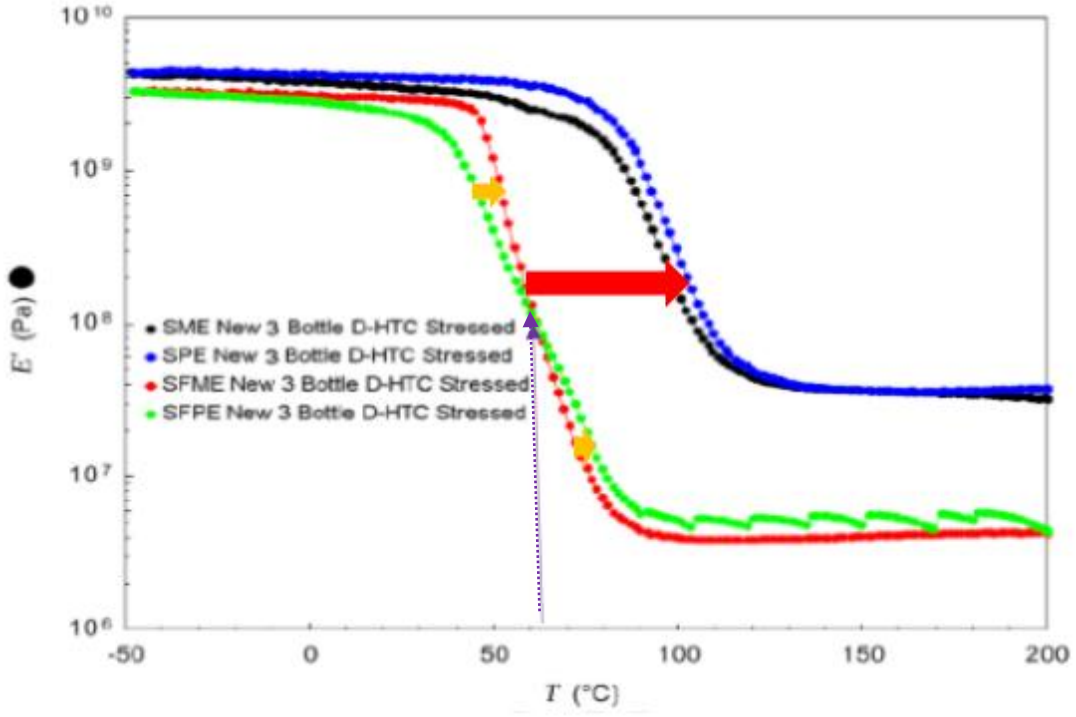

Figure 91 D. M.A Overlay of tensile storage modulus Vs temperature curve for the four formulations – Hygrothermal Stressed

Figure 91 shows an overlay comparing the E' values as a function of temperature for the four formulations for wet stressed condition. As observed in Figure 91, there was change in E' signals for the formulations occurring between 30 to 105 ^{o}C, which represented the ranges over the Tg. The signals of SFPE and SFME intersected at 62 ^{o}C as shown by the purple arrow. As indicated by the orange arrow direction to the right, above the intersection, SFME slightly leads SFPE. In contrast, below the intersection, SFME lags SFPE. However, as indicated by the red arrow direction to the right, SME and SPE shifted significantly from SFME and SFPE. In addition, SPE shifted slightly to the right from SME. Comparing the four formulations for this exposure condition, SPE and SME shifted significantly to the right from SFPE and SFME. Again, this trend indicates the effect of the ageing process due to loss or release of retained solvents and additional crosslinking of residuals. Furthermore, the signals demonstrated that SPE and SME exhibited more rate and capacity to change following post cure while SFPE and SFME exhibited much less.

5.5.2 Thermo-mechanical analysis

(a) Glass transition temperature

As illustrated in Figure 92 and Table 37, Tgs were also measured using TMA. For the TMA specimens labelled reference films, it was observed that the values of Tg ranged from 53.8 °C to 66.7 °C. SME exhibited the highest Tg while SFME which had approximately same value with SFPE showed the lowest. SPE showed a Tg value of 55.6 °C. The following Tg trend could be drawn:

SME > SPE > SFPE ≈ SFME

This ranking of reference specimens from the TMA when compared to that obtained using either the DSC or the DMA is not in agreement. However, all analyses show a consistency for ranking SME as the highest Tg. Also the ranking of TMA reference specimens for set 1 is inconsistent to that of set 2.

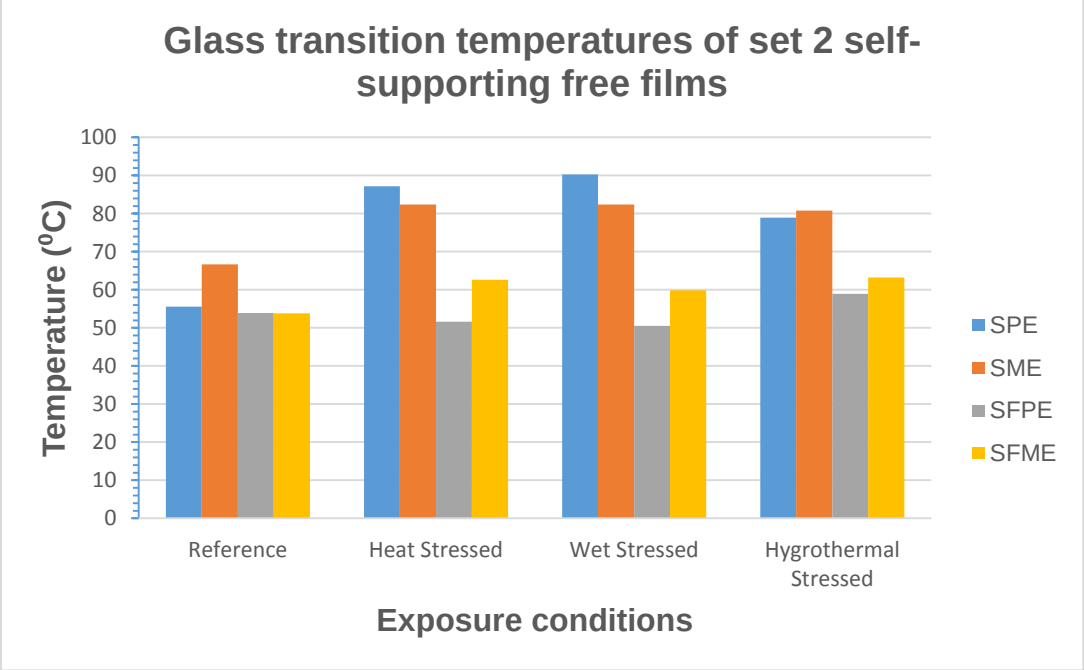

Figure 92 Bar chart plot of Tg measured using TMA

Table 37 Values of glass transition temperature (Tg) measured using TMA

Formulations \ Exposure Conditions		Set 2 TMA specimens: Self-supporting Free Films (°C)			
		Unaged	Aged		
		Reference (Ambient Cured)	Heat Stressed	Wet Stressed	Hygro-thermal Stressed
Pure Epoxy	Solvent Containing (SPE)	55.6	87.2	90.3	78.9
	Solvent Free (SFPE)	53.9	51.6	50.5	58.9
Modified Epoxy	Solvent Containing (SME)	66.7	82.4	82.4	80.8
	Solvent Free (SFME)	53.8	62.6	59.9	63.2

For the TMA specimens labelled heat stressed, it was observed that SFPE displayed the lowest Tg value while SPE exhibited the highest Tg value. Also, SME and SFME presented Tgs between those of SPE and SFPE. The following Tg trend could be drawn:

SPE > SME > SFME > SFPE

This ranking is inconsistent with that obtained for set 1 TMA specimens labelled heat stressed. However, the ranking is closely related to that obtained from the DSC second scan and the DMA rankings of set 2 specimens labelled heat stressed.

For the TMA specimens labelled wet stressed, the following Tg trend could be drawn:

SPE > SME > SFME > SFPE

This ranking is inconsistent with that from set 1 TMA specimens labelled wet stressed.

For the TMA specimens labelled hygrothermal stressed, the following Tg trend was exhibited:

SME > SPE > SFME > SFPE

As shown in Figure 93, this Tg ranking of TMA set 2 specimens labelled hygrothermal stressed is in agreement with the Tg ranking of TMA set 1 specimens labelled hygrothermal stressed 1 and hygrothermal stressed 2.

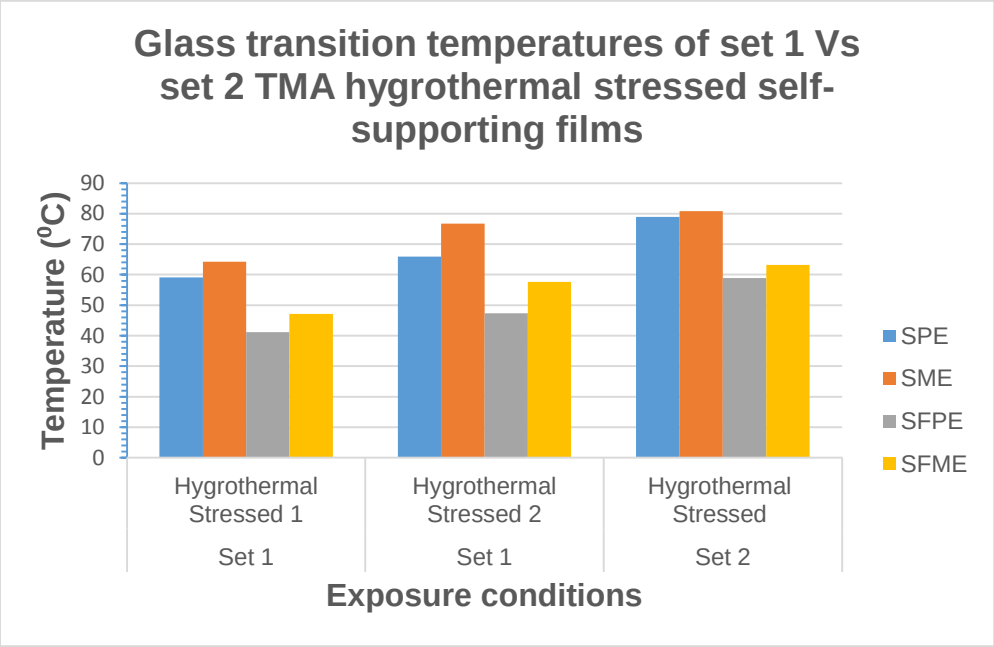

Figure 93 Tg values of hygrothermal stressed specimens for set 1 and set 2 using TMA

Table 38 illustrates the summary of the glass transition temperature Tg using TMA.

Table 38 Summary of glass transition temperature, Tg using TMA

Reference	SME > SPE > SFPE ≈ SFME
Heat Stressed	SPE > SME >> SFME >SFPE
Wet Stressed	SPE > SME >> SFME > SFPE
Hygrothermal Stressed	SME > SPE > SFME > SFPE

(b) Coefficient of thermal expansion

Table 39 shows the values of coefficient of thermal expansion (CTE) obtained for set 2 TMA specimens using TMA. For the TMA specimens labelled reference, it was observed that the values of CTE ranged from 53.3

µm/m°C to 74.4 µm/m°C. SFPE exhibited the highest CTE while SPE showed the lowest. SME and SFME showed CTE values of 56.6 µm/m°C and 63.6 µm/m°C respectively. For the TMA specimens labelled reference, the following CTE trend could be drawn:

SFPE > SFME > SME > SPE

This TMA ranking for CTE of reference specimens from the set 2 is consistent with that obtained from set 1 specimens labelled reference.

Table 39 Values of coefficient of thermal expansion (CTE) measured using TMA

Formulations \ Exposure Conditions		Set 2 TMA specimens: Self-supporting Free Films (µm/m°C)			
		Unaged	Aged		
		Reference (Ambient Cured)	Heat Stressed	Wet Stressed	Hygro- thermal Stressed
Pure Epoxy	Solvent Containing (SPE)	54.1	39.6	40.0	42.2
	Solvent Free (SFPE)	70.2	70.1	73.6	71.7
Modified Epoxy	Solvent Containing (SME)	61.8	54.0	54.9	54.4
	Solvent Free (SFME)	65.1	73.8	60.4	77.6

Table 39 shows the values of coefficient of thermal expansion obtained using TMA. Also, Figures 94 and 95 show the bar plots using TMA.

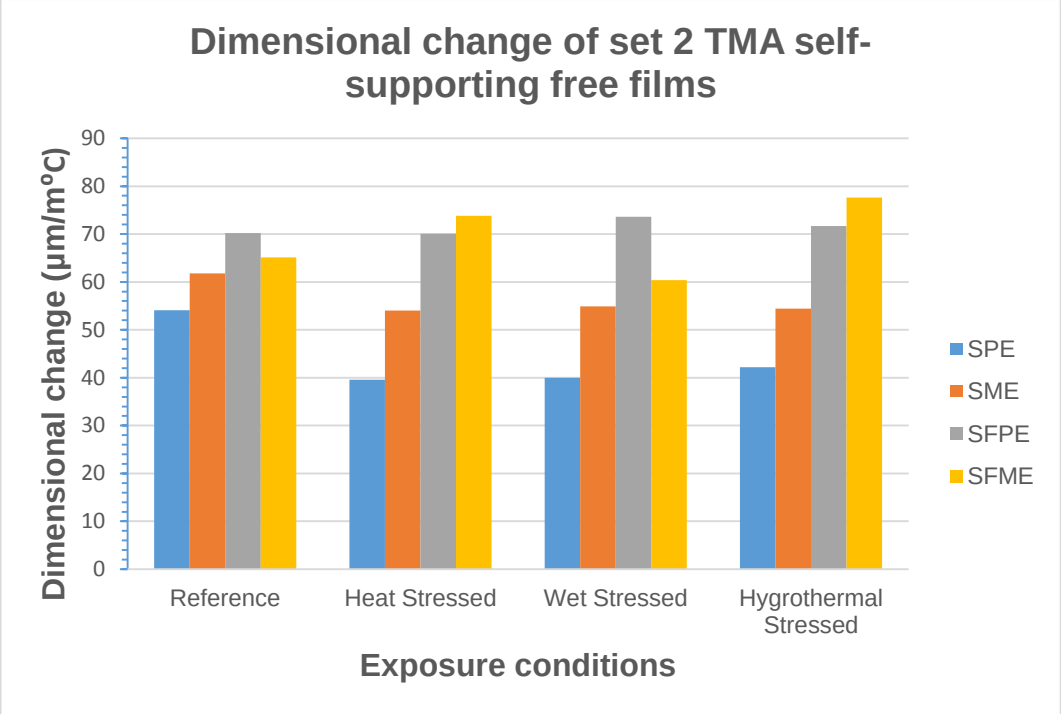

Figure 94 Dimensional change values of set 2 using TMA

For the TMA specimens labelled heat stressed, the observed ranking is as follows:

SFME > SFPE > SME > SPE

This ranking is inconsistent with that from the TMA ranking for reference specimens of set 1.

For the TMA specimens labelled wet stressed, the observed ranking trend is as follows:

SFPE > SFME > SME > SPE

This ranking is consistent with that obtained from the TMA specimens labelled wet stressed for set 1. This ranking is also in agreement with that obtained for TMA specimens labelled hygrothermal stressed 1 and hygrothermal stressed 2 of set 1.

For the TMA specimens labelled hygrothermal stressed, the ranking exhibited is as follows:

SFME > SFPE > SME > SPE

This TMA ranking closely related to that from set 1 specimens labelled hygrothermal stressed 1 and hygrothermal stressed 2. However, for set 1 specimens, SFPE exhibited the highest CTE value in both cases while for set 2, SFME displayed the highest CTE value.

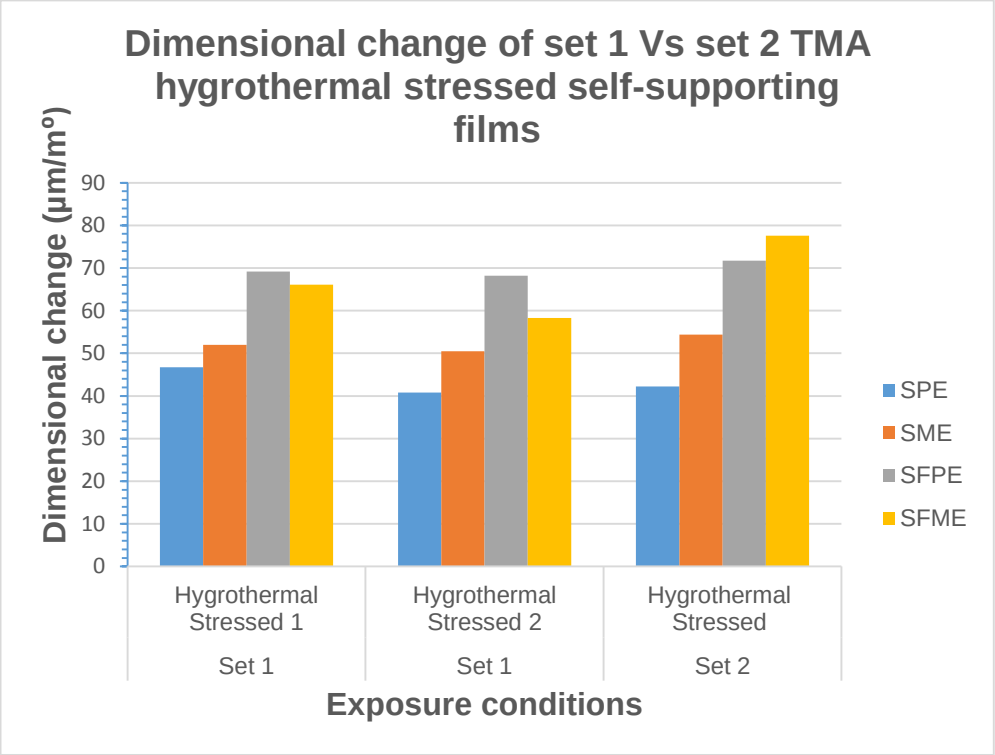

Figure 95 Dimensional changes values of set 1 Vs set 2 using TMA

Furthermore, it can be inferred that SFPE and SFME had higher CTEs in most exposure cases considered while SPE and SME had less CTEs when compared to SFPE and SFME. Table 40 illustrates the summary of the CTE using TMA.

Table 40 Summary of coefficient of thermal expansion, CTE using TMA

Reference	SFPE > SFME > SME > SPE
Heat Stressed	SFME > SFPE > SME > SPE
Wet Stressed	SFPE > SFME > SME > SPE
Hygrothermal Stressed	SFME > SFPE > SME > SPE

Figures 96 provides an overlay TMA plots of dimensional change for coefficient of thermal expansion as a function of temperature obtained for the four formulations after exposure to different defined laboratory conditions.

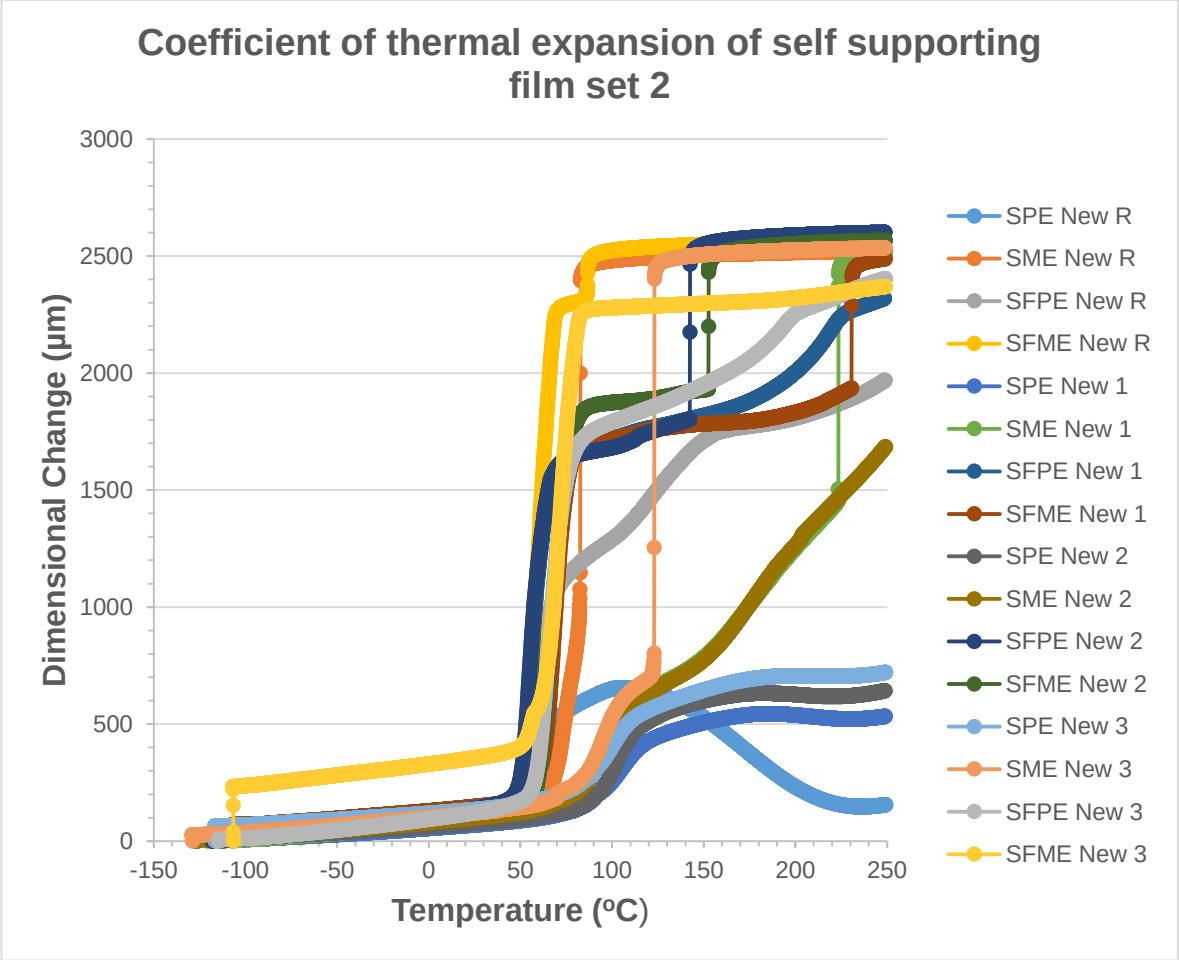

Figure 96 Overlay plot of CTE measured using TMA for set 2 free films

The average CTE from the exposure conditions are 71.40 x 10^{-6} ºC, 69.23 x 10^{-6} ºC, 56.28 x 10^{-6} ºC and 43.98 x 10^{-6} ºC for SFPE, SFME, SME and SPE respectively. Comparing the average CTE of each formulation to the CTE of structural steel (12 x 10^{-6} ºC) [104], it was observed that the difference (or mismatch) in CTE are 59.4 x 10^{-6} ºC, 57.23 x 10^{-6} ºC, 44.28 x 10^{-6} ºC and 31.98 x 10^{-6} ºC for SFPE, SFME, SME and SPE respectively. In relating the

mismatch CTE values to the result from the fatigue test in sections 5.2.1 and 5.4.1, a plausible conclusion is that the mismatched CTE had the least effect on SFPE. On the contrary, SPE with the lowest average mismatched CTE was adversely affected by cracking after one cycle of the fatigue test. Furthermore, it was observed that SPE and SME containing higher pigment content had lower CTE compared to SFPE and SFME with lower pigment content. It is highly likely that the pigments retained a substantial amount of heat energy, thereby allowing a smaller amount of dissipated energy at the interface. In addition, as the ultimate Tg of SFPE and SFME were much lesser than the top cycling temperature of 100 ^{o}C (T > Tg), there is a high mobility of the segmental molecular binders resulting in a stress relieve state. For SPE and SME, this was not the case. SPE developed the most stress following film formation and more with ageing from residual solvent loss and further cross-linking. In conclusion, formulations (SFPE and SFME) with the higher CTE and more mismatched to steel performed much better than those (SPE and SME) with lower CTE and less mismatch.

5.6 Statistical Analysis

Having completed the experimental characterisation, a statistical analysis was performed on the data to evaluate the effect of the fatigue test from the numbers of cycles to failure and the effect of volume loss on DFT of the four formulations. For the statistical analysis, ANOVA (a parametric analysis of variances) was used to analyse and compare the mean effect of the fatigue test resulting in number of cycles to failure as well as the mean volume loss from DFT measurements before and after completing the fatigue test on the participants of four formulations: SPE, SFPE, SME and SFME. The homogeneity of variances (levene's test) and the significant effect parametric Post Hoc Tukey were applied at .05 significance level [101,102].

5.6.1 SPSS Output 1 for fatigue test

SPSS Output 1 comprises of the descriptive statistics, tests between subject effects and the post hoc test from the effect of the proposed fatigue test on formulation type. Table 41 illustrates the descriptive statistics from one-way ANOVA with each formulation, the number of participants i.e. T specimens (N), the means, standard deviation and standard errors of the means for each formulation and confidence intervals (CI) limit within which the means of 95 out of 100 samples would fall.

Table 41 Descriptive statistics for numbers of cycles to failure

Formulation	N	Mean	Std. Deviation	Std. Error	95% Confidence interval for Mean	
					Lower bound	Upper bound
SPE	12	1.00	.000	.392	.211	1.789
SME	12	39.50	2.611	.392	38.711	40.289
SFPE	12	59.50	.522	.392	58.711	60.289
SFME	12	59.50	.522	.392	58.711	60.289

In Table 41, the column labelled standard deviation indicates the sampling distribution of the data. Thus, for SPE group, the means of the samples has a standard deviation of .000. The column labelled confidence interval offers the limits within which the means of 95 out of 100 sample would fall. For SPE group, 95 of the samples has a mean number of cycles to failure between .211 and 1.789. For SME group, the means of the samples has a standard deviation of 2.611 while both SFPE and SFME have a standard deviation of .522. For the column labelled confidence interval, SME has a mean number of cycles to failure between 38.711 and 40.289 while both SFPE and SFME have a mean number of cycles to failure between 58.711 and 60.289.

Table 42 Tests of between-subjects effects for number of cycles to failure

Source	Sum of squares	df	Mean squares	F	Sig.	Eta squared
Formulation	27380.250	3	9126.750	4947.741	.000	.997
Error	81.000	44	1.841			
Total	27461.250	47				

Table 42 presents the SPSS output 1 for the main ANOVA summary with the between-group effects. This table has six labelled columns: source, sum of squares, df, mean squares, F, sig., and eta squared. The sum of squares for the model (the total experimental effect) is 27380.250 and the degree of freedom on which the sum of squares are based (df) is 3. The mean sum of squares is associated with the experimental effect (the systematic variance) is 9126.750. The sum of squared errors and associated degree of freedom are 81.000 and 44 respectively. The F ratio representing the ratio of systematic variance to unsystematic variance is 4957.741. Lastly, the probability of obtaining an F-ratio of such magnitude by chance alone is .000. Therefore, as the observed significance value is less than .05, it was concluded that there was a significant effect of the fatigue test on the number of cycles to failure on formulation type.

Having established that the ANOVA was significant, a post hoc test was performed using Dunnett C.

Post Hoc Test: Formulation

Table 43 Multiple comparison of number of cycles to failure using Dunnett C

(I) Formulation	(J) Formulation	Mean Difference (I-J)	Std. Error	Sig.	95% Confidence interval	
					Lower bound	Upper bound
SPE	SME	-38.50*	.754		-40.77	-36.23
	SFPE	-58.50*	.151		-58.95	58.05
	SFME	-58.50*	.151		-58.95	58.05
SME	SPE	38.50*	.754		36.23	40.77
	SFPE	-20.00*	.769		-22.31	-17.69
	SFME	-20.00*	.769		-22.31	-17.69

SFPE	SPE	58.50*	.151		58.05	58.95
	SME	20.00*	.769		17.69	22.31
	SFME	.00	.213		-.64	.64
SFME	SPE	58.50*	.151		58.05	58.95
	SME	20.00*	.769		17.69	22.31
	SFPE	.00	.213		-.64	.64

*.The mean difference is significant at the .05 level

Table 43 illustrates the SPSS output 1 from the Dunnett C post hoc. In this table, each formulation in column labelled I is compared to the other formulations in column labelled J. For each pair of formulations, the difference between the formulation means, the standard error of the difference, the significance level of the difference and a 95% confidence interval are produced. First, SPE is compared to SME, SFPE and SFME. A significant difference was revealed in all cases. Next, SME was compared to the other formulations. Again all comparisons were significant. Similarly, SFPE was compared to other formulations. Likewise, SFME was compared to other formulations. All comparisons demonstrated a high significance. The comparison between SFPE and SFME indicated that the means of both SFPE and SFME are related in performance regarding numbers of cycles to failure from the fatigue test. However, the means of SFPE and SFME were significantly different from those of SPE and SME. Both SFPE and SFME produced a higher mean than SME and SPE while SME was moderate.

Leven's test indicated that the assumption of homogeneity of variance had been violated, F (3, 44) = -, p < .05. The results of the ANOVA showed that formulation was significantly affected by the fatigue test, F (3, 44) = 4957.741, p < .05, r = .998. The effect size indicated that the effect of the fatigue test on formulation types was substantial.

Dunnett C post hoc tests revealed significant differences in performance between all formulations (p < .05 for all tests) with SFPE and SFME exhibiting related behaviour.

The results of the ANOVA analysis supports the conclusion that there is a statistically significant and strong relationship between numbers of cycles to failure from the fatigue test and formulation type.

5.6.2 SPSS Output 2 for volume loss

SPSS Output 2 shows the table of descriptive statistics, test of between subject effects and post hoc test from ANOVA on the effect of volume loss on DFT of formulation type measured before and after subjecting participants (specimens) to the designed fatigue test. The four formulations had participants representing the target DFTs of 640 µm and 960 µm.

(a) Volume loss for 640 µm DFT

Table 44 shows the descriptive statistics for volume loss for 640 µm with the columns labelled formulation, N (number of participants), standard deviation, standard error and 95% confidence interval (CI). For SPE group, the means of the samples has a standard deviation of 34.39. For the column labelled 95% CI, SPE group has a mean difference between 95.387 and 111.530. For SME group, the means of the samples has a standard deviation of 25.02 while SFPE and SFME have a standard deviation of 18.20 and 50.51 respectively. For the column labelled confidence interval, SME has a mean difference in volume loss between 50.609 and 66.752 while SFPE has a mean difference in volume loss between 31.975 and 49.659; and SFME between 64.637 and 80.780.

Table 44 volume loss for 640 µm DFT measurement

Formulation	N	Mean	Std. Deviation	Std. Error	95% Confidence interval for Mean	
					Lower bound	Upper bound
SPE	72	103.46	34.39	4.100	95.387	111.530

Formulation	N	Mean	Std. Deviation	Std. Error	95% Confidence interval for Mean	
					Lower bound	Upper bound
SME	72	58.68	25.02	4.100	50.609	66.752
SFPE	60	40.82	18.20	4.491	31.975	49.659
SFME	72	72.71	50.51	4.100	64.637	80.780

Table 45 presents the SPSS output 2 for the main ANOVA summary with the between-group effects for 640 µm DFT. The sum of squares for the model (the total experimental effect) is 141449.382 and the degree of freedom on which the sum of squares are based (df) is 3. The mean sum of squares is associated with the experimental effect (the systematic variance) is 47149.794. The sum of squared errors and associated degree of freedom are 329185.386 and 272 respectively. The F ratio representing the ratio of systematic variance to unsystematic variance is 38.959. Lastly, the probability of obtaining an F-ratio of such magnitude by chance alone is .000. Therefore, as the observed significance value is less than .05, it was concluded that there was a significant effect of volume loss on formulation after the participants were subjected to the fatigue test.

Table 45 Tests of between-subjects effects of volume loss for 640 µm DFT

Source	Sum of squares	df	Mean squares	F	Sig.	Eta squared
Formulation	141449.382	3	47149.794	38.959	.000	.301
Error	329185.386	272	1210.240			
Total	470634.768	275				

Having established that the ANOVA was significant, a post hoc test was performed using Games-Howell.

Post Hoc Test: Formulation

Table 46 Multiple comparisons of volume loss for 640 µm DFT

Games-Howell

(I) Formulation	(J) Formulation	Mean Difference (I-J)	Std. Error	Sig.	95% Confidence interval	
					Lower bound	Upper bound
SPE	SME	44.7778*	5.01265	.000	31.7316	57.8239
	SFPE	62.6417*	4.68526	.000	50.4217	74.8616
	SFME	30.7500*	7.20237	.000	11.9959	49.5041
SME	SPE	-44.7778*	5.01265	.000	-57.8239	-31.7316
	SFPE	17.8639*	3.77074	.000	8.0481	27.6797
	SFME	-14.0278	6.64387	.156	-31.3757	3.3201
SFPE	SPE	-62.6417*	4.68526	.000	-74.8616	-50.4217
	SME	-17.8639*	3.77074	.000	-27.6797	-8.0481
	SFME	-31.8917*	6.40047	.000	-48.6387	-15.1446
SFME	SPE	-30.7500*	7.20237	.000	-49.5041	-11.9959
	SME	14.0278	6.64387	.156	-3.3201	31.3757
	SFPE	31.8917*	6.40047	.000	15.1446	48.6387

*.The mean difference is significant at the .05 level

Table 46 illustrates the SPSS output 2 from the Games-Howell post hoc for 640 µm DFT. In this table, each formulation in column labelled I is compared to the other formulations in column labelled J. For each pair of formulations, the difference between the formulation means, the standard error of the difference, the significance level of the difference and a 95% confidence interval are produced. First, SPE is compared to SME, next to SFPE and last to SFME. This process of comparison was followed with other formulations. Following this process of comparison for SPE, a significant difference was revealed in all cases. Next, SME was compared to the other formulations, with the exception for SFME, other comparisons were significant. For SFPE, all comparisons were significant. For SFME, with the exception for SME, other comparisons were significant. In summary, all comparisons demonstrated a high significance except the comparison between SME and SFME that was non-significant indicating that the means of both SME and SFME had related amount of volume loss at 640 µm. However, the means of SPE and SFPE were significantly different from those of SME and SFME. SFPE produced the lowest amount of volume loss while SPE produced the highest volume loss. SFME and SME produced volume loss that were between.

Leven's test indicated that the assumption of homogeneity of variance had been violated, F (3, 272) = 4.413, p < .05. The results of the ANOVA identified SFPE formulation as having the lowest volume loss compared to SPE, SME and SFME. Volume loss is significantly affected by formulation type, F (3, 272) = 38.959, p < .05, r = .549. The effect size indicated that the effect of volume loss on formulation was substantial.

Games-Howell post hoc tests revealed significant differences between all formulations (p < .05 for all tests) except between SME and SFME (not significant).

The results of the ANOVA confirms the conclusion that there is a statistically significant and strong relationship between volume loss for 640 µm DFT and formulation type after undergoing the fatigue test.

(b) Volume loss for 940 µm DFT

Table 47 shows the descriptive statistics for volume loss for 960 µm with the columns labelled formulation, N (number of participants), standard deviation,

standard error and 95% confidence interval (CI). For SPE group, the means of the samples has a standard deviation of 46.59. For the column labelled 95% CI, SPE group has a mean difference between 110.772 and 130.200. For SME group, the means of the samples has a standard deviation of 45.17 while SFPE and SFME have a standard deviation of 38.11 and 36.11 respectively. For the column labelled confidence interval, SME has a mean difference in volume loss between 100.744 and 120.173 while SFPE has a mean difference in volume loss between 60.744 and 80.173; and SFME between 92.369 and 111.798.

Table 47 Descriptive statistics of volume loss for 960µm DFT

Formulation	N	Mean	Std. Deviation	Std. Error	95% Confidence interval for Mean	
					Lower bound	Upper bound
SPE	72	120.49	46.59	4.935	110.772	130.200
SME	72	110.49	45.17	4.935	100.744	120.173
SFPE	72	70.46	38.11	4.935	60.744	80.173
SFME	72	102.08	36.11	4.935	92.369	111.798

Table 48 presents the SPSS output 2 for the main ANOVA summary with the between-group effects for 960 µm. The sum of squares for the model (the total experimental effect) is 101021.010 and the degree of freedom on which the sum of squares are based (df) is 3. The mean sum of squares is associated with the experimental effect (the systematic variance) is 33673.670. The sum of squared errors and associated degree of freedom are 498045.236 and 284 respectively. The F ratio representing the ratio of systematic variance to unsystematic variance is 19.202. Lastly, the probability of obtaining a F-ratio of such magnitude by chance alone is .000. Therefore, as the observed significance value is less than .05, it was concluded that there was a significant effect of volume loss on formulation from the fatigue test.

Table 48 Tests of between-subjects effects of volume loss for 960µm DFT

Source	Sum of squares	df	Mean squares	F	Sig.	Eta squared
Formulation	101021.010	3	33673.670	19.202	.000	.169
Error	498045.236	284	1753.680			
Total	599066.246	287				

Having established that the ANOVA was significant, a post hoc test was performed using Games-Howell.

Post Hoc Test: Formulation

Table 49 Multiple comparisons of volume loss for 960µm DFT

Games-Howell

(I) Formulation	(J) Formulation	Mean Difference (I-J)	Std. Error	Sig.	95% Confidence interval	
					Lower bound	Upper bound
SPE	SME	10.0278	7.64712	.557	-9.8528	29.9083
	SFPE	50.0278*	7.13976	.000	31.4591	68.5965
	SFME	18.4028*	6.94678	.044	.3298	36.4758
SME	SPE	-10.0278	7.64712	.557	-29.9083	9.8528
	SFPE	40.0000*	7.01206	.000	21.7656	58.2344
	SFME	8.3750	6.81547	.610	-9.3535	26.1035

SFPE	SPE	-50.0278*	7.13976	.000	-68.5965	-35.4591
	SME	-40.0000*	7.01206	.000	-58.2344	-21.7656
	SFME	-31.6250*	6.24085	.000	-47.8504	-15.3996
SFME	SPE	-18.4028*	6.94678	.044	-36.4758	-.3298
	SME	-8.3750	6.81547	.610	-26.1035	9.3535
	SFPE	31.6250*	6.24085	.000	15.3996	47.8504

*.The mean difference is significant at the .05 level

Table 49 shows the SPSS output 2 from the Games-Howell post hoc for 960 µm DFT. Similarly, in this table, each formulation in column labelled I is compared to the other formulations in column labelled J. For each pair of formulations, the difference between the formulation means, the standard error of the difference, the significance level of the difference and a 95% confidence interval are produced. A similar process of comparison as used for the 640 µm DFT was followed. First, SPE was compared to SME, next to SFPE and last to SFME. The outcome of the comparison for SPE showed that a significant difference was revealed in other cases except with SME indicating that the means of both SPE and SME had related volume loss at 960 µm DFT. Next, SME, SFPE and SFME were compared to the other formulations respectively. Only SFPE comparison was significant in all cases unlike the comparisons of others. The comparisons from SME was significant he except the comparison between SME and SFME that was non-significant indicating that the means of both SME and SFME had related volume loss at 960 µm DFT. However, the means of SPE and SFPE were significantly different from those of SME and SFME. Again, SFPE produced the lowest amount of volume loss while SPE produced the highest volume loss. SFME and SME produced volume loss that were between.

Leven's test indicated that the assumption of homogeneity of variance had not been violated, F (3, 284) = .571, p > .05. The results of the ANOVA identified SFPE formulation as having the lowest volume loss than SPE, SME and SFME. Volume loss is significantly affected by formulation type, F

(3, 287) = 19.202, $p < .05$, $r = .411$. The effect size indicated that the effect of volume loss on formulation was substantial.

Games-Howell post hoc tests revealed significant differences in volume loss between SFPE and other formulations ($p < .05$ for all tests). However, differences in volume loss are related between SME and SFME (not statistically significant). Similarly, difference between SPE and SME are related (not statistically significant).

The results of the ANOVA confirms the conclusion that there is a statistically significant and strong relationship between volume loss for 960 µm DFT of SFPE and other formulations after undergoing the fatigue test.

Specifically, the volume loss of SFPE for 640 µm DFT ($M = 40.82$, $SD = 18.20$) was less than that of 960 µm DFT ($M = 70.46$, $SD = 38.73$). Equally, the volume loss of SFME for 640 µm DFT ($M = 72.70$, $SD = 50.52$) was less than that for 960 µm DFT ($M = 102.08$, $SD = 36.11$). Also, the volume loss of SME for 640 µm DFT ($M = 58.68$, $SD = 25.02$) was less than for 960 µm DFT ($M = 110.46$, $SD = 45.17$). Similarly, the volume loss of SPE for 640 µm DFT ($M = 103.46$, $SD = 34.39$) was less than the 960 µm DFT ($M = 120.47$, $SD = 46.59$). In both DFTs considered for volume loss, SFPE has the lowest volume loss while SPE had the highest volume loss. These findings confirms that the effect of volume loss following the fatigue test differed between the formulations and showed that there is an increase in volume loss with increase in DFT.

CHAPTER 6
NUMERICAL MODELLING OF COATING FORMULATIONS

6.1 Finite Element Analysis

Prior to in service use of materials, numerical modelling could also be applied in understanding the anticipated behavioural response and performance of materials to loadings such as structural and thermal. Depending on the loading conditions, there are a number of analysis available to users of numerical modelling. For a structure experiencing thermal loading, applying numerical modelling in the area of thermal analysis will likely provide insight into either the distribution of temperature, the distribution of heat flux or the thermal stress. In addition, for structures experiencing either thermal expansion or contraction and/or both such as the case of the T specimens exposed to the fatigue testing based on hygrothermal cycling, it could be advantageous to simulate and evaluate them for thermal stress (and corresponding thermal strain) as this could offer structural responses concerning change in temperature conditions. However, numerical modelling techniques strongly rely on input parameters or material properties that are derived from experimental characterisation.

Finite Element Analysis (also known as Finite Element Method) is a numerical modelling technique utilised in obtaining approximate solutions of complex engineering problems that are unsolvable by basic theories. The concept of Finite Element Analysis (FEA) is based on dividing a complicated geometry into pieces that are much smaller and less complicated. These smaller pieces are glued together using complex mathematics to yield approximate solution. Thus, FEA breaks a complicated geometry into simpler blocks called elements and the shape of the elements is defined by nodes which are points. Zienkiewicz [105] presented an historic account on the development of FEA and of computational mechanics. Some of the key developments, which shaped FEA for today's application are as follows:

- 1943 – Courant (Variational methods that set the foundation for FEA)
- 1956 – Turner, Clough, Martin, and Topp (Stiffness method)
- 1960 – Clough devised the term "Finite Element" in solving plane problems

- 1970s – Mainframe computers were utilised for the application of FEA
- 1980s – Microcomputers, development of pre-processors and post-processors (Graphical User Interface)
- 1990s – Analysis of large structural systems, dynamic and nonlinear problems
- 2000s – Analysis of multiscale and multiphysics system problems

6.1.1 A typical FEA procedure

A typical FEA procedure irrespective of the simulation type follows the basic steps outlined below:

- Specify the type of analysis system
- Create or attach the geometry model
- Divide the geometry model into nodes and elements (meshing)
- Assign material properties and boundary conditions including loads
- Solve
- Select Results
- Review and interpret Results

The principal difference in the above approach of an FEA simulation is the application of load type(s) specific to an analysis system and the evaluation of results as per the analysis system. In a commercial FEA package such as ANSYS, the above listed steps are sorted into the following stages:

- Pre-processing (building of FEA models, specifying element properties; and applying boundary constrains and loads)
- Processing - FEA solver (assembling and solving FEA equations, calculating element results)
- Post-processing (sorting and displaying the results)

Advantages of FEA include: reducing the number of prototype testing, simulating designs that are unsuitable for prototype testing, measuring parameters such as temperature, stress, safety factor and deformation at points of interest in the geometrical model, optimising of a design and representing the result from an analysis in graphical format. A potential disadvantage of FEA is the inability to offer exact solution.

6.1.2 An overview of ANSYS Workbench

The simulation interface used in this research for the numerical modelling is ANSYS Workbench hence; this section offers a brief overview to the main features of the graphical user interface in ANSYS Workbench. The graphical user interface of ANSYS Workbench consists of the following: Title bar, Menu bar, Standard toolbar, Project Schematic window, Toolbar and Status bar.

6.1.2.1 Menu bar

The menu bar is positioned horizontally at the top of the Workbench user interface. It offers the following labelled tabs: File, View, Tools, Units, Extensions and Help.

6.1.2.2 Toolbox

The Toolbox contains four sections: Analysis systems, Component systems, Custom systems and Design Exploration. As constituents from the analysis systems and the component systems were the only ones utilised in the modelling simulation for this research, both are emphasised on next.

(a) Analysis systems

Analysis systems are utilised to build a project. Analysis systems include transient thermal, static structural, fluid flow and steady-state thermal.

(b) Component systems

Components systems are utilised to either build or expand an analysis system. Component systems include mesh, geometry and engineering data.

6.1.2.3 Project schematic window

The project schematic window is an empty space prior to housing one system or more.

A typical simulation in ANSYS Workbench is performed by dragging a system from any of the four sections in the toolbox and dropping it

on the project schematic window. A system refers to the item on the Project Schematic window.

A simple system such as geometry has a cell while a complex system has cells and links. Each cell contributes to achieving the simulation objective of an FEA modelling project and each cell is activated typically from top to bottom of the system by double clicking.

6.1.2.4 Cells in a system

Generally, in ANSYS Workbench, systems such as thermal static, thermal transient and static structural have cells labelled from top to bottom with the following labels: Engineering Data, Geometry, Model, Setup, Solution and Results.

(a) Engineering data

The cell labelled Engineering Data is utilised in defining the material properties such as Young's modulus, Poisson's ratio and Density of the model. Engineering data is activated by double clicking on it.

(b) Geometry

The cell labelled Geometry is utilised in either creating, importing or editing a geometrical model that is utilised in a system during simulation. One of the methods in creating a geometrical model in ANSYS Workbench is to double click on the Geometry cell that will subsequently open the graphics window of DesignModeler as shown in Figure 97.

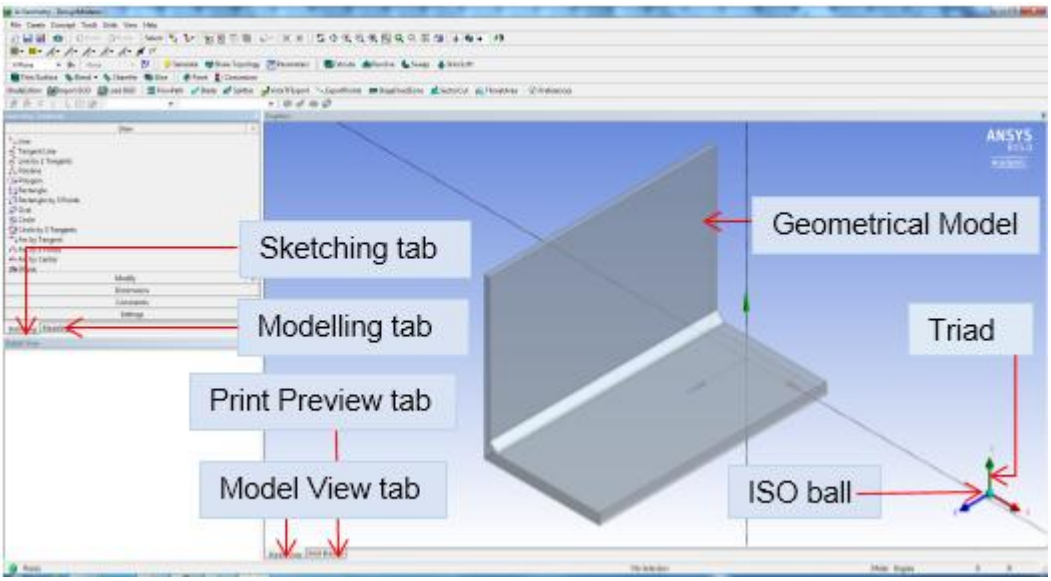

Figure 97 Graphics window of DesignModeler containing a Geometrical Model

DesignModeler allows two basic modes: Sketching and Modelling. The sketching tab within DesignModeler is used to switch to the sketching mode where drawing a two-dimensional sketch in the graphics window is performed. It contains five toolbox sections: draw, modify, dimension, constraint and setting. Each section has specific constituents that are utilised when in the sketching mode to create, modify and dimension a sketch. The modelling tab within DesignModeler is used to switch to the modelling mode where either a part or an assembly model is generated using the outline sketch(s) from the graphic window in sketching mode. The modelling mode contains features/tools such as extrude, chamfer, fillet and revolve. Other features within the DesignModeler are as follows: Tree Outline (which has the three default planes: XY, YZ and ZX and a summary of any other operation carried out in building a model), Triad, Ruler, Status bar, Model View and Print View.

(c) Model

The cell labelled Model when launched by double clicking, opens up in Mechanical window and is utilised in breaking a complex geometrical model into smaller elements to yield an appropriate mesh density. This cell is linked to meshing.

(d) Setup

The cell labelled Setup is utilised in specifying the boundary conditions such as loads and constraints specific to an analysis system. When this cell is invoked, it opens in Mechanical window.

(e) Solution

The cell labelled Solution utilises the FEA solver in solving the simulated problem of an analysis system. Data fed from the other cells (geometry, mesh, assigned material properties and boundary conditions) above it are utilised during this process. The cell also opens in Mechanical window.

(f) Results

The cell labelled Results is utilised in displaying the obtained results after solving the simulated analysis system. This cell also opens in Mechanical window.

6.2 Coupled Field Analysis Systems

As a coupled field system analysis comprising of both a transient thermal analysis system and a static structural analysis system was modelled in ANSYS Workbench, a brief review of transient thermal analysis system will be discussed further.

A coupled field analysis system has two or more single analysis fields in a numerical modelling project and considers the mutual interaction between the systems. It applies similar principle as for a single analysis system where the user walks through cells of a system from top to bottom as described in section 6.1.2.4 previously.

6.2.1 Thermal analysis

The thermal analysis part of the coupled field analysis systems was used to determine the temperature distribution that was fed as input for thermal stress evaluation. Hence, it was considered appropriate to discuss briefly some related theoretical background such as the heat transfer modes and analysis types.

For thermal problems, there are primarily three heat transfer modes: conduction, convection and radiation that are encountered either alone or in

combination. Conduction is a heat transfer mode where heat is transferred within a body or between bodies in contact as a consequence of temperature gradient. Convection is another heat transfer mode in which the medium of heat exchange is between a fluid and a body while radiation is a heat transfer mode in which the heat is transferred through space. Each heat transfer mode can be modelled using any of the two thermal analysis types: Steady state thermal analysis and Transient thermal analysis. In steady state thermal analysis, the applied thermal loads are invariable with respect to time whereas, in transient thermal analysis the applied loads vary as a function of time *t* and space (*x, y, z* in the Cartesian coordinates).

ANSYS manual [102, 103] provides a heat balance equation for transient thermal analysis based on the conservation of energy as shown in eq 7 below.

$$k\,(\partial^2 T/\partial x^2) + k\,(\partial^2 T/\partial y^2) + q = \rho c\,((\partial T/\partial t) \quad \textbf{(7)}$$

Where *k* is thermal conductivity coefficient (W/(m°C)), q is heat generation rate (J/(m^{3}s), ρ is density (Kg/m^3) and c is specific heat capacity (J/(kg°C)).

6.2.2 Thermal stress analysis

Thermal stress is induced when a structure is constrained. The relationship between the temperature variation and corresponding thermal strain from the response of the structure can be expressed in eq 8 as follows:

$$\varepsilon_{th} = \alpha \Delta T \quad \textbf{(8)}$$

Where, α is the coefficient of thermal expansion (°C^{-1}), ε_{th} is the thermal strain and $\Delta T = T_2 - T_1$ is the change in temperature (°C).

The total strain is given in eq 9 by

$$\varepsilon = \varepsilon_e + \varepsilon_{th} \quad \textbf{(9)}$$

In which ε_e is the elastic strain arising from mechanical load.

$$\varepsilon_e = E^{-1}\sigma \quad \textbf{(10)}$$

Therefore, substituting eqs 8 and 10 into eq 9 gives the total strain in eq 11 as:

$$\varepsilon = E^{-1}\sigma + \alpha\Delta T \quad \textbf{(11)}$$

Then rearranging eq 11 and making stress (σ) the subject of the formula gives eq 12:

$$\sigma = E\,(\varepsilon - \varepsilon_{th}) \quad \textbf{(12)}$$

Further theorem details linked to these equations can be obtained in ANSYS manual [106, 107].

6.3 Modelling of Coupled Field Analysis Systems

Having reviewed some background, the behavioural response of adhered epoxy coating formulations: SPE, SME, SFPE and SFME on steel substrate was evaluated using the coupled analysis system. The analysis utilised the commercial ANSYS software. Two dry film thickness of the four epoxy coating formulations: 960 µm (i.e. 0.000960 m) and 640 µm (i.e. 0.000640 m) adhered to steel substrate were modelled respectively. Furthermore, the fundamental assumptions are that displacement values will be small so that a linear solution is valid, material properties will remain in the linear region and the coating film/steel substrate is homogenous.

6.3.1 Engineering aata

Each of the four coating formulations: SPE, SME, SFPE and SFME were added as a new material to in the outline schematic of Engineering Data interface. Also, the corresponding values of material properties were entered in the outline schematic of Engineering Data.

6.3.2 Geometrical model

A three dimensional L shaped geometrical model of a T specimen was considered for this modelling. Due to symmetry and gains in computation time without sacrificing accuracy, only half of the T specimen was modelled. The L shaped model consisted of the steel substrate and one specific dry film thickness of each epoxy coating formulation is shown in Figure 98.

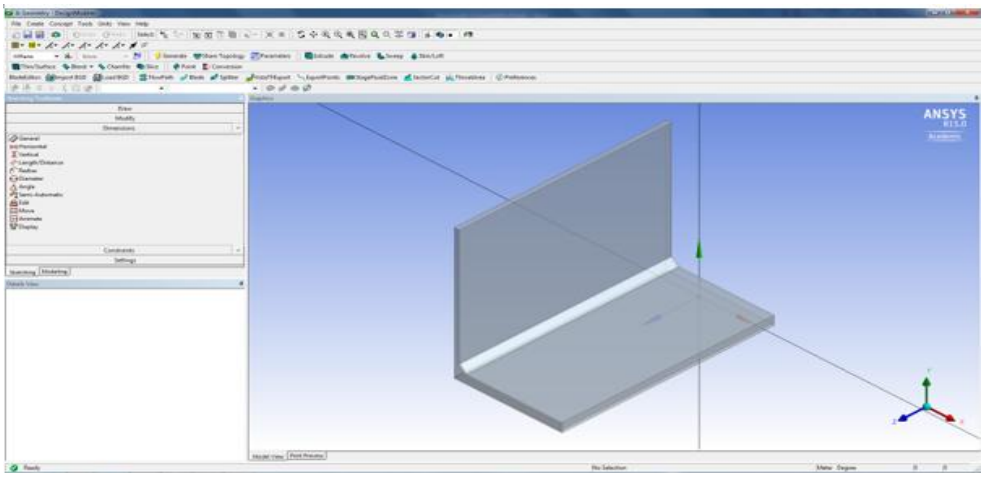

Figure 98 L shaped Geometrical model

The geometrical dimensions of the L steel substrate model, for flange (L: 0.0725 m, W: 0.005 m, D: 0.145 m) and for web (L: 0.0025 m, W: 0.095 m, D: 0.145 m). The dry film thickness of the four epoxy coating formulations: 0.000960 m and 0.000640 m respectively. Each coating formulation was assigned as a material to the geometrical model in Workbench.

6.3.3 Meshing

Meshing was mapped on the L shaped model using a higher order solid element. Both the coating and steel substrate were meshed using a three-dimensional 20node hexahedron (brick) element. Areas around the fillet weld were further refined. The generated mesh amounted to 29,700 elements and 171,552 nodes. The mesh is shown in Figure 99.

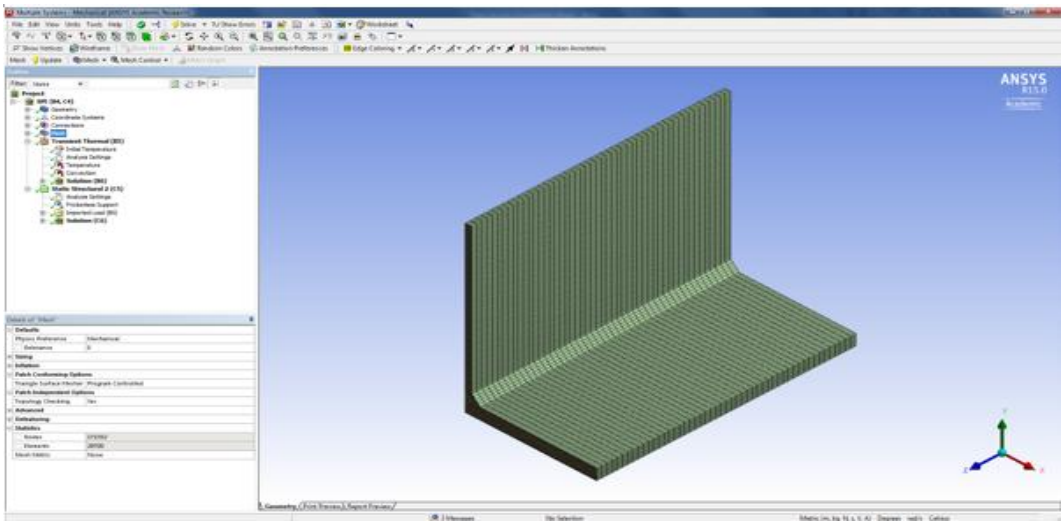

Figure 99 Meshed L shaped Geometrical model

For stress concentration problems, higher order solid elements such as 20node hexahedron element is ideal and suitable in modelling corners. The element exhibits quadratic behaviour.

6.3.4 Boundary conditions

In the transient thermal analysis system, thermal loads of 100 ºC for initial temperature of the L specimen and 22 ºC ambient temperature was modelled. Also, the surrounding temperature of the stagnant water was modelled by convective film coefficient of 1200 W/m^{2}ºC at 22 ºC. In the structural analysis system, rigid body was avoided using frictionless support.

6.3.5 Solution and results

A coupled field analysis system was used in solving the problem. The computed thermal history from the transient thermal system was imported to the static structural system. Results were scoped with contour legends showing the maximum and minimum for stress and strain encountered for this modelling. The next section will present the results.

CHAPTER 7
NUMERICAL RESULTS

7.1 FEA Simulation

The scoped numerical results from simulating the L specimen model with adhered films of the respective four formulations: SPE, SME, SFPE and SFME are presented in this section. Two coating dry film thicknesses: 960 µm (i.e. 0.000960 m) and 640 µm (i.e. 0.000640 m) of each formulation are considered for comparison. Figures 102 to 109 show the contour plots with corresponding legends displayed in the graphic screens for Equivalent strain. The legend shows a band of colours in a column arranged from top to bottom. Each band of colour indicates a specific value. For example, the colour blue in the legend depicts the minimum value while colour red represents the maximum value.

7.1.1 Equivalent (von Mises) stress

Presented in Figure 100 is the bar chart plot of Equivalent (von Mises) stress for SPE, SME, SFPE and SFME.

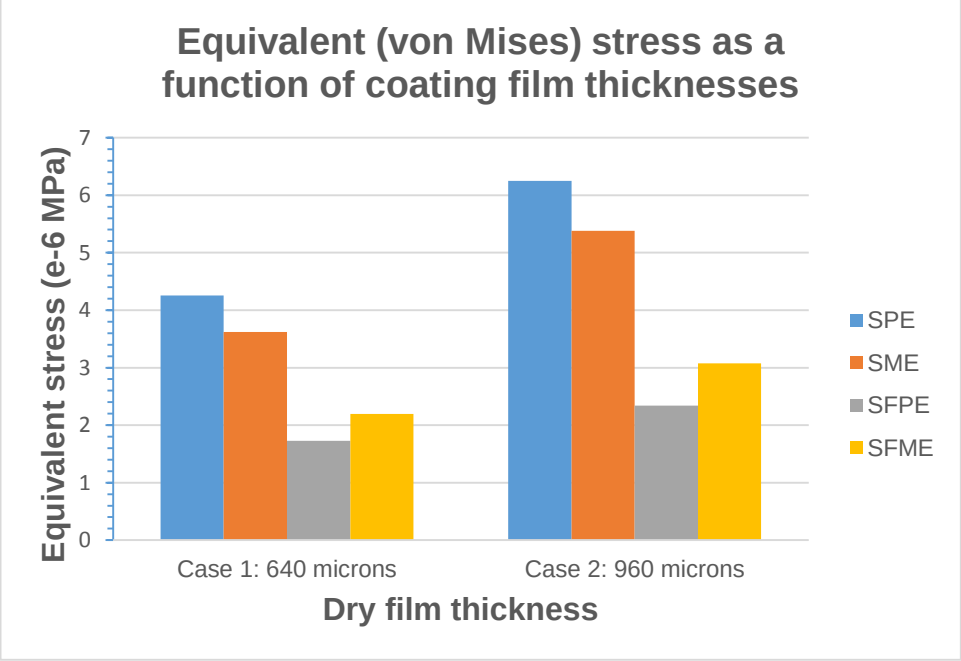

Figure 100 Bar chart plot of case 1 and case 2 equivalent stress on simulated L specimens

The Equivalent (von Mises) Stress is a common criterion utilised in understanding the effect of all the directional stresses acting at the point under consideration. It represents the response of the model as either able to sustain or unable (fails) to sustain the applied stress at specific location(s).

For case1 with L specimen having 640 µm adhered film, it was observed that the magnitudes of the minimum Equivalent stress occurred uniformly on the coating film and ranged from approximately 1.725e-6 MPa to 4.258e-6 MPa. SPE displayed the highest while SFPE exhibited the lowest. Both SME and SFME displayed magnitudes of 3.62e-6 MPa and 2.195e-6 MPa respectively. The following trend in minimum Equivalent stress was drawn:

SPE > SME > SFME > SFPE

For case2 with L specimen having 960 µm adhered film, it was observed that the magnitudes of the minimum Equivalent stress ranged from approximately 2.340e-6 MPa to 6.25e-6 MPa. SPE displayed the highest while SFPE exhibited the lowest. Both SME and SFME displayed magnitudes of 5.383e-6 MPa and 3.073e-6 MPa respectively. There is some increase in stress in the four formulations for the 960 µm film when compared to that of the 640 µm film. However, the increase is more significant in the solvent containing formulations: SPE and SME formulations than the solvent free formulations: SFPE and SFME. The following trend in minimum Equivalent stress was drawn:

SPE > SME > SFME > SFPE

The ranking of Equivalent (von Mises) stress in both cases simulated compares very well. Also, this ranking agrees with the general view that thicker films are likely to show more stress than thinner ones. This ranking also confirms that exhibited in the fatigue testing and the view that formulations with a higher stress has much lesser capacity to withstand further additional load/stress from the external source or environment.

Furthermore, the maximum Equivalent (von Mises) stress of approximately 0.35 MPa occurred in the steel substrate in all cases considered, which is

much higher than that for the coating formulations of both thicknesses simulated.

7.1.2 Equivalent elastic strain

Presented in Figure 101 is the bar chart plot of Equivalent Elastic Strain for SPE, SME, SFPE and SFME.

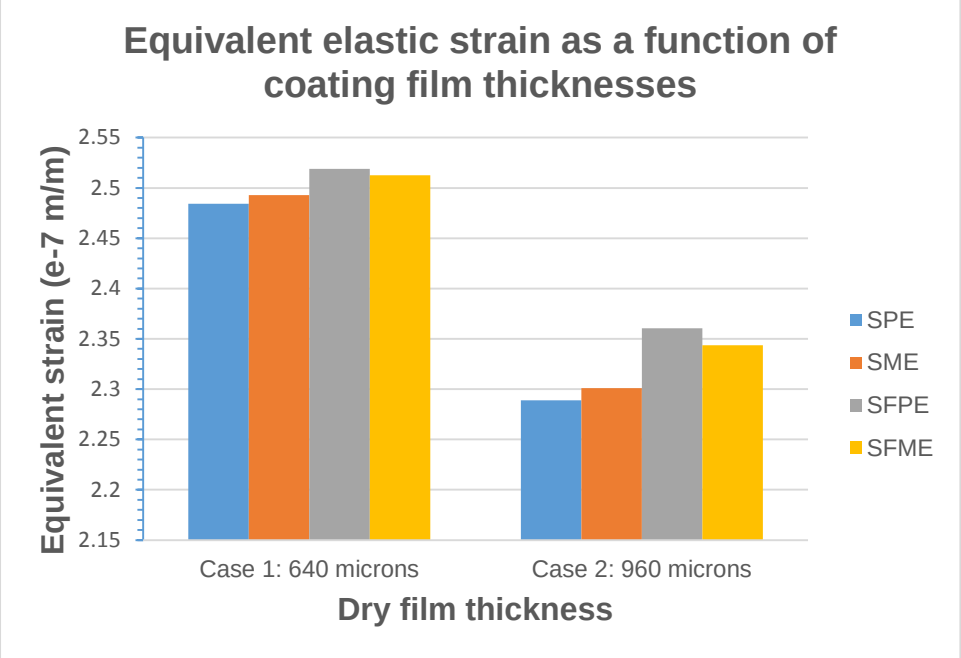

Figure 101 Bar chart plot of Case 1 and Case 2 Equivalent Strain on Simulated L specimens

For case1 with L specimen having 640 µm DFT, it was observed that the magnitudes of the maximum Equivalent strain ranged from approximately 2.484e-7 m/m to 2.158e-7 m/m. SFPE displayed the highest while SPE exhibited the lowest. Both SME and SFME displayed magnitudes of 2.492e-7 m/m and 2.512e-7 m/m respectively. The following trend in maximum Equivalent strain emerged:

SFPE > SFME > SME > SPE

Presented in Figures 102 to 105 are the graphic display of the Equivalent strain computed for 640 µm films in this numerical simulation.

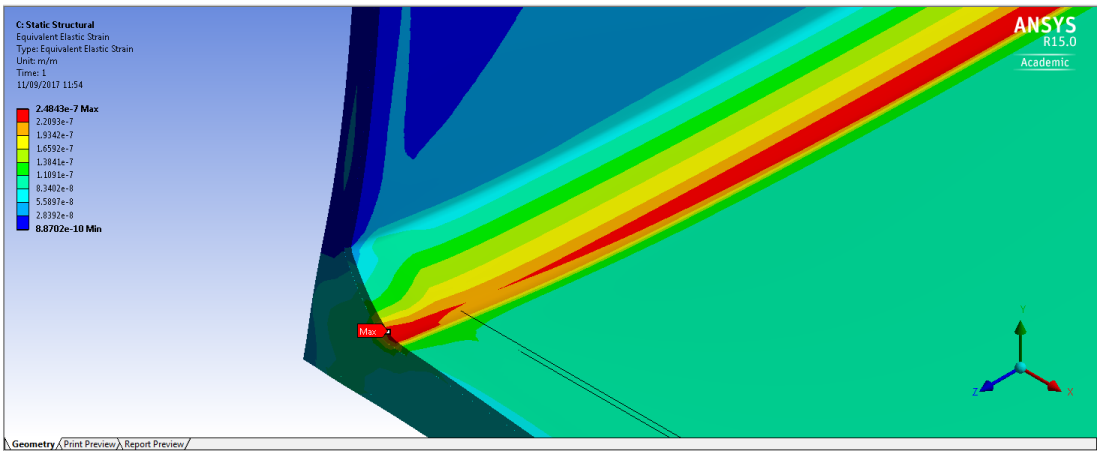

Figure 102 Undeformed and deformed model views of equivalent strain for SPE with 640 microns DFT

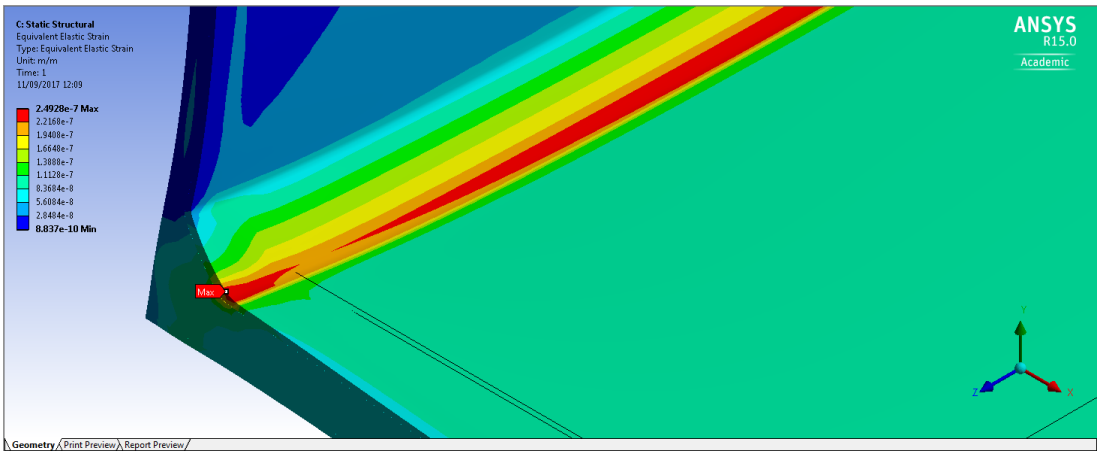

Figure 103 Undeformed and deformed model views of equivalent strain for SME with 640 microns DFT

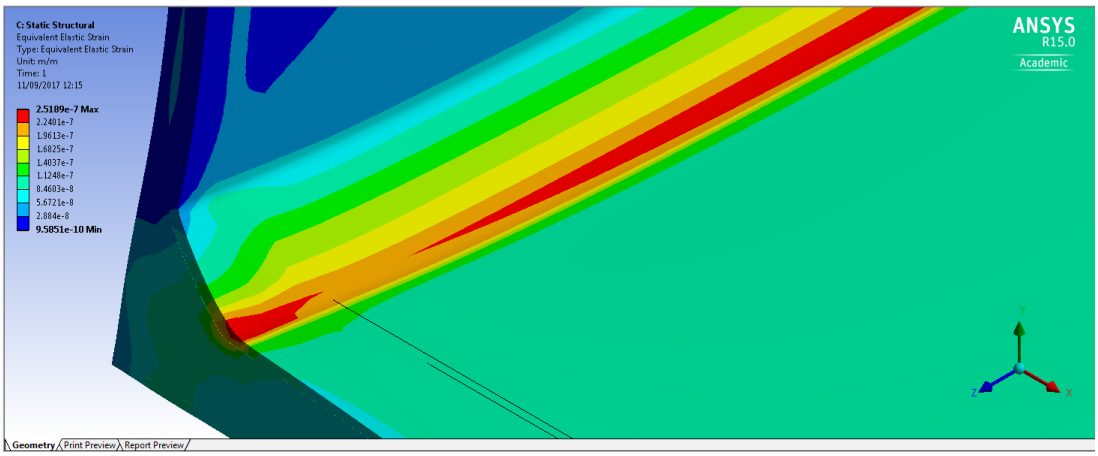

Figure 104 Undeformed and deformed model views of equivalent strain for SFPE with 640 microns DFT

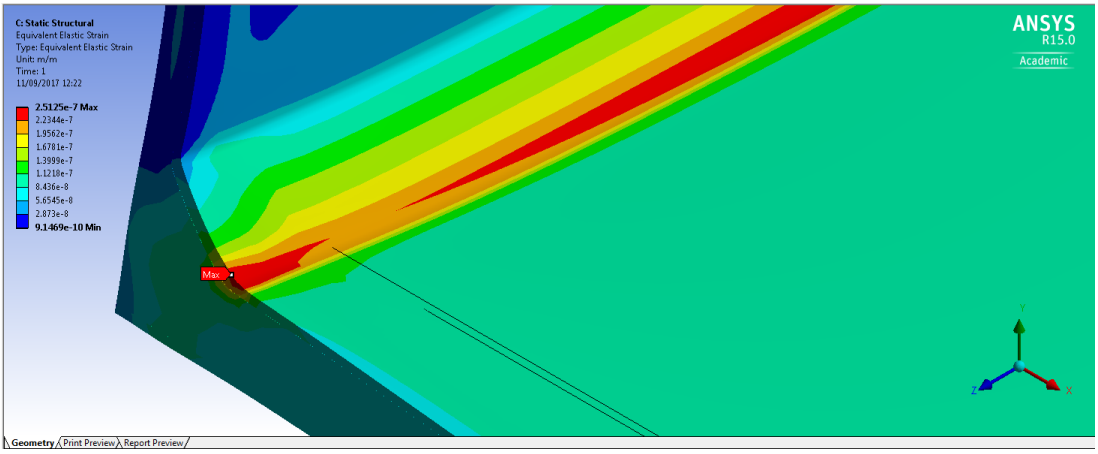

Figure 105 Undeformed and deformed model views of equivalent strain for SFME with 640 microns DFT

For case2 with L specimen having 960 µm DFT, it was observed that the magnitudes of the maximum Equivalent strain ranged from approximately 2.289e-7 m/m to 2.360e-7 m/m. SFPE displayed the highest while SPE exhibited the lowest. Both SME and SFME displayed magnitudes of 2.300e-7 m/m and 2.343e-7 m/m respectively. The following trend in maximum Equivalent strain emerged:

SFPE > SFME > SME > SPE

Presented in Figures 106 to 109 are the graphic display of the Equivalent strain computed for 960 µm films in this numerical simulation.

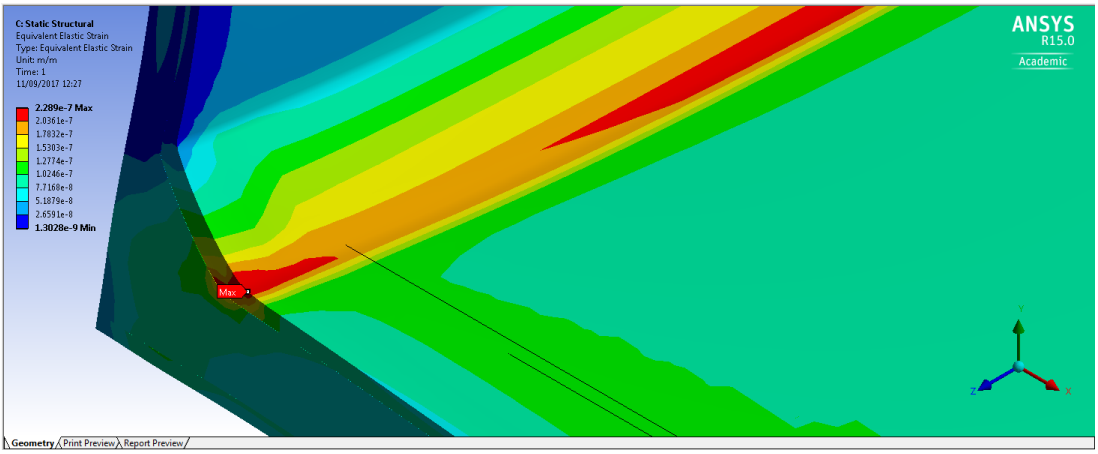

Figure 106 Undeformed and deformed model views of equivalent strain for SPE with 960 microns DFT

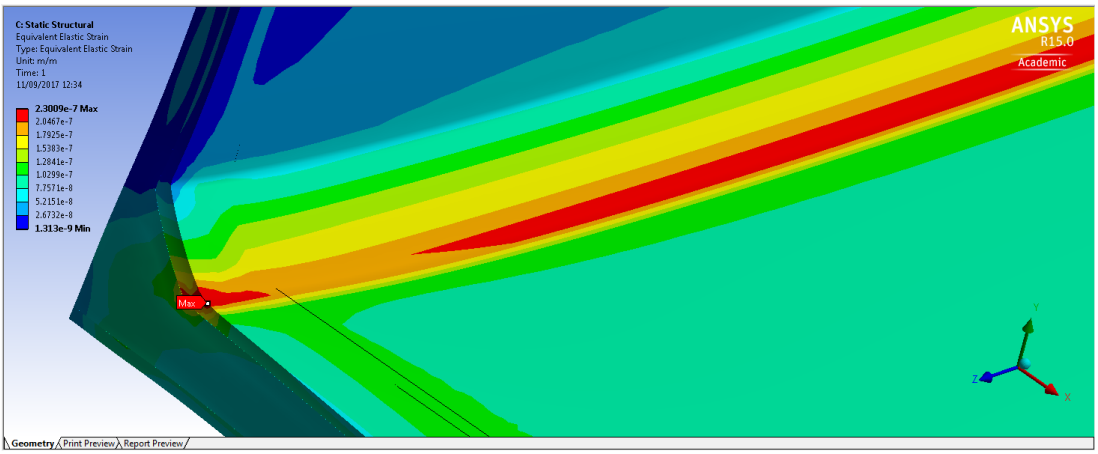

Figure 107 Undeformed and deformed model views of equivalent strain for SME with 960 microns DFT

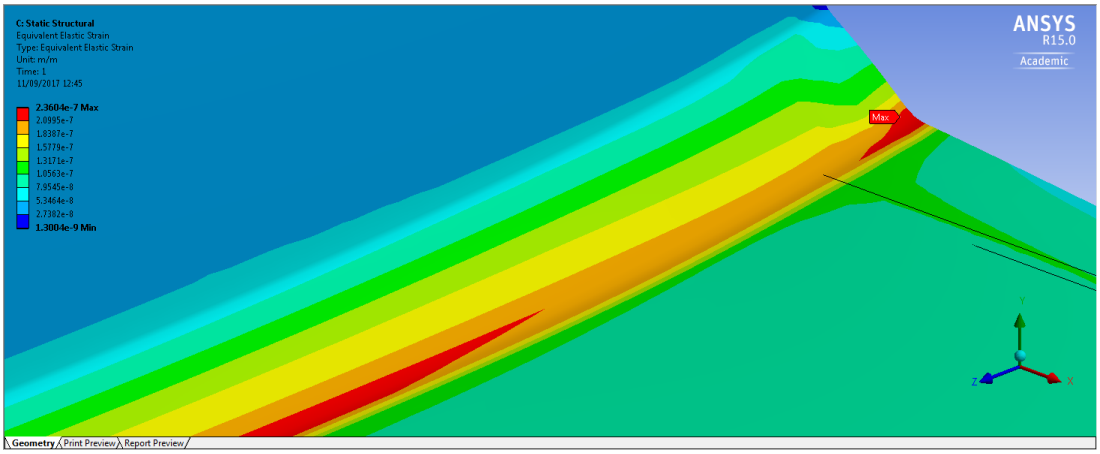

Figure 108 Undeformed and deformed model views of equivalent strain for SFPE with 960 microns DFT

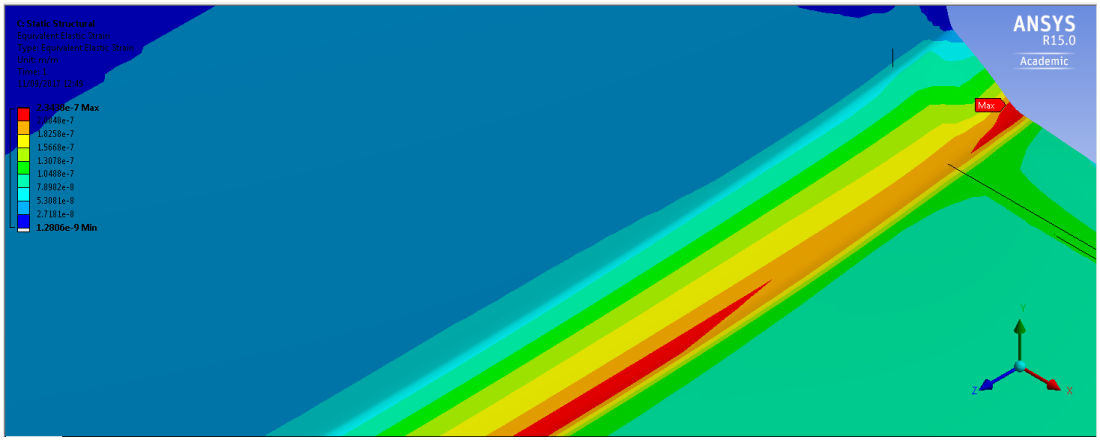

Figure 109 Undeformed and deformed model views of equivalent strain for SFME with 960 microns DFT

The ranking in both cases simulated compares very well. It indicates that the 640 µm DFT L model could sustain more strain that the 960 µm DFT L model. Also, the maximum strain occurs locally at the weld intersection of the L model on the coating film which confirms the influence of geometry.

CHAPTER 8
DISCUSSION OF RESULTS

8.1 Experimental Characterisation of Coating Formulations

In this study, following exposure of test specimens to defined laboratory conditions, the protective durability of four WBT coating formulations (SPE, SFPE, SME and SFME) all based on epoxy-amine technology has been evaluated against cracking failure (or resistance to cracking). The performance of the four WBT coating formulations was characterised by using a fatigue test (based on hygrothermal cycling) and test specimens designed around a number of variables identified as being the most significant from literatures reviewed and industry experience. Two sets of test specimens comprising of T specimens (T sectional substrates with adherent films) and free films (self-supporting and non-self-supporting) were prepared as representatives of the four WBT formulations and subjected to similar conditions. The fatigue test comprising - ambient temperature cure, dry conditioning period, wet conditioning period and hygrothermal cycling conditions with rapid rates of change - was designed to cause potential changes by maximising the stress development within the T specimens. This ultimately resulted in loss of the protective ability and coating integrity by cracking after a certain number of cycles from heating and immersing as seen in WBT in service. In conjunction, thermal analysis - from DSC, DMA, and TMA - was used to characterise properties such as glass transition temperature Tg, storage moduli and coefficient of thermal expansion of the free films. Furthermore, mechanical analysis – from uniaxial tensile analyser – was used to evaluate tensile fracture strength and elongation to fracture of dog bone shaped free films.

8.1.1 Fatigue test and order of resistance to cracking

The fatigue test produced a specific rank order in terms of resistance to cracking and did so twice with very good agreement between the two sets of tests. Following exposure of T specimens to the fatigue test, it was observed that the effects of hygrothermal cyclic stress on SFPE and SFME formulations was not as severe as on SME and SPE formulations. Based on the number of cycles to failure particularly at the weld intersection of the web and flange for both set 1 and set 2 specimens, it was observed that all six

specimens of SPE failed in one (1) cycle. All six specimens of SME in set 1 failed in forty two (42) cycles and those for set 2 failed at thirty seven (37) cycles while all specimens for SFME and some of SFPE failed in fifty nine (59) cycles for set 1 and sixty (60) cycles for set 2. Also, surface cracks (referred to in practice as checking) appeared on the flat faces of the specimens for SFME and SFPE as a result of the fatigue test. Based on the findings from the fatigue test between two set of tests, the fatigue test has demonstrated strong correlation between the rank order: (**SFPE > SFME > SME > SPE**) and number of cycles to failure. Thus, the fatigue test has offered an established means for characterising (or distinguishing) between WBT coating formulations regarding the resistance to cracking. However, the rank order of resistance to cracking produced from this fatigue test was not in agreement with industry expectations that modified epoxy formulations (i.e. either SME or SFME) are worse than pure epoxy formulations (i.e. either SPE or SFPE). Rather, it showed that the solvent containing pure epoxy formulation, SPE to be the worst while solvent free pure, SFPE outperformed other formulations Thus, indicating that formulation is a major contributor in determining WBT coating performance regarding resistance to cracking and it is unsafe to generalise behaviour based on the description of one constituent of the formulation.

8.1.2 Resistance to cracking and corrosion

The cracking failure on the T specimens of SPE formulation was more intense than on the other formulations as their crack size was significantly larger. Also, the cracks ran parallel and perpendicular on the weld intersection of the flange and web as well as the top flange weld. In addition, the cracks propagated from the coating surface to the steel sectional substrate. In contrast to SPE formulation, SME formulation showed significant resistance before failure and the crack size was smaller but still propagated to the steel substrate. For SME, the cracks only ran parallel to the weld intersection and were visually smaller in both size and length. For SFPE and SFME formulations, surface cracks appeared on the flat surfaces of T specimens for both formulation. In addition, cracks appeared on the weld intersection of all T specimens coated with SFME formulation while cracks at the weld intersection only appeared on 2 specimen of SFPE. Furthermore, over the duration of the test, the cracks did not penetrate through the film to the steel substrate of both SFPE and SFME T specimens

which was evident following removal of the coating film using hammer and chisel at the end of the test. The bare steel substrates of SFME and SFPE did not show any brown rust from corrosion unlike those of SPE and SME which had brown rust on. Although the cracks did not penetrate the coating film to the steel substrate, they are considered as fatigue cracks generated by the fatigue test. Considering the number of cycles to failure, both solvent free formulations – SFPE and SFME performed better than the solvent containing formulations – SPE and SME as both cracked earliest (with SPE formulation been the first to crack) from the fatigue testing. This view is in agreement with the study by Ingle et al. [108] on the performance of solvent containing and solvent free epoxy coatings applied in WBT in-service. Thus, fatigue resistance to cracking through a high number of cycles to film failure is an important property for durability in WBT environment.

8.1.3 Resistance to cracking and volume loss from film thickness measurements

An attempt was made to evaluate and compare formulations (SPE and SME) which cracked the earliest to those (SFPE and SFME) that cracked much later through the amount of volume loss or shrinkage which was analysed from DFT readings that were obtained before and after fatigue testing of the T specimens. The comparison of the volume loss (DFT reduction) of T specimens coated in the solvent containing formulations (SPE and SME) and those coated in solvent free formulations (SFPE and SFME) indicated that SPE and SME formulations underwent more shrinkage than SFPE and SFME formulations. Both SPE and SME formulations contained solvents: xylene and butanol but SME formulation also contained a solid non-reactive diluent. The content of solvent (volatile organic compounds – VOCs) in SME formulation was approximately 300 g/L while that in SPE formulation was approximately 264 g/L. Although both SPE and SME formulations contained the same type of solvents and SPE had slightly less amount, SPE formulation cracked earliest at one cycle while SME formulations resisted thirty six cycles before cracking.

ANOVA statistics was used to analysed the mean effect of volume loss before and after fatigue test. The measurement of volume loss from DFTs taken before and after fatigue testing indicated a decrease in all four formulations for both 640 µm DFT and 960 µm DFT. The results of the

ANOVA for 640 µm DFT and 960 µm DFT identified that the mean effect of volume loss on SFPE formulation was significantly lesser than for SPE, SME and SFME. On the contrary, SPE showed the highest volume loss. For the 640 µm DFT, F (3, 272) = 38.959, $p < .05$, $r = .549$. Similarly, for the 960 µm DFT, F (3, 287) = 19.202, $p < .05$, $r = .411$. In addition, the effect size in both DFTs indicated that the mean effect of volume loss on formulation was substantial.

Specifically, the volume loss of SFPE for 640 µm DFT (M = 40.82, SD = 18.20) was less than that of 960 µm DFT (M = 70.46, SD = 38.73). Equally, the volume loss of SFME for 640 µm DFT (M = 72.70, SD = 50.52) was less than that for 960 µm DFT (M = 102.08, SD = 36.11). Also, the volume loss of SME for 640 µm DFT (M = 58.68, SD = 25.02) was less than for 960 µm DFT (M = 110.46, SD = 45.17). Similarly, the volume loss of SPE for 640 µm DFT (M = 103.46, SD = 34.39) was less than the 960 µm DFT (M = 120.47, SD = 46.59). In both DFTs considered for volume loss, SFPE had significantly the lowest volume loss while SPE had the highest volume loss. The findings suggested that the amount of volume loss for particular formulation increases with DFT increase and confirmed that the effect of volume loss following the fatigue test differed between the formulations.

Comparing the solvent containing formulations, SME had a shrinkage less than that in SPE. A potential explanation ascribed for this behaviour is related to the fact that the non-reactive diluent in SME formulation is a solid with a very low vapour pressure, and therefore remains within the dry film even after post curing. It is therefore possible that this constituent provided a plasticising effect in SME formulation which was been diminished from subsequent cycles of fatigue exposure during testing until the endurance limit of SME was exhausted. Also, the difference in glass transition temperature (initial (Tgi) and ultimate (Tg∞)) obtained for SPE and SME formulations further supports this view as the difference between Tgi and Tg∞ of SPE was twice that for SME. This difference in Tgs was earlier presented on Table 14 of section 5.2.1.

Comparing the pure epoxy formulations, SFPE (solvent free formulation) and SPE (solvent containing formulation), while all the SPE failed in one cycle, many of SFPE endured fifty eight cycles before cracking. This finding is attributed to the greater flexibility and lower Tg and possibly reduced stress

in SFPE. A principal formulation difference is that SFPE does not contain solvents but a mono-functional reactive diluent which acts as a chain stopper and reduces cross link density. This is evident in the difference between the Tgi and Tg∞ recorded as that for SFPE was much reduced when compared to that of SPE. Also, shown on Table 14 of Section 5.2.1.

Similarly, comparing the modified epoxy formulations, SFME (solvent free formulation) and SME (solvent containing formulation), it was observed that SFME endured much more cycles before failure despite both formulations contained non-reactive diluent. A significant difference between the two formulations is that the diluent used in the SME formulation is a solid at room temperature while that used in the SFME formulation is liquid. Another principal difference in the two formulations is the inclusion of solvent in SME formulation.

Thus, cracking resistance can be linked to higher levels of retained solvent which was later released on heating after post curing, inducing shrinkage and increasing stress which leaves less capacity to cope with subsequent exposure conditions in service. Furthermore, it could be implied that the films with the most potential to change through chemical and/or physical mechanism which are highly interdependent have the potential to develop a higher initial stress which in turn means they might fail more quickly under the extreme conditions such as that within a WBT environment.

8.1.4 Resistance to cracking: Surface preparation and effect of geometry

Also, surface preparation and effect of geometry (welded intersection corners) are other factors considered for enhanced coating integrity and performance. The performance of the four WBT formulations was evaluated further to understand the influence of surface preparation and effect of geometry using T specimens that were both blasted and power tooled at welds.

From the study, there is a significant correlation between the effect of geometry - especially at weld corners/or intersection with higher dry film thicknesses applied on power tooled areas - and resistance to cracking. Cracks occurred the most on the intersection welds (or corners) of the web and flange of coated T specimens at specified cycles as reported. However,

there is less evidence to suggest that the effect of surface preparation from power tooling significantly influenced coating performance/integrity because most of the coated T specimens for SME, SFPE and SFME formulation showed no signs of cracking failure on the power tooled fillet weld placed on the top of the flange. Even when the coating integrity on the power tooled areas of the fillet weld at the intersection of the web and flange had failed by cracking. Also, most of the T specimens coated with solvent containing formulations – SPE and SME had cracks occurring at the toe of their blasted weld but not on the flat surface which were blasted to the same Sa 2.5 standard. Thus, the effect of surface preparation from power tooling and/or grit blasting could be dependent on the geometry found in areas such as welded corners which produces out of plane stresses on and around welds. This finding is also confirmed by Park et al. [109] who found that the standard of surface preparation had less influence on the coating performance compared to the formulation of the coating material which had a significant effect on performance.

8.1.5 Resistance to cracking and glass transition temperature (Tg)

The measurement of glass transition temperatures (Tg) is a fundamental technique used to characterise polymers and coating formulations. It follows that low Tg values from the initial temperature scan can be indicative of high levels of retained solvent and/or unreacted functional groups which can be unbeneficial to performance where exposure conditions are related to heating/cooling and/or immersing. Post curing can achieve the desired complete reaction of these residual groups as well as increase the values of Tg to reach the ultimate (Tg∞). Also, coating formulations which are highly cross-linked would give generally higher Tgs as demonstrated following the re-scan process with DSC analysis and use of oven dry conditioned specimens in DMA and TMA thermal analysis.

Thus, in general from the characterisation of free films (both self-supporting and non-self-supporting) using thermal analysis (DSC, DMA and TMA), the Tg∞ values obtained for the solvent containing formulations (SPE and SME) were much higher than that of the solvent free formulations (SFPE and SFME). However, comparing Tg∞ values against performance for the formulations (SPE and SME) with the higher Tgs and those (SFPE and

SFME) with the lower Tgs, SPE and SME formulations exhibited poor performance with less cycles to failure (with the occurrence of cracks) in the fatigue testing. It is worth emphasising that the initial Tg results from the thermal analysis cannot be solely relied on in predicting the performance of coating. Similarly, the Tg∞ cannot be used alone to predict performance. However, a significant difference between initial Tg and ultimate Tg (i.e. ΔTg) may be useful for initial screening as it is indicative of the capacity of the coating film to change on further heating, either by loss of solvents or additional reaction from residuals, after initial cure at ambient temperature. Such environment for further heating are found in WBTs with shared heated bulkheads.

8.1.6 Resistance to cracking: storage modulus and pigment Volume Concentration

The storage modulus measured from free film specimens using DMA (before and after exposure to the fatigue test) showed that the solvent containing formulations had the higher moduli values while the solvent free formulations was much less. The higher moduli values recorded for the solvent containing formulations (SPE and SME) can be attributed to the higher content of pigments, fillers (rigid particles) resulting in an increased pigment volume concentration (PVC) when compared to the solvent free formulations (SFPE and SFME). The PVCs are 27.88%, 26.21%, 10.65% and 8.96% for SPE, SME, SFPE and SFME respectively.

In general, the solvent containing formulations (SPE and SME) with higher PVC and higher moduli experienced worse cracking while the solvent free formulations (SFPE and SFME) with lower PVC and lower moduli showed the reverse in behaviour.

8.1.7 Resistance to cracking: the effect of dry film thickness DFT

The influence of dry film thickness (DFT) using 640 µm and 960 µm film thicknesses was not apparent as all T specimens with these two film thicknesses for a particular formulation that showed crack did so at the same number of cycles following exposure to the fatigue test. It could also be that the dry film thicknesses are already above the critical level for cracking where a significant difference can be observed.

8.1.8 Elongation to fracture and resistance to cracking

The elongation to fracture shows that SFPE had the highest elongation while SME was the least for the specimens labelled reference and SFME was least for the heat stressed ones. SPE was position as having a better elongation to fracture that SFME and SME yet SPE had the worst resistance to cracking from the fatigue test. Furthermore, the heat stressed specimens of the four formulations had their elongation to fracture significantly diminished that the four formulations could not be significantly characterised (or distinguished) by this means.

8.1.9 Tensile fracture strength and resistance to cracking

The Tensile Fracture Strength of the heat stress specimens for the 960 µm DFT was in agreement with the resistance to cracking as demonstrated by the fatigue test. Similarly, the reference specimens for the 960 µm DFT was in agreement with the ranking of the fatigue test. The fracture strength increased of all formulations after post curing with SPE most affected.

8.1.10 Resistance to cracking and the effect of stoichiometry

Amongst the four epoxy-based formulations, SPE formulation had the highest stoichiometric ratio while SME had the least stoichiometric ratio. SFPE and SFME had stoichiometric ratios that were within that of SPE and SME.

For the solvent containing formulations, SPE with the highest stoichiometric ratio of 90% failed at the early stages of the fatigue testing (1 cycle) while SME with the least stoichiometric ratio of 70% endured much more cycles to failure than SPE. In contrast to the solvent containing formulations, the solvent free formulations: SFPE and SFME (which had stoichiometric ratios of 85% and 80% respectively) resisted much more cycles than both SPE and SME before failure.

Based on these stoichiometric ratios, there is a weak correlation between the stoichiometric ratio (i.e. the quantitative relationship governing the amount of epoxy resin and amine curing agent required to react with one another) and performance with regards to cracking. However, if the capacity for change in properties between application and after being in service (cycling between hot/cold or heating/cooling and/ or immersing) is related to

cracking failure, then having excess epoxy gives more potential for change including homopolymerisation (epoxy reacting with itself resulting in brittleness of film) – could be guidance for formulators. Therefore, it will be unwise to speculate any further and it will be best to investigate stoichiometric ratio(s) further.

8.1.11 Coefficient of thermal expansion and resistance to cracking

Coefficient of thermal expansion (CTE) can generate adverse stress within a structure when heated and kept at constant length or between to dissimilar materials from rapid heating and cooling as in this cased the coated T substrate. Generally, the CTE value of mild steel falls below those of the four formulations with SPE showing the lowest values and SFPE showing the highest values. SPE with the lowest average mismatched CTE was adversely affected by cracking after one cycle of the fatigue test. Furthermore, it was observed that SPE and SME containing higher pigment content had lower CTE compared to SFPE and SFME with lower pigment content. It is highly likely that the pigments retained a substantial amount of heat energy, thereby allowing a smaller amount of dissipated energy at the interface. In addition, as the ultimate Tg of SFPE and SFME were much lesser than the top cycling temperature of 100 ^{o}C (T > Tg), there is a high mobility of the segmental molecular binders resulting in a stress relieve state. For SPE and SME, this was not the case. SPE developed the most stress following film formation and more with ageing from residual solvent loss and further cross-linking. In conclusion, better performance of WBT formulations was dependent on higher CTE and more mismatched to steel (as seen for SFPE and SFME) than with lower CTE and less mismatch (SPE and SME).

8.1.12 Resistance to cracking and the effect of curing agent

The amine curing agents used to co-react the base epoxy paints are:

- Ancamine 2519 ® - Modified cycloaliphatic amine adduct with benzyl alcohol
- Ancamine 2712M ® – Mixed aliphatic - cycloaliphatic amine, no benzyl alcohol 100% solids
- Cardolite NX-4709E ® - Phenalkamine

For the solvent containing formulations, Ancamine 2519 ® was co-reacted with SPE while Cardolite NX-4709E ® was co-reacted with SME. For the solvent free formulations, Ancamine 2712M ® was co-reacted with SFPE and SFME. It was not possible to establish in this research project any clear pattern of advantageous performance for crack resistance from curing agents used.

However, the inclusion of benzyl alcohol in a formulation must be treated with caution as it will be lost from the film on heating.

In conclusion, it is important to consider the formulation when evaluating performance in terms of resistance to cracking as all of the constituents play a significant role in this regards. The performance characterised by this research demonstrates that SFPE and SFME formulations seem to show closely related in endurance limits. However, within the test parameters, SFPE with few failed T specimen would offer a better choice for coating integrity and steel substrate protection where the challenges of premature cracking is prevalent from fatigue cycling between ambient temperature and elevated temperature as seen in WBT of merchant vessels especially crude oil and chemical tankers.

8.2 Numerical Characterisation of Coating Formulations

In this study, following the coupled transient thermal structural simulation of the L specimen model with adhered coating of dry film thicknesses of 640 µm and 960 µm of each formulation, the obtained Equivalent (von Mises) stress and Equivalent strain are linked to the performance of the formulations from the fatigue test.

8.2.1 Equivalent stress and order of resistance to cracking

The Equivalent stress produced the same ranking for the two cases of DFT compared. The ranking also compares well with that produced from the experimental characterisation using the fatigue test where the solvent containing formulations showed less resistance to cracking and the solvent free formulations exhibited the most resistance to cracking. The Equivalent stress that occurred on the coating film indicates that the solvent containing formulations: SPE and SME showed more stress than that showed by the solvent free formulations: SFPE and SFME. SPE showed the highest

magnitude of stress amongst the four formulations in both dry film thicknesses simulated and compared. Thus, confirming the reason while SPE with much more accumulated stress was unable to sustain as many cycles in the fatigue testing as the other formulations prior to failure. Unlike SPE, SME showed less stress than SPE but exhibited more than SFPE and SFME. A likely deduction from the less stress in SME than SPE is that the magnitude of stress for SME was within the range where much more cycles to failure than SPE could be sustained with the fatigue testing. SFME exhibited much less stress than SME but more than SFPE. SFPE showed the least stress and was the most resistant to cracking amongst the four formulations compared. From the simulation, a possible explanation would be that SFPE had the least stress magnitude and so could accommodate much more stress which was demonstrated in the cycles to failure in the fatigue test. However, the performance of SFPE was very close to that of SFME from the fatigue test.

8.2.2 Equivalent strain and order of resistance to cracking

The Equivalent strain from the simulation further justify the order of resistance to cracking especially locally at the weld intersection. The Equivalent strain on the coating film shows that the solvent free formulations have the capacity to accumulate more strain locally at the weld intersection compared to the solvent containing formulations. SFPE has the most capacity of strain. SFME closely follows SFPE in the capacity to accommodate strain. Next to SFPE and SFME is SME. SPE show the least capacity to accumulated strain.

From the results of the FEA, it could be implied that formulation is a significant influence to stress bearing and performance in terms of resistance to cracking. In addition, the influence of geometry was evident as the strain locally was more.

CHAPTER 9
CONCLUSIONS & RECOMMENDATIONS

9.1 Conclusions

Following the experimental, numerical and statistical results in this research project, several conclusions emerged:

- The designed fatigue test characterised the performance and durability of four WBT coating formulations (SPE, SFPE, SME and SFME) against cracking/embrittlement and established a specific rank order of performance with very good agreement between two separate runs. The fatigue test demonstrated that hygrothermal cycling accompanied with thermal shock exacerbates embrittlement and cracking failure of WBT epoxy formulations especially at the welded corners with higher DFT.
- Based on the specific rank order of cracking failure (**SFPE > SFME > SME > SPE**) produced twice by the fatigue test, this fatigue test is proposed as a potential and convenient means for the PSPC to evaluate loss of flexibility of WBT coatings against embrittlement and cracking failure.
- On average between the two runs from the fatigue test, all the T specimens representing SPE, SME and SFME failed at welded corners at 1, 39.5 and 59.5 cycles respectively while some of SFPE failed at 59.5 cycles. This result revealed that WBT epoxy formulations have different levels of performance and durability as SFPE outperformed the other formulations whereas SPE performed worst. Within the parameters of the fatigue test, SFPE emerged as the formulation with superior performance in meeting the PSPC recommendation on withstanding thermal fatigue resistance - repeated heating and cooling without brittle failure.
- The rank order of cracking failure produced from this fatigue test was contrary to industry expectations that modified formulations are worse than pure formulations. The implication from this finding was that the entire constituent of the formulation (as a whole) should be considered in determining crack resistance performance and it was unsafe to generalise behaviour based on the premise of one constituent of the formulation as in the industry's view.
- The statistical results of the ANOVA test confirmed that formulation was significant as each formulation endured different numbers of cycle in the

fatigue test, F (3, 44) = 4957.741, $p < .05$, $r = .998$. The effect size indicated that the effect of the fatigue test on formulation was substantial. SFPE formulation had a performance that was statistically significant in all cases compared to other formulations.

- The measurement of volume loss from DFTs taken before and after fatigue testing indicated a decrease in all four formulations for both 640 µm DFT and 960 µm DFT. The results of the ANOVA for 640 µm DFT and 960 µm DFT identified that the mean effect of volume loss on SFPE formulation was significantly lesser than for SPE, SME and SFME. On the contrary, SPE showed the highest volume loss. For the 640 µm DFT, F (3, 272) = 38.959, $p < .05$, $r = .549$. Similarly, for the 960 µm DFT, F (3, 287) = 19.202, $p < .05$, $r = .411$. In addition, the effect size in both DFTs indicated that the mean effect of volume loss on formulation was substantial.
- Glass transition temperature (Tg) measurement for unaged and aged free films were not invariable with a mix of increase and decrease in magnitude. With DSC measurement, the aged free films of SPE increased by 2 times the unaged while those of SME increased by 1.5 times the unaged. In contrast, the aged free films of SFPE and SFME decreased by 0.22 and 0.17 times the unaged respectively. With TMA and DMA analysers for specimens that were post cured at 50 ºC, SFPE showed almost invariable Tg magnitude of 47.3 ºC and 51 ºC respectively while SFME, SME and SPE varied. Furthermore, Tg magnitudes were lesser from TMA analyses compared to DMA and DSC confirming that the process of measurement was different with each analyser.
- The initial glass transition temperature (Tgi) from the unaged specimen cannot be used alone as a performance indicator for crack resistance. Similarly, the measurement of the ultimate glass transition temperature (Tg∞) from the aged specimen cannot be used alone as a performance indicator for crack resistance. However, the difference between the Tgi and Tg∞ (i.e. ΔTg) as measured on free films by DSC, DMA and TMA could be an indicator for initial screening as films with significant ΔTg showed the most potential to change through chemical and/or physical mechanisms as demonstrated by SPE. Such formulations containing significant solvent and residual functional group after initial film formation have a propensity to fail more quickly under extreme conditions such as that within a WBT environment.

- Coefficient of thermal expansion (CTE) measurement using TMA showed that aged specimens of SFPE and SFME produced higher CTE magnitudes up to 71.7 and 77.6 µm/m°C respectively. In contrast, SPE and SME produced lower CTE magnitudes of 42.2 and 54.4 µm/m°C respectively.
- Plasticisation was mostly apparent on measured properties of free film specimens that were post cured at 50 ºC compared to those post cured at 100 ºC.
- Tensile moduli of unaged and aged free film specimens measured using DMA showed an increase of up to 1.3 times of unaged for SPE and 2 times of unaged for SME. In contrast, SFPE and SFME exhibited a drop of 0.5 times and 0.9 times of the unaged respectively.
- Tensile testing revealed that exposure temperature significantly influence fracture strength and elongation to fracture as in this case at 100 ºC. The fracture strength of the aged dogbone specimen increased for all formulations. SPE increased significantly to approximately 9 times of the unaged while SME increased to 4 times of the unaged. SFPE and SFME increased approximately 2 and 3 times of the unaged respectively. The elongation to fracture decreased significantly for all formulations. The elongation to fracture of SFPE diminished to 1.87% while the other formulations diminished to approximately 1%.
- The simulated FEA model correlates the influence of geometry and higher film thickness as demonstrated with the higher stress at the welded corner.
- Following the use of various methods to analyse the performance of 4 WBT formulations using unaged and aged specimens, the required properties for durability are : minor volume loss of DFT after post cure, low Tg_{∞} (around 25 to 30 ºC above ambient temperature), increased CTE, reduced fracture strength, increased elongation to fracture, low moduli and increased cycles to failure.
- Overall, the fatigue test has established and delivered an enhanced performance testing for evaluating and selecting durable coating systems against embrittlement and cracking.

9.2 Recommendations

Following on from this research project, some areas are recommended for further work:

- The effect of mechanical fatigue testing on ambient cured and post cured supported films should be investigated to determine a correlation with thermal cycling.
- The properties of in-service coatings that have been subjected to natural ageing should be evaluated and correlated to those that have been subjected to artificial ageing.
- A much larger sample space of epoxy based formulations used in WBT could be further investigated using the proposed fatigue test.
- The material properties used in the modelling are based on tensile uniaxial testing hence it will be also beneficial to apply material properties based on cyclic uni-axial testing for further investigation.

REFERENCES

[1] **EMSA (2005)** *Double Hull Tankers: High Level Panel of Experts Report*. European Maritime Safety Agency.

[2] **TSCF (1992)** *Condition Evaluation and Maintenance of Tanker Structures.* London: Witherby & Co. Tanker Structural Co-operative Forum.

[3] **TSCF (1995)** *Guidelines for Inspection and Maintenance of Double Hull Tanker Structures*. London: Witherby & Co. Tanker Structural Co-operative Forum.

[4] **IMO (1999)** *Focus on IMO: IMO and the Safety of Bulk Carriers.* International Maritime Organisation.

[5] **SSC (2002)** *BULK CARRIERS*: *Design, Operation, and Maintenance Concerns for Structural Safety of Bulk Carriers.* Ship Structure Committee. [Online] Available at: www.shipstructure.org/case_studies/BulkCarriers.pdf *(*Accessed 10 February 2016).

[6] **Void, H. (1997)** 'Evaluating Protective Coating for Ballast Tanks', *PCE*, pp. 16 – 22.

[7] **Azevedo, J. (2006)** 'A New Approach for Ballast & Cargo Tank Coatings: A Solvent Free and Humidity Tolerant Epoxy System with Edge-Retentive Properties'. In: *The Royal Institution of Naval Architects (RINA) Conference on Advanced Materials and Coatings, London*.

[8] **IACS (2006)** *Recommendation 87, Guidelines for Coating Maintenance & Repairs for Ballast Tanks and Combined Cargo/Ballast Tanks on Oil Tankers*, *Rev.1*. London: International Association of Classification Societies.

[9] **Dickins, D. F. (1995)** *The Double Hull Issue and Oil Spill Risk on the Pacific West Coast*. [Online] Available at: http://www2.gov.bc.ca/assets/gov/environment/air-land-water/spills-and-environmental-emergencies/docs/double_hull_issue.pdf (Accessed 12 January 2016).

[10] **Terhune, K. (2011)** 'Tanker Technology*:* limitations of double hulls', *A Report by Living Oceans Society*, pp. 1 - 25.

[11] **ABS (2007)** *Guidance Notes on the Inspection, Maintenance and Application of Marine Coating Systems*. Houston TX: American Bureau of Shipping.

[12] **Mills, G. & Eliasson, J. (2006)** 'Factors Influencing Early Crack Development in Marine Cargo and Ballast Tank Coatings', *Journal of Protective Coatings & Linings /PCE*, pp. 10 – 21.

[13] **Eliasson, J., Rauta, B. & Gunner, T. (2005)** 'Ballast Water Tank Coatings for the Future', *Corrosion2005*, 05001, Houston TX: NACE International, pp. 1 – 30.

[14] **I M O (2006)** *Resolution MSC. 215(82), Performance Standard for Protective Coatings for Dedicated Seawater Ballast Tanks In All Types of Ships and Double-Sided Skin Spaces of Bulk Carriers (PSPC)*, adopted 8 December 2006. London: International Maritime Organisation.

[15] **Askheim, E., Nokleby, J. O., Carlsson, L. & Palm, M. (2001)** 'Why Do Paints Crack', *PCE,* pp. 49 – 55.

[16] **Eliasson, J. & Towers, R. (2008)** 'The Future of Ballast Tank Coatings', *Journal of Protective Coatings & Linings*, pp. 28 – 36.

[17] **OCIMF (1997)** *Factors Influencing Accelerated Corrosion of Cargo Oil Tanks*. Oil Companies International Marine Forum. [Online] Available at: https://www.ocimf.org/library/information-papers/ (Accessed: 12 September 2014).

[18] **Guan, S. W., Liu, D., Moreno, M. & Garneau, R. (2004)** '100% Solids Rigid Polyurethane Coatings Technology for Corrosion Protection of Ballast Tanks', *Corrosion2004*, 04029, Houston TX: NACE International, pp. 1 – 12.

[19] **Melchers, R. E. & Jiang, X. (2006)** 'Estimation of Models for Durability of Epoxy Coatings in Water Ballast Tanks', *Ships and Offshore Structures*, 1 (1), pp. 61 – 70.

[20] **Fedrizzi, L., Bergo, A., Defloricon, F. & Valentinelli, L. (2003)** 'Assessment of Protective Properties of Organic Coatings by Thermal Cycling', *Progress in Organic Coatings*, 48, pp. 271-280.

[21] **Mitchell, M. J., Clayton, D. & Ward, D. (2005)** 'A Critical Review of Current Performance Tests for Offshore Anti-Corrosive Coatings', *Corrosion2005*, 05021, Houston TX: NACE International, pp. 1 - 17.

[22] **Winter, M. (2011)** 'Laboratory Test methods for Offshore Coatings: A Review of a Round Robin Study', *Corrosion2011*, 11041, Houston TX: NACE International, pp. 1 – 14.

[23] **Phillippe, L. C. & Nathalie, L. (2005)** 'Evaluating Coating Performance in Severe Marine Environments: Investigating the Test Method', *Journal of Protective Coatings & Linings /PCE*, pp. 29 – 38.

[24] **IACS (2007)** *Recommendation 96 Double Hull Oil Tankers – Guidelines for Surveys, Assessment & Repair of Hull Structures*. London: International Association of Classification Societies.

[25] **National Research Council (1996)** *Stemming the Tide: Controlling Introductions of Nonindigenous Species by Ships' Ballast Water*, Washington D.C: National Academies Press, pp. 22.

[26] **DNV (1998)** *DNV-98-P009 rev 1.0 Classification Focus on Protective Coating*. Hovik: Det Norske Veritas.

[27] **Marrion, A. R. (2004)** *The Chemistry and Physics of Coatings*, 2nd edn. Cambridge: The Royal Society of Chemistry.

[28] **Hare, C. H. (1995)** 'The Glass Transition', *Journal of Protective Coatings & Linings*, pp. 83 – 96.

[29] **Cook, M., Lohe, M. & Klippstein, A. (2002)** 'Novel Technology for 2K Water Vapour Permeable Epoxy Floor Systems: A European Perspective', *Journal of Protective Coatings & Linings /PCE*, pp. 51 – 56.

[30] **Hare, C. H. (1996)** 'Free Volume', *Journal of Protective Coatings & Linings*, pp. 67 - 80.

[31] **Hare, C. H. (1996)** 'Thermal Stresses', *Journal of Protective Coatings & Linings*, pp. 89 - 101.

[32] **ABS (2004)** *Guidance Notes on the Application and Maintenance of Marine Coating Systems*. Houston, TX: American Bureau of Shipping.

[33] **Hare, C. H. (1995)** 'The Molecular Structure of Polymeric Binders' *Journal of Protective Coatings & Linings*, pp. 67 - 78.

[34] **'Epoxy' *Etymonline.com* (2013)** [Online] Available at www.etymonline.com (Accessed: 24 November 2013)

[35] **Hamerton, I. (1996)** *Recent Developments in Epoxy Resins*, Report 91, Rapra Review Reports, Expert Overviews Covering the Science and Technology of Rubber and Plastics. Shropshire: Rapra Technology Limited, pp. 5

[36] **Salem, L. S. (1996)** 'Epoxies for Steel. Generic Coating Types', *Journal of Protective Coatings & Linings*, pp. 77 - 98.

[37] **Kline, H. H. (1996)** 'Inorganic Zinc-Rich' *Journal of Protective Coatings & Linings*, pp. 73 - 105.

[38] **Freewebs.com (2015)** *Epichlorohydrin* [Figure] [Online] Available at: www.freewebs.com/greengrip/Bisphenol%20A+Epichlorohydrin.doc (Accessed: 26 February 2015)

[39] **Boyle, M. A., Martin, C. J. & Neuner, J. D. (2001)** *Epoxy Resins*, Composites, Vol. 21, ASM Handbook. ASM International, p 78

[40] **Bhatnagar, M. S. (1996)** 'Epoxy Resins (Overview)'. *The Polymeric Materials Encyclopedia,* Boca Raton: CRC Press, pp. 1 – 11.

[41] **Air Products & Chemicals, Inc. (2013)** *Epoxy Additives Training Manual***.**

[42] **Bauer, R. S., Marx, E. J. & Watkins, M. J. (1995)** 'Epoxy resins in Coatings', In: Koleske, J. V. (editor), *Paint and Coating Testing Manual*, 14th edn. of Gardner-Sward handbook. Philadelphia: ASTM International, pp. 74 - 78.

[43] **Odell, L. B. & Siegmund, A. (1995)** 'Pipeline Coating', In Koleske, J. V. (editor), *Paint and Coating Testing Manual*, 14th edn. of Gardner-Sward handbook. Philadelphia: ASTM International, pp. 731 – 734.

[44] **O'Donoghue, M., Garrett R. & Schilling, M. S. (2001) '**Understanding coating materials – The Myth of Generic Equivalency and other short stories', In: *SSPC National Conference*, Atlanta.

[45] **International Paints Limited** *Intershield 300: Abrasion Resistant Aluminum Pure Epoxy* [Online] Available at https://www.yumpu.com/en/document/view/19746506/intershield-300-brochure-shipserv/7 (Accessed: 20 September 2015)

[46] **HEMPEL** *Epoxy Encyclopaedia: Strong Protection at all Points*.

[47] **Struik, L. C. E. (1977)** 'Physical Aging in Plastics and Other Glassy Materials', *Polymer Engineering and Science*, 17(3) pp. 165 – 173.

[48] **Perera, D. Y. (2003)** 'Physical Ageing of Organic Coatings', *Progress in Organic Coatings,* 47 pp. 61 – 76.

[49] **Hare, C. H. (1996)** 'Viscoelasticity', *Journal of Protective Coatings & Linings*, pp. 103 - 113.

[50] **Ringsberg, J. W. (1997)** 'On Mechanical interaction between Steel and Coating in Welded Structures' PhD Thesis, School of Mechanical and Vehicular Engineering, Chalmers University of Technology, Goteborg, Sweden.

[51] **Coldie, B. & Kok, B. (2008)** 'A practical solution to ballast tank coatings', *Drydock,* pp. 24 - 32.

[52] **Wei, C., Eliasson, J., Jansen, E., Wang, G. & Basu, R. I. (2011)** 'IMO PSPC Implementation and 15 Years of Target Useful Coating Life', *Corrosion2011*, 11418, Houston TX: NACE International, pp. 1 – 15.

[53] **Perera, D. Y. (2003)** 'Stress Phenomenon in Organic Coating', In: Koleske, J. V. (editor), *Paint and Coating Testing Manual, 14th edn. of the Gardner-Sward Handbook*, Philadelphia: ASTM, pp. 585 – 599.

[54] **Zhang, B. J., Lim, C., Kim, B. C. & Lee, D. G. (2005)** 'Stress Analysis and Evaluation of Cracks Developed on Coatings for Welded Joints of Water Ballast Tanks', *Corrosion2005*, 05015, Houston TX: NACE International, pp. 1 - 10.

[55] **Gunter, B. (2001)** 'High-Performance Coatings for Protection of Hydraulic Steel Structures in Waterways', *JPCL*, pp. 54 – 61.

[56] **Tator, K. B. (2004)** 'Risk Assessment and Economic Considerations When Coating Ballast Tanks', In: Smith, C., Siewart, T., Mishra, B., Olson, D. & Lassiegne, A. (editors) *Coatings for Corrosion Protection: Offshore Oil and Gas Operation Facilities, Marine Pipeline and Ship Structures*, Mississippi: NIST Special Publication, pp. 101 – 114.

[57] **Hare, C. H. (1997)** 'Internal Stress: Part I' *Aircraft Paint Stripping News*, 2(2), pp. 2 – 6.

[58] **Hare, C. H. (1996)** 'Internal Stress: Part II' *Journal of Protective Coatings & Linings*, pp. 101 - 115.

[59] **Hare, C. H. (1996)** 'Hygroscopic Stresses', *Journal of Protective Coatings & Linings*, pp. 59 – 70.

[60] **Croll, S. G. (1978)** 'Internal Stress In a Solvent-Cast Thermoplastic Coating', *Journal of Coatings Technology*, 50(638), pp.33 – 38.

[61] **Song, E. H., Lee, H. I., Chung, M. K., Park, C. S., Lee, C. H., Shin, C. S., Lee, S. K. & Baek, K. K. (2006) '**Why Do We Have Cracks in Epoxy Coatings for Water Ballast Tanks', *Corrosion2006*, 06015, pp. 1 - 13.

[62] **Knudsen, O. O., Bjorgum, A., Polanco-Loria, M., Oyen, A. & Johnsen, R. (2007)** 'Internal Stress and Mechanical Properties of Paint Films', *Corrosion2007*, 07003, Houston TX: NACE International, pp.

[63] **Negele, O. & Funke, W. (1 9 9 6)** 'Internal Stress and Wet Adhesion of Organic Coatings', *Progress In Organic Coatings,* 28, pp. 285-289

[64] **Korobov, Y. & Salem, L. (1990)** 'Stress Analysis as a Tool in Coatings Research', *Material Performance*, pp. 30 – 45.

[65] **Husain, A., Al-Shamali, O. & Abduljaleel, A. (2004)** 'Investigation of Marine Related Deterioration of Coal Tar Epoxy Paint on Tubular Steel Pilings' *Desalination*, 166 pp. 295 - 304.

[66] **Shifler, D. A. & Aylor, D. M. (2005)** 'Factors Affecting Corrosion Performance and Testing of Materials and Components in Seawater', *Corrosion2005*, 05224, Houston TX: NACE International, pp. 1 – 15.

[67] **Merlatti, C., Perrin, F. X., Aragon, E. & Margaillan, A. (2008)** 'Evaluation of Physio-Chemical Changes in Sub-Layers of Multi-layer Anticorrosive Marine Paint Systems: Plasticizer and Solvent Release' *Progress in Organic Coatings*, 61 pp. 53 - 62.

[68] **Grossman, D. M. (1996)** 'More Realistic Test for Atmospheric Corrosion', *ASTM Standardisation News*, pp. 34 – 39.

[69] **Brownlee, K., Speed, C. & Whitehead, R. (2004)** 'Decision Making in Coating Selection in Marine/Offshore Environments', In: Smith, C., Siewart, T.,

Mishra, B., Olson, D. & Lassiegne, A. (editors) *Coatings for Corrosion Protection: Offshore Oil and Gas Operation Facilities, Marine Pipeline and Ship Structures*, Mississippi: NIST Special Publication, pp.115 – 133.

[70] **ASTM International (2010)** *ASTM D5894-10:2010 Standard Practice for Cyclic Salt Fog/UV Exposure of Painted Metal, (Alternating Exposures in a Fog/Dry cabinet and a UV/Condensation Cabinet).* West Conshohocken: ASTM International.

[71] **ISO (2009)** *ISO 20340:2009(E)**,** Paints and Varnishes – Performance Requirements for Protective Paint Systems for Offshore and Related Structures.* Geneva: International Standardization Organisation.

[72] **NORSOK (2012)** *NORSOK M-501:2012, Surface Preparation and Protective Coating.* Lysaker: STANDARDS NORSOK.

[73] **NORDTEST (2002)** *NORDTEST Method NT POLY 185:2002*, *Determination of Flexibility and Fatigue Resistance of Aged Ballast Tank Coatings.* Espoo: NORDTEST.

[74] **NACE (2004)** *NACE Standard TM0304:2004, Offshore Platform Atmospheric and Splash Zone Maintenance Coating System Evaluation.* Houston: NACE International.

[75] **NACE (2004)** *NACE Standard TM0104:2004, Offshore Platform Ballast Water Tank Coating System Evaluation.* Houston: NACE International.

[76] **Weber, P.F. (2010)** 'An Overview of the Tanker Structure Cooperative Forum', *TSCF Shipbuilders Meeting*

[77] **Lohmann, T. (2009)** 'Implementing the IMO PSPC for Ballast Water Tanks', *Journal of Protective Coatings & Linings*, pp.12 – 21.

[78] **Hoppe, H.** "Development of Mandatory IMO Performance Standards for Protective Coatings On Ships: An Overview", pp. 1 – 11. [Online]. Available at: www.imo.org/blast/blastdatahelper.asp?data_id=1482 (Accessed: 15th April 2014)

[79] **GL (2010)** *Guidelines for Corrosion Protection and Coating Systems - Rules for Classification and Construction vi -10*. Hamburg: Germanischer Lloyd AG.

[80] **SAFINAH (2009)** Safinah Limited, Internal Report

[81] **Oriaifo, E. A., Perera, N, Guy, A., Leung, P. S. and Tan, K. T. (2014) '**A Review of Test Protocols for Assessing Coating Performance of Water Ballast Tank Coatings', World Academy of Science, Engineering and Technology, International Science Index 94, *International Journal of Mechanical, Aerospace, Industrial, Mechatronics and Manufacturing Engineering*, 8(10), pp.1610 – 1615.

[82] **'High-speed-disperser' *indiamart.com* (2014)** [Online] Available at https://dir.indiamart.com/pune/high-speed-disperser.html (Accessed:16 February 2014).

[83] **Hare, C. H. (2001)** 'The Effects of Pigment Dispersion and Flocculation on Coatings' *Journal of Protective Coatings & Linings*, pp. 69 - 94.

[84] **'Vortex movement of paint' *menzcn.com* (2014)** [Online] Available at http://www.menzcn.com (Accessed: 20 February 2014).

[85] **Solly, R. (2001)** 'Construction', In *SUPERTANKERS: Anatomy and Operation*. London: Witherby & Co. Ltd, pp. 23

[86] **Baldwin, L. (1997)** 'Improving Coating Processes In the Shipbuilding Industry' *PCE,* pp. 23 – 25.

[87] **Kattan, M. R. (2007)** 'Matching the Coating Process to Shipyard Need' *Shipbuilding Technology ISST 2007*, Osaka.

[88] **Kattan, M. R., Blakey, J., Panosky, M. & CeVinney, S. (2007)** 'Time and Cost Effects of the Coating Process' *Journal of Ship Production*, 19 (4).

[89] **Graco (2012) '**The Basics of Airless Spraying: Information on Basic Components, Spray Techniques and Safety'. Minnesota: Graco

[90] **ASTM International (1996)** *ASTM E 376 – 96**,** Standard Practice for Measuring Coating Thickness by Magnetic – Field or Eddy – Current (Electromagnetic) Test Methods.* West Conshohocken: ASTM International

[91] **ISO (2012)** *ISO 19840:2012**,** Paints and Varnishes – Corrosion Protection of Steel Structures by Protective Paint Systems – Measurement of and Acceptance Criteria for Thickness of Dry Films on Rough Surfaces.* Geneva: International Standardization Organisation.

[92] **ASTM International (2003)** *ASTM D 1640-03:2003 Standard Test Methods for Drying, Curing, or Film Formation of Organic Coatings at Room Temperature.* West Conshohocken: ASTM International.

[93] **Wunderlich, B. (1990)** *Thermal Analysis*. London: Academic Press.

[94] **Menard, K. P. (1999)** *Dynamic Mechanical Analysis: A Practical Introduction*. Boca Raton: CRC Press.

[95] **Wendlandt, W. W. (1986)** *Thermal Analysis,* New York, NY: Wiley.

[96] **ASTM International (2014)** *ASTM E1356-08:2014 Standard Test Method for Assignment of the Glass Transition Temperatures by Differential Scanning Calorimetry.* West Conshohocken: ASTM International.

[97] **Leng, K. (2008)** *Material Characterisation: Introduction to Microscopic and Spectroscopic Methods*. Singapore: John Wiley & Sons.

[98] **ASTM International (2013)** *ASTM E1640-13:2013 Standard Test Method for Assignment of the Glass Transition Temperature by Dynamic Mechanical Analysis.* West Conshohocken: ASTM International.

[99] **ASTM International (2014)** *ASTM E1545-05:2005 Standard Test Method for Assignment of the Glass Transition Temperature by Thermomechanical Analysis.* West Conshohocken: ASTM International.

[100] **ASTM International (2002)** *ASTM E638-02a:2002 Standard Test Method for Tensile Properties of Plastics.* West Conshohocken: ASTM International

[101] **Morgan, G. A., Griego, O. V & Gloeckner, G. W., (2001)** *SPSS For Windows*, London: Lawrence Erlbaum Associates

[102] **Field, A., (2000)** Discovering Statistics Using SPSS For Windows, London: Sage Publication

[103] **Hinton, P. R., (1995)** *Statistics Explained*, London: Routledge

[104] **ASM International (1998)** Metals Handbook. Ohio: ASM International.

[105] **Zienkiewicz, O. C., (2004)** 'The Birth of The Finite Element Method and of Computational Mechanics' *International Journal for Numerical Methods in Engineering,* 60, pp. 3 – 10

[106] **ANSYS Inc. (2010)** *Ansys Mechanical APDL and Mechanical Application Theory Reference.* Release 13.0. Canonsburg: Ansys, Inc.

[107] **ANSYS Inc. (2015)** *Ansys Workbench User Manual.* Release 16. Canonsburg: Ansys, Inc.

[108] **Ingle, M., Slebodnick, P. & Martin, J. (2011), '**High Solids Coating Performance and Service History', *Corrosion2011*, 11421, pp. 1 – 8.

[109] **Park, C. S., Son, S. M., Shin, C. S., Chung, M. K. & Baek, K. K. (2007) '**Effects of Surface Preparation Methods and Protective Coating Types on the Performance of Erection Joint Weld Seams in Water Ballast Tanks', *Corrosion2007*, 07004, Houston TX: NACE International, pp. 1 - 14.

APPENDIX I - PUBLICATIONS

[1] **Oriaifo, E. A., Perera, N, Guy, A., Leung, P. S. & Tan, K. T., 2014. '**A Review of Test Protocols for Assessing Coating Performance of Water Ballast Tank Coatings'. World Academy of Science, Engineering and Technology, International Science Index 94*, International Journal of Mechanical, Aerospace, Industrial, Mechatronics and Manufacturing Engineering*, 8(10), pp. 1610 – 1615.

[2] **Perera, N, Oriaifo, A. E., Guy, A., Leung, P. S. & Tan, K. T., 2015. '**Investigating the Accelerated Test Conditions to Produce Cracking Failure of Water Ballast Tank Coatings*'*. Paris, In: *The 6th International Congress of Energy and Environment Engineering and Management.*

APPENDIX II - COATING FORMULATIONS (PART A)

Data sheet for solvent containing pure epoxy (SPE)

Vol% Solids	70.73	**Wt% Solids**	82.91
PVC	27.88	**Wt% Pigment**	45.45
Specific Gravity	1.55	**VOC (European)**	264.42
Stoichiometry	90.45	**Mix Ratio (By Volume)**	7.11:1
Soluble: Insoluble Pigment Ratio	0 : 100	**Mix Ratio (By Volume)**	4.50 : 1
Cost per Litre	2.38	**Cost Type (region + cost set)**	Felling
Cost / m^2 at specified DFT	0.00	**Dry Film Thickness, micrometres**	No Information
Formula Cost Type UOM:	£LT	**Batch Size (LT)**	1.00
Vol% Binder	63:1:12:4:21	**Vol% Biocide**	0.00

No.	Code	Wt Pnt	Wt %	Vol%	DryVol%	Cost%	Std Cost
1	**RE 1553**	374.66	24.21	32.16	45.47	32.13	√
2	**KS 0922**	8.68	0.56	0.92	0.63	1.04	√
3	**CB 0004**	67.80	4.38	7.84	0.00	2.42	√
4	**CA 0005**	18.72	1.21	2.30	0.00	0.71	√
5	**RE 0474**	86.68	5.60	7.88	8.31	7.21	√
6	**FT 1917**	290.56	18.78	10.19	14.41	3.79	√

7	**QT 1143**	20.35	1.31	2.01	2.85	8.51	√
8	**FB 0233**	326.08	21.07	7.41	10.47	3.98	√
9	**PT 0297**	86.68	5.60	2.11	2.99	8.23	√
10	**CB 0004**	13.56	0.88	1.57	0.00	1.45	√
11	**CB 0004**	40.68	2.63	4.70	0.00	0.83	√
12	**CA 0005**	21.97	1.42	2.71	0.00	1.45	√
	Totals	1,356.42	87.66	81.82	85.13	70.79	√

No.	**Code**	**Wt Pnt**	**Wt %**	**Vol%**	**DryVol%**	**Cost%**	**Std Cost**
13	**KH6636**	190.91	12.34	18.18	14.87	29.21	√
Totals		190.91	12.34	18.18	14.87	29.21	√

Data sheet for solvent containing modified epoxy (SME)

Vol% Solids	65.17	**Wt% Solids**	79.35
PVC	26.21	**Wt% Pigment**	42.45
Specific Gravity	1.44	**VOC (European)**	296.65
Stoichiometry	70.04	**Mix Ratio (By Volume)**	4.83 : 1
Soluble: Insoluble Pigment Ratio	0 : 100	**Mix Ratio (By Volume)**	2.87 : 1
Cost per Litre	1.41	**Cost Type (region + cost set)**	Felling
Cost / m^2 at specified	0.00	**Dry Film Thickness,**	No

DFT		**micrometres**	Information
Formula Cost Type UOM:	£LT	**Batch Size (LT)**	1.00
Vol% Binder	37:6:24:4:30	**Vol% Biocide**	0.00

No.	Code	Wt Pnt	Wt %	Vol%	DryVol%	Cost%	Std Cost
1	**RE 1553**	206.30	14.36	17.71	27.17	28.06	√
2	**CB 0004**	58.33	4.06	6.74	0.00	2.97	√
3	**CA 0005**	16.66	1.16	2.05	0.00	1.06	√
4	**KS 0922**	3.74	0.26	0.40	0.30	0.75	√
5	**RE 0474**	41.95	2.92	3.81	4.36	5.53	√
6	**BH 0082**	123.26	8.58	11.36	17.43	9.34	√
7	**FT 1917**	250.83	17.46	8.80	13.51	5.15	√
8	**FB 0233**	285.89	19.90	6.50	9.97	6.08	√
9	**QT 1143**	17.24	1.20	1.78	2.74	9.53	√
10	**PT 0297**	73.12	5.09	1.78	2.74	9.53	√
11	**CB 0004**	13.22	0.92	1.53	0.00	0.67	√
12	**CB 0004**	38.07	2.65	4.40	0.00	1.94	√
13	**CA 0005**	19.83	1.38	2.44	0.00	1.26	√
14	**CB 0004**	31.31	2.18	3.62	0.00	1.60	√
15	**CA 0005**	10.49	0.73	1.29	0.00	0.67	√
	Totals	1,190.24	82.85	74.15	78.10	81.15	√

No.	Code	Wt Pnt	Wt %	Vol%	DryVol%	Cost%	Std Cost
16	**KH3154**	246.38	17.15	25.85	21.90	18.85	√
Totals		246.38	17.15	25.85	21.90	18.85	√

Data sheet for solvent free pure epoxy (SFPE)

Vol% Solids	97.78	**Wt% Solids**	98.30
PVC	10.65	**Wt% Pigment**	28.25
Specific Gravity	1.32	**VOC (European)**	22.53
Stoichiometry	84.66	**Mix Ratio (By Volume)**	3.87 : 1
Soluble: Insoluble Pigment Ratio	0 : 100	**Mix Ratio (By Volume)**	2.68 : 1
Cost per Litre	2.06	**Cost Type (region + cost set)**	Felling
Cost / m^2 at specified DFT	0.00	**Dry Film Thickness, micrometres**	No Information
Formula Cost Type UOM:	£LT	**Batch Size (LT)**	1.00
Vol% Binder	46:2:20:31	**Vol% Biocide**	0.00

No.	Code	Wt Pnt	Wt %	Vol%	DryVol%	Cost%	Std Cost
1	**RE 0583**	477.73	36.13	40.49	41.41	61.09	√

No.	Code	Wt Pnt	Wt %	Vol%	DryVol%	Cost%	Std Cost
2	**KS 0974**	6.83	0.52	0.72	0.01	1.87	√
3	**QT 0110**	17.86	1.35	1.80	1.84	4.34	√
4	**FT 0770**	142.05	10.74	5.07	5.19	1.65	√
5	**FB 1839**	181.64	13.74	4.13	4.22	2.64	√
6	**PT 2058**	49.85	3.77	1.22	1.24	4.03	√
7	**CA 0041**	10.51	0.79	1.01	0.00	0.82	√
8	**KX 0854**	158.70	12.00	17.89	18.29	23.14	√
9	**CA 0041**	5.25	0.40	0.50	0.00	0.41	√
	Totals	1,050.42	79.45	72.83	72.21	100.00	√

No.	Code	Wt Pnt	Wt %	Vol%	DryVol%	Cost%	Std Cost
10	**MK01/00001**	271.74	20.55	27.17	27.79	0.00	√
	Totals	271.74	20.55	27.17	27.79	0.00	√

Data sheet for solvent free modified epoxy (SFME)

Vol% Solids	99.37	**Wt% Solids**	99.54
PVC	8.96	**Wt% Pigment**	24.55
Specific Gravity	1.31	**VOC (European)**	5.98
Stoichiometry	79.47	**Mix Ratio (By Volume)**	5.19 : 1
Soluble: Insoluble	0 : 100	**Mix Ratio (By Volume)**	3.71 : 1

Pigment Ratio			
Cost per Litre	2.27	**Cost Type (region + cost set)**	Felling
Cost / m^2 at specified DFT	0.00	**Dry Film Thickness, micrometres**	No Information
Formula Cost Type UOM:	£LT	**Batch Size (LT)**	1.00
Vol% Binder	45:30:2:23	**Vol% Biocide**	0.00

No.	Code	Wt Pnt	Wt %	Vol%	DryVol%	Cost%	Std Cost
1	**RE 0583**	475.26	36.18	40.27	40.53	55.30	√
2	**KS 0974**	6.04	0.46	0.64	0.00	1.50	√
3	**BH 0050**	278.44	21.20	27.03	27.20	32.15	√
4	**QT 0110**	19.04	1.45	1.92	1.94	4.21	√
5	**FT 1917**	121.20	9.23	4.25	4.28	1.55	√
6	**FB 1839**	157.95	12.02	3.59	3.61	2.09	√
7	**PT 2058**	43.38	3.30	1.06	1.06	3.19	√
	Totals	1,101.31	83.84	78.63	78.63	100.00	√

No.	Code	Wt Pnt	Wt %	Vol%	DryVol%	Cost%	Std Cost
8	**MK01/00001**	212.31	16.16	21.23	21.37	0.00	√
	Totals	212.31	16.16	21.23	21.37	0.00	√

Graco Code	Raw Material Name
BH 0082	SUN-TACK C9
BH 0050	PL-400 HYDROCARBON RESIN
CA 0005	N-BUTANOL
CA 0041	BENZYL ALCOHOL
CB 0004	XYLENE
FB 0233	AW15
FT 1839	TALC CM2P
FT 1917	TALC POWDER TL-3
FB 1839	BARIFINE B20
KS 0922	EFKA-5044
KS 0974	EFKA-2725
KX 0854	EPODIL 748 DILUENT
PT 0297	TIONA 595
PT 2058	KRONOS 2090
QT 1143	DISPARLON 6650
QT 0110	CRAYVALLAC MT
RE 1553	DER 331 EPOXY RESIN
RE 0474	DER 660-X80 EPOXY RESIN
RE 0583	EPIKOTE 862

APPENDIX III - CURING AGENTS (PART B)

Graco Code	Raw Material Name
KH 3154	CARDOLITE NX – 4709E
KH 6636	ANCAMINE 2519
MK 01/00001	ANCAMINE 2712M